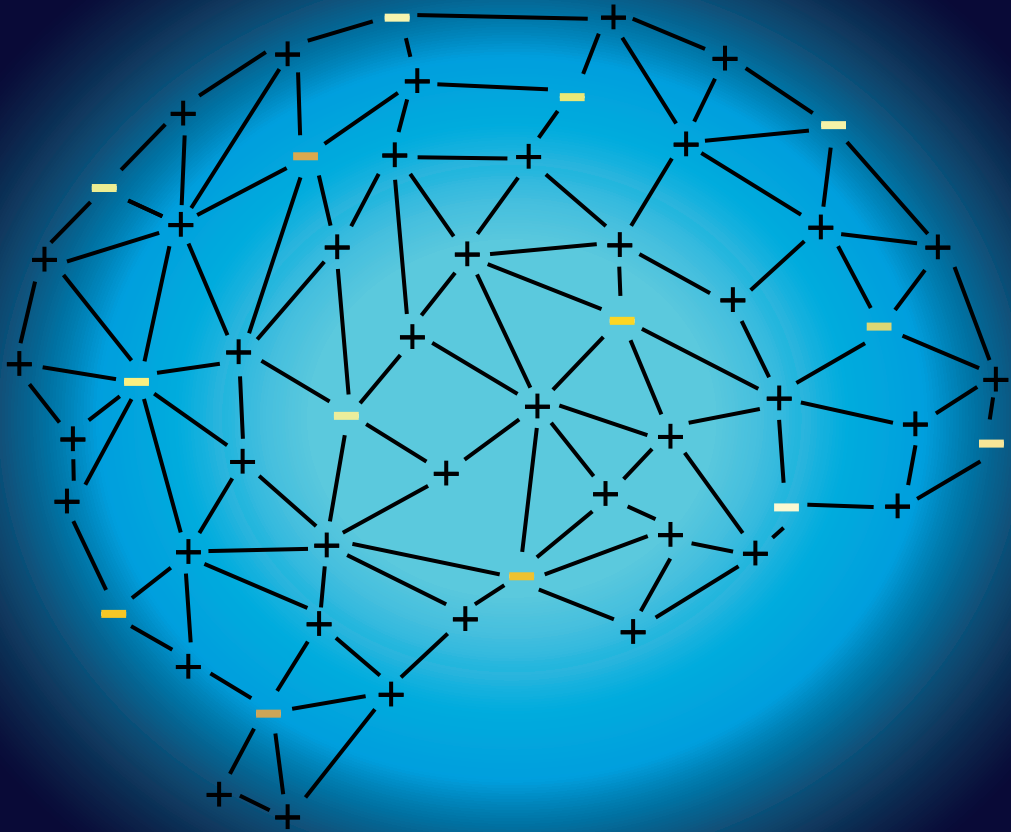


Need for Negativity:

The role of chloride homeostasis and the GABA shift in brain development

Carlijn Peerboom



Need for Negativity: The role of chloride homeostasis and the GABA shift in brain development

Carlijn Nicolle Elise Peerboom

The studies described in the thesis were performed at the division of Cell Biology at the Faculty of Science of Utrecht University, The Netherlands. This research was supported by a TOP grant from ZonMW (#91216021) and by the Nederlandse Organisatie voor Wetenschappelijk Onderzoek (NWO; #OCENW.KLEIN.150).

Author: Carlijn Peerboom

Cover lay-out: Carlijn Peerboom

Provided by thesis specialist Ridderprint, ridderprint.nl

Printing: Ridderprint

Layout and design: Michèle Duquesnoy, persoonlijkproefschrift.nl

ISBN: 978-94-6483-284-6

Copyright 2023 © Carlijn Peerboom

The Netherlands. All rights reserved. No parts of this thesis may be reproduced, stored in a retrieval system or transmitted in any form or by any means without permission of the author.

**Need for Negativity:
The role of chloride homeostasis and the GABA shift
in brain development**

**Noodzakelijke Negativiteit:
De rol van chloride homeostase en de GABA shift in hersenontwikkeling
(met een samenvatting in het Nederlands)**

Proefschrift

ter verkrijging van de graad van doctor aan de
Universiteit Utrecht
op gezag van de
rector magnificus, prof.dr. H.R.B.M. Kummeling,
ingevolge het besluit van het college voor promoties
in het openbaar te verdedigen op

woensdag 30 augustus 2023 des middags te 4.15 uur

door

Carlijn Nicolle Elise Peerboom

geboren op 22 januari 1993
te Geleen

Promotoren:

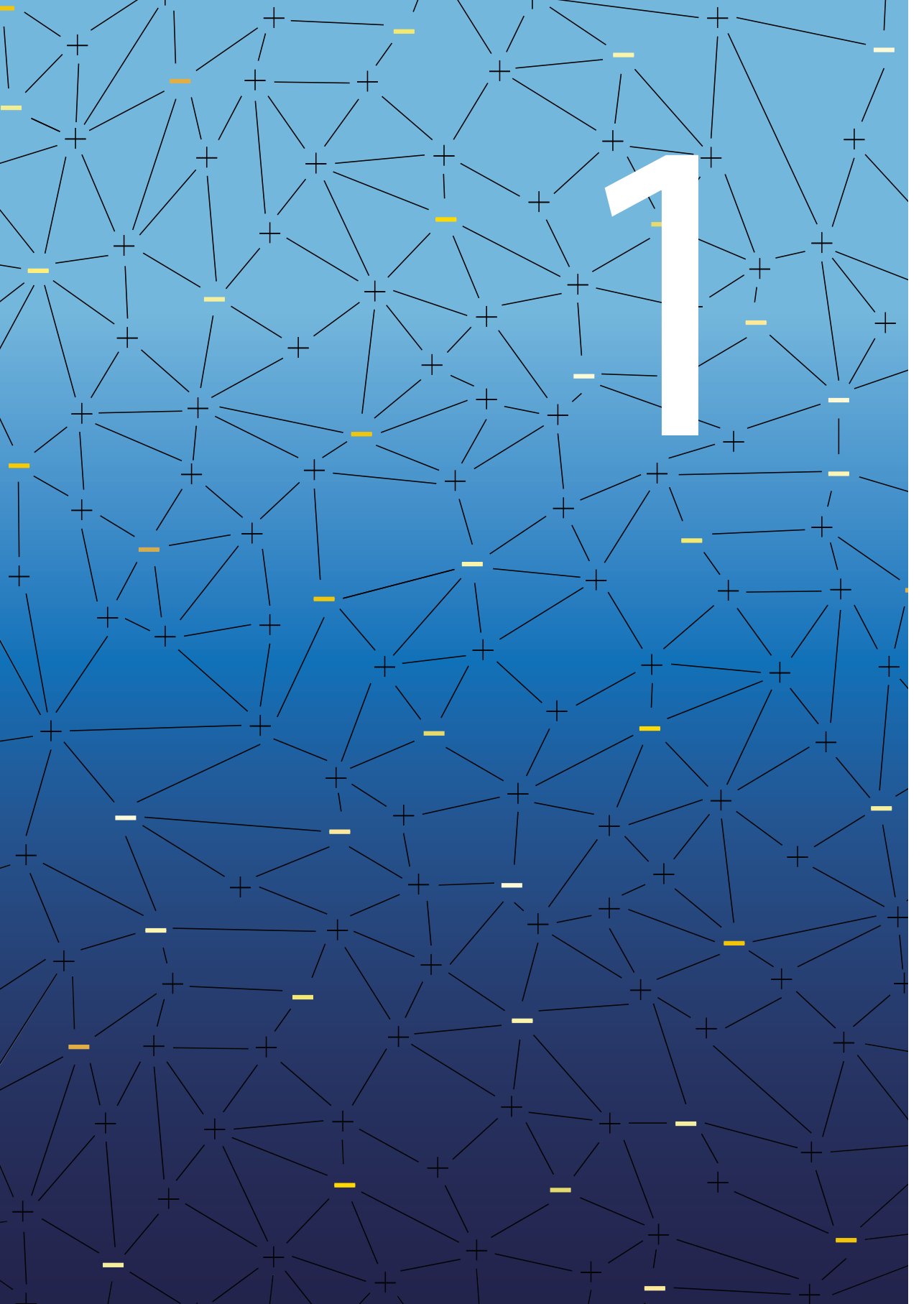
Prof. dr. A.S. Akhmanova
Prof. dr. C.J. Wierenga

Beoordelingscommissie:

Prof. dr. J.P.H. Burbach
Prof. dr. F.E. Hoebeek
Prof. dr. C.A. Lohmann
Prof. dr. N. Nadif Kasri
Dr. G.M. van Woerden

Index

Chapter 1	Introduction	07
Chapter 2	The postnatal GABA shift: a developmental perspective.....	29
Chapter 3	Using SuperClomeleon to measure changes in intracellular chloride during development and after early life stress	71
Chapter 4	Delaying the GABA shift indirectly affects membrane properties in the developing hippocampus	95
Chapter 5	Treatment with furosemide indirectly increases inhibitory transmission in the developing hippocampus.....	139
Chapter 6	Discussion	167
Addendum	Summary	198
	Nederlandse samenvatting	200
	Curriculum Vitae	202
	List of publications.....	203
	Acknowledgements	204



1

Introduction

Carlijn Peerboom

Our brain is a fascinatingly complex organ that enables us to process information from the outside world and to respond through actions, thoughts, ideas and emotions. The architecture of our adult brain, is set up during brain development which starts approximately two weeks after conception already (Fig. 1). First, molecular cues and spontaneously generated electrical activity set up a rough layout of the network. Later, sensory experiences start contributing to the electrical activity in the neuronal network, further refining it. This sequence of cues that guide the formation of our brain is highly conserved across species, including rodents.

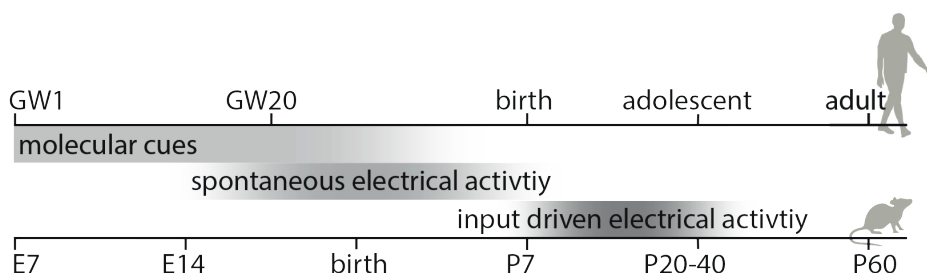


Figure 1. Schematic representation of the processes guiding the development of the human and rodent brain.

The development of the brain follows roughly the same maturational steps in humans and mice. It is initially guided by molecular interactions, but their importance declines with age. Spontaneous electrical activity contributes to network development slightly later, until input driven activity becomes the main contributor to brain development. Abbreviations: GW, gestational week; E, embryonic day; P, postnatal day.

A relatively recently discovered cue that is thought to play a critical role in brain development, is the shift in the function of neurotransmitter γ -aminobutyric acid (GABA). During the development of rodent, frog, turtle, rabbit, bird, and most likely also human brain, GABA shifts from being depolarizing to hyperpolarizing. Work in the animal brain, primarily of rodents, suggest that depolarizing GABA plays an important role as in promoting initial network assembly. Only later on, hyperpolarizing GABA is required for maintaining electrical homeostasis. These findings imply that the timing of the GABA shift is crucial for brain development and thereby also for brain architecture and function in adulthood. Yet, the consequences of a delayed GABA shift, a common feature in neurodevelopmental disorders (NDDs), remain unclear. In this thesis, I aim to improve our understanding of the consequences of a mistimed GABA shift for brain development.

1.1 GABAergic inhibition is crucial for the functioning of neurons and network in the adult brain

Decades of neuroscientific research have enabled us to begin to understand the workings of the fundamental building blocks of our brains, and to appreciate their complex, collective functioning. The mature human brain is a network of approximately 10^{11} neurons (and approximately the same number non-neuronal cells) (Azevedo et al., 2009). Neurons communicate with each other, particularly at specialized sites called synapses through molecules called neurotransmitters. Each synapse consists of a pre-synapse, a synaptic cleft, and a post-synapse. Neurotransmitters are released from the presynaptic terminal and diffuse across the synaptic cleft to activate receptors at the post-synapse. Many postsynaptic receptors are ligand-gated ion channels that transform chemical signals into electrical signals. Neurons and their synapses can be classified into two major subclasses based on the neurotransmitter they release and electrical signal they induce. Excitatory neurons, releasing excitatory neurotransmitters such as glutamate, cause the membrane potential of the postsynaptic neuron to be transiently elevated or depolarized. In contrast, inhibitory neurons, mostly using the neurotransmitter GABA, typically hyperpolarize the postsynaptic membrane in a mature brain (inducing a negative fluctuation in the membrane potential). In the postsynaptic neuron, all incoming excitatory and inhibitory fluctuations of the membrane potential are integrated. If the membrane of the postsynaptic neuron is sufficiently depolarized and a threshold potential is reached, the neuron will fire an action potential and activate its own synapses to propagate the signal onto downstream neurons.

Just try to imagine that each of the 10^{11} neurons in our brains continuously receives and processes thousands of excitatory and inhibitory inputs. How do neurons cope with this constant bombardment of incoming signals? For proper neuronal and network functioning it is crucial that inhibition, which limits action potential firing, counteracts or balances excitatory transmission. Inhibition enables the network to filter relevant from irrelevant inputs (Pouille and Scanziani, 2001; Wehr and Zador, 2003; Kanold and Shatz, 2006; Pan-vazquez et al., 2020). In addition, inhibition keeps action potential frequencies within neurons in a functional range to generate network responses that are linear to external input strength (Turrigiano and Nelson, 2004; Maffei and Fontanini, 2009; Herstel and Wierenga, 2021).

1.2 GABA functions as an excitatory signal during brain development

An important exception is during early brain development, when excitation is not balanced by inhibition yet. In the embryonic brain, the number of excitatory synapses is still relatively low, and the excitatory synapses that have been formed are not functional yet. The immature synapses lack α -amino-3-hydroxy-5-methyl-4-isoxazolepropionic acid (AMPA) type glutamate receptors and their N-methyl-D-aspartate (NMDA) type glutamate receptors are mostly inactive. Instead of glutamate, GABA functions as the primary excitatory signal during this period. Excitatory GABA promotes network assembly during embryonic development, before GABA will become the main inhibitory neurotransmitter in the adult brain.

The advantage of depolarizing GABA signaling in the developing brain is that GABAergic transmission can promote action potential firing and be excitatory during development. Depolarizing and excitatory GABA functions as an important molecular cue during brain development, allowing for the growth of the neuronal network. Excitatory GABA mediates stem cell proliferation, neuronal migration and promotes the formation and maturation of excitatory synapses (see chapter 2) (Peerboom and Wierenga, 2021). If depolarizing GABA also mediates the formation of inhibitory synapses remains less clear. Some studies suggest that depolarizing GABA promotes the formation of GABAergic synapses and recruitment of GABA receptors (Akerman and Cline, 2006; Nakanishi et al., 2007; Wang and Kriegstein, 2008, 2011; Oh et al., 2016; Pisella et al., 2019), while others shows that depolarizing GABA limits GABAergic transmission instead (Chudotvorova et al., 2005; Pisella et al., 2019).

1.3 The GABA shift plays a crucial role in network development

To prevent the developing brain from becoming hyperactive by continuously generating more excitatory neurons and excitatory synapses, a break on network growth and activity is required. With the decrease in intraneuronal chloride levels, hyperpolarizing GABA starts inhibiting neuronal activity and providing the opposing force that is required to balance excitation. Since hyperpolarizing GABA permits that only relevant inputs are processed by the network, and less relevant inputs are filtered out, hyperpolarizing GABA is important for the experience-dependent refinement of the network (see chapter 2) (Pouille and Scanziani, 2001; Wehr and Zador, 2003; Kanold and Shatz, 2006; Pan-vazquez et al., 2020).

Thus, the shift in the function of GABA signaling is a crucial event in brain development, as it defines GABA's molecular and electrical role, while matching the circumstances and needs of the developing network. This implies that proper timing of the GABA shift is crucial for brain development.

1.4 The GABA shift is a result of a decrease in intraneuronal chloride concentrations

How can GABA_A function switch from being excitatory in the immature brain, but being inhibitory later on? GABA signals primarily via ionotropic GABA_A receptors, which are ion channels that are mainly permeable for chloride ions. In the immature brain, intraneuronal chloride levels are high. As a result, activation of GABA_A receptors leads to an outflow of negatively charged chloride ions and depolarization of the postsynaptic neuron. Also in humans cortical neurons, GABA has been shown to be excitatory at gestational week 22 (Chen and Kriegstein, 2015). During development, intracellular chloride levels decrease and in the mature brain intraneuronal chloride levels are low. Therefore, activation of a GABA_A receptors results in an influx of chloride resulting in membrane hyperpolarization and GABA exerts its typical inhibitory action. The developmental decrease in chloride levels causes a gradual drop in the reversal potential for GABA_A currents below resting membrane potential, which shifts GABA currents from being depolarizing to hyperpolarizing. This phenomenon is called the GABA shift (Fig. 2).

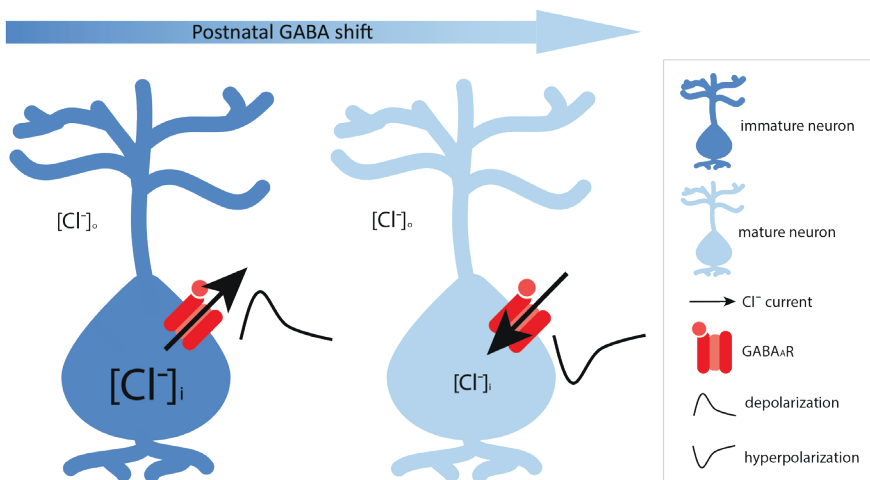


Figure 2. GABA shifts due to a decrease in intracellular chloride concentration.

The direction of the flow of chloride ions through GABA_A receptors depends on the electrochemical chloride gradient. Left: In the immature brain, the intracellular chloride concentration ($[Cl^-]_i$) is relatively high. Activation of GABA_A receptors results in an outflow of chloride, resulting in membrane depolarization. Right: During development, intracellular chloride levels decrease. As a result, activation of GABA_A receptors leads to an entry of chloride and GABAergic signaling results in hyperpolarization of mature neurons.

The GABA shift is the result of a change in the relative contributions of the chloride transporters Na-K-2Cl cotransporter isoform 1 (NKCC1) and the K-Cl cotransporter isoform 2 (KCC2). In the immature brain chloride transport over the membrane is dominated by chloride importer NKCC1. During development, intracellular chloride decreases, due to increase in chloride exporter KCC2. In humans, the change in chloride co-transporter expression takes usually place in the first year after birth (Dzhala et al., 2005; Sedmak et al., 2016). In rodents, GABA shifts during the first two postnatal weeks (Rivera et al., 1999; Stein et al., 2004; Ben-Ari et al., 2007; Romo-Parra et al., 2008; Glykys et al., 2009; Kirmse et al., 2015; Sulis Sato et al., 2017).

To determine when the GABA shift occurs intracellular chloride levels need to be measured. This is impossible in humans, but in animal models several methods exist to evaluate the GABA shift. The shift has classically been measured using electrophysiology. The developmental decrease of intracellular chloride in rodent neurons can be inferred from measurements of the reversal potential of the GABA_A current using perforated patch clamp recordings (Ebihara et al., 1995; Ben-Ari et al., 2007; Tyzio et al., 2007). Antibiotics (e.g., gramicidin or amphotericin B) in the patch pipette form small pores in the membrane which leaves intracellular chloride concentration intact (Fig. 3 (Ebihara et al., 1995)). However, the reversal potential only provides an estimate of the intracellular chloride concentration as GABAergic currents contain not only a chloride, but also a bicarbonate component of approximately 20-40%. The bicarbonate reversal potential is much more positive than the chloride reversal potential (at around -10 mV) and maintained by pH-dependent mechanisms. As a result, the contribution of bicarbonate to the GABA_A reversal potential increases with the developmental decrease of the chloride reversal potential (Misgeld and Frotscher, 1986; Bormann et al., 1987; Kaila et al., 1993). Assuming that chloride reversal potentials equal the GABA reversal potentials results in an overestimation of chloride concentrations, especially in mature neurons. In addition, perforated patch clamp recordings are labor intensive. It is technically extremely challenging to measure chloride concentrations in large populations of neurons, while big individual differences can exist between neurons and many recordings may be required to get a good population estimate (Tyzio et al., 2007; Sulis Sato et al., 2017).

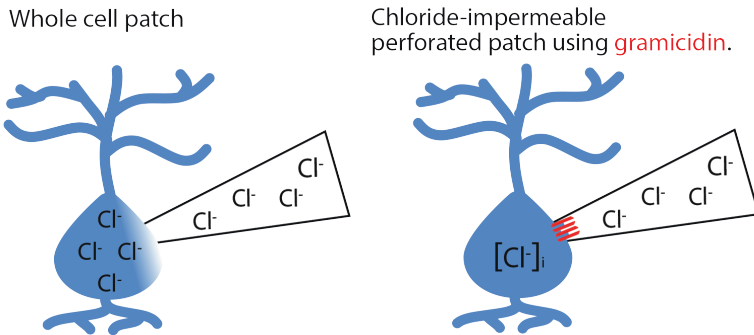


Figure 3. Assessing intracellular chloride concentrations using perforated patch clamp.

With the patch clamp technique, one gets electrical access to neurons. In the whole cell configuration, the intraneuronal chloride concentration is affected by the concentration of chloride in the pipette solution. In the perforated patch clamp configuration, the antibiotic gramicidin in the patch pipette forms small pores in the neuronal membrane leaving intracellular chloride intact.

As a promising alternative, fluorescent biosensors have been developed in recent years. The best biosensors today are for calcium, as a proxy of neuronal activity. Calcium sensors have contributed immensely to our understanding of neuronal signaling (Day-Cooney et al., 2022; Dong et al., 2022). However, recent technological developments have generated a number of other useful biosensors, including for chloride. In theory, the recently developed chloride sensor SuperClomeleon (SCLm) enables noninvasive assessment of chloride in multiple neurons simultaneously, overcoming the disadvantages of perforated patch clamp recordings (Grimley et al., 2013; Boffi et al., 2018; Rahmati et al., 2021). In this thesis, we investigated the applicability of the SCLm sensor to measure the developmental changes in chloride in the mouse brain.

1.5 Molecular and environmental factors regulate the timing of the GABA shift

An important open question is how the shift in GABA's function is triggered in developing neurons (Medina et al., 2014). The shift also occurs in neuronal cultures and organotypic slices (Rivera et al., 1999; Salmon et al., 2020), indicating that it is (at least partly) induced by an intrinsic molecular program. Some molecular factors (described in more detail in chapter 2) have been found able to prevent GABA from shifting too early, while other factors assure the postnatal GABA shift is not too late. On top of the molecular program, the shift is adjusted by hormones (such as the sex hormones and thyroid hormone), neuronal activity and early life experience. For instance, stress

during early life was shown to alter the timing of the GABA shift (Veerawatananan et al., 2016; Furukawa et al., 2017; Hu et al., 2017b) and poses an increased risk for aberrant brain function in later life (Teicher et al., 2016; Joëls et al., 2018).

1.6 The timing of the GABA shift is altered in neurodevelopmental disorders

Intriguingly, NDDs are associated with a mistimed chloride maturation and GABA shift (Talós et al., 2012; Duarte et al., 2013; Bruining et al., 2015; Ruffolo et al., 2018; Molnár et al., 2020; Wang et al., 2021; Birey et al., 2022). NDDs represent a broad range neurological and psychiatric conditions, including autism spectrum disorder, Rett, Fragile X and Down syndrome, typically manifesting in the first three years after birth. Numerous genetic risks for NDDs are known, particularly in synaptic genes and regulators of neurodevelopment (e.g. chromatin remodelers and members of the mammalian target of rapamycin (mTOR) pathway) (Parenti et al., 2020). The risk for NDDs is also conferred by exposure to environmental risk factors, such as *in utero* infections, drug exposure and hypoxia (Parenti et al., 2020). In NDD patients alterations in the chloride co-transporters have been reported (Talós et al., 2012; Duarte et al., 2013; Deidda et al., 2015b; Ruffolo et al., 2018), suggesting that the GABA shift is altered. Work in animal models for NDDs also shows that NDD risks or mutations often converge to a delayed GABA shift (He et al., 2014; Tyzio et al., 2014; Banerjee et al., 2016; Corradini et al., 2017; Fernandez et al., 2018; Roux et al., 2018; Lozovaya et al., 2019; Bertoni et al., 2020), an imbalance in excitation and inhibition (Gogolla et al., 2009; Antoine et al., 2019) and alterations in sensory sensitivity (Meredith, 2015; Molnár et al., 2020). These observations suggest that a delay in the GABA shift during early postnatal development may affect early network development, disturb the coordination between excitation and inhibition and result in an altered network responsiveness in adulthood (Meredith, 2015; Molnár et al., 2020).

1.7 The consequences of a delayed GABA shift remain unclear

The role of depolarizing GABA in network assembly and excitatory synapse formation and maturation (LoTurco et al., 1995; Leinekugel et al., 1997; Haydar et al., 2000; Bortone and Polleux, 2007; Andäng et al., 2008; Luhmann et al., 2015; Oh et al., 2016) and of hyperpolarizing GABA in network refinement (Pouille and Scanziani, 2001; Wehr and Zador, 2003; Kanold and Shatz, 2006; Pan-vazquez et al., 2020) were discovered in rodents by manipulating GABA signaling up until the first week after birth or advancing the GABA shift. In contrast, the consequences of a delayed GABA shift, as often observed in NDDs, remain mostly unclear. It is often assumed that the effects of excitatory GABA are exacerbated when the GABA shift is delayed. A delayed GABA shift would then lead to excessive excitatory synapse formation and an excitation and inhibition imbalance. However, this has not yet been addressed experimentally.

To examine the consequences of a delayed GABA shift, previous studies have used knock out and knock down approaches targeting the KCC2 protein. These studies revealed that KCC2 supports neuronal maturation through a physical interaction with various other proteins, including the actin cytoskeleton to facilitate activity-induced spine growth (Li et al., 2007; Llano et al., 2015), glutamatergic AMPA receptors to support their insertion and confinement in the synapse (Gauvain et al., 2011; Chevy et al., 2015) and potassium channels to hyperpolarize the resting membrane potential (Chevy et al., 2015; Goutierre et al., 2019). Importantly, spine development could be rescued by expression of a chloride-transport-deficient KCC2 mutant (Li et al., 2007; Llano et al., 2015) and AMPA receptors or potassium channels were not affected by pharmacological inhibition of KCC2 (Gauvain et al., 2011; Chevy et al., 2015; Goutierre et al., 2019). This shows that KCC2 also mediates neuronal maturation, independently of its role in mediating ion transport.

The consequences of a delayed GABA shift have also been studied mouse models with a genetically altered KCC2 phosphorylation. Interestingly, these mice have NDD-resembling phenotypes, such as altered social behavior, memory retention and an increased seizure susceptibility (Moore et al., 2019; Pisella et al., 2019). Restoration of the postnatal GABA shift through pharmacological inhibition of NKCC1 rescued some but not all phenotypes in these mice. This suggests that deregulation of KCC2 phosphorylation itself contributes to the alterations in these mice (Pisella et al., 2019). These examples show that it remains technically challenging to examine the consequences of a delayed GABA shift, independently of KCC2 structural role or phosphorylation status.

1.8 Examining the consequences of a delayed GABA shift through overexpression of NKCC1

In my PhD project I set out to examine the consequences of a delayed GABA shift without interfering with KCC2's structural role. Our initial approach was to overexpress the chloride importer NKCC1. An increased expression of NKCC1 has been found in specific genetic mouse models for NDDs, including schizophrenia, Fragile X and Down Syndrome (Deidda et al., 2015b; He et al., 2018; Kim et al., 2021), as well as in patients with Schizophrenia and Down Syndrome (Dean et al., 2007; Deidda et al., 2015b). In addition, a gain-of-function mutation in NKCC1 predisposes for Schizophrenia (Merner et al., 2016). This suggests that OE of NKCC1 would be a valuable approach, with direct relevance for NDDs.

We successfully overexpressed YFP-NKCC1 in HEK cells using polyethylenimine and in neurons using lipofectamine (Fig. 4A,B). Unfortunately, these transfection reagents are not efficient in slices, so we had to revert to viral approaches or electroporation. We first set out to produce lentivirus for YFP-NKCC1. However, we were not successful

in producing the lentivirus in our HEK cells. We considered that virus production may have been hampered by the high intracellular chloride in HEK cells resulting from the NKCC1 overexpression. We therefore added 200 μM of NKCC1 blocker bumetanide or 200 μM furosemide to the cultured HEK cells. However, this did not improve virus production. We reasoned that the large size of the NKCC1 construct (FUGW21-YFP-NKCC1 is 8438 kb between Long Terminal Repeats) impaired virus production. Though lentiviral vectors can incorporate constructs up to 10 kb in size, vector titer is known to decrease with an increasing insert length (Kumar et al., 2001). We therefore sought another approach.

As an alternative, we used slice electroporation for overexpression of pCAG-YFP-NKCC1. However, in our hands, electroporated slices looked unhealthy. In addition, cells that expressed YFP-NKCC1 mostly displayed glial morphologies. We optimized electroporation parameters to target as many neurons as possible (see methods). However, we could not improve slice health and achieved a maximum of five neurons per slice (Fig. 4C,D). Thus, we were not successful in effectively transfecting neurons in slice cultures with this method.

As a third option, we used *in utero* electroporation to overexpress pCAG-YFP-NKCC1 in the visual cortex, in collaboration with the Lohmann lab at the Netherlands Institute for Neuroscience. In a first trial 10 to 200 YFP positive neurons were visible in in layer 2/3 of organotypic slices of the visual cortex (Fig. 4E). We conclude that *in utero* electroporation would be the preferred method to overexpress NKCC1. Unfortunately we were unable to functionally validate the overexpression of NKCC1 in these neurons as collaboration experiments had to be stopped due to the COVID-19 pandemic. We therefore resorted to the pharmacological approach that I describe briefly below and in more detail in chapter 4 and 5.

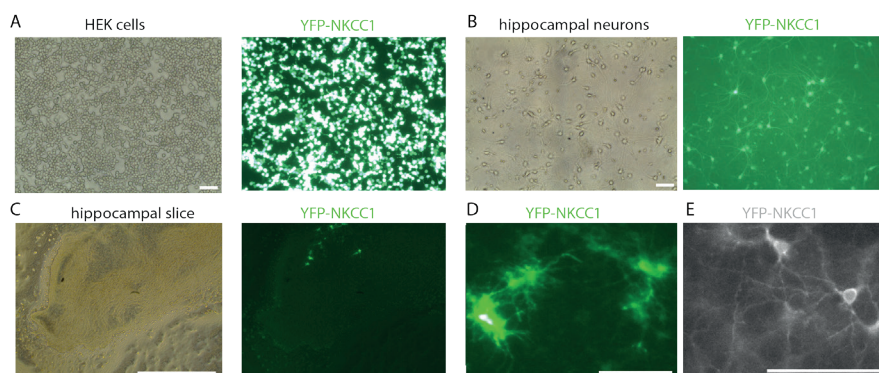


Figure 4. Overexpression of NKCC1 via lentivirus was not successful, but could be achieved using *in utero* electroporation.

A) Overexpression of YFP-NKCC1 in HEK cells. Scale bar=100 μm .

B) Overexpression of YFP-NKCC1 in dissociated hippocampal neurons. Scale bar=100 μm .

C) Example organotypic hippocampal culture at DIV9 in after slice electroporation of YFP-NKCC1. Scale bar=1000 μm

D) Cells that express YFP-NKCC1 after slice electroporation have glial morphology. Scale bar=100 μm .

E) Expression of YFP-NKCC1 in the visual cortex after *in utero* electroporation. Scale bar=100 μm .

As an alternative to overexpression of the chloride exporter NKCC1, we set out to delay the GABA shift by blocking the chloride importer KCC2. We therefore used VU0463271 (VU), a specific KCC2 antagonist (Delpire et al., 2012) and assessed the consequences of a delayed GABA shift on the development of both excitatory and inhibitory synapses. In a parallel study, we used furosemide, an inhibitor of both KCC2 and NKCC1 to examine the role of chloride in the development of GABAergic synapses.

Methods used for the experiments described in this introduction

For slice cultures and in utero electroporations, C57Bl/6J mice of both sexes were used. For dissociated neuronal cultures, male and female Wistar rats were used (Janvier Labs). Slice cultures were prepared as described in chapters 3, 4 and 5. Dissociated neuronal cultures were prepared as described in (Cunha-Ferreira et al., 2018)

Transfections

HEK293 cells were transfected with pFUGW-YFP-NKCC1 (cloned from Addgene YFP-NKCC1 plasmid #49085) polyethylenimine (PEI; 1 µg/µl; Polysciences). Hippocampal neurons were transfected using Lipofectamine 2000 (Invitrogen) at DIV8. pFUGW-YFP-NKCC1 (~ 0.5 µg/well) was mixed with 10 µl Lipofectamine2000 in 200 µl Neurobasal medium (NB), incubated for 25 minutes and added to the neurons in 800 µl NB at 37°C and 5% CO₂ for 45 minutes. Next, neurons were washed in preheated NB and transferred back to their original medium for at least 48 h.

Virus production and infection

HEK293 cells were maintained at a high growth rate in DMEM supplemented with 10% FCS and 1% pen/strep. At 1 day after plating, cells were transfected using PEI (1 µg/µl; Polysciences) with second-generation LV packaging plasmids (psPAX2 and 2MD2.G) and pFUGW-YFP-NKCC1 (cloned from Addgene YFP-NKCC1 plasmid #49085) at a 1:1:1 molar ratio. Six hours after transfection, cells were washed once with PBS, and medium was replaced with DMEM containing 1% pen/strep. In some experiments, DMEM was supplemented with 200µM bumetanide or 200µM furosemide. At 48 hours after transfection, the supernatant was harvested and briefly centrifuged at 700g to remove cell debris. The supernatant was concentrated using Amicon Ultra 15 100K MWCO columns (Milipore) and frozen at -80°C until infection. For primary cultures, 0.5-2 µl virus was added per coverslip at DIV. For organotypic hippocampal slice cultures, virus was injected into the CA1 region at DIV1 using an Eppendorf Femtojet injector.

Hippocampal slice electroporation

Electroporation was performed using a pCAG-YFP-NKCC1 plasmid (cloned from Addgene NKCC1 plasmid #49085). Slice electroporation was performed in organotypic cultures at DIV1. A slice was transferred to preheated HBSS. Fast Green (5%, F7252, Sigma) was added to the plasmid solution (1 $\mu\text{g}/\mu\text{l}$) to enable visual inspection of the injection. This mixture was injected onto the pyramidal cells layer in CA1 using a glass micropipette and a picospritzer. An electroporator (ECM 830 Electro-Square-Porator, Harvard Apparatus) and platinum plated tweezer-electrodes (Nepagene) were used. The positive pole of tweezer-like electrodes was placed above the slice. A drop of warm HBSS was added onto the slice. Rectangular pulses (5 pulses 25V, 5ms duration with an interval of 995ms (personal communication Helene Becq (Clot-Faybesse), Inserm, Marseille, France), or 3 pulses 32V, 100 ms duration with an interval of 100 ms (Will et al., 2019), or 5 pulses 27V, 1ms duration with an interval of 100ms (Niculescu et al., 2018) or 3 pulses at 5V, 1 ms duration with an interval of 999 ms as a test for minimal electroporation) were applied to the slice via a drop of warm HBSS. Helene Becq's protocol was optimal for hitting neurons over glia, though neuronal transfection rates remained low (maximum five neurons per slice). After electroporation, slices were placed back into the incubator.

In utero electroporation

Pyramidal neurons in layer 2/3 of the visual cortex were transfected with a pCAG-YFP-NKCC1 plasmid (1 mg/ml) using in utero electroporation at E16.5 (Harvey et al., 2009). Pregnant mice were anesthetized with isoflurane and an incision (1.5–2 cm) was made in the abdominal wall. The uterine horns were removed from the abdomen. DNA was injected into the lateral ventricle of embryos using a sharp glass electrode. Voltage pulses (five square wave pulses, 30 V, 50-ms duration, 950-ms interval, custom-built electroporator) were delivered across the brain with tweezer electrodes covered in conductive gel. Embryos were rinsed with warm saline solution and placed back into the abdomen. Muscle and skin of the pregnant dam were sutured. Organotypic slices of the visual cortex were made on P5 following the procedure described above. Slices were evaluated at DIV3-8.

1.9 Scope of this thesis

The maturation of neuronal chloride levels is considered a key event in brain development. However, our means to study intracellular chloride in large populations of neurons are limited and the consequences of a delayed chloride maturation as commonly observed in NDDs, remain unclear. During my PhD, I aimed to improve our understanding the consequences of a mistimed GABA shift for brain development. We examined the applicability of the novel SClm sensor to assess intracellular chloride levels in many neurons during development. In addition, we manipulated the maturation of neuronal chloride levels and examined its consequences for network development.

In **chapter 2** we summarize the current knowledge on the role of intracellular chloride and the GABA shift during brain development. We argue that the shift from depolarizing to hyperpolarizing GABA represents the final shift in a sequence of GABA shifts, regulating proliferation, migration, differentiation, and finally plasticity of developing neurons. Once the rough layout has been set up and activity becomes driven by sensory inputs, hyperpolarizing GABA is required to carefully select the optimal neural representations from many competing inputs that increasingly bombard the developing brain. We summarize the factors that promote or inhibit the GABA shift, though the precise molecular trigger remains to be elucidated. We also discuss the evidence for alterations of the GABA shift in NDDs.

In **chapter 3** we examine the applicability of the SClm sensor to study intracellular chloride in large neuronal populations. We show that we can measure a clear developmental decrease in intracellular chloride in cultured brain slices as well as an increase in intracellular chloride after early life stress in acute slices. Although conversion from SClm fluorescence to absolute chloride concentrations proved difficult, this chapter shows that the SClm sensor is a powerful tool to measure physiological changes in chloride levels in brain slices.

In **chapter 4** we examine the consequences of a delayed GABA shift using KCC2 blocker VU in cultured brain slices. We show that elevated chloride levels do not have any direct effects on the function and structure of synapses and neurons. However, after normalization of neuronal chloride levels, slices exhibited an elevated inhibitory transmission, and neurons showed subtle, cell-specific alterations in their membrane properties. Our study underscores a role of chloride homeostasis beyond synapse formation, and implicates a link between chloride levels and membrane conductance.

In **chapter 5** we treated slice cultures for one week with furosemide, blocking both KCC2 as well as NKCC1. Again, the function and structure of inhibitory synapses was not affected directly after the treatment, further confirming that postnatal chloride

levels do not directly affect synapse formation. However, after normalization of GABA signaling, we observed that inhibitory transmission was enhanced, presumably due to an increased number of inhibitory synapses. Furthermore, we found some indications for altered cell swelling. This study sheds new light on the mechanisms of action of furosemide as an anti-epileptic. Increasing the number of inhibitory synapses might constitute a mechanism by which furosemide reduces seizure susceptibility.

In **chapter 6** I discuss the findings presented in Chapter 2-5 in light of the overall question of this thesis: what are the consequences of a mistimed GABA shift for brain development? I will discuss the pros and cons of the methods used in this thesis to follow the developmental chloride trajectory. I also highlight technical advancements that may further enhance to our understanding of the GABA shift. These advancements include improved chloride indicators, which could make it easier to follow the chloride development in many neurons, and CRISPR/Cas9-mediated genome editing, which may enable us to follow NKCC1, KCC2 and other proteins involved in the GABA shift in living brain tissue in the future. In addition, I discuss how the environment may affect the timing of the GABA shift, how the timing of the GABA shift may direct brain development, the implications of our findings for neurodevelopmental disorders and the implications of our findings on furosemide as a possible treatment for epilepsy. At this moment, we are only beginning to understand how genetic mutations and early life experience that affect the timing of the GABA shift, may push brain development into different directions. A more precise understanding of the consequences of a mistimed GABA shift may be useful for the creation of targeted therapies to alleviate behavioral burden in neurodevelopmental disorders.

1.10 References

- Akerman, C.J., Cline, H.T., 2006. Depolarizing GABAergic conductances regulate the balance of excitation to inhibition in the developing retinotectal circuit in vivo. *J. Neurosci.* 26, 5117–5130. <https://doi.org/10.1523/JNEUROSCI.0319-06.2006>
- Andäng, M., Hjerling-Leffler, J., Moliner, A., Lundgren, T.K., Castelo-Branco, G., Nanou, E., Pozas, E., Bryja, V., Halliez, S., Nishimaru, H., Wilbertz, J., Arenas, E., Koltzenburg, M., Charnay, P., Manira, A. El, Ibañez, C.F., Ernfors, P., 2008. Histone H2AX-dependent GABAA receptor regulation of stem cell proliferation. *Nature* 451, 460–464. <https://doi.org/10.1038/nature06488>
- Antoine, M.W., Langberg, T., Schnepel, P., Feldman, D.E., 2019. Increased Excitation-Inhibition Ratio Stabilizes Synapse and Circuit Excitability in Four Autism Mouse Models - supplemental. *Neuron* 101, 648-661.e4. <https://doi.org/10.1016/j.neuron.2018.12.026>
- Azevedo, F.A.C., Carvalho, L.R.B., Grinberg, L.T., Farfel, J.M., Ferretti, R.E.L., Leite, R.E.P., Filho, W.J., Lent, R., Herculano-Houzel, S., 2009. Equal numbers of neuronal and nonneuronal cells make the human brain an isometrically scaled-up primate brain. *J. Comp. Neurol.* 513, 532–541. <https://doi.org/10.1002/cne.21974>
- Banerjee, A., Rikhye, R. V., Breton-Provencher, V., Tang, X., Li, C., Li, K., Runyan, C.A., Fu, Z., Jaenisch, R., Sur, M., 2016. Jointly reduced inhibition and excitation underlies circuit-wide changes in cortical processing in Rett syndrome. *Proc. Natl. Acad. Sci.* 113, E7287–E7296. <https://doi.org/10.1073/pnas.1615330113>
- Ben-Ari, Y., Gaiarsa, J.-L., Tyzio, R., Khazipov, R., 2007. GABA: A Pioneer Transmitter That Excites Immature Neurons and Generates Primitive Oscillations. *Physiol. Rev.* 87, 1215–1284. <https://doi.org/10.1152/physrev.00017.2006>
- Bertoni, A., Schaller, F., Tyzio, R., Gaillard, S., Santini, F., Xolin, M., Diabira, D., Vaidyanathan, R., Matarazzo, V., Medina, I., Hammock, E., Zhang, J., Chini, B., Gaiarsa, J.-L., Muscatelli, F., 2020. Acute neonatal oxytocin impacts hippocampal network development and restores adult social memory deficits in a mouse model of autism spectrum disorder. *BioRxiv*.
- Birey, F., Li, M.Y., Gordon, A., Thete, M. V., Valencia, A.M., Revah, O., Paşca, A.M., Geschwind, D.H., Paşca, S.P., 2022. Dissecting the molecular basis of human interneuron migration in forebrain assembloids from Timothy syndrome. *Cell Stem Cell* 29, 248-264. e7. <https://doi.org/10.1016/j.stem.2021.11.011>
- Boffi, J.C., Knabbe, J., Kaiser, M., Kuner, T., 2018. KCC2-dependent steady-state intracellular chloride concentration and pH in cortical layer 2/3 neurons of anesthetized and awake mice. *Front. Cell. Neurosci.* 12, 1–14. <https://doi.org/10.3389/fncel.2018.00007>
- Bormann, J., Hamill, O.P., Sakmann, B., 1987. Mechanism of anion permeation through channels gated by glycine and gamma-aminobutyric acid in mouse cultured spinal neurones. *J. Physiol.* 385, 243–286.
- Bortone, D., Polleux, F., 2007. KCC2 Expression Promotes the Termination of Cortical Interneuron Migration in a Voltage-Sensitive Calcium-Dependent Manner supplemental. *Environ. Microbiol.* 9, 1523–1534. <https://doi.org/10.1111/j.1462-2920.2007.01271.x>
- Bruining, H., Passtoors, L., Goriounova, N., Jansen, F., Hakvoort, B., de Jonge, M., Poil, S.S.-S., 2015. Paradoxical Benzodiazepine Response: A Rationale for Bumetanide in Neurodevelopmental Disorders? *Pediatrics* 136, e539-43. <https://doi.org/10.1542/peds.2014-4133>


- Chen, J., Kriegstein, A.R., 2015. A GABAergic projection from the zona incerta to cortex promotes cortical neuron development. *Science* (80-.). 350, 554–558. <https://doi.org/10.1126/science.aac6472>
- Chevy, Q., Heubl, M., Goutierre, M., Backer, S., Moutkine, I., Eugene, E., Bloch-Gallego, E., Levi, S., Poncer, J.C., 2015. KCC2 Gates Activity-Driven AMPA Receptor Traffic through Cofilin Phosphorylation. *J. Neurosci.* 35, 15772–15786. <https://doi.org/10.1523/JNEUROSCI.1735-15.2015>
- Chudotvorova, I., Ivanov, A., Rama, S., Christian, A.H., Pellegrino, C., 2005. Early expression of KCC2 in rat hippocampal cultures augments expression of functional GABA synapses 3, 671–679. <https://doi.org/10.1113/jphysiol.2005.089821>
- Corradini, I., Focchi, E., Rasile, M., Morini, R., Desiato, G., Tomasoni, R., Lizier, M., Ghirardini, E., Fesce, R., Morone, D., Barajon, I., Antonucci, F., Pozzi, D., Matteoli, M., 2017. Maternal Immune Activation Delays Excitatory-to-Inhibitory Gamma-Aminobutyric Acid Switch in Offspring. *Biol. Psychiatry* 83, 1–12. <https://doi.org/10.1016/j.biopsych.2017.09.030>
- Cunha-Ferreira, I., Chazeau, A., Buijs, R.R., Stucchi, R., Will, L., Pan, X., Adolfs, Y., van der Meer, C., Wolthuis, J.C., Kahn, O.I., Schätzle, P., Altelaar, M., Pasterkamp, R.J., Kapitein, L.C., Hoogenraad, C.C., 2018. The HAUS Complex Is a Key Regulator of Non-centrosomal Microtubule Organization during Neuronal Development. *Cell Rep.* 24, 791–800. <https://doi.org/10.1016/j.celrep.2018.06.093>
- Day-Cooney, J., Dalangin, R., Zhong, H., Mao, T., 2022. Genetically encoded fluorescent sensors for imaging neuronal dynamics in vivo. *J. Neurochem.* 1–25. <https://doi.org/10.1111/jnc.15608>
- Dean, B., Keriakous, D., Scarr, E., Thomas, E. a., 2007. From Subjects With Gene expression profiling in Brodmann's area 46 from subjects with schizophrenia Brian. *Aust. N. Z. J. Psychiatry* 41, 308–320.
- Deidda, G., Parrini, M., Naskar, S., Bozarth, I.F., Contestabile, A., Cancedda, L., 2015. Reversing excitatory GABAAR signaling restores synaptic plasticity and memory in a mouse model of Down syndrome. *Nat. Med.* 21, 318–326. <https://doi.org/10.1038/nm.3827>
- Delpire, E., Baranczak, A., Waterson, A.G., Kim, K., Kett, N., Morrison, R.D., Scott Daniels, J., David Weaver, C., Lindsley, C.W., 2012. Further optimization of the K-Cl cotransporter KCC2 antagonist ML077: Development of a highly selective and more potent in vitro probe. *Bioorganic Med. Chem. Lett.* 22, 4532–4535. <https://doi.org/10.1016/j.bmcl.2012.05.126>
- Dong, C., Zheng, Y., Long-Iyer, K., Wright, E.C., Li, Y., Tian, L., 2022. Fluorescence Imaging of Neural Activity, Neurochemical Dynamics, and Drug-Specific Receptor Conformation with Genetically Encoded Sensors. *Annu. Rev. Neurosci.* 45, 273–294. <https://doi.org/10.1146/annurev-neuro-110520-031137>
- Duarte, S.T., Armstrong, J., Roche, A., Ortez, C., Pérez, A., O'Callaghan, M. del M., Pereira, A., Sanmartí, F., Ormazábal, A., Artuch, R., Pineda, M., García-Cazorla, A., 2013. Abnormal Expression of Cerebrospinal Fluid Cation Chloride Cotransporters in Patients with Rett Syndrome. *PLoS One* 8, 1–7. <https://doi.org/10.1371/journal.pone.0068851>
- Dzhala, V.I., Talos, D.M., Sdrulla, D.A., Brumback, A.C., Mathews, G.C., Benke, T.A., Delpire, E., Jensen, F.E., Staley, K.J., 2005. NKCC1 transporter facilitates seizures in the developing brain. *Nat. Med.* 11, 1205–1213. <https://doi.org/10.1038/nm1301>
- Ebihara, S., Shirato, K., Harata, N., Akaike, N., 1995. Gramicidin-perforated patch recording: GABA response in mammalian neurones with intact intracellular chloride. *J. Physiol.* 484, 77–86. <https://doi.org/10.1113/jphysiol.1995.sp020649>

- Fernandez, A., Dumon, C., Guimond, D., Fernandez, A., Burnashev, N., Tyzio, R., Lozovaya, N., Ferrari, D.C., Bonifazi, P., Ben-Ari, Y., 2018. The GABA Developmental Shift Is Abolished by Maternal Immune Activation Already at Birth. *Cereb. Cortex* 29, 3982–3992. <https://doi.org/10.1093/cercor/bhy279>
- Furukawa, M., Tsukahara, T., Tomita, K., Iwai, H., Sonomura, T., Miyawaki, S., Sato, T., 2017. Neonatal maternal separation delays the GABA excitatory-to-inhibitory functional switch by inhibiting KCC2 expression. *Biochem. Biophys. Res. Commun.* 493, 1243–1249. <https://doi.org/10.1016/j.bbrc.2017.09.143>
- Gauvain, G., Chamma, I., Chevy, Q., Cabezas, C., Irinopoulou, T., Bodrug, N., Carnaud, M., Levi, S., Poncer, J.C., 2011. The neuronal K-Cl cotransporter KCC2 influences postsynaptic AMPA receptor content and lateral diffusion in dendritic spines. *Proc. Natl. Acad. Sci.* 108, 15474–15479. <https://doi.org/10.1073/pnas.1107893108>
- Glykys, J., Dzhalal, V.I., Kuchibhotla, K.V., Feng, G., Kuner, T., Augustine, G., Bacskai, B., Staley, K., 2009. Differences in cortical vs. subcortical GABAergic signaling: a candidate mechanism of electroclinical dissociation of neonatal seizures. *Neuron*. 63, 657–672. <https://doi.org/10.1016/j.neuron.2009.08.022>. Differences
- Gogolla, N., LeBlanc, J.J., Quast, K.B., Südhof, T.C., Fagiolini, M., Hensch, T.K., 2009. Common circuit defect of excitatory-inhibitory balance in mouse models of autism. *J. Neurodev. Disord.* 1, 172–181. <https://doi.org/10.1007/s11689-009-9023-x>
- Goutierre, M., Al Awabdh, S., Donneger, F., François, E., Gomez-Dominguez, D., Irinopoulou, T., Menendez de la Prida, L., Poncer, J.C., 2019. KCC2 Regulates Neuronal Excitability and Hippocampal Activity via Interaction with Task-3 Channels. *Cell Rep.* 28, 91–103. <https://doi.org/10.1016/j.celrep.2019.06.001>
- Grimley, J.S., Li, L., Wang, W., Wen, L., Beese, L.S., Hellinga, H.W., Augustine, G.J., 2013. Visualization of Synaptic Inhibition with an Optogenetic Sensor Developed by Cell-Free Protein Engineering Automation. *J. Neurosci.* 33, 16297–16309. <https://doi.org/10.1523/JNEUROSCI.4616-11.2013>
- Haydar, T.F., Wang, F., Schwartz, M.L., Rakic, P., 2000. Differential Modulation of Proliferation in the Neocortical Ventricular and Subventricular Zones. *J. Neurosci.* 20, 5764–5774. <https://doi.org/10.1523/JNEUROSCI.20-15-05764.2000>
- He, Q., Arroyo, E.D., Smukowski, S.N., Xu, J., Piochon, C., Savas, J.N., Portera-Cailliau, C., Contractor, A., 2018. Critical period inhibition of NKCC1 rectifies synapse plasticity in the somatosensory cortex and restores adult tactile response maps in fragile X mice. *Mol. Psychiatry* 24, 1732–1747. <https://doi.org/10.1038/s41380-018-0048-y>
- He, Q., Nomura, T., Xu, J., Contractor, A., 2014. The Developmental Switch in GABA Polarity Is Delayed in Fragile X Mice. *J. Neurosci.* 34, 446–450. <https://doi.org/10.1523/JNEUROSCI.4447-13.2014>
- Herstel, L.J., Wierenga, C.J., 2021. Network control through coordinated inhibition. *Curr. Opin. Neurobiol.* 67, 34–41. <https://doi.org/10.1016/j.conb.2020.08.001>
- Hu, Yu, Z.L., Zhang, Y., Han, Y., Zhang, W., Lu, L., Shi, J., 2017. Bumetanide treatment during early development rescues maternal separation-induced susceptibility to stress. *Sci. Rep.* 7, 1–16. <https://doi.org/10.1038/s41598-017-12183-z>
- Joëls, M., Karst, H., Sarabdjitsingh, R.A., 2018. The stressed brain of humans and rodents. *Acta Physiol.* 223, 1–10. <https://doi.org/10.1111/apha.13066>
- Kaila, K., Voipio, J., Paalasmaa, P., Pasternack, M., Deisz, R.A., 1993. The role of bicarbonate in GABAA receptor-mediated IPSPs of rat neocortical neurones. *J. Physiol.* 464, 273–289.

- Kanold, P.O., Shatz, C.J., 2006. Subplate Neurons Regulate Maturation of Cortical Inhibition and Outcome of Ocular Dominance Plasticity. *Neuron* 51, 627–638. <https://doi.org/10.1016/j.neuron.2006.07.008>
- Kim, H.R., Rajagopal, L., Meltzer, H.Y., Martina, M., 2021. Depolarizing GABAA current in the prefrontal cortex is linked with cognitive impairment in a mouse model relevant for schizophrenia. *Sci. Adv.* 7, 1–10. <https://doi.org/10.1126/sciadv.aba5032>
- Kirmse, K., Kummer, M., Kovalchuk, Y., Witte, O.W., Garaschuk, O., Holthoff, K., 2015. GABA depolarizes immature neurons and inhibits network activity in the neonatal neocortex in vivo. *Nat. Commun.* 6, 1–13. <https://doi.org/10.1038/ncomms8750>
- Kumar, M., Keller, B., Makalou, N., Sutton, R.E., 2001. Systematic determination of the packaging limit of lentiviral vectors. *Hum. Gene Ther.* 12, 1893–1905. <https://doi.org/10.1089/104303401753153947>
- Leinekugel, X., Medina, I., Khalilov, I., Ben-Ari, Y., Khazipov, R., 1997. Ca²⁺ Oscillations Mediated by the Synergistic Excitatory Actions of GABA. *Neuron* 18, 243–255.
- Li, H., Khirug, S., Cai, C., Ludwig, A., Blaesse, P., Kolikova, J., Afzalov, R., Coleman, S.K., Lauri, S., Airaksinen, M.S., Keinänen, K., Khiroug, L., Saarma, M., Kaila, K., Rivera, C., 2007. KCC2 Interacts with the Dendritic Cytoskeleton to Promote Spine Development. *Neuron* 56, 1019–1033. <https://doi.org/10.1016/j.neuron.2007.10.039>
- Llano, O., Smirnov, S., Soni, S., Golubtsov, A., Guillemain, I., Hotulainen, P., Medina, I., Nothwang, H.G., Rivera, C., Ludwig, A., 2015. KCC2 regulates actin dynamics in dendritic spines via interaction with β -PIX. *J. Cell Biol.* 209, 671–686. <https://doi.org/10.1083/jcb.201411008>
- LoTurco, J.J., Owens, D.F., Heath, M.J.S., Davis, M.B.E., Kriegstein, A.R., 1995. GABA and glutamate depolarize cortical progenitor cells and inhibit DNA synthesis. *Neuron* 15, 1287–1298. [https://doi.org/10.1016/0896-6273\(95\)90008-X](https://doi.org/10.1016/0896-6273(95)90008-X)
- Lozovaya, N., Nardou, R., Tyzio, R., Chiesa, M., Pons-Bennaceur, A., Eftekhari, S., Bui, T.T., Billon-Grand, M., Rasero, J., Bonifazi, P., Guimond, D., Gaiarsa, J.L., Ferrari, D.C., Ben-Ari, Y., 2019. Early alterations in a mouse model of Rett syndrome: the GABA developmental shift is abolished at birth. *Sci. Rep.* 9, 1–16. <https://doi.org/10.1038/s41598-019-45635-9>
- Luhmann, H.J., Fukuda, A., Kilb, W., 2015. Control of cortical neuronal migration by glutamate and GABA. *Front. Cell. Neurosci.* 9, 1–15. <https://doi.org/10.3389/fncel.2015.00004>
- Maffei, A., Fontanini, A., 2009. Network homeostasis: a matter of coordination. *Curr. Opin. Neurobiol.* 19, 168–173. <https://doi.org/10.1016/j.conb.2009.05.012>
- Medina, I., Friedel, P., Rivera, C., Kahle, K.T., Kourdougli, N., Uvarov, P., Pellegrino, C., 2014. Current view on the functional regulation of the neuronal K⁺-Cl⁻ cotransporter KCC2. *Front. Cell. Neurosci.* 8, 1–18. <https://doi.org/10.3389/fncel.2014.00027>
- Meredith, R.M., 2015. Sensitive and critical periods during neurotypical and aberrant neurodevelopment: A framework for neurodevelopmental disorders. *Neurosci. Biobehav. Rev.* 50, 180–188. <https://doi.org/10.1016/j.neubiorev.2014.12.001>
- Merner, N.D., Mercado, A., Khanna, A.R., Hodgkinson, A., Bruat, V., Awadalla, P., Gamba, G., Rouleau, G.A., Kahle, K.T., 2016. Gain-of-function missense variant in SLC12A2, encoding the bumetanide-sensitive NKCC1 cotransporter, identified in human schizophrenia. *J. Psychiatr. Res.* 77, 22–26. <https://doi.org/10.1016/j.jpsychires.2016.02.016>
- Misgeld, U., Frotscher, M., 1986. Postsynaptic GABAergic inhibition of non-pyramidal neurons in the guinea-pig hippocampus. *Neuroscience* Sep 19, 193–206.
- Molnár, Z., Luhmann, H.J., Kanold, P.O., 2020. Transient cortical circuits match spontaneous and sensory-driven activity during development. *Science* (80-.). 370. <https://doi.org/10.1126/science.abb2153>

- Moore, Y.E., Conway, L.C., Wobst, H.J., Brandon, N.J., Deeb, T.Z., Moss, S.J., 2019. Developmental Regulation of KCC2 Phosphorylation Has Long-Term Impacts on Cognitive Function. *Front. Mol. Neurosci.* 12, 1–11. <https://doi.org/10.3389/fnmol.2019.00173>
- Nakanishi, K., Yamada, J., Takayama, C., Oohira, A., Fukuda, A., 2007. NKCC1 Activity Modulates Formation of Functional Inhibitory Synapses in Cultured Neocortical Neurons. *Synapse* 411, 401–411. <https://doi.org/10.1002/syn>
- Niculescu, D., Michaelsen-Preusse, K., Güner, Ü., van Dorland, R., Wierenga, C.J., Lohmann, C., 2018. A BDNF-Mediated Push-Pull Plasticity Mechanism for Synaptic Clustering. *Cell Rep.* 24, 2063–2074. <https://doi.org/10.1016/j.celrep.2018.07.073>
- Oh, W.C., Lutzu, S., Castillo, P.E., Kwon, H.B., 2016. De novo synaptogenesis induced by GABA in the developing mouse cortex - supplemental. *Science (80-)*. 353, 1037–1040. <https://doi.org/10.1126/science.aaf5206>
- Pan-vazquez, A., Wefelmeyer, W., Sabater, V.G., Neves, G., Burrone, J., 2020. Activity-Dependent Plasticity of Axo-axonic Synapses at the Axon Initial Segment. *Neuron* 106, 1–12. <https://doi.org/10.1016/j.neuron.2020.01.037>
- Parenti, I., Rabaneda, L.G., Schoen, H., Novarino, G., 2020. Neurodevelopmental Disorders: From Genetics to Functional Pathways. *Trends Neurosci.* 43, 608–621. <https://doi.org/10.1016/j.tins.2020.05.004>
- Peerboom, C., Wierenga, C.J., 2021. The postnatal GABA shift: A developmental perspective. *Neurosci. Biobehav. Rev.* 124, 179–192. <https://doi.org/10.1016/j.neubiorev.2021.01.024>
- Pisella, Gaiarsa, Diabira, Zhang, Khalilov, Duan, Kahle, Medina, 2019. Impaired regulation of KCC2 phosphorylation leads to neuronal network dysfunction and neurodevelopmental pathology. *Sci. Signal.* 12. <https://doi.org/10.1126/scisignal.aay0300>
- Pouille, F., Scanziani, M., 2001. Enforcement of temporal fidelity in pyramidal cells by somatic feed-forward inhibition. *Science (80-)*. 293, 1159–1163. <https://doi.org/10.1126/science.1060342>
- Rahmati, N., Normoyle, K.P., Glykys, J., Dzhalal, V.I., Lillis, K.P., Kahle, K.T., Raiyyani, R., Jacob, T., Staley, K.J., 2021. Unique actions of gaba arising from cytoplasmic chloride microdomains. *J. Neurosci.* 41, 4967–4975. <https://doi.org/10.1523/JNEUROSCI.3175-20.2021>
- Rivera, C., Voipio, J., Payne, J. a, Ruusuvoori, E., Lahtinen, H., Lamsa, K., Pirvola, U., Saarma, M., Kaila, K., 1999. The K⁺/Cl⁻ co-transporter KCC2 renders GABA hyperpolarizing during neuronal maturation. *Nature* 397, 251–255. <https://doi.org/10.1038/16697>
- Romo-Parra, H., Treviño, M., Heinemann, U., Gutiérrez, R., 2008. GABA actions in hippocampal area CA3 during postnatal development: Differential shift from depolarizing to hyperpolarizing in somatic and dendritic compartments. *J. Neurophysiol.* 99, 1523–1534. <https://doi.org/10.1152/jn.01074.2007>
- Roux, S., Lohof, A., Ben-Ari, Y., Poulain, B., Bossu, J.-L., 2018. Maturation of GABAergic Transmission in Cerebellar Purkinje Cells Is Sex Dependent and Altered in the Valproate Model of Autism. *Front. Cell. Neurosci.* 12, 1–14. <https://doi.org/10.3389/fncel.2018.00232>
- Ruffolo, G., Cifelli, P., Roseti, C., Thom, M., van Vliet, E.A., Limatola, C., Aronica, E., Palma, E., 2018. A novel GABAergic dysfunction in human Dravet syndrome. *Epilepsia* 59, 2106–2117. <https://doi.org/10.1111/epi.14574>
- Salmon, C.K., Pribiag, H., Gizowski, C., Farmer, W.T., Cameron, S., Jones, E. V., Mahadevan, V., Bourque, C.W., Stellwagen, D., Woodin, M.A., Murai, K.K., 2020. Depolarizing GABA Transmission Restrains Activity-Dependent Glutamatergic Synapse Formation in the Developing Hippocampal Circuit. *Front. Cell. Neurosci.* 14, 1–16. <https://doi.org/10.3389/fncel.2020.00036>

- Sedmak, G., Puskarjov, N.J.-M.M., Ulapec, M., Krušlin, B., Kaila, K., Judaš, M., 2016. Developmental Expression Patterns of KCC2 and Functionally Associated Molecules in the Human Brain. *Cereb. Cortex* 27, 4060–4072. <https://doi.org/10.1093/cercor/bhw218>
- Stein, V., Hermans-Borgmeyer, I., Jentsch, T.J., Hübner, C.A., 2004. Expression of the KCl Cotransporter KCC2 Parallels Neuronal Maturation and the Emergence of Low Intracellular Chloride. *J. Comp. Neurol.* 468, 57–64. <https://doi.org/10.1002/cne.10983>
- Sulis Sato, S., Artoni, P., Landi, S., Cozzolino, O., Parra, R., Pracucci, E., Trovato, F., Szczurkowska, J., Luin, S., Arosio, D., Beltram, F., Cancedda, L., Kaila, K., Ratto, G.M., 2017. Simultaneous two-photon imaging of intracellular chloride concentration and pH in mouse pyramidal neurons in vivo. *Proc. Natl. Acad. Sci.* 114, E8770–E8779. <https://doi.org/10.1073/pnas.1702861114>
- Talos, D.M., Sun, H., Kosaras, B., Joseph, A., Folkerth, R.D., Poduri, A., Madsen, J.R., Black, P.M., Jensen, F.E., 2012. Altered inhibition in tuberous sclerosis and type IIb cortical dysplasia. *Ann. Neurol.* 71, 539–551. <https://doi.org/10.1002/ana.22696>
- Teicher, M.H., Samson, J.A., Anderson, C.M., Ohashi, K., 2016. The effects of childhood maltreatment on brain structure, function and connectivity. *Nat. Rev. Neurosci.* 17, 652–666. <https://doi.org/10.1038/nrn.2016.111>
- Turrigiano, G.G., Nelson, S.B., 2004. Homeostatic plasticity in the developing nervous system. *Nat. Rev. Neurosci.* 5, 97–107. <https://doi.org/10.1038/nrn1327>
- Tyzio, R., Holmes, G.L., Ben-Ari, Y., Khazipov, R., 2007. Timing of the developmental switch in GABA mediated signaling from excitation to inhibition in CA3 rat hippocampus using gramicidin perforated patch and extracellular recordings. *Epilepsia* 48, 96–105. <https://doi.org/10.1111/j.1528-1167.2007.01295.x>
- Tyzio, R., Nardou, R., Ferrari, D., Tsintsadze, T., Shahrokhi, A., Eftekhari, S., Khalilov, I., Tsintsadze, V., Brouchoud, C., Chazal, G., Lemonnier, E., Lozovaya, N., Burnashev, N., Y., B.-A., 2014. Oxytocin-Mediated GABA Inhibition During Delivery Attenuates Autism Pathogenesis in Rodent Offspring. *Science* (80-.). 343, 675–680.
- Veerawatananan, B., Surakul, P., Chutabhakdikul, N., 2016. Maternal restraint stress delays maturation of cation-chloride cotransporters and GABA receptor subunits in the hippocampus of rat pups at puberty. *Neurobiol. Stress* 3, 1–7. <https://doi.org/10.1016/j.jynstr.2015.12.001>
- Wang, D.D., Kriegstein, A.R., 2011. Blocking early GABA depolarization with bumetanide results in permanent alterations in cortical circuits and sensorimotor gating deficits. *Cereb. Cortex* 21, 574–587. <https://doi.org/10.1093/cercor/bhq124>
- Wang, D.D., Kriegstein, A.R., 2008. GABA Regulates Excitatory Synapse Formation in the Neocortex via NMDA Receptor Activation. *J. Neurosci.* 28, 5547–5558. <https://doi.org/10.1523/JNEUROSCI.5599-07.2008>
- Wang, T., Shan, L., Miao, C., Xu, Z., Jia, F., 2021. Treatment Effect of Bumetanide in Children With Autism Spectrum Disorder: A Systematic Review and Meta-Analysis. *Front. Psychiatry* 12, 1–11. <https://doi.org/10.3389/fpsy.2021.751575>
- Wehr, M., Zador, A.M., 2003. Balanced inhibition underlies tuning and sharpens spike timing in auditory cortex. *Nature* 426, 442–446. <https://doi.org/10.1038/nature02116>
- Will, L., Portegies, S., Van Schelt, J., Van Luyk, M., Jaarsma, D., Hoogenraad, C.C., 2019. Dynein activating adaptor BICD2 controls radial migration of upper-layer cortical neurons in vivo. *Acta Neuropathol. Commun.* 7, 1–23. <https://doi.org/10.1186/s40478-019-0827-y>



2

The postnatal GABA shift: a developmental perspective

C. Peerboom¹ and C.J. Wierenga^{1,2}

¹ Cell Biology, Neurobiology and Biophysics, Biology department, Utrecht University, 3584CH, Utrecht, the Netherlands,

² Current address: Faculty of Science & Donders Institute, Radboud University, 6525 AJ, Nijmegen, the Netherlands

This chapter has been published in *Neuroscience & Biobehavioral Reviews*, 2021, May (124), doi: [10.1016/j.neubiorev.2021.01.024](https://doi.org/10.1016/j.neubiorev.2021.01.024)

2.1 Abstract

GABA is the major inhibitory neurotransmitter that counterbalances excitation in the mature brain. The inhibitory action of GABA relies on the inflow of chloride ions (Cl^-), which hyperpolarizes the neuron. In early development, GABA signaling induces outward Cl^- currents and is depolarizing. The postnatal shift from depolarizing to hyperpolarizing GABA is a pivotal event in brain development and its timing affects brain function throughout life. Altered timing of the postnatal GABA shift is associated with several neurodevelopmental disorders. Here, we argue that the postnatal shift from depolarizing to hyperpolarizing GABA represents the final shift in a sequence of GABA shifts, regulating proliferation, migration, differentiation, and finally plasticity of developing neurons. Each developmental GABA shift ensures that the instructive role of GABA matches the circumstances of the developing network. Sensory drive may be a crucial factor in determining proper timing of the postnatal GABA shift. A developmental perspective is necessary to interpret the full consequences of a mismatch between connectivity, activity and GABA signaling during brain development.

2.2 Introduction

The direction of γ -aminobutyric acid (GABA) currents through ionotropic GABA receptors reverses during brain development from depolarizing to hyperpolarizing. This developmental change is often referred to as the postnatal GABA shift, and is caused by a change in the expression of the two major chloride (Cl⁻) transporters, Na-K-2Cl cotransporter isoform 1 (NKCC1) and the K-Cl cotransporter isoform 2 (KCC2) (Fig. 1). Conservation of the GABA shift across brain structures and species, including frogs, turtles, mice, rats, rabbits, birds, and most likely also humans, suggests that the GABA shift has been preserved during evolution and is essential for brain development (Ben-Ari et al., 2007; Tang, 2020). Defects in the GABA shift are associated with a wide variety of neurodevelopmental disorders, including autism (Schulte et al., 2018). Recent experimental studies have suggested postnatal GABA signaling as an interesting common therapeutic target for neurodevelopmental disorders. In animal models of Fragile X (He et al., 2018), Down syndrome (Deidda et al., 2015b) and Rett syndrome (Banerjee et al., 2016), restoring inhibitory GABA signaling during a restricted postnatal period yielded significant and long lasting improvements in brain function. Pilot studies in human patients (Bruining et al., 2015; Lemonnier et al., 2017; Khademullah et al., 2020) have also been encouraging. These promising findings are raising renewed attention to the central role for GABA signaling in brain development. Why is the postnatal GABA shift so important and when exactly does GABA need to shift? To answer these questions we first examine the role of depolarizing GABA in the developing hippocampus and cortex. Consecutively, depolarizing GABA instructs proliferation, migration and differentiation of immature neurons during early neuronal development. In addition, depolarizing GABA can contribute to spontaneous activity in some brain areas. We conclude that the postnatal GABA shift represents one of a series of developmental shifts in the roles of GABA during brain development. In the second part of the review, we focus on the postnatal shift to hyperpolarizing GABA, which is required at later stages to regulate activity and to tighten plasticity rules to optimize neuronal networks to process (sensory) information throughout life. We discuss how sensory drive may be a crucial factor in determining proper timing of the postnatal GABA shift and how a developmental perspective will help to interpret the consequences of a mismatch between connectivity, activity and GABA signaling during brain development.

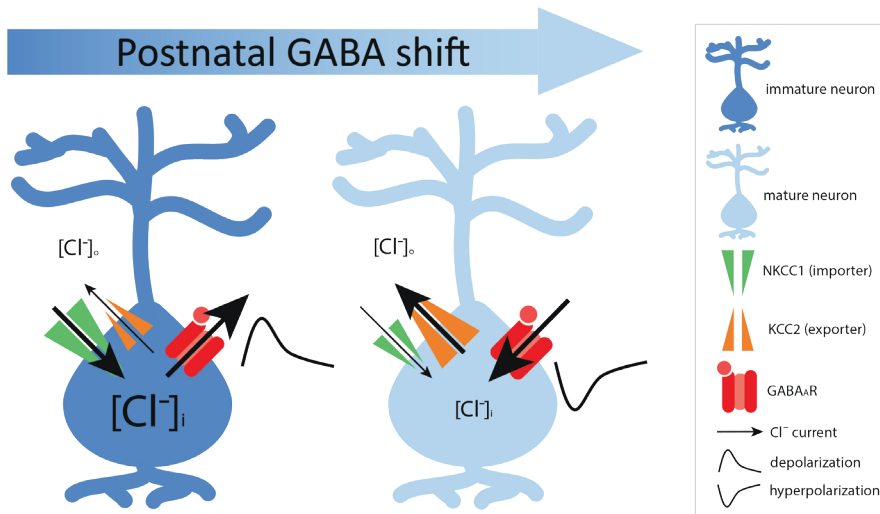


Figure 1. The postnatal GABA shift is due to a decrease in intracellular chloride (Cl^-) concentration. The direction of the flow of Cl^- ions through GABA_A receptors depends on the electrochemical Cl^- gradient. Left: In the immature brain, the intracellular Cl^- concentration is relatively high, as Cl^- transport over the membrane is dominated by NKCC1. Activation of GABA_A receptors results in an outflow of Cl^- resulting in membrane depolarization. Right: During development, intracellular Cl^- levels decrease, due to increased expression and activity of KCC2. As a result, activation of GABA_A receptors leads to an entry of Cl^- and GABAergic signaling results in hyperpolarization of mature neurons.

2.3 Depolarizing GABA mediates early neuronal development

GABA signaling is present already early in development, long before neurons form networks via synapses. For instance, embryonic and neuronal crest stem cells release and respond to GABA via GABA_A receptors in an autocrine way (Andäng et al., 2008; Wang and Kriegstein, 2008). In the following, we will describe the multiple roles of GABA in brain development in rodents (mostly mice). When other model organisms were used, we will state them explicitly. From around mouse embryonic day (E)9, GABA is released from growth cones of interneurons (Taylor and Gordon-Weeks, 1991; Gao and Pol, 2000). The earliest depolarizing GABAergic synaptic responses are measured approximately one week later (at E16-20) in the cortical plate (CP) and hippocampus, when the first GABAergic synapses emerge (LoTurco et al., 1995; Owens et al., 1996, 1999; Demarque et al., 2002; Gozlan and Ben-Ari, 2003). As GABA is depolarizing at this stage, GABA signaling can activate voltage-gated calcium (Ca^{2+}) channels (LoTurco et al., 1995; Owens et al., 1996; Kirmse et al., 2010, 2015; Tyzio et al., 2014; Furukawa et al., 2017). As we will describe below, depolarizing GABA and GABA-induced Ca^{2+} influx are important instruction signals to regulate development of the embryonic brain

(Fig. 2). Rather than simply promoting developmental processes in young neurons, GABA governs developmental switching points, from proliferation to migration, from migration to differentiation, and finally from differentiation to synapse formation. Thus, while being depolarizing, GABA's instructive role shifts in each step of early network development.

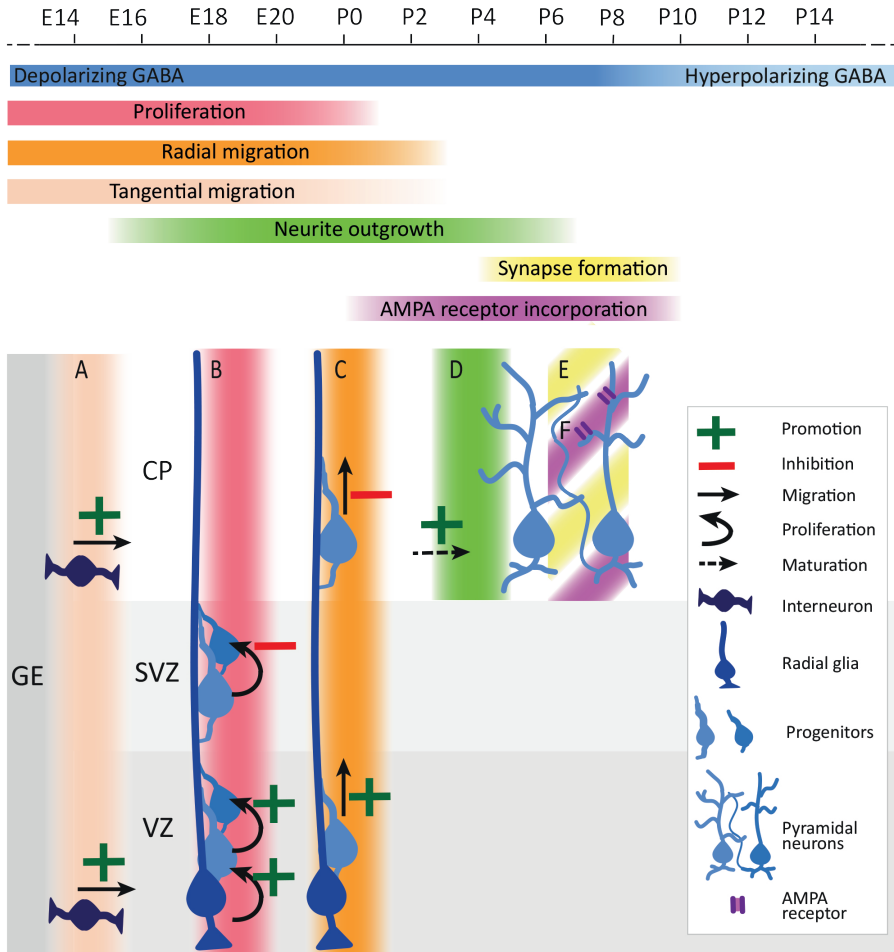


Figure 2. Developmental switching points, instructed by GABA signaling.

Depolarizing GABA guides the construction of the brain early in development by mediating the migration, proliferation and maturation of synapses of neuronal precursors and interneurons in the developing cortex. GE = ganglionic eminence, CP = cortical plate, SVZ = subventricular zone, VZ = ventricular zone.

Depolarizing GABA mediates proliferation

An important role for GABA in early development is to mediate cell cycle progression of stem cells in the developing brain (Fig. 2B). Neurons are generated within the developing cortex from neural stem cells. The primary neural stem cells, the radial glia cells, are located in the ventricular zone (VZ), while the subventricular zone (SVZ) is a secondary proliferative region where intermediate progenitor cells reside. Whereas depolarizing GABA promotes proliferation of primary stem cells in the VZ (Haydar et al., 2000; Ikeda-Matsuo et al., 2012), GABA signaling actually inhibits the proliferation of intermediate precursors in the SVZ (Haydar et al., 2000). The negative effect in SVZ seems stronger, which explains the observed decrease in progenitor proliferation in slices containing both regions after depolarization with GABA or high extracellular potassium (K^+) (LoTurco et al., 1995; Haydar et al., 2000; Liu et al., 2005). GABA has been shown to inhibit cell cycle progression by mediating the expression levels of different cell cycle regulators in a wide variety of neurons, both *in vitro* and *in vivo* (Nguyen et al., 2003; Andäng et al., 2008; Cesetti et al., 2011; Duveau et al., 2011; Fernando et al., 2011; Song et al., 2012). However, the precise molecular pathways used by GABA to promote proliferation in VZ and inhibit proliferation in the SVZ remain to be elucidated.

Depolarizing GABA mediates migration

Newborn neurons migrate away from the VZ and SVZ through the intermediate zone (IZ) to the developing CP. This migration is also regulated by depolarizing GABA (reviewed by (Luhmann et al., 2015)) (Fig. 2C). Depolarization, either by GABA or via high extracellular K^+ , promotes migration of dissociated embryonic cortical neurons in chemotaxis chambers (Behar et al., 1996, 1998) whereas interference with GABAergic depolarization reduces migration of cortical neurons *in vivo* (Inoue et al., 2012). Evidence from embryonic cortical slice cultures shows that depolarizing GABA promotes migration from VZ via $GABA_A-\rho$ receptors (Behar et al., 2000; Denter et al., 2010). $GABA_A-\rho$ receptors are ionotropic receptors that produce slow, but large and sustained Cl^- currents when activated (Woodward et al., 1993). $GABA_A-\rho$ receptors are only transiently expressed by migrating neurons and replaced by more conventional $GABA_A$ receptors once neurons reach the CP (Denter et al., 2010). Inhibiting conventional $GABA_A$ receptors with bicuculline, which does not block $GABA_A-\rho$ receptors (Woodward et al., 1993), actually increases the number of neurons reaching the CP (Behar et al., 2000; Bolteus, 2004; Heck et al., 2007; Denter et al., 2010), suggesting that $GABA_A$ receptor signaling inhibits the migration of neurons once $GABA_A-\rho$ receptors are downregulated. GABA also limits migration in the olfactory bulb and in newborn granule cells in the adult hippocampus (Fueshko et al., 1998; Duveau et al., 2011).

GABAergic interneurons are generated in the ganglionic eminences of the ventral telencephalon and follow a tangential migration route into the developing cortex and hippocampus between approximately E10 and E16 (Hu et al., 2017a). Depolarizing

GABA also promotes the tangential migration of interneurons (Fig. 2A) (Bortone and Polleux, 2009; Inada et al., 2011). Once interneurons start expressing KCC2, Ca²⁺ signaling decreases due to hyperpolarizing GABA and migration slows down (Bortone and Polleux, 2009). GABA_A- ρ receptors are also expressed in GABAergic interneurons (Semyanov and Kullmann, 2002; Martinez-Delgado et al., 2010), but their role in interneuron migration has not been explored.

Depolarizing GABA promotes neurite growth and synapse formation

After young pyramidal neurons have reached their final destination, depolarizing GABA induced Ca²⁺ influx promotes outgrowth of neurites (reviewed by (Sernagor et al., 2010)) (Fig. 2D) in cultures (Barbin et al., 1993; Maric et al., 2001; Gascon et al., 2006; Reynolds et al., 2008; Ageta-Ishihara et al., 2009; Nakajima and Marunaka, 2016) and *in vivo* (Cancedda et al., 2007; Wang and Kriegstein, 2008, 2011; Ikeda-Matsuo et al., 2012). GABA also promotes dendritic arborization in newborn neurons in the adult hippocampus and olfactory bulb (Duveau, 2011; Ge, 2006; Gascon, 2006). In addition, GABA promotes the formation of synapses (Fig. 2E). Blockade of GABAergic transmission with bicuculline for 24 hours in cultured intact hippocampi prevented the developmental increase in the frequency of inhibitory synaptic currents that normally occurs after birth (Colin-Le Brun et al., 2004). In addition, local depolarizing GABA signaling can induce the formation of excitatory and inhibitory synapses on young dendrites (Oh et al., 2016). Depolarizing GABA also promotes synapse formation onto newborn neurons in the dentate gyrus of adult mice (Ge, 2006).

GABA-induced postsynaptic depolarization can trigger activity-dependent structural plasticity and neurite growth via Ca²⁺ influx (Sernagor et al., 2010; Oh et al., 2016), implying GABA is merely used as a source of depolarization. However, specific and Ca²⁺ independent GABA signaling was also recently reported. Depolarizing GABA was found to induce intracellular Mg²⁺ release from mitochondria to promote neuronal maturation (Yamanaka et al., 2018). In addition, mitochondrial activity can result in sequestration of GABA within mitochondria in flies, possibly limiting excessive GABAergic signaling (Kanellopoulos et al., 2020). Future studies should further explore this intriguing link between mitochondrial and GABA signaling in the developing brain.

Depolarizing GABA promotes synapse maturation

Glutamatergic synapses in the early postnatal brain often lack AMPA-type glutamate receptors. Synapses that only contain NMDA receptors, which are blocked by Mg²⁺ at negative membrane potentials, are often called 'silent' synapses (Wang and Kriegstein, 2009). Glutamatergic synapses can be 'unsilenced' by insertion of AMPA receptors after NMDA receptor activation. GABAergic depolarization removes the Mg²⁺ block, thereby facilitating unsilencing of immature glutamatergic synapses of rodents and *Xenopus* (Leinekugel et al., 1997; Akerman and Cline, 2006; Chancey et al., 2013; van Rheede et al., 2015). The AMPA/NMDA receptor ratio increases drastically after birth until

around postnatal day (P)10 in rodents (Durand et al., 1996; Isaac et al., 1997; Rumpel et al., 1998; Itami et al., 2003) and between stage 40 and 49 in *Xenopus* tadpoles (Wu et al., 1996; Akerman and Cline, 2006; van Rheede et al., 2015), which corresponds with the period just before GABA becomes hyperpolarizing (Fig. 2F). The frequency of spontaneous glutamatergic currents increases substantially during this period, probably reflecting a combination of an increased number of glutamatergic synapses and increased insertion of AMPA receptors in rodents and *Xenopus* (Durand et al., 1996; Wu et al., 1996; Isaac et al., 1997; Akerman and Cline, 2006; van Rheede et al., 2015). When postnatal GABA depolarization is chronically impaired, AMPA-mediated synaptic currents eventually develop normally (Chudotvorova et al., 2005; Ge et al., 2006; Nakanishi et al., 2007; Wang and Kriegstein, 2008, 2011; Pfeiffer et al., 2009), suggesting that other factors besides GABA can provide the required depolarization to promote glutamatergic synapse formation.

In summary, GABA plays pivotal roles in the initial formation of neuronal networks in the embryonic and early postnatal brain. Depolarizing GABA provides the Ca^{2+} influx to mediate the initial steps of network construction at a time when glutamatergic signaling is still scarce. GABA signaling also provides more specific instructions, but our current understanding remains incomplete. Depolarization by GABA or high K^+ promotes the proliferation of early neuronal precursors, but concomitantly limits proliferation at later stages. In a similar dichotomic fashion, GABA and high K^+ promote migration of newborn neurons, but limit migration of older neurons. In addition, depolarization by GABA promotes the integration of young neurons into networks along with their maturation, possibly not only through Ca^{2+} , but also Mg^{2+} signaling. Thus, developing neurons use GABA as an instructive signal to accomplish a sequence of developmental processes. The instruction given by GABA depends on the intrinsic properties of the developing neurons, such as the expression of specific receptors and Cl^- transporters, which change as the neurons mature. Currently, only a few of these cell-intrinsic factors are known (e.g. the transient expression of GABA_A - ρ receptors in migrating neurons). In addition, local cues may modulate the GABAergic instruction signal or indirectly affect intrinsic properties of the neurons in a region-specific manner. It will be important for future research to identify the precise molecular factors and mechanisms that enable a relatively constant GABA signal to trigger a specific sequence of developmental processes in young neurons.

2.4 Roles of GABA in early activity

The contribution of depolarizing GABA to neuronal activity is rather complex. It is important to realize that GABA-induced depolarization and Ca^{2+} influx do not necessarily go hand in hand with neuronal excitation as the opening of GABA_A receptors inevitably results in an increase in membrane conductance: the membrane becomes 'leaky'. This means that glutamate-induced depolarizations are attenuated

when traveling from the dendrite to the soma, which is generally referred to as 'shunting'. Shunting reduces overall excitation, regardless of the direction of Cl^- flux through the GABA_A receptors. Depolarizing GABA will be excitatory or shunting depending on the exact interplay between Cl^- levels, activity levels and the number of excitatory and inhibitory synapses onto developing neurons (Staley and Mody, 1992; Gao et al., 1998; Morita et al., 2006; Le Magueresse and Monyer, 2013). This complex interplay likely explains the discrepancies in GABA's actions found in slices versus *in vivo* and differences between brain regions.

There is ample evidence for GABA-induced excitation in brain slices. Application of GABA induces firing and increases excitatory postsynaptic current (EPSC) frequency in E18-P13 neocortical and hippocampal slices (Owens et al., 1996; Gozlan and Ben-Ari, 2003; Khazipov et al., 2004; Rheims et al., 2008; Kirmse et al., 2010) and optogenetic activation of GABAergic interneurons increases EPSC frequency in hippocampal and cortical slices from P2-9 mice (Valeeva et al., 2016). Thus, in brain slices of newborn rodents GABA-induced depolarization is sufficient to induce action potential firing and GABA can be truly excitatory. Excitatory GABA can also support spontaneous oscillations in immature brain slices. During the first days after birth spontaneous oscillations are characterized by giant depolarizing potentials (GDPs) (Blankenship and Feller, 2010). Hippocampal GDPs increase when GABAergic depolarization is enhanced (Spoljaric et al., 2019). In contrast, hippocampal and cortical GDPs transform into epileptiform discharges after loss of depolarizing GABA (Ben-Ari et al., 1989; Khalilov et al., 1997, 2015; Leinekugel et al., 1997; Wells et al., 2000; Dzhalala et al., 2005; Mohajerani and Cherubini, 2005; Sipila et al., 2006; Allène et al., 2008; Rheims et al., 2008; Pfeffer et al., 2009; Valeeva et al., 2010). This is because the action of GABA changes from depolarizing to hyperpolarizing during a GDP due to the large reduction in intracellular Cl^- concentration when many GABA_A channels open. GDPs are therefore driven, but at the same time also limited by, GABA signaling (Khalilov et al., 2015; Lombardi et al., 2018). Around P8-10 the frequency of GDPs starts to decrease, until GDPs fully disappear after P12 (Ben-Ari et al., 1989; Khazipov et al., 2004; Rheims et al., 2008). Around the same time, GABA shifts from being mainly excitatory to being shunting during baseline activity in these slices (Valeeva et al., 2016; Salmon et al., 2020).

In the first weeks after birth, activity in the hippocampus of living rodent pups is characterized by sharp waves (SWs) during rest, the *in vivo* counterpart of GDPs in hippocampal slices (Leinekugel et al., 2002). Chemogenetic suppression of GABAergic interneurons in the hippocampus of P3 mice decreases SW frequency and amplitude (Murata and Colonnese, 2020). Moreover, SWs are acutely blocked when GABA-induced depolarization is abolished (Sipila et al., 2006). This clearly demonstrates that depolarizing GABA contributes to spontaneous postnatal hippocampal activity

in vivo. The shift to inhibitory GABA in the hippocampus occurs around P7 (Murata and Colonnese, 2020).

The situation in the postnatal cortex seems different. Release of GABA in the cortex of anaesthetized mice at P3-7 induces Ca^{2+} influx, but decreases neuronal firing (Kirmse et al., 2015; Valeeva et al., 2016; Che et al., 2018; Murata and Colonnese, 2020). These observations suggest that in the postnatal cortex GABA is depolarizing, but acts mostly inhibitory via shunting. This is consistent with studies showing that depolarizing GABA is not involved in early oscillations in the newborn cortex *in vivo* (Minlebaev et al., 2006, 2011; Kirmse et al., 2015; Marguet et al., 2015). These cortical oscillations depend strongly on AMPA receptor activation and are modulated by cholinergic activity (Yang et al., 2016).

So whereas GABA-induced depolarization and Ca^{2+} influx do promote network formation on a cellular level across the brain, the precise impact of GABA-induced depolarization and Ca^{2+} influx on the network highly dependent on both Cl^- levels and locally ongoing activity. The activity of glutamatergic, GABAergic and other inputs determine the distribution of conductance across the neuronal membrane and thereby the impact of GABAergic signaling. As a result, the shift from depolarizing to hyperpolarizing GABA signaling is not simply accompanied by a shift from GABAergic excitation to inhibition. Depolarization by GABA can induce action potentials when activity is relatively low, for instance in brain slices. In the intact brain, regional heterogeneity is important. GABA can induce firing and amplify spontaneous activity in the perinatal hippocampus. With the increase in hippocampal activity levels and decrease in Cl^- levels during the second postnatal week, inhibitory actions of GABA are assured. In the newborn cortex, depolarizing GABA is mostly shunting and therefore inhibitory.

2.5 Hyperpolarizing GABA: Development of input sensitivity

In the first weeks after birth, spontaneous activity in the sensory cortex of rodents decreases and the network becomes more susceptible to sensory input. The shift to hyperpolarizing GABA is tightly coupled to the recruitment of interneurons by thalamocortical input. In P3-5 slices, when GABA is still depolarizing, GABAergic cells in layer IV of barrel cortex are hardly engaged by thalamocortical input. Only by P7 thalamocortical input activates feedforward GABAergic transmission, which is then hyperpolarizing (Daw et al., 2007). Without thalamic input, for instance after subplate ablation, the shift to hyperpolarizing GABA does not occur (Kanold and Shatz, 2006). In this way, hyperpolarizing GABAergic responses are assured when the cortex becomes receptive to sensory input and spontaneous activity decreases (Toyoizumi et al., 2013; Lohmann and Kessels, 2014). With increasing sensory input, hyperpolarizing GABA becomes essential to enhance sensory sensitivity, improve

temporal precision and sharpen the tuning to sensory stimuli (Pouille and Scanziani, 2001; Wehr and Zador, 2003), and to sharpen the coincidence window for plasticity in the developing network (Kanold and Shatz, 2006; Pan-vazquez et al., 2020). The GABA shift also makes GABAergic signaling faster. During development, GABA_A receptor $\alpha 3$ subunits are replaced by the faster $\alpha 1$ subunits, resulting in a faster decay of GABAergic synaptic currents (Laurie et al., 1992; Taketo and Yoshioka, 2000). This change in subunit composition depends on the developmental decrease in the Cl⁻ concentration, independently of GABA_A receptor signaling (Kanold and Shatz, 2006; Succol et al., 2012).

Together, these studies suggest that GABAergic interneurons become engaged by thalamocortical input in the cortex around the time when GABA shifts. The shift to hyperpolarizing GABA increases input sensitivity of the network and short hyperpolarizing GABAergic responses tighten plasticity rules and improve temporal precision. The shift from depolarizing to hyperpolarizing GABA signaling seems therefore tightly linked to the connectivity and activity in the local network, and the shift may be closely aligned to the period when circuits are shaped by external (sensory) inputs. In the second part of this review we will examine what is known about how the timing of postnatal GABA shift is regulated and how subsequent development of synaptic connections are altered when the timing is off.

2.6 Timing of the postnatal GABA shift

The postnatal decrease in Cl⁻ concentration has been measured using fluorescent Cl⁻ indicators and by determining the driving force for GABAergic transmission using cell attached or perforated patch recordings. The average Cl⁻ driving force shifts from positive to negative around P10-14 in pyramidal neurons of hippocampal and cortical slices (Rivera et al., 1999; Stein et al., 2004; Tyzio et al., 2007; Romo-Parra et al., 2008; Kirmse et al., 2015; Sulis Sato et al., 2017; Pisella et al., 2019). Interestingly, *in vivo* Cl⁻ levels decrease approximately 4 days earlier in the cortex than in the hippocampus (Murata and Colonnese, 2020). Moreover, Cl⁻ levels decrease approximately a week earlier in GABAergic cells compared to pyramidal cells (Banke and McBain, 2006; Bortone and Polleux, 2009), although hippocampal PV cells seem to synchronize with pyramidal neurons (Sauer and Bartos, 2010). In female hippocampal and midbrain slices the GABA shift is several days earlier compared to males (approximately P6-10 in females and P14-17 in males) (Kyrozis et al., 2006; Nuñez and McCarthy, 2007; Galanopoulou, 2008), while the GABA shift in the cerebellum is actually advanced in males by 4 days (Roux et al., 2018). Thus the timing of the GABA shift appears strongly dependent on cell type, sex and brain region. It should also be noted, that the variance in intracellular Cl⁻ concentration found between individual neurons is large (Kyrozis et al., 2006; Galanopoulou, 2008; He et al., 2014), both *in vivo* and *in vitro* and across methods used to measure Cl⁻ levels (Owens et al., 1996; Rivera et al., 1999; Stein et

al., 2004; Yamada et al., 2004; Galanopoulou, 2006; Romo-Parra et al., 2008; He et al., 2014; Kirmse et al., 2015; Sulis Sato et al., 2017; Pisella et al., 2019) and that the Cl^- concentration in individual neurons also varies over time and is dependent on activity in the network (Khalilov et al., 2015; Lombardi et al., 2018). The Cl^- concentration is even non-uniformly distributed within a single pyramidal neuron and GABAergic reversal potentials become progressively more negative from the Axon Initial Segment (AIS) to the soma, but less negative from the soma into the dendrites (Romo-Parra et al., 2008; Khirug, 2012; Rinetti-Vargas et al., 2017; Pan-vazquez et al., 2020). This illustrates that the postnatal GABA shift is not a simple switch that takes place at a certain moment in postnatal development, but rather reflects a gradual change in neuronal Cl^- homeostasis, such that GABA signaling gradually becomes more hyperpolarizing within local neuronal networks.

Developmental expression pattern of chloride transporters

The developmental decrease in intracellular Cl^- concentration is established by an increase in the relative expression and activity of postnatal chloride exporter KCC2 compared to importer NKCC1 (Fig. 1) in both excitatory and inhibitory neurons (Rivera et al., 1999; Gulyás et al., 2001; Yamada et al., 2004; Sauer and Bartos, 2010; Otsu et al., 2020). The effect of NKCC1 inhibitor bumetanide on the GABAergic driving force decreases with development in excitatory neurons, indicating that the relative contribution of NKCC1 to GABA function decreases (Banke and McBain, 2006). It remains unresolved if the decrease in NKCC1 function reflects a decrease in its expression. While some studies report a developmental downregulation of NKCC1 mRNA and protein levels over the first postnatal weeks (Shimizu-okabe et al., 2002; Yamada et al., 2004; Dzhala et al., 2005), others have reported that NKCC1 levels actually increase over development (Clayton et al., 1998; Sun and Murali, 1999; Yan et al., 2001). The discrepancy may be explained by differences in probe sequences and antibodies used for detection of NKCC1, which may result in different sensitivity for the two main NKCC1 isoforms (NKCC1a and b). Inclusion of male and female animals might aggravate discrepancies in NKCC1 expression patterns, as levels of NKCC1 are elevated in embryonic and newborn male hippocampi and midbrains compared to females (Damborsky and Winzer-serhan, 2012; Murguía-Castillo et al., 2013). Inclusion of glia in the samples may also contribute, as NKCC1 mRNA is also present in astrocytes (Yan et al., 2001).

KCC2 is exclusively expressed by neurons and not by glia (Payne et al., 1996). KCC2s mRNA and protein levels increase during postnatal rodent development (Lu et al., 1999; Rivera et al., 1999; Shimizu-okabe et al., 2002; Stein et al., 2004; Dzhala et al., 2005; Lee, 2010; Kovács et al., 2014). This is due to an increase in expression of KCC2b levels, while KCC2a levels remain constant (Uvarov et al., 2007). Total KCC2 expression levels are increased in early postnatal interneurons versus pyramidal neurons (Bortone and Polleux, 2009) and in female compared to male brains (Murguía-Castillo et al.,

2013; Kang et al., 2015). Posttranslational modifications further contribute to the developmental increase in KCC2 function (Schulte et al., 2018). For instance, KCC2 becomes dephosphorylated at threonine residues T906 and T1007 (Rinehart et al., 2009; Kahle et al., 2013; Friedel et al., 2015; Moore et al., 2019; Pisella et al., 2019), while it gets phosphorylated at serine residue S940 (Lee et al., 2007; Kahle et al., 2013; Moore et al., 2019) during postnatal development. These modifications enhance KCC2 function and membrane stability.

KCC2: more than a chloride transporter

The postnatal upregulation of KCC2 serves other roles in brain development in addition to inducing low internal Cl⁻ levels. In mature neurons, KCC2 proteins are enriched near synapses (Gulyás et al., 2001; Báldi et al., 2010; Chamma et al., 2013; Kovács et al., 2014). KCC2 resides in a multi-protein complex in the neuronal membrane, and is coupled to numerous other proteins, including ion channels, neurotransmitter receptors (Huang et al., 2012; Wright et al., 2017; Garand et al., 2019), cytoskeleton associated proteins and various enzymes (Blaesse and Schmidt, 2015; Smalley et al., 2020b). The developmental increase in KCC2 levels therefore supports neuronal maturation via various structural roles, independent of Cl⁻ transport. For instance, KCC2 indirectly contributes to the hyperpolarization of the resting membrane potential in developing neurons by stabilizing Task-3 potassium channels in the neuronal membrane (Goutierre et al., 2019). In addition, KCC2 facilitates activity-induced spine growth via interactions with the actin cytoskeleton. KCC2 promotes actin dynamics in spines, and supports AMPA receptor insertion and confinement (Gauvain et al., 2011; Chevy et al., 2015). Importantly, all of these roles were shown to be independent of the KCC2 function in transporting Cl⁻, but rely on the structural interaction of KCC2 with other proteins. Interestingly, the structural function of KCC2 and its role in Cl⁻ transport sometimes have opposite effects. For instance, KCC2 overexpression in the developing cortex leads to an increase in spine density, via its interaction with actin (Fiumelli et al., 2013; Puskarjov et al., 2017; Awad et al., 2018). However, the KCC2-induced increase in spine density is prevented by boosting the Cl⁻ transport function of the overexpressed KCC2, presumably because spine growth is counteracted by an increase in GABAergic inhibition in the network (Awad et al., 2018).

2.7 What triggers the postnatal GABA shift?

An important open question is how the shift from NKCC1 to KCC2 dominated Cl⁻ transport is triggered in developing neurons (Medina et al., 2014). As the shift also occurs in neuronal cultures and organotypic slices (Rivera et al., 1999; Ganguly et al., 2001; Kelsch et al., 2001; Perrot-Sinal et al., 2001; Titz et al., 2003; Khirug et al., 2005; Ludwig et al., 2011a, 2011b; Sun et al., 2013; Dumon et al., 2018), the GABA shift is (at least partly) induced by an intrinsic developmental program.

Molecular factors regulating the GABA shift

One intriguing study has suggested that neuroligin-2 (NL2) plays a key role in triggering the GABA shift. NL2 is a postsynaptic cell adhesion molecule specific for GABAergic synapses (Blundell et al., 2009). Expression of NL2 increases during postnatal cortical development. Interestingly, the increase in NL2 expression was found to precede the increase in KCC2 expression and NL2 levels directly influence KCC2 expression, independent of network activity. Knockdown of NL2 decreases KCC2 expression and results in GABAergic depolarization, even in mature cortical neurons (Sun et al., 2013). This strongly suggests that NL2 directly regulates KCC2 expression and is required for the maintenance of KCC2 function and GABAergic inhibition (Blundell et al., 2009). The mechanism via which NL2 enhances KCC2 function and the trigger for the developmental increase in NL2 levels have not been resolved.

In addition to NL2, many factors have been identified that do not directly regulate KCC2 expression, but that are able to promote or repress the postnatal GABA shift. Leptin, estradiol and Brain-Derived Neurotrophic Factor (BDNF) precursor pro-BDNF inhibit KCC2 function and may thereby repress a precocious GABA shift. Leptin is a hormone that regulates energy levels and immune responses in the mature brain, but functions as a neurotrophic signal during brain development (Dumon et al., 2018). Plasma leptin levels decrease during the second postnatal week when GABA becomes hyperpolarizing. Leptin weakens expression of KCC2 and its stability in the plasma membrane (Dumon et al., 2018). Estradiol is a testosterone derivative. Its levels decrease gradually in the first two weeks after birth of male and female rats (Konkle and McCarthy, 2011). Estradiol acutely increases NKCC1 function and decreases KCC2 expression in slices (Perrot-Sinal et al., 2001, 2007; Galanopoulou and Moshé, 2003; Nakamura et al., 2004). In the mature brain BDNF promotes neuronal survival and outgrowth (Ghosh et al., 1994). However, in the first postnatal week, its precursor protein pro-BDNF, which exhibits proapoptotic functions, constitutes the main isoform in the brain (Yang et al., 2009; Menshanov et al., 2015). In utero electroporation of a cleavage-resistant pro-BDNF, which cannot be processed into BDNF, decreased KCC2 expression and kept GABA depolarizing in the cortex (Riffault et al., 2018). Together, these results suggest that abundance of leptin, estradiol and pro-BDNF during the first postnatal week help to keep KCC2 expression low.

In sharp contrast with its precursor, mature BDNF promotes KCC2 function in young neurons via neurotrophin/tropomyosin kinase B (TrkB) receptors (Carmona et al., 2006). Treatment with BDNF increases KCC2 levels (Ludwig et al., 2011a) and KCC2 levels are increased in BDNF-overexpressing mice (Aguado et al., 2003). However, KCC2 function is not affected in BDNF knockout (KO) mice (Puskarjov et al., 2015), indicating that BDNF can accelerate the GABA shift, but that its presence is not absolutely required. Together, these findings suggest that the postnatal shift from pro-BDNF to BDNF

regulates the timing of the GABA shift by releasing the negative control by pro-BDNF and by actively promoting KCC2 expression via TrkB receptors.

Other factors that have been shown to actively promote the GABA shift by increasing KCC2 function include neurturin (Ludwig et al., 2011b), TGF β 2 (Roussa et al., 2016), sonic hedgehog receptor Smo (Delmotte et al., 2019), nicotine (Liu et al., 2006; Damborsky and Winzer-serhan, 2012), IGF1 (Kelsch et al., 2001; Baroncelli et al., 2017), allopregnanolone (Mòdol et al., 2014), thyroid hormone (Friauf et al., 2008; Sawano et al., 2013), testosterone and its derivative dihydrotestosterone (Galanopoulou and Moshé, 2003), and oxytocin (Leonzino et al., 2016). Many of these factors likely cooperate to promote KCC2 function and the postnatal GABA shift. For instance, upregulation of KCC2 by neurturin and BDNF is mediated by activation of a common pathway involving ERK1/2 and the transcription factor Egr4 (Ludwig et al., 2011b, 2011a) and activation of nicotinic acetylcholine receptors, Smo, IGF1 receptors and thyroid hormone receptors increase BDNF levels (Carro et al., 2000; Landi et al., 2009; Shulga et al., 2009; Radzikinas et al., 2011; Damborsky and Winzer-serhan, 2012).

In conclusion, the timing of the GABA shift is tightly regulated in the developing brain through external and internal factors, as well as hormones. Specific factors prevent GABA from shifting too early, while other factors assure the postnatal GABA shift is not too late.

Spontaneous and externally-driven neuronal activity promote the GABA shift

Even before sensory input drives neuronal activity, the developing brain displays various forms of spontaneous activity. Many of the factors that promote the postnatal GABA shift are activity-dependent, including BDNF and IGF1 (Cao et al., 2011; Porcher et al., 2011). This means that the timing of the GABA shift is coordinated with early network activity. For instance, disruption of spontaneously generated activity in the cochlea prior to the onset of auditory input results in decreased KCC2 function and prevents the GABA shift in newborn animals (Kotak and Sanes, 1996; Vale and Sanes, 2000; Vale et al., 2003; Shibata et al., 2004).

Cortical BDNF and IGF1 levels increase via sensory input (Castren et al., 1992; Tropea et al., 2006; Landi et al., 2009) and GABAergic maturation is strongly influenced by early life experience. For instance, prenatal maternal restraint stress as well as repeated separations of newborn pups from their mother from P2 to P14 or during the first 3 postnatal weeks induce a delay in the GABA shift of newborn mice (Veerawatananan et al., 2016; Furukawa et al., 2017; Hu et al., 2017b). In contrast, maternal separations from P4 to P6 for 6 hours per day advance the GABA shift by decreasing activity of NKCC1 and increasing expression of KCC2 (Galanopoulou, 2008). Decreased expression of NKCC1 versus KCC2 also occurs when mice are growing up in an enriched environment, with enhanced sensory and social stimuli (He et al., 2010; Baroncelli et al., 2017).

The instructive role of sensory experience becomes even more clear in animal models in which the connection between sensory input and the cortex is demolished during development, for example through ablation of the subplate. The subplate is formed by a population of transient cells that indirectly link thalamic (sensory) input to layer 4 neurons (Friauf et al., 1990). Ablation of the subplate right before eye opening prevents visual input to drive cortical activity. This prevents the postnatal increase in KCC2, including its (indirect) effects on neuronal maturation (Kanold and Shatz, 2006; Jantzie et al., 2015). A similar delay was found after sensory deprivation in turtles. Continuous dark rearing of turtles for four weeks from hatching onwards reduced KCC2 levels in the retina and prolonged the period when GABAergic responses were depolarizing (Sernagor et al., 2003).

Together, these studies demonstrate that the maturation of GABAergic signaling is tightly regulated by an intrinsic developmental program that employs trophic and other factors as signaling molecules. These intrinsic programs are under constant adjustment by hormones, (spontaneous) neuronal activity and sensory input. Future studies should further unravel the molecular mechanisms by which sensory input affects the postnatal GABA shift.

2.8 Consequences of a precocious or delayed GABA shift on network development

As explained above, hyperpolarizing GABA is crucial for gating synaptic plasticity (Pouille and Scanziani, 2001; Wehr and Zador, 2003; Capogna et al., 2020). The timing of the shift to hyperpolarizing GABA is therefore crucial in determining the capacity of the network to undergo developmental changes in response to (sensory) input. To gain insight into the importance of precise timing of the GABA shift, many studies have advanced or delayed the GABA shift and studied the effects on network development and behavior. The shift has been advanced experimentally by increasing the expression of KCC2 or by decreasing the expression or function of NKCC1 using genetic or pharmacological approaches. A delay in the shift has been achieved by decreasing KCC2 levels or its activity. When interpreting experimental results, it is important to realize that manipulations of KCC2 not only affect the postnatal GABA shift, but will inevitably also alter the functions of KCC2 that are independent of Cl⁻. In addition, when accelerating the GABA shift to an earlier timepoint, the influence of depolarizing GABA as a trophic factor will be automatically reduced. We will review the consequences of these manipulations in the next sections and we have summarized our conclusions in Table 1.

Advancing the postnatal GABA shift

Advancing the GABA shift prenatally has severe consequences for the development of glutamatergic synapses. Knockdown or pharmacological inhibition of NKCC1 from

E15, which induces hyperpolarizing GABAergic responses already at P0, results in a reduction in glutamatergic synapses 2-4 weeks after birth, which lasts until adulthood (Table 1). Timing is crucial, as miniature EPSC frequency is not affected when NKCC1 is blocked only embryonically (E15-19) or only postnatally (P0-7) (Wang and Kriegstein, 2008, 2011). The effect of depolarizing GABA on glutamatergic synapse formation depends on its ability to activate NMDA receptors (Wang and Kriegstein, 2008). A similar decrease in glutamatergic synapses was found after advancing the GABA shift via early overexpression of KCC2 in rodents and *Xenopus* (Akerman and Cline, 2006; Awad et al., 2018). Importantly, in both studies this effect was shown to depend on Cl⁻ transport. As explained above, the developmental shift in intracellular Cl⁻ does not precisely parallel the shift from excitatory to inhibitory GABA. During the transition period in which GABA is still depolarizing, but already inhibits network activity through shunting, depolarizing GABA actually constrains glutamatergic synapse formation in the hippocampus. Blocking GABA for 48 hours during this period therefore results in an increase in miniature EPSCs and spine density (Salmon et al., 2020). Together, these results show that depolarizing GABA promotes the formation of glutamatergic synapses via NMDA receptor activation during a short developmental window, which closes when GABA signaling becomes inhibitory. Missing this window, by shifting GABA too early, perturbs glutamatergic connectivity for life.

The role of depolarizing GABA in inhibitory synapse formation seems more complex. A precocious GABA shift by decreasing NKCC1 activity reduces the number of inhibitory synapses only transiently (Nakanishi et al., 2007; Wang and Kriegstein, 2011; Deidda et al., 2015a). This transient decrease occurs three to four weeks after the onset of the NKCC1 manipulation and may reflect an indirect effect of glutamatergic alterations (Wang and Kriegstein, 2008). However, when a precocious GABA shift is induced via early overexpression of KCC2, the opposite occurs: GABAergic transmission actually increases (Chudotvorova et al., 2005; Akerman and Cline, 2006). Importantly, these effects are mediated by changes in intracellular Cl⁻ (Akerman and Cline, 2006). In contrast to the transient and delayed decrease in GABAergic transmission seen after removal of NKCC1, overexpression of KCC2 results in an immediate increase in GABAergic transmission. It is possible that low levels of KCC2 limit the development of inhibitory synapses during early postnatal development. A mechanism remains elusive, but it would be interesting to further explore interactions between KCC2 and GABA_A receptor subunit $\alpha 1$ (Huang et al., 2012) and NL2 (Blundell et al., 2009).

Delaying the postnatal GABA shift

It is technically more challenging to delay the GABA shift. Complete KO of KCC2 in mice is lethal after birth as a result of respiratory failure (Hübner et al., 2001). Therefore, complete absence of KCC2 can only be investigated in embryonic tissue. Synaptic changes have been reported in KCC2 KO embryos, even though embryonic KCC2 levels do not affect GABAergic reversal potentials at this age (Li et al., 2007; Khalilov

et al., 2011). Several alternative mouse models have been developed in which KCC2 expression is not absent, but strongly reduced (5-20% remaining expression) (Woo et al., 2002; Tornberg et al., 2005; Anacker et al., 2019). Alterations in glutamatergic and GABAergic transmission have been described in these models, but it remains unclear if these are due to a loss of KCC2s structural role or insufficient GABAergic hyperpolarization (Riecki et al., 2008; Anacker et al., 2019). To study the consequences of a delayed GABA shift while preserving the Cl⁻-independent function of KCC2, mouse models are developed recently in which KCC2 activity is decreased by interfering with post-translational modifications of KCC2. In KCC2 S940A mice KCC2 levels are normal, but KCC2 phosphorylation at serine (S) residue 940 is prevented, resulting in a postnatal delay of the GABA shift by approximately 6 days (Moore et al., 2019). In KCC2^{E/+} mice, phosphomimic mutations of KCC2 at threonine (T) residues 906 and 1007 result in a delay of the postnatal GABA shift by ~4 days in the hippocampus (Pisella et al., 2019). At P15, excitatory transmission is increased in KCC2^{E/+} slices, whereas inhibitory transmission is decreased compared to controls, but excitatory and inhibitory transmission were comparable to control again at P30 after the GABA shift was complete (Pisella et al., 2019).

Table 1. Effects of manipulations of the GABA shift on excitatory and inhibitory synaptic transmission.

Timing GABA shift	Type manipulation	Effect on transmission	References
Advanced GABA shift			
Embryonically	KD NKCC1, Block NKCC1, OE KCC2	Excitatory transmission decreased in adult	Akerman and Cline, 2006; Awad et al., 2018; Wang and Kriegstein, 2008; Wang and Kriegstein, 2011
Embryonically or first week after birth	Block NKCC1	Inhibitory transmission transiently decreased ~4 weeks after manipulation	Deidda et al., 2015a; Nakanishi et al., 2007*; Wang and Kriegstein, 2008; Wang and Kriegstein, 2011
Embryonically or first week after birth	OE KCC2	Inhibitory transmission increased ~5-12 days after manipulation	Akerman and Cline, 2006; Chudotvorova, 2005*
Second week after birth	Block NKCC1, OE KCC2	Inhibitory transmission normal ~7 days after manipulation	Succol et al., 2012*
Second week after birth	Block shunting GABA	Excitatory transmission increased 5 days after manipulation	Salmon et al., 2020
Delayed GABA shift			
Third week after birth	KD KCC2	Inhibitory transmission normal ~7 days after manipulation	Succol et al., 2012*
Third week after birth	Block KCC2	Inhibitory transmission decreased ~7 days after manipulation	Succol et al., 2012*
Fourth week after birth	KCC2E/+ mice	Excitatory transmission transiently increased at P15 Inhibitory transmission transiently decreased at P15	Pisella et al, 2019

* These studies were performed in dissociated cultures. Indicated timing is equivalent *in vivo* timing (e.g. manipulations starting at DIV0 in cultures made from P7 mice are considered equivalent to the second week after birth), but developmental timing may partially reset in culture.

Behavioral consequences

The measured effects on synaptic currents after an early or late postnatal GABA shift are relatively subtle and sometimes only transient. However, these synaptic changes occur at a developmental period in which crucial decisions are made for adult connectivity and function (Takesian and Hensch, 2013). A postnatal GABA shift which is not coordinated with cortical activity patterns and sensory input may cause permanent alterations in brain connectivity and therefore function. Subtle changes in synaptic drive or activity can gate developmental plasticity and may therefore have long-lasting consequences for neuronal circuits. Indeed, several studies have demonstrated that small changes to the timing of the postnatal GABA shift, in either direction, are associated with alterations in behavior that last until adulthood. For instance, mice with an accelerated GABA shift through inhibition of NKCC1 or enhanced KCC2 function show a developmental delay in motor coordination and strength, decrease in anxiety, enhanced auditory reactivity, increased social behavior, a slight acceleration in the rate of learning and improved long-term memory function in adulthood (Wang and Kriegstein, 2011; Moore et al., 2019). A transient reduction in inhibitory transmission after bumetanide treatment from P3-8 was shown to prolong the critical period for visual plasticity (Deidda et al., 2015a). On the other hand, mice with reduced KCC2 levels display reduced social behavior and impaired sensory sensitivity and long term memory, along with increased anxiety-like behavior and seizure susceptibility and decreased social interaction (Delpire and Mount, 2002; Tornberg et al., 2005; Anacker et al., 2019; Moore et al., 2019; Pisella et al., 2019). These studies clearly underscore the importance of proper timing. A recent study showed that behavioral defects in adulthood are also evoked by a transient elevation in neuronal activity, induced with kainic acid after birth (P6 to P15) (Friedman and Kahen, 2019). Together, these results show that the timing of the postnatal GABA shift needs to be coordinated with cortical activity patterns and sensory input to assure proper network development and life-long function.

2.9 Implications for translational research

Expression studies on postmortem brains indicate that a developmental increase in the function of KCC2 versus NKCC1 also takes place in the first year after birth of humans (Kharod et al., 2019). In patients with autism spectrum disorder (ASD) and other neurodevelopmental disorders (NDDs) altered expression levels of Cl⁻ transporters have been found. ASD is associated with an elevated risk for epilepsy and other electroencephalography abnormalities (Buckley and Holmes, 2016), along with perturbations in the regulatory domain of KCC2 (Merner et al., 2015a). Down syndrome is associated with increased NKCC1 levels (Deidda et al., 2015b), Rett syndrome with reduced KCC2 levels (Duarte et al., 2013) and Tuberous Sclerosis Complex and Dravet syndrome with both increased NKCC1 and reduced KCC2 levels (Talós et al., 2012; Ruffolo et al., 2016, 2018). These findings suggest that the GABA shift is delayed or

perhaps even entirely absent in patients with various NDDs. In addition, excessive leptin or inadequate thyroid hormone or oxytocin signaling, which may also delay the GABA shift, have been implicated in the development of ASD (Ashwood et al., 2008; Modi and Young, 2012; Román et al., 2013).

A delay in the GABA shift due to an elevated ratio of NKCC1 to KCC2 activity has also been observed in several monogenetic animal models of NDDs, including mouse models for Fragile X syndrome (FMR1 KO mice) (He et al., 2014; Tyzio et al., 2014; Smalley et al., 2020a) and DiGeorge syndrome (Lgdel^{+/-} mice) (Amin et al., 2017), as well in environmental ASD rodent models, in which mice and rats have been exposed in utero to immunogenic stimuli (Corradini et al., 2017; Fernandez et al., 2018) or valproate (Tyzio et al., 2014; Roux et al., 2018). The postnatal GABA shift seems to be even completely absent in rodent models for Rett (Mecp2 KO mice) and Down syndrome (Ts65Dn mice), in which depolarizing GABAergic actions and an elevated ratio of NKCC1 versus KCC2 were found in adulthood (Duarte et al., 2013; Deidda et al., 2015b; Banerjee et al., 2016; Tang et al., 2016; Lozovaya et al., 2019).

In an increasing number of studies, administration of the NKCC1 inhibitor bumetanide around birth is used to restore postnatal GABAergic driving force and to correct early alterations in network activity (Amin et al., 2017; Fernandez et al., 2018; Pisella et al., 2019). In many cases, inhibition of NKCC1 results in a (partial) rescue of many behavioral defects in mice (Tyzio et al., 2014; He et al., 2018; Lozovaya et al., 2019; Savardi et al., 2020). The first studies in human patients also indicate that administration of NKCC1 inhibitor bumetanide to young ASD patients can attenuate the severity of their symptoms, with no major side effects on cognitive performance in multiple clinical trials (Lemonnier and Ben-Ari, 2010; Lemonnier et al., 2012, 2017; Hadjikhani et al., 2018; van Andel et al., 2020; Zhang et al., 2020) (recently reviewed by (Kharod et al., 2019)). This underscores the crucial impact of precise timing of the postnatal GABA shift on brain function and behavior later in life. It remains unclear how the precise therapeutic window and expected effects depend on the underlying cause for the delayed shift.

These results corroborate that sustained GABAergic depolarization affects early postnatal activity levels, with long-lasting consequences for behavior. An incomplete or delayed GABA shift may contribute to behavioral symptoms in (a subset of) NDD patients. Rectifying postnatal activity by decreasing intracellular Cl⁻ levels may constitute a promising therapy for these patients. Another interesting, but mostly unexplored, possibility would be to rescue the GABA shift through sensory enrichment (He et al., 2010; Weitlauf et al., 2017).

2.10 Conclusions and final remarks

In the mature brain, hyperpolarizing GABAergic inhibition is essential for regulating information processing by counterbalancing glutamatergic excitatory transmission. Glutamatergic synapses emerge around birth in the rodent brain, but crucial neurodevelopmental events take place already when glutamatergic transmission is still scarce and most neuronal activity is locally and spontaneously generated, independent of external sensory input. At this stage depolarizing GABAergic currents instruct the entire developmental sequence of local network establishment. The function of depolarizing GABA changes during each step, from facilitating the proliferation of stem cells, mediating the migration of precursors, outgrowth of neurites and maturation of synapses and sustaining early activity patterns in the hippocampus.

Once the rough layout is present and postnatal activity becomes sensory driven (Toyoizumi et al., 2013; Lohmann and Kessels, 2014) KCC2 activity increases and GABA shifts from being depolarizing to hyperpolarizing. This postnatal GABA shift represents the last shift in a series of developmental GABA shifts. Hyperpolarizing GABA is required to carefully select the optimal neural representations from many competing inputs that increasingly bombard the developing brain. When the postnatal GABA shift and increase in thalamocortical inputs are not mutually coordinated, network function remains altered for life.

Although some factors have been identified that guide the developmental GABA shifts, the precise molecular mechanisms by which these factors and input do so, remain to be elucidated, in particular for the postnatal shift to hyperpolarizing GABA. It also remains unclear when GABAergic hyperpolarization is exactly required and why the timing of the postnatal GABA shift is altered in ASD and related NDDs. It is unknown if altered levels of the Cl⁻ cotransporters are a direct effect of genetic or environmental factors, or that the shift is delayed because earlier developmental 'checkpoints' are missed. Subtle changes in the perinatal network may cause failure to activate signaling programs that normally promote the rise in KCC2 expression and shift to hyperpolarizing GABA. It will be particularly interesting to further examine the link between sensory input and the timing of the postnatal GABA shift, particularly in the context of NDDs. Improving our understanding of GABAergic signaling in brain development may open up new strategies to alleviate behavioral impairments in ASD and related NDDs in the future.

2.11 Author Contributions

CP and CJW conceived and wrote the paper together.

2.12 Declaration of Interests

The authors declare no competing interests.

2.13 Acknowledgements

This research was supported by a TOP grant 9126021 from ZonMw. The authors thank Christian Lohmann, Martien Kas and Lotte Herstel for critically reading the manuscript.

2.14 References

- Ageta-Ishihara, N., Takemoto-Kimura, S., Nonaka, M., Adachi-Morishima, A., Suzuki, K., Kamijo, S., Fujii, H., Mano, T., Blaeser, F., Chatila, T.A., Mizuno, H., Hirano, T., Tagawa, Y., Okuno, H., Bito, H., 2009. Control of cortical axon elongation by a GABA-driven Ca^{2+} /calmodulin-dependent protein kinase cascade. *J. Neurosci.* 29, 13720–13729. <https://doi.org/10.1523/JNEUROSCI.3018-09.2009>
- Aguado, F., Carmona, M.A., Pozas, E., Aguiló, A., Martínez-Guijarro, F.J.F., Alcántara, S., Borrell, V., Yuste, R., Ibañez, C.C.F., Soriano, E., 2003. BDNF regulates spontaneous correlated activity at early developmental stages by increasing synaptogenesis and expression of the $\text{K}^{+}/\text{Cl}^{-}$ co-transporter KCC2. *Development* 130, 1267–1280. <https://doi.org/10.1242/dev.00351>
- Akerman, C.J., Cline, H.T., 2006. Depolarizing GABAergic conductances regulate the balance of excitation to inhibition in the developing retinotectal circuit in vivo. *J. Neurosci.* 26, 5117–5130. <https://doi.org/10.1523/JNEUROSCI.0319-06.2006>
- Allène, C., Cattani, A., Ackman, J.B., Bonifazi, P., Aniksztejn, L., Ben-Ari, Y., Cossart, R., 2008. Sequential generation of two distinct synapse-driven network patterns in developing neocortex. *J. Neurosci.* 28, 12851–12863. <https://doi.org/10.1523/JNEUROSCI.3733-08.2008>
- Amin, H., Marinaro, F., De Pietri Tonelli, D., Berdondini, L., 2017. Developmental excitatory-to-inhibitory GABA-polarity switch is disrupted in 22q11.2 deletion syndrome: a potential target for clinical therapeutics. *Sci. Rep.* 7, 15752.
- Anacker, A.M.J., Moran, J.T., Santarelli, S., Forsberg, C.G., Rogers, T.D., Stanwood, G.D., Hall, B.J., Delpire, E., Veenstra-VanderWeele, J., Saxe, M.D., 2019. Enhanced Social Dominance and Altered Neuronal Excitability in the Prefrontal Cortex of Male KCC2b Mutant Mice. *Autism Res.* 9999, 1–12. <https://doi.org/10.1002/aur.2098>
- Andäng, M., Hjerling-Leffler, J., Moliner, A., Lundgren, T.K., Castelo-Branco, G., Nanou, E., Pozas, E., Bryja, V., Halliez, S., Nishimaru, H., Wilbertz, J., Arenas, E., Koltzenburg, M., Charnay, P., Manira, A. El, Ibañez, C.F., Ernfors, P., 2008. Histone H2AX-dependent GABAA receptor regulation of stem cell proliferation. *Nature* 451, 460–464. <https://doi.org/10.1038/nature06488>
- Ashwood, P., Kwong, C., Hansen, R., Hertz-Picciotto, I., Croen, L., Krakowiak, P., Walker, W., Pessah, I.N., Van De Water, J., 2008. Brief report: Plasma leptin levels are elevated in autism: Association with early onset phenotype? *J. Autism Dev. Disord.* 38, 169–175. <https://doi.org/10.1007/s10803-006-0353-1>
- Awad, P.N., Amegandjin, C.A., Szczurkowska, J., Carriço, J.N., Fernandes do Nascimento, A.S., Baho, E., Chattopadhyaya, B., Cancedda, L., Carmant, L., Di Cristo, G., 2018. KCC2 Regulates Dendritic Spine Formation in a Brain-Region Specific and BDNF Dependent Manner. *Cereb. Cortex* 1–14. <https://doi.org/10.1093/cercor/bhy198>
- Báldi, R., Varga, C., Tamás, G., 2010. Differential distribution of KCC2 along the axo-somato-dendritic axis of hippocampal principal cells. *Eur. J. Neurosci.* 32, 1319–1325. <https://doi.org/10.1111/j.1460-9568.2010.07361.x>
- Banerjee, A., Rikhye, R.V., Breton-Provencher, V., Tang, X., Li, C., Li, K., Runyan, C.A., Fu, Z., Jaenisch, R., Sur, M., 2016. Jointly reduced inhibition and excitation underlies circuit-wide changes in cortical processing in Rett syndrome. *Proc. Natl. Acad. Sci.* 113, E7287–E7296. <https://doi.org/10.1073/pnas.1615330113>
- Banke, T.G., McBain, C.J., 2006. GABAergic input onto CA3 hippocampal interneurons remains shunting throughout development. *J. Neurosci.* 26, 11720–11725. <https://doi.org/10.1523/JNEUROSCI.2887-06.2006>

- Barbin, G., Pollard, H., Gaiarsa, J.L., Ben-Ari, Y., 1993. Involvement of GABAA receptors in the outgrowth of cultured hippocampal neurons. *Neurosci. Lett.* 152, 150–154. [https://doi.org/10.1016/0304-3940\(93\)90505-F](https://doi.org/10.1016/0304-3940(93)90505-F)
- Baroncelli, L., Cenni, M.C., Melani, R., Deidda, G., Landi, S., Narducci, R., Cancedda, L., Maffei, L., Berardi, N., 2017. Early IGF-1 primes visual cortex maturation and accelerates developmental switch between NKCC1 and KCC2 chloride transporters in enriched animals. *Neuropharmacology* 113, 167–177. <https://doi.org/10.1016/j.neuropharm.2016.02.034>
- Behar, T.N., Schaffner, A.E., Scott, C.A., Greene, C.L., Barker, J.L., 2000. GABA receptor antagonists modulate postmitotic cell migration in slice cultures of embryonic rat cortex. *Cereb. Cortex* 10, 899–909.
- Behar, T.N., Schaffner, A.E., Scott, C.A., O'Connell, C., Barker, J.L., 1998. Differential Response of Cortical Plate and Ventricular Zone Cells to GABA as a Migration Stimulus. *J. Neurosci.* 18, 6378–6387. <https://doi.org/10.1523/jneurosci.18-16-06378.1998>
- Behar, T.N., Tran, H.T., Ma, W., 1996. GABA Stimulates Cortical Neurons Chemotaxis and Chemokinesis of Embryonic via Calcium-Dependent Mechanisms 16, 1808–1818.
- Ben-Ari, Y., Cherubini, E., Corradetti, R., Gaiarsa, J., 1989. Giant synaptic potentials in immature rat CA3 hippocampal neurones. *J. Physiol. Sep.* 303–325.
- Ben-Ari, Y., Gaiarsa, J.-L., Tyzio, R., Khazipov, R., 2007. GABA: A Pioneer Transmitter That Excites Immature Neurons and Generates Primitive Oscillations. *Physiol. Rev.* 87, 1215–1284. <https://doi.org/10.1152/physrev.00017.2006>
- Blaesse, P., Schmidt, T., 2015. K-Cl cotransporter KCC2 — a moonlighting protein in excitatory and inhibitory synapse development and function 615–624. <https://doi.org/10.1007/s00424-014-1547-6>
- Blankenship, A.G., Feller, M.B., 2010. Mechanisms underlying spontaneous patterned activity in developing neural circuits. *Nat. Rev. Neurosci.* 11, 18–29. <https://doi.org/10.1038/nrn2759>
- Blundell, J., Tabuchi, K., Bolliger, M.F., Blaiss, C.A., Liu, X., Südhof, T.C., Powell, C.M., 2009. Increased Anxiety-like Behaviour in Mice Lacking the Inhibitory Cell Adhesion Molecule Neuroligin 2. *Brain* 8, 114–126. <https://doi.org/10.1111/j.1601-183X.2008.00455.x>. Increased
- Bolteus, A.J., 2004. GABA Release and Uptake Regulate Neuronal Precursor Migration in the Postnatal Subventricular Zone. *J. Neurosci.* 24, 7623–7631. <https://doi.org/10.1523/JNEUROSCI.1999-04.2004>
- Bortone, D., Polleux, F., 2009. KCC2 Expression Promotes the Termination of Cortical Interneuron Migration in a Voltage-Sensitive Calcium-Dependent Manner. *Neuron* 62, 53–71. <https://doi.org/10.1016/j.neuron.2009.01.034>
- Bruining, H., Passtoors, L., Goriounova, N., Jansen, F., Hakvoort, B., de Jonge, M., Poil, S.S.-S., 2015. Paradoxical Benzodiazepine Response: A Rationale for Bumetanide in Neurodevelopmental Disorders? *Pediatrics* 136, e539–43. <https://doi.org/10.1542/peds.2014-4133>
- Buckley, A.W., Holmes, G.L., 2016. Epilepsy and autism. *Cold Spring Harb. Perspect. Med.* 6, 1–18. <https://doi.org/10.1101/cshperspect.a022749>
- Cancedda, L., Fiumelli, H., Chen, K., Poo, M., 2007. Excitatory GABA Action Is Essential for Morphological Maturation of Cortical Neurons In Vivo. *J. Neurosci.* 27, 5224–5235. <https://doi.org/10.1523/JNEUROSCI.5169-06.2007>
- Cao, P., Maximov, A., Südhof, T.C., 2011. Activity-dependent IGF-1 exocytosis is controlled by the Ca²⁺-sensor synaptotagmin-10. *Cell* 145, 300–311. <https://doi.org/10.1016/j.cell.2011.03.034>

- Capogna, M., Castillo, P.E., Maffei, A., 2020. The ins and outs of inhibitory synaptic plasticity: Neuron types, molecular mechanisms and functional roles. *Eur. J. Neurosci.* 1–20. <https://doi.org/10.1111/ejn.14907>
- Carmona, M.A., Pozas, E., Martínez, A., Espinosa-Parrilla, J.F., Soriano, E., Aguado, F., 2006. Age-dependent spontaneous hyperexcitability and impairment of GABAergic function in the hippocampus of mice lacking *trkB*. *Cereb. Cortex* 16, 47–63. <https://doi.org/10.1093/cercor/bhi083>
- Carro, E., Nuñez, A., Busiguina, S., Torres-Aleman, I., 2000. Circulating insulin-like growth factor I mediates effects of exercise on the brain. *J. Neurosci.* 20, 2926–33.
- Castren, E., Zafra, F., Thoenen, H., Lindholm, D., 1992. Light regulates expression of brain-derived neurotrophic factor mRNA in rat visual cortex. *Proc. Natl. Acad. Sci.* 89, 9444–9448. <https://doi.org/10.1073/pnas.89.20.9444>
- Cesetti, T., Fila, T., Obernier, K., Bengtson, C.P., Li, Y., Mandl, C., Hözl-Wenig, G., Ciccolini, F., 2011. GABAA receptor signaling induces osmotic swelling and cell cycle activation of neonatal prominin+ precursors. *Stem Cells* 29, 307–319. <https://doi.org/10.1002/stem.573>
- Chamma, I., Heubl, M., Chevy, Q., Renner, M., Moutkine, I., Eugene, E., Poncer, J.C., Levi, S., 2013. Activity-Dependent Regulation of the K/Cl Transporter KCC2 Membrane Diffusion, Clustering, and Function in Hippocampal Neurons. *J. Neurosci.* 33, 15488–15503. <https://doi.org/10.1523/jneurosci.5889-12.2013>
- Chancey, J.H., Adlaf, E.W., Sapp, M.C., Pugh, P.C., Wadiche, J.I., Overstreet-Wadiche, L.S., 2013. GABA Depolarization Is Required for Experience-Dependent Synapse Unsilencing in Adult-Born Neurons. *J. Neurosci.* 33, 6614–6622. <https://doi.org/10.1523/JNEUROSCI.0781-13.2013>
- Che, A., Babij, R., Iannone, A.F., Fetcho, R.N., Ferrer, M., Liston, C., Fishell, G., De Marco García, N. V., 2018. Layer I Interneurons Sharpen Sensory Maps during Neonatal Development. *Neuron* 99, 98–116. <https://doi.org/10.1016/j.neuron.2018.06.002>
- Chevy, Q., Heubl, M., Goutierre, M., Backer, S., Moutkine, I., Eugene, E., Bloch-Gallego, E., Levi, S., Poncer, J.C., 2015. KCC2 Gates Activity-Driven AMPA Receptor Traffic through Cofilin Phosphorylation. *J. Neurosci.* 35, 15772–15786. <https://doi.org/10.1523/JNEUROSCI.1735-15.2015>
- Chudotvorova, I., Ivanov, A., Rama, S., Christian, A.H., Pellegrino, C., 2005. Early expression of KCC2 in rat hippocampal cultures augments expression of functional GABA synapses 3, 671–679. <https://doi.org/10.1113/jphysiol.2005.089821>
- Clayton, G.H., Owens, G.C., Wolff, J.S., Smith, R.L., 1998. Ontogeny of cation-Cl-cotransporter expression in rat neocortex. *Dev. Brain Res.* 109, 281–292. [https://doi.org/10.1016/S0165-3806\(98\)00078-9](https://doi.org/10.1016/S0165-3806(98)00078-9)
- Colin-Le Brun, I., Ferrand, N., Caillard, O., Tosetti, P., Ben-Ari, Y., Gaiarsa, J.-L., Brun, I.C., Ferrand, N., Caillard, O., Tosetti, P., Ben-Ari, Y., 2004. Spontaneous synaptic activity is required for the formation of functional GABAergic synapses in the developing rat hippocampus. *J. Physiol.* 559, 129–139. <https://doi.org/10.1113/jphysiol.2004.065060>
- Corradini, I., Focchi, E., Rasile, M., Morini, R., Desiato, G., Tomasoni, R., Lizier, M., Ghirardini, E., Fesce, R., Morone, D., Barajon, I., Antonucci, F., Pozzi, D., Matteoli, M., 2017. Maternal Immune Activation Delays Excitatory-to-Inhibitory Gamma-Aminobutyric Acid Switch in Offspring. *Biol. Psychiatry* 83, 1–12. <https://doi.org/10.1016/j.biopsych.2017.09.030>
- Damborsky, J.C., Winzer-serhan, U.H., 2012. Effects of sex and chronic neonatal nicotine treatment on Na²⁺/K⁺/Cl⁻ co-transporter 1, K⁺/Cl⁻ co-transporter 2, brain-derived neurotrophic factor, NMDA receptor subunit 2A and NMDA receptor subunit 2B mRNA expression in the postnatal rat hippocampus. *Neuroscience* 225, 105–117. <https://doi.org/10.1016/j.neuroscience.2012.09.002>

- Daw, M.I., Ashby, M.C., Isaac, J.T.R., 2007. Coordinated developmental recruitment of latent fast spiking interneurons in layer IV barrel cortex. *Nat. Neurosci.* 10, 453–461. <https://doi.org/10.1038/nn1866>
- Deidda, G., Allegra, M., Cerri, C., Naskar, S., Bony, G., Zunino, G., Bozzi, Y., Caleo, M., Cancedda, L., 2015a. Early depolarizing GABA controls critical-period plasticity in the rat visual cortex. *Nat. Neurosci.* 18, 87–96. <https://doi.org/10.1038/nn.3890>
- Deidda, G., Parrini, M., Naskar, S., Bozarth, I.F., Contestabile, A., Cancedda, L., 2015b. Reversing excitatory GABAAR signaling restores synaptic plasticity and memory in a mouse model of Down syndrome. *Nat. Med.* 21, 318–326. <https://doi.org/10.1038/nm.3827>
- Delmotte, Q., Medina, I., Hamze, M., Buhler, E., Zhang, J., Belgacem, Y.H., Porcher, C., 2019. Sonic Hedgehog Signaling (Shh) regulates the developmental shift of GABA polarity in rat somatosensory cortex. *BioRxiv* <https://doi.org/10.1101/799015>. <https://doi.org/https://doi.org/10.1101/799015>
- Delpire, E., Mount, D.B., 2002. Human and Murine Phenotypes Associated with Defects in Cation-Chloride Cotransport. *Annu. Rev. Physiol.* 64, 803–843. <https://doi.org/10.1146/annurev.physiol.64.081501.155847>
- Demarque, M., Represa, A., Lè Ne Becq, H., Khalilov, I., Ben-Ari, Y., Aniksztejn, L., 2002. Paracrine Intercellular Communication by a Ca²⁺-and SNARE-Independent Release of GABA and Glutamate Prior to Synapse Formation cones in developing networks. *Neuron* 36, 1051–1061.
- Denter, D.G., Heck, N., Riedemann, T., White, R., Kilb, W., Luhmann, H.J., 2010. GABAC receptors are functionally expressed in the intermediate zone and regulate radial migration in the embryonic mouse neocortex. *Neuroscience* 167, 124–134. <https://doi.org/10.1016/j.neuroscience.2010.01.049>
- Duarte, S.T., Armstrong, J., Roche, A., Ortez, C., Pérez, A., O'Callaghan, M. del M., Pereira, A., Sanmartí, F., Ormazábal, A., Artuch, R., Pineda, M., García-Cazorla, A., 2013. Abnormal Expression of Cerebrospinal Fluid Cation Chloride Cotransporters in Patients with Rett Syndrome. *PLoS One* 8, 1–7. <https://doi.org/10.1371/journal.pone.0068851>
- Dumon, C., Diabira, D., Chudotvorova, I., Bader, F., Sahin, S., Zhang, J., Porcher, C., Wayman, G., Medina, I., Gaiarsa, J.L., 2018. The adipocyte hormone leptin sets the emergence of hippocampal inhibition in mice. *Elife* 7, 1–20. <https://doi.org/10.7554/eLife.36726>
- Durand, G.M., Kovalchuk, Y., Konnerth, A., 1996. LTP and functional synapse in developing hippocampus. *Nature* 381, 71–75.
- Duveau, V., Laustela, S., Barth, L., Gianolini, F., Vogt, K.E., Keist, R., Chandra, D., Homanics, G.E., Rudolph, U., Fritschy, J.M., 2011. Spatiotemporal specificity of GABAA receptor-mediated regulation of adult hippocampal neurogenesis. *Eur. J. Neurosci.* 34, 362–373. <https://doi.org/10.1111/j.1460-9568.2011.07782.x>
- Dzhala, V.I., Talos, D.M., Sdrulla, D.A., Brumback, A.C., Mathews, G.C., Benke, T.A., Delpire, E., Jensen, F.E., Staley, K.J., 2005. NKCC1 transporter facilitates seizures in the developing brain. *Nat. Med.* 11, 1205–1213. <https://doi.org/10.1038/nm1301>
- Fernandez, A., Dumon, C., Guimond, D., Fernandez, A., Burnashev, N., Tyzio, R., Lozovaya, N., Ferrari, D.C., Bonifazi, P., Ben-Ari, Y., 2018. The GABA Developmental Shift Is Abolished by Maternal Immune Activation Already at Birth. *Cereb. Cortex* 29, 3982–3992. <https://doi.org/10.1093/cercor/bhy279>
- Fernando, R.N., Eleuteri, B., Abdelhady, S., Nussenzweig, A., Andäng, M., Ernfors, P., 2011. Cell cycle restriction by histone H2AX limits proliferation of adult neural stem cells. *Proc. Natl. Acad. Sci. U. S. A.* 108, 5837–5842. <https://doi.org/10.1073/pnas.1014993108>

- Fiumelli, H., Briner, A., Puskarjov, M., Blaesle, P., Belem, B., Dayer, A., Kaila, K., Martin, J., Vutskits, L., 2013. An Ion Transport-Independent Role for the Cation-Chloride Cotransporter KCC2 in Dendritic Spinogenesis In Vivo. *Cereb. Cortex* 23, 378–388.
- Friauf, E., McConnell, S.K., Shatz, C.J., 1990. Functional synaptic circuits in the subplate during fetal and early postnatal development of cat visual cortex. *J. Neurosci.* 10, 2601–2613.
- Friauf, E., Wenz, M., Oberhofer, M., Nothwang, H.G., Balakrishnan, V., Knipper, M., Löhrike, S., 2008. Hypothyroidism impairs chloride homeostasis and onset of inhibitory neurotransmission in developing auditory brainstem and hippocampal neurons. *Eur. J. Neurosci.* 28, 2371–2380. <https://doi.org/10.1111/j.1460-9568.2008.06528.x>
- Friedel, P., Kahle, K.T., Zhang, J., Hertz, N., Pisella, L.I., Buhler, E., Schaller, F., Duan, J., Khanna, A.R., Bishop, P.N., Shokat, K.M., Medina, I., 2015. WNK1-regulated inhibitory phosphorylation of the KCC2 cotransporter maintains the depolarizing action of GABA in immature neurons. *Sci. Signal.* 8, ra65. <https://doi.org/10.1126/scisignal.aaa0354>
- Friedman, L., Kahen, B.A., 2019. Chronic Subconvulsive Activity during Early Postnatal Life Produces Autistic Behavior in the Absence of Neurotoxicity in the Juvenile Weanling Period. *Behav Brain Res* 374:112046.
- Fueshko, S.M., Key, S., Wray, S., 1998. GABA Inhibits Migration of Luteinizing Hormone-Releasing Hormone Neurons in Embryonic Olfactory Explants. *J. Neurosci.* 18, 2560–2569. <https://doi.org/10.1523/jneurosci.18-07-02560.1998>
- Furukawa, M., Tsukahara, T., Tomita, K., Iwai, H., Sonomura, T., Miyawaki, S., Sato, T., 2017. Neonatal maternal separation delays the GABA excitatory-to-inhibitory functional switch by inhibiting KCC2 expression. *Biochem. Biophys. Res. Commun.* 493, 1243–1249. <https://doi.org/10.1016/j.bbrc.2017.09.143>
- Galanopoulou, A.S., 2008. Dissociated gender-specific effects of recurrent seizures on GABA signaling in CA1 pyramidal neurons: Role of GABAA receptors. *J. Neurosci.* 28, 1557–1567. <https://doi.org/10.1523/JNEUROSCI.5180-07.2008>
- Galanopoulou, A.S., 2006. Sex- and cell-type-specific patterns of GABAA receptor and estradiol-mediated signaling in the immature rat substantia nigra. *Eur. J. Neurosci.* 23, 2423–2430. <https://doi.org/10.1111/j.1460-9568.2006.04778.x>
- Galanopoulou, A.S., Moshé, S.L., 2003. Role of sex hormones in the sexually dimorphic expression of KCC2 in rat substantia nigra. *Exp. Neurol.* 184, 1003–1009. [https://doi.org/10.1016/S0014-4886\(03\)00387-X](https://doi.org/10.1016/S0014-4886(03)00387-X)
- Ganguly, K., Schinder, A., Wong, S., Poo, M., 2001. GABA itself promotes the developmental switch of neuronal GABAergic responses from excitation to inhibition. *Cell* 105, 521–32.
- Gao, X.-B., Chen, G., van den Pol, A.N., 1998. GABA-Dependent Firing of Glutamate-Evoked Action Potentials at AMPA/Kainate Receptors in Developing Hypothalamic Neurons. *J. Neurophysiol.* 79, 716–726. <https://doi.org/10.1152/jn.1998.79.2.716>
- Gao, X., Pol, A.N. Van Den, 2000. GABA release from mouse axonal growth cones. *J. Physiol.* 523, 629–637.
- Garand, D., Mahadevan, V., Woodin, M.A., 2019. Ionotropic and metabotropic kainate receptor signalling regulates Cl⁻ homeostasis and GABAergic inhibition. *J. Physiol.* 597, 1677–1690. <https://doi.org/10.1113/JP276901>
- Gascon, E., Dayer, A.G., Sauvain, M.O., Potter, G., Jenny, B., De Roo, M., Zraggen, E., Demaurex, N., Muller, D., Kiss, J.Z., 2006. GABA regulates dendritic growth by stabilizing lamellipodia in newly generated interneurons of the olfactory bulb. *J. Neurosci.* 26, 12956–12966. <https://doi.org/10.1523/JNEUROSCI.4508-06.2006>

- Gauvain, G., Chamma, I., Chevy, Q., Cabezas, C., Irinopoulou, T., Bodrug, N., Carnaud, M., Levi, S., Poncer, J.C., 2011. The neuronal K-Cl cotransporter KCC2 influences postsynaptic AMPA receptor content and lateral diffusion in dendritic spines. *Proc. Natl. Acad. Sci.* 108, 15474–15479. <https://doi.org/10.1073/pnas.1107893108>
- Ge, S., Goh, E.L.K., Sailor, K.A., Kitabatake, Y., Ming, G.L., Song, H., 2006. GABA regulates synaptic integration of newly generated neurons in the adult brain. *Nature* 439, 589–593. <https://doi.org/10.1038/nature04404>
- Ghosh, A., Carnahan, J., Greenberg, M.E., 1994. Requirement for BDNF in Activity-Dependent Survival of Cortical Neurons 263, 1618–1623.
- Goutierre, M., Al Awabdh, S., Donneger, F., François, E., Gomez-Dominguez, D., Irinopoulou, T., Menendez de la Prida, L., Poncer, J.C., 2019. KCC2 Regulates Neuronal Excitability and Hippocampal Activity via Interaction with Task-3 Channels. *Cell Rep.* 28, 91–103. <https://doi.org/10.1016/j.celrep.2019.06.001>
- Gozlan, H., Ben-Ari, Y., 2003. Interneurons are the source and the targets of the first synapses formed in the rat developing hippocampal circuit. *Cereb. Cortex* 13, 684–692. <https://doi.org/10.1093/cercor/13.6.684>
- Gulyás, A.I., Sík, A., Payne, J.A., Kaila, K., Freund, T.F., 2001. The KCl cotransporter, KCC2, is highly expressed in the vicinity of excitatory synapses in the rat hippocampus. *Eur. J. Neurosci.* 13, 2205–2217. <https://doi.org/10.1046/j.0953-816X.2001.01600.x>
- Hadjikhani, N., Åsberg Johnels, J., Lassalle, A., Zürcher, N.R., Hippolyte, L., Gillberg, C., Lemonnier, E., Ben-Ari, Y., 2018. Bumetanide for autism: More eye contact, less amygdala activation. *Sci. Rep.* 8, 8–15. <https://doi.org/10.1038/s41598-018-21958-x>
- Haydar, T.F., Wang, F., Schwartz, M.L., Rakic, P., 2000. Differential Modulation of Proliferation in the Neocortical Ventricular and Subventricular Zones. *J. Neurosci.* 20, 5764–5774. <https://doi.org/10.1523/JNEUROSCI.20-15-05764.2000>
- He, Q., Arroyo, E.D., Smukowski, S.N., Xu, J., Piochon, C., Savas, J.N., Portera-Cailliau, C., Contractor, A., 2018. Critical period inhibition of NKCC1 rectifies synapse plasticity in the somatosensory cortex and restores adult tactile response maps in fragile X mice. *Mol. Psychiatry* 24, 1732–1747. <https://doi.org/10.1038/s41380-018-0048-y>
- He, Q., Nomura, T., Xu, J., Contractor, A., 2014. The Developmental Switch in GABA Polarity Is Delayed in Fragile X Mice. *J. Neurosci.* 34, 446–450. <https://doi.org/10.1523/JNEUROSCI.4447-13.2014>
- He, S., Ma, J., Liu, N., Yu, X., 2010. Early enriched environment promotes neonatal GABAergic neurotransmission and accelerates synapse maturation. *J. Neurosci.* 30, 7910–7916. <https://doi.org/10.1523/JNEUROSCI.6375-09.2010>
- Heck, N., Kilb, W., Reiprich, P., Kubota, H., Furukawa, T., Fukuda, A., Luhmann, H.J., 2007. GABA-A receptors regulate neocortical neuronal migration in vitro and in vivo. *Cereb. Cortex* 17, 138–148. <https://doi.org/10.1093/cercor/bhj135>
- Hu, J.S., Vogt, D., Sandberg, M., Rubenstein, J.L., 2017. Cortical interneuron development: A tale of time and space. *Dev.* 144, 3867–3878. <https://doi.org/10.1242/dev.132852>
- Hu, Yu, Z.L., Zhang, Y., Han, Y., Zhang, W., Lu, L., Shi, J., 2017. Bumetanide treatment during early development rescues maternal separation-induced susceptibility to stress. *Sci. Rep.* 7, 1–16. <https://doi.org/10.1038/s41598-017-12183-z>
- Huang, Y., Ko, H., Cheung, Z.H., Yung, K.K.L., Yao, T., Wang, J.J., Morozov, A., Ke, Y., Ip, N.Y., Yung, W.H., 2012. Dual actions of brain-derived neurotrophic factor on GABAergic transmission in cerebellar Purkinje neurons. *Exp. Neurol.* 233, 791–798. <https://doi.org/10.1016/j.expneurol.2011.11.043>
- Hübner, C. a, Stein, V., Hermans-Borgmeyer, I., Meyer, T., Ballanyi, K., Jentsch, T.J., 2001. Disruption of KCC2 reveals an essential role of K-Cl cotransport already in early synaptic inhibition. *Neuron* 30, 515–524.

- Ikeda-Matsuo, Y., Bordey, A., Wu, S., Taylor, M.M., Kubera, C., Young, S.Z., 2012. NKCC1 Knockdown Decreases Neuron Production through GABAA-Regulated Neural Progenitor Proliferation and Delays Dendrite Development. *J. Neurosci.* 32, 13630–13638. <https://doi.org/10.1523/jneurosci.2864-12.2012>
- Inada, H., Watanabe, M., Uchida, T., Ishibashi, H., Wake, H., Nemoto, T., Yanagawa, Y., Fukuda, A., Nabekura, J., 2011. GABA regulates the multidirectional tangential migration of GABAergic interneurons in living neonatal mice. *PLoS One* 6, e27048. <https://doi.org/10.1371/journal.pone.0027048>
- Inoue, K., Furukawa, T., Kumada, T., Yamada, J., Wang, T., Inoue, R., Fukuda, A., 2012. Taurine inhibits K⁺-Cl⁻ cotransporter KCC2 to regulate embryonic Cl⁻ homeostasis via with-no-lysine (WNK) protein kinase signaling pathway. *J. Biol. Chem.* 287, 20839–20850. <https://doi.org/10.1074/jbc.M111.319418>
- Isaac, J.T.R., Crair, M.C., Nicoll, R.A., Malenka, R.C., 1997. Silent synapses during development of thalamocortical inputs. *Neuron* 18, 269–280. [https://doi.org/10.1016/S0896-6273\(00\)80267-6](https://doi.org/10.1016/S0896-6273(00)80267-6)
- Itami, C., Kimura, F., Kohno, T., Matsuoka, M., Ichikawa, M., Tsumoto, T., Nakamura, S., 2003. Brain-derived neurotrophic factor-dependent unmasking of “silent” synapses in the developing mouse barrel cortex. *Proc. Natl. Acad. Sci.* 100, 13069–13074. <https://doi.org/10.1073/pnas.2131948100>
- Jantzie, L.L., Corbett, C.J., Firl, D.J., Robinson, S., 2015. Postnatal erythropoietin mitigates impaired cerebral cortical development following subplate loss from prenatal hypoxia-ischemia. *Cereb. Cortex* 25, 2683–2695. <https://doi.org/10.1093/cercor/bhu066>
- Kahle, K.T., Deeb, T.Z., Puskarjov, M., Silayeva, L., Liang, B., 2013. Modulation of neuronal activity by phosphorylation of the K-Cl cotransporter KCC2 36, 726–737. <https://doi.org/10.1016/j.tins.2013.08.006> Modulation
- Kanellopoulos, A.K., Mariano, V., Spinazzi, M., Woo, Y.J., Mclean, C., Pech, U., Li, K.W., Armstrong, J.D., Giangrande, A., Callaerts, P., Smit, A.B., Abrahams, B.S., Fiala, A., Achsel, T., Bagni, C., 2020. Aralar Sequesters GABA into Hyperactive Article Aralar Sequesters GABA into Hyperactive Mitochondria , Causing Social Behavior Deficits. *Cell* 180, 1178–1197. <https://doi.org/10.1016/j.cell.2020.02.044>
- Kang, S.K., Markowitz, G.J., Kim, S.T., Johnston, M. V., Kadam, S.D., 2015. Age- and sex-dependent susceptibility to phenobarbital-resistant neonatal seizures: Role of chloride co-transporters. *Front. Cell. Neurosci.* 9, 1–16. <https://doi.org/10.3389/fncel.2015.00173>
- Kanold, P.O., Shatz, C.J., 2006. Subplate Neurons Regulate Maturation of Cortical Inhibition and Outcome of Ocular Dominance Plasticity. *Neuron* 51, 627–638. <https://doi.org/10.1016/j.neuron.2006.07.008>
- Kelsch, W., Hormuzdi, S., Straube, E., Lewen, A., Monyer, H., Misgeld, U., 2001. Insulin-like growth factor 1 and a cytosolic tyrosine kinase activate chloride outward transport during maturation of hippocampal neurons. *J. Neurosci.* 21, 8339–47.
- Khademullah, C.S., Aqrabawi, A.J., Place, K.M., Dargaei, Z., Liang, X., Pressey, J.C., Bedard, S., Yang, J.W., Garand, D., Keramidis, I., Gasecka, A., Côté, D., De Koninck, Y., Keith, J., Zinman, L., Robertson, J., Kim, J.C., Woodin, M.A., 2020. Cortical interneuron-mediated inhibition delays the onset of amyotrophic lateral sclerosis. *Brain* 143, 800–810. <https://doi.org/10.1093/brain/awaa034>
- Khalilov, I., Chazal, G., Chudotvorova, I., Pellegrino, C., Corby, S., Ferrand, N., Gubkina, O., Nardou, R., Tyzio, R., Yamamoto, S., Hentsch, T., Hübner, C., Gaiarsa, J., Ben-Ari, Y., Medina, I., 2011. Enhanced synaptic activity and epileptiform events in the embryonic KCC2 deficient hippocampus. *Front. Cell. Neurosci.* 5.

- Khalilov, I., Khazipov, R., Esclapez, M., Ben-Ari, Y., 1997. Bicuculline induces ictal seizures in the intact hippocampus recorded in vitro. *Eur. J. Pharmacol.* 319, 5–6. [https://doi.org/10.1016/S0014-2999\(96\)00964-8](https://doi.org/10.1016/S0014-2999(96)00964-8)
- Khalilov, I., Minlebaev, M., Mukhtarov, M., Khazipov, R., 2015. Dynamic Changes from Depolarizing to Hyperpolarizing GABAergic Actions during Giant Depolarizing Potentials in the Neonatal Rat Hippocampus. *J. Neurosci.* 35, 12635–12642. <https://doi.org/10.1523/jneurosci.1922-15.2015>
- Kharod, S.C., Kang, S.K., Kadam, S.D., 2019. Off-Label Use of Bumetanide for Brain Disorders: An Overview. *Front. Neurosci.* 13, doi: 10.3389/fnins.2019.00310. <https://doi.org/10.3389/fnins.2019.00310>
- Khazipov, R., Khalilov, I., Tyzio, R., Morozova, E., Ben-Ari, Y., Holmes, G.L., 2004. Developmental changes in GABAergic actions and seizure susceptibility in the rat hippocampus. *Eur. J. Neurosci.* 19, 590–600. <https://doi.org/10.1111/j.0953-816X.2003.03152.x>
- Khirug, 2012. GABAergic Depolarization of the Axon Initial Segment in Cortical Principal Neurons Is Caused by the Na–K–2Cl Cotransporter NKCC1. *Indian J. Nat. Prod. Resour.* 3, 467–476. <https://doi.org/10.1523/JNEUROSCI.0908-08.2008>
- Khirug, S., Huttu, K., Ludwig, A., Smirnov, S., Voipio, J., Rivera, C., Kaila, K., Khiroug, L., 2005. Distinct properties of functional KCC2 expression in immature mouse hippocampal neurons in culture and in acute slices. *Eur. J. Neurosci.* 21, 899–904. <https://doi.org/10.1111/j.1460-9568.2005.03886.x>
- Kirmse, K., Kummer, M., Kovalchuk, Y., Witte, O.W., Garaschuk, O., Holthoff, K., 2015. GABA depolarizes immature neurons and inhibits network activity in the neonatal neocortex in vivo. *Nat. Commun.* 6, 1–13. <https://doi.org/10.1038/ncomms8750>
- Kirmse, K., Witte, O.W., Holthoff, K., 2010. GABA depolarizes immature neocortical neurons in the presence of the ketone body β -hydroxybutyrate. *J. Neurosci.* 30, 16002–16007. <https://doi.org/10.1523/JNEUROSCI.2534-10.2010>
- Konkle, A.T.M., McCarthy, M.M., 2011. Developmental time course of estradiol, testosterone, and dihydrotestosterone levels in discrete regions of male and female rat brain. *Endocrinology* 152, 223–235. <https://doi.org/10.1210/en.2010-0607>
- Kotak, V.C., Sanes, D.H., 1996. Developmental influence of glycinergic transmission: Regulation of NMDA receptor-mediated EPSPs. *J. Neurosci.* 16, 1836–1843. <https://doi.org/10.1523/jneurosci.16-05-01836.1996>
- Kovács, K., Basu, K., Rouiller, I., Sík, A., 2014. Regional differences in the expression of K⁺-Cl⁻ 2 cotransporter in the developing rat cortex. *Brain Struct. Funct.* 219, 527–538. <https://doi.org/10.1007/s00429-013-0515-9>
- Kyrozis, A., Chudomel, O., Moshé, S.L., Galanopoulou, A.S., 2006. Sex-dependent maturation of GABA_A receptor-mediated synaptic events in rat substantia nigra reticulata. *Neurosci. Lett.* 398, 1–5. <https://doi.org/10.1016/j.neulet.2005.12.018>
- Landi, S., Ciucci, F., Maffei, L., Berardi, N., Cenni, M.C., 2009. Setting the Pace for Retinal Development: Environmental Enrichment Acts Through Insulin-Like Growth Factor 1 and Brain-Derived Neurotrophic Factor. *J. Neurosci.* 29, 10809–10819. <https://doi.org/10.1523/jneurosci.1857-09.2009>
- Laurie, D.J., Wisden, W., Seeburg, P.H., 1992. The distribution of thirteen GABA_A receptor subunit mRNAs in the rat brain. III. Embryonic and postnatal development. *J. Neurosci.* 12, 4151–72.
- Le Magueresse, C., Monyer, H., 2013. GABAergic Interneurons Shape the Functional Maturation of the Cortex. *Neuron* 77, 388–405. <https://doi.org/10.1016/j.neuron.2013.01.011>

- Lee, 2010. Possible involvement of DNA methylation in NKCC1 gene expression during postnatal development and in response to ischemia. 114, 520–529. <https://doi.org/10.1111/j.1471-4159.2010.06772.x>
- Lee, H.H.C., Walker, J.A., Williams, J.R., Goodier, R.J., Payne, J.A., Moss, S.J., 2007. Direct protein kinase C-dependent phosphorylation regulates the cell surface stability and activity of the potassium chloride cotransporter KCC2. *J. Biol. Chem.* 282, 29777–29784. <https://doi.org/10.1074/jbc.M705053200>
- Leinekugel, X., Khazipov, R., Cannon, R., Hirase, H., Buzsáki, G., 2002. Correlated Bursts of Activity in the Neonatal Hippocampus in Vivo. *Science (80-.)*. 296, 2049–2052.
- Leinekugel, X., Medina, I., Khalilov, I., Ben-Ari, Y., Khazipov, R., 1997. Ca²⁺ Oscillations Mediated by the Synergistic Excitatory Actions of GABA. *Neuron* 18, 243–255.
- Lemonnier, E., Ben-Ari, Y., 2010. The diuretic bumetanide decreases autistic behaviour in five infants treated during 3 months with no side effects. *Acta Paediatr.* 99, 1885–1888. <https://doi.org/10.1111/j.1651-2227.2010.01933.x>
- Lemonnier, E., Degrez, C., Phelep, M., Tyzio, R., Josse, F., Grandgeorge, M., Hadjikhani, N., Ben-Ari, Y., 2012. A randomised controlled trial of bumetanide in the treatment of autism in children. *Transl. Psychiatry* 2, e202-8. <https://doi.org/10.1038/tp.2012.124>
- Lemonnier, E., Villeneuve, N., Sonie, S., Serret, S., Rosier, A., Roue, M., Brosset, P., Viellard, M., Ernoux, D.B., Rondeau, S., Thummler, S., Ravel, D., Ben-Ari, Y., 2017. Effects of bumetanide on neurobehavioral function in children and adolescents with autism spectrum disorders. *Transl. Psychiatry* 7, e1056-9. <https://doi.org/10.1038/tp.2017.10>
- Leonzino, M., Busnelli, M., Antonucci, F., Verderio, C., Mazzanti, M., Chini, B., 2016. The Timing of the Excitatory-to-Inhibitory GABA Switch Is Regulated by the Oxytocin Receptor via KCC2. *Cell Rep.* 15, 96–103. <https://doi.org/10.1016/j.celrep.2016.03.013>
- Li, H., Khirug, S., Cai, C., Ludwig, A., Blaesse, P., Kolikova, J., Afzalov, R., Coleman, S.K., Lauri, S., Airaksinen, M.S., Keinänen, K., Khiroug, L., Saarma, M., Kaila, K., Rivera, C., 2007. KCC2 Interacts with the Dendritic Cytoskeleton to Promote Spine Development. *Neuron* 56, 1019–1033. <https://doi.org/10.1016/j.neuron.2007.10.039>
- Liu, X., Wang, Q., Haydar, T.F., 2005. Nonsynaptic GABA signaling in postnatal subventricular zone controls proliferation of GFAP-expressing progenitors 8, 1179–1187. <https://doi.org/10.1038/nm1522>
- Liu, Z., Neff, R.A., Berg, D.K., 2006. Sequential Interplay of Nicotinic and GABAergic Signaling Guides Neuronal Development. *Science (80-.)*. 314, 1610–1614.
- Lohmann, C., Kessels, H.W., 2014. The developmental stages of synaptic plasticity. *J. Physiol.* 592, 13–31. <https://doi.org/10.1113/jphysiol.2012.235119>
- Lombardi, A., Jedlicka, P., Luhmann, H.J., Kilb, W., 2018. Giant depolarizing potentials trigger transient changes in the intracellular Cl⁻ concentration in CA3 pyramidal neurons of the immature mouse hippocampus. *Front. Cell. Neurosci.* 12, 1–15. <https://doi.org/10.3389/fncel.2018.00420>
- LoTurco, J.J., Owens, D.F., Heath, M.J.S., Davis, M.B.E., Kriegstein, A.R., 1995. GABA and glutamate depolarize cortical progenitor cells and inhibit DNA synthesis. *Neuron* 15, 1287–1298. [https://doi.org/10.1016/0896-6273\(95\)90008-X](https://doi.org/10.1016/0896-6273(95)90008-X)
- Lozovaya, N., Nardou, R., Tyzio, R., Chiesa, M., Pons-Bennaceur, A., Eftekhari, S., Bui, T.T., Billon-Grand, M., Rasero, J., Bonifazi, P., Guimond, D., Gaiarsa, J.L., Ferrari, D.C., Ben-Ari, Y., 2019. Early alterations in a mouse model of Rett syndrome: the GABA developmental shift is abolished at birth. *Sci. Rep.* 9, 1–16. <https://doi.org/10.1038/s41598-019-45635-9>

- Lu, J., Karadsheh, M., Delpire, E., 1999. Developmental regulation of the neuronal-specific isoform of K-Cl cotransporter KCC2 in postnatal rat brains. *J. Neurobiol.* 39, 558–568. [https://doi.org/10.1002/\(SICI\)1097-4695\(19990615\)39:4<558::AID-NEU9>3.0.CO;2-5](https://doi.org/10.1002/(SICI)1097-4695(19990615)39:4<558::AID-NEU9>3.0.CO;2-5)
- Ludwig, A., Uvarov, P., Soni, S., Thomas-Crusells, J., Airaksinen, M.S., Rivera, C., 2011a. Early Growth Response 4 Mediates BDNF Induction of Potassium Chloride Cotransporter 2 Transcription. *J. Neurosci.* 31, 644–649. <https://doi.org/10.1523/jneurosci.2006-10.2011>
- Ludwig, A., Uvarov, P., Soni, S., Thomas-Crusells, J., Airaksinen, M.S., Rivera, C., 2011b. Neurturin evokes MAPK-dependent upregulation of Egr4 and KCC2 in developing neurons. *Neural Plast.* 2011, 1–8. <https://doi.org/10.1155/2011/641248>
- Luhmann, H.J., Fukuda, A., Kilb, W., 2015. Control of cortical neuronal migration by glutamate and GABA. *Front. Cell. Neurosci.* 9, 1–15. <https://doi.org/10.3389/fncel.2015.00004>
- Marguet, S.L., Morellini, F., Hanganu-Opatz, I.L., Merseburg, A., Le-Schulte, V.T.Q., Neu, A., Ivanov, A., Jakovcevski, I., Bernard, C., Eichler, R., Isbrandt, D., 2015. Treatment during a vulnerable developmental period rescues a genetic epilepsy. *Nat. Med.* 21, 1436–1444. <https://doi.org/10.1038/nm.3987>
- Maric, D., Liu, Q.Y., Maric, I., Chaudry, S., Chang, Y.H., Smith, S. V, Sieghart, W., Fritschy, J.M., Barker, J.L., 2001. GABA expression dominates neuronal lineage progression in the embryonic rat neocortex and facilitates neurite outgrowth via GABA(A) autoreceptor/Cl⁻ channels. *J. Neurosci.* 21, 2343–60.
- Martinez-Delgado, G., Estrada-Mondragon, A., Miledi, R., Martinez-Torres, A., 2010. An Update on GABA rho Receptors. *Curr. Neuropharmacol.* 8, 422–433.
- Medina, I., Friedel, P., Rivera, C., Kahle, K.T., Kourdougli, N., Uvarov, P., Pellegrino, C., 2014. Current view on the functional regulation of the neuronal K⁺-Cl⁻ cotransporter KCC2. *Front. Cell. Neurosci.* 8, 1–18. <https://doi.org/10.3389/fncel.2014.00027>
- Menshanov, P.N., Lanshakov, D.A., Dygalo, N.N., 2015. proBDNF is a major product of bdnf gene expressed in the perinatal rat cortex. *Physiol. Res.* 64, 925–934.
- Merner, N., Chandler, M., Bourassa, C., Liang, B., Khanna, A., Dion, P., Rouleau, G., Kahle, K., 2015. Regulatory domain or CpG site variation in SLC12A5, encoding the chloride transporter KCC2, in human autism and schizophrenia. *Front. Cell. Neurosci.* 9, 386.
- Minlebaev, M., Ben-Ari, Y., Khazipov, R., 2006. Network Mechanisms of Spindle-Burst Oscillations in the Neonatal Rat Barrel Cortex In Vivo. *J. Neurophysiol.* 97, 692–700. <https://doi.org/10.1152/jn.00759.2006>
- Minlebaev, M., Colonnese, M., Tsintsadze, T., Sirota, A., Khazipov, R., 2011. Early Gamma Oscillations Synchronize Developing Thalamus and Cortex. *Science (80-.)*. 334, 226–229. <https://doi.org/10.1126/science.1210574>
- Modi, M.E., Young, L.J., 2012. The oxytocin system in drug discovery for autism: Animal models and novel therapeutic strategies. *Horm. Behav.* 61, 340–350. <https://doi.org/10.1038/jid.2014.371>
- Mòdol, L., Casas, C., Llidó, A., Navarro, X., Pallarès, M., Darbra, S., 2014. Neonatal allopregnanolone or finasteride administration modifies hippocampal K⁺ Cl⁻ co-transporter expression during early development in male rats. *J. Steroid Biochem. Mol. Biol.* 143, 343–347. <https://doi.org/10.1016/j.jsbmb.2014.05.002>
- Mohajerani, M.H., Cherubini, E., 2005. Spontaneous recurrent network activity in organotypic rat hippocampal slices. *Eur. J. Neurosci.* 22, 107–118. <https://doi.org/10.1111/j.1460-9568.2005.04198.x>

- Moore, Y.E., Conway, L.C., Wobst, H.J., Brandon, N.J., Deeb, T.Z., Moss, S.J., 2019. Developmental Regulation of KCC2 Phosphorylation Has Long-Term Impacts on Cognitive Function. *Front. Mol. Neurosci.* 12, 1–11. <https://doi.org/10.3389/fnmol.2019.00173>
- Morita, K., Tsumoto, K., Aihara, K., 2006. Bidirectional modulation of neuronal responses by depolarizing GABAergic inputs. *Biophys. J.* 90, 1925–1938. <https://doi.org/10.1529/biophysj.105.063164>
- Murata, Y., Colonnese, M.T., 2020. GABAergic interneurons excite neonatal hippocampus in vivo. *Sci. Adv.* 6, 1–10.
- Murguía-Castillo, J., Beas-Zárate, C., Rivera-Cervantes, M.C., Feria-Velasco, A.I., Ureña-Guerrero, M.E., 2013. NKCC1 and KCC2 protein expression is sexually dimorphic in the hippocampus and entorhinal cortex of neonatal rats. *Neurosci. Lett.* 552, 52–57. <https://doi.org/10.1016/j.neulet.2013.07.038>
- Nakajima, K. ichi, Marunaka, Y., 2016. Intracellular chloride ion concentration in differentiating neuronal cell and its role in growing neurite. *Biochem. Biophys. Res. Commun.* 479, 338–342. <https://doi.org/10.1016/j.bbrc.2016.09.075>
- Nakamura, N.H., Rosell, D.R., Akama, K.T., McEwen, B.S., 2004. Estrogen and ovariectomy regulate mRNA and protein of glutamic acid decarboxylases and cation-chloride cotransporters in the adult rat hippocampus. *Neuroendocrinology* 80, 308–323. <https://doi.org/10.1159/000083657>
- Nakanishi, K., Yamada, J., Takayama, C., Oohira, A., Fukuda, A., 2007. NKCC1 Activity Modulates Formation of Functional Inhibitory Synapses in Cultured Neocortical Neurons. *Synapse* 411, 401–411. <https://doi.org/10.1002/syn>
- Nguyen, L., Malgrange, B., Breuskin, I., Bettendorff, L., Moonen, G., Belachew, S., Rigo, J.-M., 2003. Autocrine/Paracrine Activation of the GABA A Receptor Inhibits the Proliferation of Neurogenic Polysialylated Neural Cell Adhesion Molecule-Positive (PSA-NCAM+) Precursor Cells from Postnatal Striatum. *J. Neurosci.* 23, 3278–3294. <https://doi.org/10.1523/jneurosci.23-08-03278.2003>
- Nuñez, J.L., McCarthy, M., 2007. Evidence for an Extended Duration of GABA-Mediated Excitation in the Developing Male Versus Female Hippocampus. *Dev Neurobiol.* 67, 1879–1890. <https://doi.org/10.1080/10810730902873927>
- Oh, W.C., Lutz, S., Castillo, P.E., Kwon, H.B., 2016. De novo synaptogenesis induced by GABA in the developing mouse cortex - supplemental. *Science* (80-). 353, 1037–1040. <https://doi.org/10.1126/science.aaf5206>
- Otsu, Y., Donneger, F., Schwartz, E.J., Poncer, J.C., 2020. Cation–chloride cotransporters and the polarity of GABA signalling in mouse hippocampal parvalbumin interneurons. *J. Physiol.* 598, 1–16. <https://doi.org/10.1113/JP279221>
- Owens, D.F., Boyce, L.H., Davis, M.B.E., Kriegstein, A.R., 1996. Excitatory GABA responses in embryonic and neonatal cortical slices demonstrated by gramicidin perforated-patch recordings and calcium imaging. *J. Neurosci.* 16, 6414–6423.
- Owens, D.F., Liu, X., Kriegstein, A.R., 1999. Changing Properties of GABA A Receptor-Mediated Signaling During Early Neocortical Development. *J. Neurophysiol.* 82, 570–583. <https://doi.org/10.1152/jn.1999.82.2.570>
- Pan-vazquez, A., Wefelmeyer, W., Sabater, V.G., Neves, G., Burrone, J., 2020. Activity-Dependent Plasticity of Axo-axonic Synapses at the Axon Initial Segment. *Neuron* 106, 1–12. <https://doi.org/10.1016/j.neuron.2020.01.037>
- Payne, J., Stevenson, T., Donaldson, L., 1996. Molecular characterization of a putative K-Cl cotransporter in rat brain A neuronal-specific isoform. *J. Biol. Chem.* 271, 16245–16252.

- Perrot-Sinal, T.S., Davis, A.M., Gregerson, K.A., Kao, J.P.Y., McCarthy, M.M., 2001. Estradiol enhances excitatory gamma-butyric acid-mediated calcium signaling in neonatal hypothalamic neurons. *Endocrinology* 142, 2238–2243. <https://doi.org/10.1210/endo.142.6.8180>
- Perrot-Sinal, T.S., Sinal, C.J., Reader, J.C., Speert, D.B., McCarthy, M.M., 2007. Sex differences in the chloride cotransporters, NKCC1 and KCC2, in the developing hypothalamus. *J. Neuroendocrinol.* 19, 302–308. <https://doi.org/10.1111/j.1365-2826.2007.01530.x>
- Pfeffer, C.K., Stein, V., Keating, D.J., Maier, H., Rinke, I., Rudhard, Y., Hentschke, M., Rune, G.M., Jentsch, T.J., Hubner, C.A., 2009. NKCC1-Dependent GABAergic Excitation Drives Synaptic Network Maturation during Early Hippocampal Development. *J. Neurosci.* 29, 3419–3430. <https://doi.org/10.1523/JNEUROSCI.1377-08.2009>
- Pisella, Gaiarsa, Diabira, Zhang, Khalilov, Duan, Kahle, Medina, 2019. Impaired regulation of KCC2 phosphorylation leads to neuronal network dysfunction and neurodevelopmental pathology. *Sci. Signal.* 12. <https://doi.org/10.1126/scisignal.aay0300>
- Porcher, C., Hatchett, C., Longbottom, R.E., McAinch, K., Sihra, T.S., Moss, S.J., Thomson, A.M., Jovanovic, J.N., 2011. Positive feedback regulation between γ -aminobutyric acid type A (GABA_A) receptor signaling and brain-derived neurotrophic factor (BDNF) release in developing neurons. *J. Biol. Chem.* 286, 21667–21677. <https://doi.org/10.1074/jbc.M110.201582>
- Pouille, F., Scanziani, M., 2001. Enforcement of temporal fidelity in pyramidal cells by somatic feed-forward inhibition. *Science* (80-.). 293, 1159–1163. <https://doi.org/10.1126/science.1060342>
- Puskarjov, M., Ahmad, F., Khirug, S., Sivakumaran, S., Kaila, K., Blaesse, P., 2015. BDNF is required for seizure-induced but not developmental up-regulation of KCC2 in the neonatal hippocampus. *Neuropharmacology* 88, 103–109.
- Puskarjov, M., Fiumelli, H., Briner, A., Bodogan, T., Demeter, K., Laco, C., Mavrovic, M., Blaesse, P., Kaila, K., Vutskits, L., 2017. K-Cl Cotransporter 2-mediated Cl⁻ Extrusion Determines Developmental Stage-dependent Impact of Propofol Anesthesia on Dendritic Spine. *Anesthesiology* 126, 1–13.
- Radzikinas, K., Aven, L., Jiang, Z., Tran, T., Paez-Cortez, J., Boppidi, K., Lu, J., Fine, A., Ai, X., 2011. A Shh/miR-206/BDNF cascade coordinates innervation and formation of airway smooth muscle. *J. Neurosci.* 31, 15407–15415. doi.org/10.1523/JNEUROSCI.2745-11.2011
- Reynolds, A., Brustein, E., Liao, M., Mercado, A., Babilonia, E., Mount, D.B., Drapeau, P., 2008. Neurogenic Role of the Depolarizing Chloride Gradient Revealed by Global Overexpression of KCC2 from the Onset of Development. *J. Neurosci.* 28, 1588–1597. <https://doi.org/10.1523/jneurosci.3791-07.2008>
- Rheims, S., Minlebaev, M., Ivanov, A., Represa, A., Khazipov, R., Holmes, G.L., Ben-Ari, Y., Zilberter, Y., 2008. Excitatory GABA in rodent developing neocortex in vitro. *J. Neurophysiol.* 100, 609–619. <https://doi.org/10.1152/jn.90402.2008>
- Riekkki, R., Pavlov, I., Tornberg, J., Lauri, S.E., Airaksinen, M.S., Taira, T., 2008. Altered Synaptic Dynamics and Hippocampal Excitability but Normal Long-Term Plasticity in Mice Lacking Hyperpolarizing GABA_A Receptor-Mediated Inhibition in CA1 Pyramidal Neurons. *J. Neurophysiol.* 99, 3075–3089. <https://doi.org/10.1152/jn.00606.2007>
- Riffault, B., Kourdougli, N., Dumon, C., Ferrand, N., Buhler, E., Schaller, F., Chambon, C., Rivera, C., Gaiarsa, J.L., Porcher, C., 2018. Pro-Brain-Derived Neurotrophic Factor (proBDNF)-Mediated p75 NTR Activation Promotes Depolarizing Actions of GABA and Increases Susceptibility to Epileptic Seizures. *Cereb. Cortex* 28, 510–527. <https://doi.org/10.1093/cercor/bhw385>

- Rinehart, J., Maksimova, Y.D., Tanis, J.E., Stone, K.L., Hodson, C.A., Zhang, J., Risinger, M., Pan, W., Wu, D., Colangelo, C.M., Forbush, B., Joiner, C.H., Gulcicek, E.E., Gallagher, P.G., Lifton, R.P., 2009. Sites of Regulated Phosphorylation that Control K-Cl Cotransporter Activity. *Cell* 138, 525–536. <https://doi.org/10.1016/j.cell.2009.05.031>
- Rinetti-Vargas, G., Phamluong, K., Ron, D., Bender, K.J., 2017. Periadolescent Maturation of GABAergic Hyperpolarization at the Axon Initial Segment. *Cell Rep.* 20, 21–29. <https://doi.org/10.1016/j.celrep.2017.06.030>
- Rivera, C., Voipio, J., Payne, J. a, Ruusuvuori, E., Lahtinen, H., Lamsa, K., Pirvola, U., Saarma, M., Kaila, K., 1999. The K⁺/Cl⁻ co-transporter KCC2 renders GABA hyperpolarizing during neuronal maturation. *Nature* 397, 251–255. <https://doi.org/10.1038/16697>
- Román, G.C., Ghassabian, A., Bongers-Schokking, J.J., Jaddoe, V.W.V., Hofman, A., De Rijke, Y.B., Verhulst, F.C., Tiemeier, H., 2013. Association of gestational maternal hypothyroxinemia and increased autism risk. *Ann. Neurol.* 74, 733–742. <https://doi.org/10.1002/ana.23976>
- Romo-Parra, H., Treviño, M., Heinemann, U., Gutiérrez, R., 2008. GABA actions in hippocampal area CA3 during postnatal development: Differential shift from depolarizing to hyperpolarizing in somatic and dendritic compartments. *J. Neurophysiol.* 99, 1523–1534. <https://doi.org/10.1152/jn.01074.2007>
- Roussa, E., Speer, J., Chudotvorova, I., Khakipoor, S., Smirnov, S., Rivera, C., Kriegstein, K., 2016. The membrane trafficking and functionality of the K⁺-Cl⁻ co-transporter KCC2 is regulated by TGF- β 2. *J. Cell Sci.* 129, 3485–3498.
- Roux, S., Lohof, A., Ben-Ari, Y., Poulain, B., Bossu, J.-L., 2018. Maturation of GABAergic Transmission in Cerebellar Purkinje Cells Is Sex Dependent and Altered in the Valproate Model of Autism. *Front. Cell. Neurosci.* 12, 1–14. <https://doi.org/10.3389/fncel.2018.00232>
- Ruffolo, G., Cifelli, P., Roseti, C., Thom, M., van Vliet, E.A., Limatola, C., Aronica, E., Palma, E., 2018. A novel GABAergic dysfunction in human Dravet syndrome. *Epilepsia* 59, 2106–2117. <https://doi.org/10.1111/epi.14574>
- Ruffolo, G., Iyer, A., Cifelli, P., Roseti, C., Mühlebner, A., van Scheppingen, J., Scholl, T., Hainfellner, J., Feucht, M., Krsek, P., Zamecnik, J., Jansen, F., Spliet, W., Limatola, C., Aronica, E., Palma, E., 2016. Functional aspects of early brain development are preserved in tuberous sclerosis complex (TSC) epileptogenic lesions. *Neurobiol. Dis.* 95, 93–101.
- Rumpel, S., Hatt, H., Gottmann, K., 1998. Silent synapses in the developing rat visual cortex: Evidence for postsynaptic expression of synaptic plasticity. *J. Neurosci.* 18, 8863–8874. <https://doi.org/10.1523/jneurosci.18-21-08863.1998>
- Salmon, C.K., Pribiag, H., Gizowski, C., Farmer, W.T., Cameron, S., Jones, E. V., Mahadevan, V., Bourque, C.W., Stellwagen, D., Woodin, M.A., Murai, K.K., 2020. Depolarizing GABA Transmission Restrains Activity-Dependent Glutamatergic Synapse Formation in the Developing Hippocampal Circuit. *Front. Cell. Neurosci.* 14, 1–16. <https://doi.org/10.3389/fncel.2020.00036>
- Sauer, J.F., Bartos, M., 2010. Recruitment of early postnatal parvalbumin-positive hippocampal interneurons by GABAergic excitation. *J. Neurosci.* 30, 110–115. <https://doi.org/10.1523/JNEUROSCI.4125-09.2010>
- Savardi, A., Borgogno, M., Narducci, R., La Sala, G., Ortega, J.A., Summa, M., Armirotti, A., Bertorelli, R., Contestabile, A., De Vivo, M., Cancedda, L., 2020. Discovery of a Small Molecule Drug Candidate for Selective NKCC1 Inhibition in Brain Disorders. *Chem* 6, 2073–2096. <https://doi.org/10.1016/j.chempr.2020.06.017>
- Sawano, E., Takahashi, M., Negishi, T., Tashiro, T., 2013. Thyroid hormone-dependent development of the GABAergic pre- and post-synaptic components in the rat hippocampus. *Int. J. Dev. Neurosci.* 31, 751–761. <https://doi.org/10.1016/j.ijdevneu.2013.09.007>

- Schulte, J.T., Wierenga, C.J., Bruining, H., 2018. Chloride transporters and GABA polarity in developmental, neurological and psychiatric conditions. *Neurosci. Biobehav. Rev.* 90, 260–271. <https://doi.org/10.1016/j.neubiorev.2018.05.001>
- Semyanov, A., Kullmann, D.M., 2002. Relative picrotoxin insensitivity distinguishes ionotropic GABA receptor-mediated IPSCs in hippocampal interneurons. *Neuropharmacology* 43, 726–736. [https://doi.org/10.1016/S0028-3908\(02\)00123-5](https://doi.org/10.1016/S0028-3908(02)00123-5)
- Sernagor, E., Chabrol, F., Bony, G., Cancedda, L., 2010. Gabaergic control of neurite outgrowth and remodeling during development and adult neurogenesis: General rules and differences in diverse systems. *Front. Cell. Neurosci.* 4, 1–11. <https://doi.org/10.3389/fncel.2010.00011>
- Sernagor, E., Young, C., Eglen, S.J., 2003. Developmental Modulation of Retinal Wave Dynamics: Shedding Light on the GABA Saga. *J. Neurosci.* 23, 7621–7629. <https://doi.org/10.1523/jneurosci.23-20-07621.2003>
- Shibata, S., Kakazu, Y., Okabe, A., Fukuda, A., Nabekura, J., 2004. Experience-dependent changes in intracellular Cl⁻ regulation in developing auditory neurons. *Neurosci. Res.* 48, 211–220. <https://doi.org/10.1016/j.neures.2003.10.011>
- Shimizu-okabe, C., Okabe, A., Ikeda, M., Sato, K., Kilb, W., Luhmann, H.J., Fukuda, A., 2002. Layer-specific expression of Cl⁻ transporters and differential [Cl⁻]_i in newborn rat cortex. *October 13*, 18–22. <https://doi.org/10.1097/01.wnr.0000048007>
- Shulga, A., Blaesse, A., Kysenius, K., Huttunen, H.J., Tanhuanpää, K., Saarma, M., Rivera, C., 2009. Thyroxin regulates BDNF expression to promote survival of injured neurons. *Mol. Cell. Neurosci.* 42, 408–418. <https://doi.org/10.1016/j.mcn.2009.09.002>
- Sipila, S.T., Schuchmann, S., Voipio, J., Yamada, J., Kaila, K., 2006. The cation-chloride cotransporter NKCC1 promotes sharp waves in the neonatal rat hippocampus 3, 765–773. <https://doi.org/10.1113/jphysiol.2006.107086>
- Smalley, J.L., Kontou, G., Choi, C., Qiu Ren, D.A., Abiraman, K., Santos, M.A.R., Bope, C.E., Deeb, T.Z., Davies, P.A., Brandon, N.J., Moss, S.J., 2020a. The K-Cl co-transporter 2 is a point of convergence for multiple autism spectrum disorder and epilepsy risk gene products. *BioRxiv* <https://doi.org/10.1101/2020.03.02.973859>. <https://doi.org/10.1017/CBO9781107415324.004>
- Smalley, J.L., Kontou, G., Choi, C., Ren, Q., Albrecht, D., Abiraman, K., Santos, M.A.R., Bope, C.E., Deeb, T.Z., Davies, P.A., Brandon, N.J., Moss, S.J., 2020b. Isolation and characterization of multi-protein complexes enriched in the K-Cl co-transporter 2 from brain plasma membranes. *BioRxiv* <https://doi.org/10.1101/2020.04.30.071076>.
- Song, J., Zhong, C., Bonaguidi, M.A., Sun, G.J., Hsu, D., Gu, Y., Meletis, K., Huang, Z.J., Ge, S., Enikolopov, G., Deisseroth, K., Luscher, B., Christian, K.M., Ming, G.L., Song, H., 2012. Neuronal circuitry mechanism regulating adult quiescent neural stem-cell fate decision. *Nature* 489, 150–154. <https://doi.org/10.1038/nature11306>
- Spoljaric, I., Spoljaric, A., Mavrovic, M., Seja, P., Puskarjov, M., Kaila, K., 2019. KCC2-Mediated Cl⁻ Extrusion Modulates Spontaneous Hippocampal Network Events in Perinatal Rats and Mice. *Cell Rep.* 26, 1073-1081.e3. <https://doi.org/10.1016/j.celrep.2019.01.011>
- Staley, K.J., Mody, I., 1992. Shunting of excitatory input to dentate gyrus granule cells by a depolarizing GABA(A) receptor-mediated postsynaptic conductance. *J. Neurophysiol.* 68, 197–212. <https://doi.org/10.1152/jn.1992.68.1.197>
- Stein, V., Hermans-Borgmeyer, I., Jentsch, T.J., Hübner, C.A., 2004. Expression of the KCl Cotransporter KCC2 Parallels Neuronal Maturation and the Emergence of Low Intracellular Chloride. *J. Comp. Neurol.* 468, 57–64. <https://doi.org/10.1002/cne.10983>

- Succol, F., Fiumelli, H., Benfenati, F., Cancedda, L., Barberis, A., 2012. Intracellular chloride concentration influences the GABA A receptor subunit composition. *Nat. Commun.* 3, 710–738. <https://doi.org/10.1038/ncomms1744>
- Sulis Sato, S., Artoni, P., Landi, S., Cozzolino, O., Parra, R., Pracucci, E., Trovato, F., Szczurkowska, J., Luin, S., Arosio, D., Beltram, F., Cancedda, L., Kaila, K., Ratto, G.M., 2017. Simultaneous two-photon imaging of intracellular chloride concentration and pH in mouse pyramidal neurons in vivo. *Proc. Natl. Acad. Sci.* 114, E8770–E8779. <https://doi.org/10.1073/pnas.1702861114>
- Sun, C., Zhang, L., Chen, G., 2013. An unexpected role of neuroligin-2 in regulating KCC2 and GABA functional switch. *Mol. Brain* 6, 1–13. <https://doi.org/10.1186/1756-6606-6-23>
- Sun, D., Murali, S.G., 1999. Na⁺ + K⁺ + 2Cl⁻ cotransporter in immature cortical neurons: A role in intracellular Cl⁻ regulation. *J. Neurophysiol.* 81, 1939–1948. <https://doi.org/10.1152/jn.1999.81.4.1939>
- Takesian, A.E., Hensch, T.K., 2013. Balancing plasticity/stability across brain development. *Prog. Brain Res.* 207, 3–34. <https://doi.org/10.1016/B978-0-444-63327-9.00001-1>
- Taketo, M., Yoshioka, T., 2000. Developmental change of GABA(A) receptor-mediated current in rat hippocampus. *Neuroscience* 96, 507–514. [https://doi.org/10.1016/S0306-4522\(99\)00574-6](https://doi.org/10.1016/S0306-4522(99)00574-6)
- Talos, D.M., Sun, H., Kosaras, B., Joseph, A., Folkner, R.D., Poduri, A., Madsen, J.R., Black, P.M., Jensen, F.E., 2012. Altered inhibition in tuberous sclerosis and type IIb cortical dysplasia. *Ann. Neurol.* 71, 539–551. <https://doi.org/10.1002/ana.22696>
- Tang, X., 2020. Neuronal Chloride Transporters in Health and Disease <https://doi.org/10.1016/C2017-0-02771-4>. <https://doi.org/https://doi.org/10.1016/C2017-0-02771-4>
- Tang, X., Kim, J., Zhou, L., Wengert, E., Zhang, L., Wu, Z., Carrameu, C., Muotri, A.R., Marchetto, M.C.N., Gage, F.H., Chen, G., 2016. KCC2 rescues functional deficits in human neurons derived from patients with Rett syndrome. *Proc. Natl. Acad. Sci.* 113, 751–756. <https://doi.org/10.1073/pnas.1524013113>
- Taylor, J., Gordon-Weeks, P., 1991. Calcium-independent gamma-aminobutyric acid release from growth cones: role of gamma-aminobutyric acid transport 56, 273–80.
- Titz, S., Hans, M., Kelsch, W., Lewen, A., Swandulla, D., Misgeld, U., 2003. Hyperpolarizing inhibition develops without trophic support by GABA in cultured rat midbrain neurons. *J. Physiol.* 550, 719–730. <https://doi.org/10.1113/jphysiol.2003.041863>
- Tornberg, J., Voikar, V., Savilahti, H., Rauvala, H., Airaksinen, M.S., 2005. Behavioural phenotypes of hypomorphic KCC2-deficient mice. *Eur. J. Neurosci.* 21, 1327–1337. <https://doi.org/10.1111/j.1460-9568.2005.03959.x>
- Toyoizumi, T., Miyamoto, H., Yazaki-Sugiyama, Y., Atapour, N., Hensch, T.K., Miller, K.D., 2013. A theory of the transition to critical period plasticity: inhibition selectively suppresses spontaneous activity. *Neuron* 80, 51–63. <https://doi.org/10.1016/j.neuron.2013.07.022>
- Tropea, D., Kreiman, G., Lyckman, A., Mukherjee, S., Yu, H., Horng, S., Sur, M., 2006. Gene expression changes and molecular pathways mediating activity-dependent plasticity in visual cortex. *Nat. Neurosci.* 9, 660–668. <https://doi.org/10.1038/nn1689>
- Tyzio, R., Holmes, G.L., Ben-Ari, Y., Khazipov, R., 2007. Timing of the developmental switch in GABA mediated signaling from excitation to inhibition in CA3 rat hippocampus using gramicidin perforated patch and extracellular recordings. *Epilepsia* 48, 96–105. <https://doi.org/10.1111/j.1528-1167.2007.01295.x>

- Tyzio, R., Nardou, R., Ferrari, D., Tsintsadze, T., Shahrokhi, A., Eftekhari, S., Khalilov, I., Tsintsadze, V., Brouchoud, C., Chazal, G., Lemonnier, E., Lozovaya, N., Burnashev, N., Y., B.-A., 2014. Oxytocin-Mediated GABA Inhibition During Delivery Attenuates Autism Pathogenesis in Rodent Offspring. *Science* (80-.). 343, 675–680.
- Uvarov, P., Ludwig, A., Markkanen, M., Pruunsild, P., Kaila, K., Delpire, E., Timmusk, T., Rivera, C., Airaksinen, M., 2007. A novel N-terminal isoform of the neuron-specific K-Cl cotransporter KCC2. *J. Biol. Chem.* 282, 30570–30576.
- Vale, C., Sanes, D.H., 2000. Afferent regulation of inhibitory synaptic transmission in the developing auditory midbrain. *J. Neurosci.* 20, 1912–1921. <https://doi.org/10.1523/jneurosci.20-05-01912.2000>
- Vale, C., Schoorlemmer, J., Sanes, D.H., 2003. Deafness Disrupts Chloride Transporter Function and Inhibitory Synaptic Transmission. *J. Neurosci.* 23, 7416–75224. https://doi.org/10.1007/978-3-642-28753-4_101035
- Valeeva, G., Abdullin, A., Tyzio, R., Skorinkin, A., Nikolski, E., Ben-Ari, Y., Khazipov, R., 2010. Temporal coding at the immature depolarizing gabaergic synapse. *Front. Cell. Neurosci.* 4, 1–12. <https://doi.org/10.3389/fncel.2010.00017>
- Valeeva, G., Tressard, T., Mukhtarov, M., Baude, A., Khazipov, R., 2016. An Optogenetic Approach for Investigation of Excitatory and Inhibitory Network GABA Actions in Mice Expressing Channelrhodopsin-2 in GABAergic Neurons. *J. Neurosci.* 36, 5961–5973. <https://doi.org/10.1523/JNEUROSCI.3482-15.2016>
- van Andel, D.M., Sprengers, J.J., Oranje, B., Scheepers, F.E., Jansen, F.E., Bruining, H., 2020. Effects of bumetanide on neurodevelopmental impairments in patients with tuberous sclerosis complex: an open-label pilot study. *Mol. Autism* 11, 1–14. <https://doi.org/10.1186/s13229-020-00335-4>
- van Rheede, J.J., Richards, B.A., Akerman, C.J., 2015. Sensory-Evoked Spiking Behavior Emerges via an Experience-Dependent Plasticity Mechanism. *Neuron* 87, 1050–1062. <https://doi.org/10.1016/j.neuron.2015.08.021>
- Veerawatananan, B., Surakul, P., Chutabhakdikul, N., 2016. Maternal restraint stress delays maturation of cation-chloride cotransporters and GABAA receptor subunits in the hippocampus of rat pups at puberty. *Neurobiol. Stress* 3, 1–7. <https://doi.org/10.1016/j.yjnstr.2015.12.001>
- Wang, D.D., Kriegstein, A.R., 2011. Blocking early GABA depolarization with bumetanide results in permanent alterations in cortical circuits and sensorimotor gating deficits. *Cereb. Cortex* 21, 574–587. <https://doi.org/10.1093/cercor/bhq124>
- Wang, D.D., Kriegstein, A.R., 2009. Defining the role of GABA in cortical development. *J. Physiol.* 587, 1873–1879. <https://doi.org/10.1113/jphysiol.2008.167635>
- Wang, D.D., Kriegstein, A.R., 2008. GABA Regulates Excitatory Synapse Formation in the Neocortex via NMDA Receptor Activation. *J. Neurosci.* 28, 5547–5558. <https://doi.org/10.1523/JNEUROSCI.5599-07.2008>
- Wehr, M., Zador, A.M., 2003. Balanced inhibition underlies tuning and sharpens spike timing in auditory cortex. *Nature* 426, 442–446. <https://doi.org/10.1038/nature02116>
- Weitlauf, A.S., Sathe, N.A., McPheeters, M.L., Warren, Z., 2017. Interventions Targeting Sensory Challenges in Children With Autism Spectrum Disorder - An Update. *Comp. Eff. Rev.* 186. <https://doi.org/10.23970/AHRQEPCCER186>
- Wells, J.E., Porter, J.T., Agmon, A., 2000. GABAergic inhibition suppresses paroxysmal network activity in the neonatal rodent hippocampus and neocortex. *J. Neurosci.* 20, 8822–8830. <https://doi.org/10.1523/jneurosci.20-23-08822.2000>

- Woo, N., Lu, J., England, R., McClellan, R., Dufour, S., Mount, D., Deutch, A., Lovinger, D., Delpire, E., 2002. Hyperexcitability and epilepsy associated with disruption of the mouse neuronal-specific K-Cl cotransporter gene. *Hippocampus* 12, 258–268.
- Woodward, R.M., Polenzani, L., Miledi, R., 1993. Characterization of bicuculline/baclofen-insensitive (π -like) γ -aminobutyric acid receptors expressed in *Xenopus* oocytes. II. Pharmacology of γ -aminobutyric acid(A) and γ -aminobutyric acid(B) receptor agonists and antagonists. *Mol. Pharmacol.* 43, 609–625.
- Wright, R., Newey, S.E., Ilie, A., Wefelmeyer, W., Raimondo, J. V., Ginham, R., McIlhinney, R.A.J., Akerman, C.J., 2017. Neuronal Chloride Regulation via KCC2 Is Modulated through a GABA B Receptor Protein Complex. *J. Neurosci.* 37, 5447–5462. <https://doi.org/10.1523/JNEUROSCI.2164-16.2017>
- Wu, G.-Y., Malinow, R., Cline, H.T., 1996. Maturation of a central glutamatergic synapse. *Science* (80-.). 274, 972–976. <https://doi.org/10.1126/science.274.5289.972>
- Yamada, J., Okabe, A., Toyoda, H., Kilb, W., Luhmann, H., Fukuda, A., 2004. Cl⁻ uptake promoting depolarizing GABA actions in immature rat neocortical neurones is mediated by NKCC1. *J. Physiol.* 557, 829–841.
- Yamanaka, R., Shindo, Y., Hotta, K., Suzuki, K., Oka, K., 2018. GABA-Induced Intracellular Mg²⁺ Mobilization Integrates and Coordinates Cellular Information Processing for the Maturation of Neural Networks. *Curr. Biol.* 28, 3984–3991.e5. <https://doi.org/10.1016/j.cub.2018.10.044>
- Yan, Y., Dempsey, R.J., Sun, D., 2001. Expression of Na⁺-K⁺-Cl⁻ cotransporter in rat brain during development and its localization in mature astrocytes. *Brain Res.* 911, 43–55. [https://doi.org/10.1016/S0006-8993\(01\)02649-X](https://doi.org/10.1016/S0006-8993(01)02649-X)
- Yang, J., Siao, C.J., Nagappan, G., Marinic, T., Jing, D., McGrath, K., Chen, Z.Y., Mark, W., Tessarollo, L., Lee, F.S., Lu, B., Hempstead, B.L., 2009. Neuronal release of proBDNF. *Nat. Neurosci.* 12, 113–115. <https://doi.org/10.1038/nn.2244>
- Yang, J.W., Reyes-Puerta, V., Kilb, W., Luhmann, H.J., 2016. Spindle Bursts in Neonatal Rat Cerebral Cortex. *Neural Plast.* 2016, 3467832. <https://doi.org/10.1155/2016/3467832>
- Zhang, L., Huang, C.C., Dai, Y., Luo, Q., Ji, Y., Wang, K., Deng, S., Yu, J., Xu, M., Du, X., Tang, Y., Shen, C., Feng, J., Sahakian, B.J., Lin, C.P., Li, F., 2020. Symptom improvement in children with autism spectrum disorder following bumetanide administration is associated with decreased GABA/glutamate ratios. *Transl. Psychiatry* 10, 9. <https://doi.org/10.1038/s41398-020-0692-2>



3

Using SuperClomeleon to measure changes in intracellular chloride during development and after early life stress

L.J. Herstel^{1,*}, C. Peerboom^{1,*}, S. Uijtewaal¹, D. Selemangel¹, H. Karst² and C.J. Wierenga^{1,3}

* equal contribution

¹ Cell Biology, Neurobiology and Biophysics, Biology Department, Utrecht University, 3584 CH, Utrecht, The Netherlands.

² Utrecht Brain Center, University Medical Center Utrecht, 3584 CX, Utrecht, The Netherlands.

³ Current address: Faculty of Science & Donders Institute, Radboud University, 6525 AJ, Nijmegen, the Netherlands

This chapter has been published in eNeuro 2022, 9 (6), doi: 10.1523/ENEURO.0416-22.2022.

3.1 Abstract

Intraneuronal chloride concentrations ($[Cl^-]_i$) decrease during development resulting in a shift from depolarizing to hyperpolarizing γ -aminobutyric acid (GABA) responses via chloride-permeable GABA_A receptors. This GABA shift plays a pivotal role in postnatal brain development, and can be strongly influenced by early life experience. Here, we assessed the applicability of the recently developed fluorescent SuperClomeleon (SCLm) sensor to examine changes in $[Cl^-]_i$ using two-photon microscopy in brain slices. We used SCLm mice of both sexes to monitor the developmental decrease in neuronal chloride levels in organotypic hippocampal cultures. We could discern a clear reduction in $[Cl^-]_i$ between DIV3 and DIV9 (equivalent to the second postnatal week *in vivo*) and a further decrease in some cells until DIV22. In addition, we assessed alterations in $[Cl^-]_i$ in the medial prefrontal cortex (mPFC) of P9 male SCLm mouse pups after early life stress (ELS). ELS was induced by limiting nesting material between P2 and P9. ELS induced a shift towards higher (i.e. immature) chloride levels in layer 2/3 cells in the mPFC. Although conversion from SCLm fluorescence to absolute chloride concentrations proved difficult, our study underscores that the SCLm sensor is a powerful tool to measure physiological changes in $[Cl^-]_i$ in brain slices.

3.2 Significance Statement

The reduction of intraneuronal chloride concentrations is crucial for brain development, as it ensures a shift from the initial excitatory action of the neurotransmitter GABA in immature neurons to the inhibitory GABA signaling in the adult brain. Despite the significance of chloride maturation, it has been difficult to study this phenomenon in experiments. Recent development of chloride sensors enable direct imaging of intracellular chloride signaling in neurons. Here we assessed the applicability of the SuperClomeleon chloride sensor to measure physiologically relevant changes in chloride levels using two-photon microscopy in cultured and acute brain slices. Although we also point out some limitations, we conclude that the SuperClomeleon sensor is a powerful tool to measure physiological changes in intracellular chloride.

3.3 Introduction

During normal neuronal development, γ -aminobutyric acid (GABA) responses through ionotropic GABA_A receptors shift from depolarizing to hyperpolarizing as a result of the developmental decrease in intracellular chloride concentration. In the immature brain, the intracellular chloride concentration is high and activation of GABA_A receptors results in an outflow of chloride leading to membrane depolarization. During early postnatal development, intracellular chloride levels gradually decrease. As a result, activation of GABA_A receptors in mature neurons leads to the influx of chloride and GABAergic signaling induces membrane hyperpolarization (Rivera et al., 1999; Ben-Ari et al., 2007; Kaila et al., 2014). This shift in GABA signaling plays a pivotal role in postnatal neuronal development and its timing affects brain function throughout life (Sernagor et al., 2010; Kaila et al., 2014; Lohmann and Kessels, 2014; Peerboom and Wierenga, 2021).

In rodents the GABA shift occurs normally between postnatal day (P)10 and 14 depending on brain region and cell type (Rivera et al., 1999; Stein et al., 2004; Ben-Ari et al., 2007; Romo-Parra et al., 2008; Glykys et al., 2009; Kirmse et al., 2015; Sulis Sato et al., 2017). For example, intracellular chloride levels in the visual cortex mature several days earlier compared to the hippocampus (Murata and Colonnese, 2020), while in the prefrontal cortex the GABA shift occurs even later (Amadeo et al., 2018; Karst et al., 2019). In addition, GABAergic maturation has been shown to be strongly influenced by experiences during early life. For instance, prenatal maternal restraint stress as well as repeated separations of newborn pups from their mother induced a delay in the GABA shift in hippocampal pyramidal cells in young mice (Veerawatananan et al., 2016; Furukawa et al., 2017; Hu et al., 2017b). Early life stress (ELS) has life-long consequences on neurophysiology and behavior in both humans and rodents and poses an increased risk for psychopathology later in life (Teicher et al., 2016; Joëls et al., 2018). The medial prefrontal cortex (mPFC) is known to be very sensitive to stress early in life, with life-long consequences for anxiety and stress responses (Ishikawa et al., 2015; Karst et al., 2020). The mPFC functions as a central coordinator of stress responses across brain regions as well as the periphery (McKlveen et al., 2015). However, it is currently unclear how GABA signaling in the mPFC is affected by ELS.

In most studies intracellular chloride concentrations in neurons are determined using perforated patch clamp recordings. With this technique antibiotics (e.g. gramicidin or amphotericin B) are included in the pipette to form small pores in the membrane which leaves intracellular chloride concentration intact. However, perforated patch clamp recordings are time intensive and it is difficult to perform long recordings, as access is not stable (Arosio et al., 2010). In addition, large individual differences can exist between neurons and many individual recordings may be required to get a good population estimate (Tyzio et al., 2007; Sulis Sato et al., 2017). As a promising

alternative, biosensors are being developed which allow for the real time measurement of intracellular chloride levels in a noninvasive manner (Arosio et al., 2010). The SuperClomeleon (SCLm) sensor (Grimley et al., 2013) is a second generation chloride sensor with chloride sensitivity in the physiological range. The SCLm sensor consists of two fluorescent proteins, Cerulean (CFP mutant) and Topaz (YFP mutant), joined by a flexible linker. Depending on the binding of chloride, Fluorescence Resonance Energy Transfer (FRET) occurs from the CFP donor to the YFP acceptor (Grimley et al., 2013). FRET ratios (fluorescence intensity of YFP/CFP) are independent of expression level and imaging settings, which is a major advantage when imaging in intact brain tissue. The SCLm sensor has successfully been used to determine the steady-state intracellular chloride concentration in adult mice *in vivo* (Boffi et al., 2018) and to demonstrate the existence of cytoplasmic chloride microdomains in neurons (Rahmati et al., 2021), but it has not been used to examine chloride maturation during neuronal development.

Here, we used the SCLm sensor to detect changes in chloride during early postnatal development in organotypic hippocampal cultures of mice and in acute slices of the prefrontal cortex from young control mice and mice who experienced ELS.

3.4 Methods

Animals

SuperClomeleon^{lox/-} mice (Rahmati et al., 2021) (a gift from Kevin Staley, Massachusetts General Hospital, Boston, MA) were crossed with CamKII α ^{Cre/-} mice (Tsien et al., 1996; Casanova et al., 2001) (a gift from Stefan Berger, German Cancer Research Center, Heidelberg, Germany) and will hereafter be referred to as SCLm mice. Animals were housed at reversed day-night cycle with a room temperature of 22 ± 2 °C and humidity of approximately 65%. Food (standard chow) and water were provided *ad libitum*. We noticed that SCLm mice had poor breeding performance compared to other strains kept in the same facility. On postnatal day (P) 2 the litter was randomly assigned to either the control condition (standard housing) or the ELS condition. In the ELS condition a limited amount of nesting and bedding material was made available between P2 and P9 (Rice et al., 2008; Naninck et al., 2015; Karst et al., 2020). All animal experiments were performed in compliance with the guidelines for the welfare of experimental animals and were approved by the local authorities.

Organotypic culture preparation

Postnatal developmental changes in intracellular chloride concentration ($[Cl^-]_i$) were imaged in organotypic hippocampal cultures made from P6 control SCLm mice of both sexes. For the chloride calibration and wash-in experiments, organotypic hippocampal cultures were made from P6 WT C57BL/6 mice and SCLm expression was achieved by viral injection. Slice cultures were prepared using a method based on Stoppini *et al.* (1991). After decapitation the brain was rapidly removed and placed in ice-cold Gey's

Balanced Salt Solution (GBSS; containing (in mM): 137 NaCl, 5 KCl, 1.5 CaCl₂, 1 MgCl₂, 0.3 MgSO₄, 0.2 KH₂PO₄ and 0.85 Na₂HPO₄) with 25 mM glucose, 12.5 mM HEPES and 1 mM kynurenic acid. Transverse hippocampal slices of 400 μm thick were cut with a McIlwain tissue chopper (Brinkmann Instruments). Slices were placed on Millicell membrane inserts (Millipore) in wells containing 1 mL culture medium (consisting of 48% MEM, 25% HBSS, 25% horse serum, 25 mM glucose, and 12.5 mM HEPES, with an osmolarity of 325 mOsm and a pH of 7.3 – 7.4). Slices were stored in an incubator (35°C with 5% CO₂) and medium was replaced three times a week. Experiments were performed after 1 to 22 days in vitro (DIV).

Viral expression

An adeno-associated virus (AAV) with Cre-independent expression of SCLM under the control of the Synapsin promoter (AAV9.hSyn.sCLM; a gift from Kevin Staley, Massachusetts General Hospital, Boston, MA) was injected in the CA1 area of WT cultured hippocampal slices on DIV1. Slices were imaged on DIV9-16. Compared to slices from SCLM mice, viral expression of the SCLM sensor resulted in larger variability in neuronal FRET (YFP/CFP) ratios, probably due to variability in slice quality and viral expression levels. We optimized the viral concentration to get comparable levels of YFP and CFP fluorescent intensity as observed in the mouse line.

Acute slice preparation

Young SCLM mice were decapitated at P9, followed by quick removal of the brain. For this study we used only male mice to allow direct comparison with our earlier study in C57/BL6 mice (Karst et al., 2019). Mice were always decapitated in the morning to eliminate influences of fluctuating corticosterone (CORT) levels during the day, due to the reversed day-night cycle this means that CORT levels are high at that time. The brain was stored in ice cold artificial cerebrospinal fluid (ACSF, containing (in mM): 120 choline chloride, 3.5 KCl, 0.5 CaCl₂, 6 MgSO₄, 1.25 NaH₂PO₄, 25 D-glucose and 25 NaHCO₃). Coronal slices of 350 μm thickness were made with a vibratome (Leica VT 1000S). After placing them in ACSF (consisting of (in mM): 120 NaCl, 3.5 KCl, 1.3 MgSO₄, 1.25 NaH₂PO₄, 2.5 CaCl₂, 25 D-glucose and 25 NaHCO₃) slices were heat shocked at 32°C for 20 min. Slices were then kept at room temperature and after recovery for at least 1 h, transported individually in Eppendorf tubes filled with ACSF to the microscope room in another building with a transportation time of 10 minutes.

Two-photon imaging

Slices were transferred to the microscope chamber. The bath was continuously perfused with carbonated (95% O₂, 5% CO₂) ACSF (in mM: 126 NaCl, 3 KCl, 2.5 CaCl₂, 1.3 MgCl₂, 26 NaHCO₃, 1.25 NaH₂PO₄, 20 D-glucose and 1 Trolox, with an osmolarity of 310 ± 10 mOsm/L) at a rate of approximately 1 mL/min. Bath temperature was monitored and maintained at 30–32 °C throughout the experiment. Two-photon imaging of pyramidal neurons in layer 2/3 of the mPFC or pyramidal neurons in the

CA1 area of the hippocampus was performed on a customized two-photon laser scanning microscope (Femto3D-RC, Femtonics, Budapest, Hungary). To excite the CFP donor, a Ti-Sapphire femtosecond pulsed laser (MaiTai HP, Spectra-Physics) was tuned to 840 nm. The emission signal was split using a dichroic beam splitter at 505 nm and detected using two GaAsP photomultiplier tubes. We collected fluorescence emission of Cerulean/CFP (485 ± 15 nm) and Topaz/YFP (535 ± 15 nm) in parallel. A 60x water immersion objective (Nikon NIR Apochromat; NA 1.0) was used to locate the cell layer. Of each slice, 2-4 image z-stacks in different field of views (FOVs) were acquired at a resolution of 8.1 pixels/ μm (1024x1024 pixels, 126x126 μm) with 1 μm steps of approximately 40-85 μm in depth. To monitor acute changes in $[\text{Cl}^-]_i$, we bath applied GABA_A receptor agonist muscimol (Tocris, 10 μM) and imaged at lower resolution (every 2 minutes at a resolution of 4.1 pixels/ μm (512x512 pixels, 126x126 μm) with 1 μm steps of 30-50 μm in depth).

Imaging data analysis

Image analysis was performed using Fiji/ImageJ software and results were analyzed in Prism 9 (GraphPad). We manually determined regions of interest (ROIs) around individual neuron somata. To analyze a representative cell population, in each image z-stack we selected four z-planes at comparable depths in which three cells were identified that varied in brightness (bright, middle and dark). We subtracted the mean fluorescence intensity of the background in the same image plane from the mean fluorescence intensity of CFP and YFP before calculating the fluorescence ratio. We limited our analysis to cells which were located within 450 pixels from the center of the image, as FRET ratios showed slight aberrations at the edge of our images. We excluded cells with a FRET ratio < 0.5 or > 1.6 , to avoid the selection of unhealthy cells (59 of 1893 cells; 3.1%). We verified that inclusion of these cells did not change our conclusions. We confirmed that the FRET ratios of individual cells were uncorrelated with their fluorescence intensities (data not shown).

FRET-colored images (as shown in Fig. 1C, 2D, 3A and 4A) were made in ImageJ. We first subtracted the average background and Gaussian filtered the CFP and YFP image z-stacks separately. Next, the acceptor (YFP) image was divided by the donor (CFP) image to get the ratiometric image. A mask was created by manually drawing ROIs for each soma in the image. An average projection of the ratiometric image was made of a specific z range and multiplied by the mask. Finally, the masked ratiometric image was combined with the grayscale image. Please note that these images were made for illustration purposes only, analysis was done on the raw data.

SCLm sensor calibration

Calibrations for chloride were performed as described before (Grimley et al., 2013; Boffi et al., 2018; Rahmati et al., 2021). As SCLm mice were no longer available we used organotypic hippocampal cultures from WT mice expressing the SCLm sensor. Cultured slices were treated with ionophores (100 μM nigericin and 50 μM tributyltin acetate,

Merck) to clamp $[Cl^-]_i$ and intracellular pH to extracellular levels. Saline containing various $[Cl^-]_i$ were perfused at approximately 1 mL/min. High chloride solution consisted of (in mM): 105 KCl, 48 NaCl, 10 HEPES, 20 D-glucose, 2 Na-EGTA, and 4 $MgCl_2$, whereas the solution without chloride contained (in mM): 105 K-gluconate, 48 Na-gluconate, 10 HEPES, 20 D-glucose, 2 Na-EGTA and 4 $Mg(gluconate)_2$. The high extracellular K^+ concentrations are necessary for proper functioning of nigericin (Pressman and Fahim, 1982). Intermediate $[Cl^-]_i$ solutions (0, 5, 10, 50 and 100 mM) were prepared by mixing the two solutions. To maximally quench the SClm sensor we used a KF solution containing (in mM): 105 KF, 48 NaF, 10 HEPES, 20 D-glucose, 2 Na-EGTA and 4 $Mg(gluconate)_2$. All calibration solutions were adjusted to pH 7.4. The first calibration solution with ionophores was washed in for 20 minutes and subsequent calibration solutions with ionophores were washed in for 15 minutes. Image z-stacks were acquired every 3 minutes at a resolution of 4.1 pixels/ μm (512x512 pixels, 126x126 μm) with 1 μm steps of 30-50 μm in depth. FRET ratios reached a plateau after 10 minutes of wash in, which we assumed reflected equal intracellular and extracellular chloride concentrations. We constructed the calibration curve by plotting measured FRET ratios against extracellular chloride concentrations.

However, we noticed that FRET ratios differed widely between experiments, especially at intermediate chloride levels (5-10 mM). As this severely impaired robustness of the calibration in the most relevant chloride range, we resorted to perforated patch clamp measurements to calibrate the SClm sensor within the physiological range. We performed perforated patch clamp recordings in organotypic hippocampal cultures to determine $[Cl^-]_i$ in CA1 pyramidal cells at DIV1-3, DIV8-10 and DIV20-22 (described below). We plotted the average $[Cl^-]_i$ values against the average FRET ratios measured in cells at the same DIVs and added these data to the calibration data from the ionophores. We fitted this composite calibration curve (Fig. 1D) with the following relation between FRET ratios and $[Cl^-]_i$ (Grimley et al., 2013; Boffi et al., 2018; Rahmati et al., 2021):

$$[Cl^-]_i = K_d * \left(\frac{R_{max} - R}{R - R_{min}} \right) \quad (1)$$

(in which R is the YFP/CFP emission ratio), to obtain the dissociation constant K_d and the minimum and maximum FRET ratio R_{min} and R_{max} for our measurements.

Electrophysiology

Whole-cell patch clamp recordings were made of pyramidal neurons in the hippocampal CA1 or mPFC of acute slices from SClm mice. Recording pipettes (resistance of 4-6 $M\Omega$) were pulled from thick-walled borosilicate glass capillaries (World Precision Instruments) and filled with high chloride internal solution (in mM: 70 K-gluconate, 70 KCl, 0.5 EGTA, 10 HEPES, 4 MgATP, 0.4 NaGTP, 4 Na_2 -Phosphocreatine

with pH 7.3 and osmolarity 295 mOsm/L). Cells were kept at a holding potential of -60 mV in voltage clamp throughout the experiment.

Perforated patch clamp recordings were made from CA1 pyramidal neurons in cultured hippocampal slices from WT mice at 30-32 °C. Recording pipettes (resistance of 2-4 MΩ) were pulled from thick-walled borosilicate glass capillaries (World Precision Instruments). The pipette tip was filled with gramicidin-free KCl solution (140 mM KCl and 10 mM HEPES, pH 7.2, and osmolarity 285 mOsm/L) and then backfilled with the KCl solution containing gramicidin (60 µg/ml, Sigma). CA1 neurons were clamped at -65 mV and the access resistance of the perforated cells was monitored constantly before and during recordings. An access resistance of 50 MΩ was considered acceptable to start recording. GABAergic currents were evoked by puffs of 50 µM muscimol (Tocris) dissolved in HEPES-buffered ACSF (in mM: 135 NaCl, 3 KCl, 2.5 CaCl₂, 1.3 MgCl₂, 1.25 Na₂H₂PO₄, 20 Glucose, and 10 HEPES) in the presence of 1 µM TTX (Abcam). To determine the reversal potential of chloride, GABAergic currents were recorded at a holding potentials between -100 mV and -30 mV in 10 mV steps, upon local somatic application of the GABA_A receptor agonist muscimol (50 µM) dissolved in HEPES-buffered ACSF every 30s using a Picospritzer II. The GABA reversal potential was determined from the intersection of the current-voltage curve with the x-axis. We assumed that the chloride reversal potential E_{Cl} equals the GABA reversal potential and used the Nernst equation to determine neuronal chloride concentrations:

$$E_{Cl} = -\frac{RT}{zF} \ln \frac{[Cl^-]_o}{[Cl^-]_i} = -0.0263 \ln \frac{[Cl^-]_o}{[Cl^-]_i} \quad (2)$$

(with $[Cl^-]_o = 136.6$ mM in ACSF) to convert the measured reversal potentials to estimated $[Cl^-]_i$. We are aware that GABA_A channels are also permeable for HCO₃⁻ ions (Bormann et al., 1987; Kaila et al., 1993; Kaila, 1994). By assuming that E_{Cl} equals the GABA reversal potential, we will slightly overestimate $[Cl^-]_i$.

Statistical analysis

Statistical analysis was performed with Prism 9 (GraphPad). Normality was tested using Shapiro-Wilk tests. For unpaired samples statistical significance was evaluated using the unpaired Student's t test (T test) for normally distributed data points, or the non-parametric Mann-Whitney (MW) test otherwise. A one-way ANOVA (or the Kruskal-Wallis (KW) test for non-normal distributions) was used when more than two groups were compared. Cumulative distributions were tested with the Kolmogorov-Smirnov (KS) test. Simple linear regression analysis was used to test if FRET ratios were influenced by the depth of the soma in the slice. $P < 0.05$ was considered significant. All data is presented as mean ± SEM.

3.5 Results

Two-photon imaging of $[Cl^-]_i$

To quantify the neuronal chloride concentration, SClm expression was targeted to pyramidal neurons by crossing SuperClomeleon^{lox/-} mice (Rahmati et al., 2021) with transgenic mice in which Cre recombinase expression was driven by the calcium/calmodulin-dependent protein kinase II alpha (CamKIIa) promoter (Tsien et al., 1996; Casanova et al., 2001). CaMKIIa is mostly expressed by excitatory neurons (Sík et al., 1998) and by some glia cells (Pylayeva-Gupta, 2011). In our slices from young mice, we observed many pyramidal neurons in the hippocampus and prefrontal cortex expressing the SClm sensor (Fig 1A). It is expected that ~35% of the neurons in the adult cortex and ~70% of the neurons in the adult hippocampus express CamKIIa (Wang et al., 2013). In our slices, the fraction of SClm cells is expected to be slightly lower, because CamKIIa expression still increases between P3 and P15 (Casanova et al., 2001).

The optogenetic SClm sensor consists of two fluorescent proteins, Cerulean (CFP mutant) and Topaz (YFP mutant), joined by a flexible linker (Fig. 1B). Binding of chloride to YFP reduces the FRET from the donor CFP to the YFP acceptor (Grimley et al., 2013; Arosio and Ratto, 2014). We used two-photon fluorescence microscopy to measure the 530 nm/480 nm (YFP/CFP) emission ratio (hereafter: FRET ratio) of individual cells. We calibrated measured FRET ratios against different $[Cl^-]_i$ using a combination of perforated patch recordings and ionophore treatment (Fig. 1C,D; see methods for details). Fitting this curve with equation (1) yielded a K_d value of 24.6 mM (Fig. 1D), which is in good agreement with previous reports (Grimley et al., 2013; Rahmati et al., 2021). The range of values for R_{max} measured in different calibration experiments was between 1.30 and 1.82. R_{min} ranged between 0.38 and 0.48. We used this fit to convert measured FRET ratios into $[Cl^-]_i$, for all our experiments, but we are aware that these should be considered reasonable estimates of the actual intracellular chloride levels at best.

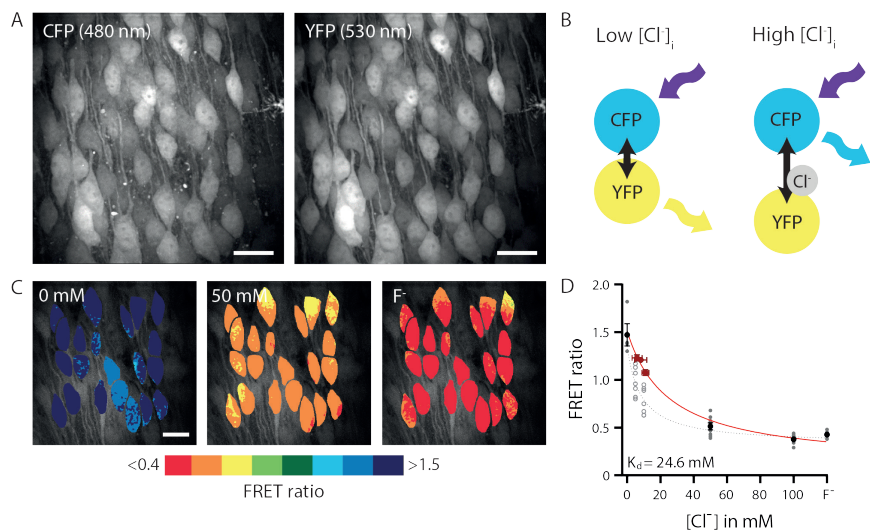


Figure 1. Two-photon imaging of $[Cl^-]_i$ in brain slices.

A) Example image of CFP (480 nm) and YFP (530 nm) fluorescence in an organotypic hippocampal culture from a SCLm mouse. Scale bar: 20 μ m.

B) Illustration of Fluorescence Resonance Energy Transfer (FRET) from CFP donor to YFP acceptor of the SCLm sensor. FRET values (YFP/CFP fluorescence ratio) decrease with higher chloride concentrations.

C) Two-photon imaging of chloride-dependent changes in the FRET ratio (530/480 nm emission) in a WT organotypic hippocampal culture with AAV SCLm expression. $[Cl^-]_i$ was clamped to the indicated external chloride concentration via ionophore treatment. Individual cells are color-coded to their FRET ratios. Scale bar: 20 μ m.

D) Calibration curve constructed from ionophore experiments (black/grey symbols) and perforated patch (red symbols) data. Data is presented as mean \pm SEM. These data were fit by equation (2), yielding the following fit parameters: $K_d = 24.6$ mM, $R_{max} = 1.51$, $R_{min} = 0.12$ (red curve; see methods for details). This calibration curve was used to convert FRET ratios into estimated chloride levels in the rest of this study.

We also show the individual data points representing individual ionophore experiments (average over 12 cells per experiment). At 5 and 10 mM extracellular chloride FRET values were highly variable (open symbols). As described in the methods, we excluded these data points from our analysis and resorted to perforated patch recordings (red symbols) for this chloride range. The grey dotted line shows the alternative calibration curve when all ionophore data are included (fit parameters $K_d = 8.4$; $R_{max} = 1.35$; $R_{min} = 0.32$; without perforated patch data). Electrophysiology data from 11 cells (DIV1-3), 9 cells (DIV8-10) and 13 cells (DIV20-22); SCLm data from 8 slices.

Acute manipulation of $[Cl^-]_i$ in brain slices

To assess the responsiveness of the SClm sensor to changes in intracellular chloride, we patched a pyramidal neuron in an acute hippocampal slice with a high concentration of chloride in the patch pipette, while monitoring changes in SClm FRET ratios. The FRET ratio in the patched cell changed immediately after break-in due to the rapid influx of chloride (Fig 2A,B). This decrease in FRET ratio was not observed in neighboring cells in the same field of view (Fig 2C). In a separate set of experiments, we monitored changes in FRET ratios during wash-in of muscimol, a specific GABA_A receptor agonist. As GABA_A receptors are chloride channels, activation of GABA_A receptors will induce influx of chloride ions, and therefore result in an increase in $[Cl^-]_i$. We observed a rapid 20% decrease in FRET ratio (indicating a 5-10 mM change in $[Cl^-]_i$) upon administration of muscimol, caused by the cellular influx of chloride (Fig 2D,E). These experiments demonstrate that the SClm sensor reliably reports rapid changes in neuronal $[Cl^-]_i$ within the physiological range.

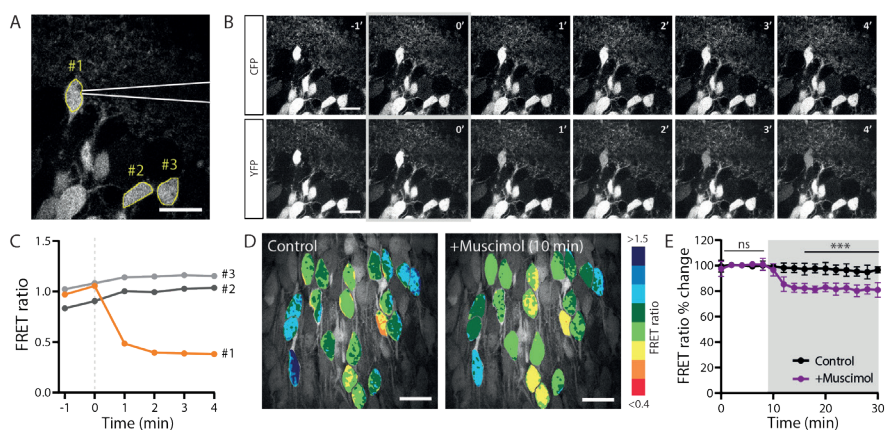


Figure 2. Monitoring acute changes in $[Cl^-]_i$ with SClm.

A) Two-photon image of CA1 pyramidal neurons in the hippocampus of an acute slice from a SClm mouse. A patch pipette (in white) is attached to cell #1 for a whole-cell recording. Two control cells are indicated with #2 and #3. Scale bar: 20 μ m.

B) Time course of CFP (upper row) and YFP (lower row) fluorescence right before and during the first minutes after break-in. After break-in (0'; gray) cell #1 rapidly fills with the high chloride internal solution (70 mM KCl) resulting in a decrease in YFP fluorescence. Scale bar: 20 μ m.

C) FRET ratio over time for cells that were infused with 70 mM KCl and neighboring controls.

D) Acute wash-in with muscimol in cultured slices with viral SClm expression, caused a decrease in FRET ratio in CA1 pyramidal neurons within 10 minutes. Scale bar: 20 μ m.

E) Average FRET ratios over time during wash-in of muscimol (grey area) and control. Data from 84 cells, 7 slices, 4 mice in both groups.

Development of neuronal $[Cl^-]_i$ levels in organotypic cultures

Next, we imaged neuronal $[Cl^-]_i$ levels in cultured hippocampal slices at different developmental stages. FRET ratios were determined at DIV2-3, DIV8-10 and DIV20-21 (Fig 3A). We observed a clear increase in FRET ratios, corresponding with a decrease in $[Cl^-]_i$, between DIV2-3 and DIV8-10 (Fig 3B,C). Although the average FRET ratio was very similar at DIV20-21 and DIV 8-10, the fraction of cells with high FRET ratios appeared larger at DIV20-21 (Fig 3D), suggesting that chloride levels in some neurons were still decreasing at this age. FRET ratios were not dependent on the depth of the somata in the slice (Fig 3E-G). This indicates that cell-to-cell differences were not due to their location in the slice and we also confirmed that FRET values are independent of fluorescence intensity (data not shown). Our results show that the GABA shift continues in organotypic hippocampal cultures during the first two weeks *in vitro*.

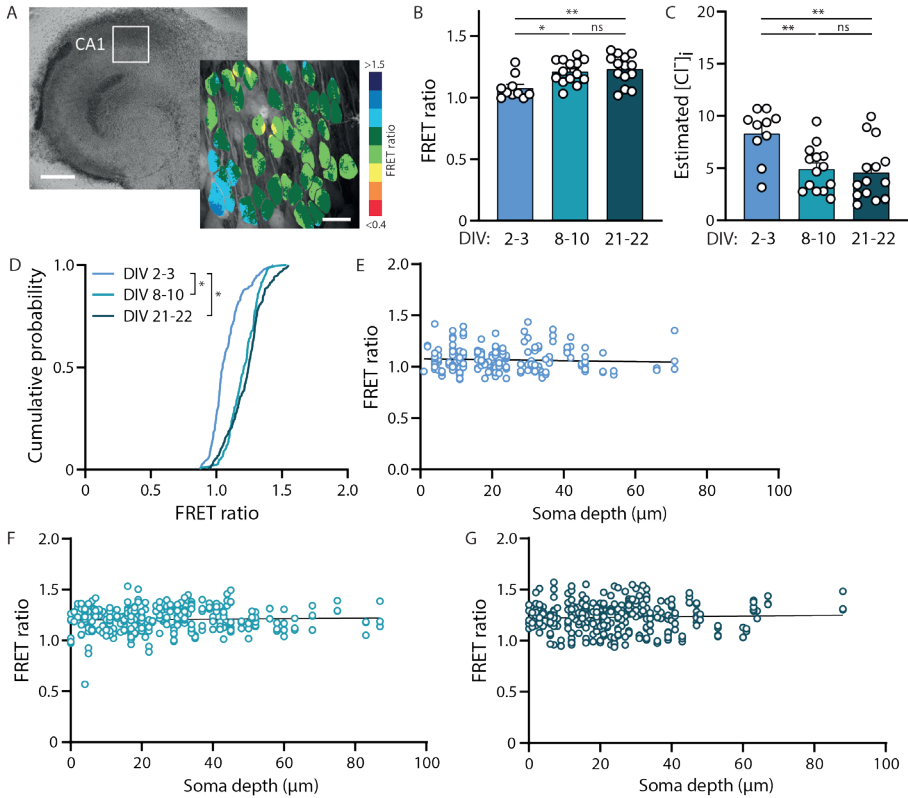


Figure 3. Developmental decrease in $[Cl^-]_i$ continues in organotypic cultures.

A) Example of an organotypic hippocampal culture from a SClm mouse at DIV8. Scale bar: 500 μ m. In the zoom an example of the FRET ratios determined in the CA1 area. Scale bar: 20 μ m.

B) Average FRET ratios of CA1 pyramidal cells at DIV2-3 ($n = 10$ slices of 6 mice), DIV8-10 ($n = 14$ slices of 8 mice) and DIV21-22 ($n = 14$ slices of 8 mice). There was a significant increase in FRET ratio over time ($p = 0.033$ DIV2-3 vs DIV8-10; $p = 0.008$ DIV2-3 vs DIV21-22; $p > 0.99$ DIV8-10 vs DIV21-22; KW test).

C) Average estimated $[Cl^-]_i$ as calculated from the FRET ratios in B. There was a significant decrease in $[Cl^-]_i$ over time ($p = 0.006$ DIV2-3 vs DIV8-10; $p = 0.003$ DIV2-3 vs DIV21-22; $p = 0.93$ DIV8-10 vs DIV21-22; one-way ANOVA).

D) Cumulative distribution of FRET ratios for individual cells at the 3 time points. For each slice 15 cells were randomly selected, making the total of number of plotted cells per condition at least 150 ($p < 0.001$ DIV2-3 vs. DIV8-10 and vs. DIV21-22; $p = 0.053$ DIV8-10 vs. DIV21-22; KS test).

E) Individual FRET ratios plotted against soma depth in slices at DIV2-3 ($n = 186$ neurons). Line represents linear regression fit ($r = 0.004$; $p = 0.41$).

F) Same as E at DIV8-10 ($n = 299$ neurons). Line represents linear regression fit ($r = 0.002$; $p = 0.48$).

G) Same as E at DIV21-22 ($n = 314$ neurons). Line represents linear regression fit ($r = 0.001$; $p = 0.50$).

Early life stress elevates neuronal $[Cl^-]_i$ at P9

We then used the SClm sensor to detect changes in intracellular chloride levels over development in the prefrontal cortex in young mice after ELS. To induce ELS in young mice, we provided a limited amount of nesting and bedding material to the mothers between P2 and P9, resulting in fragmented and unpredictable maternal care (Rice et al., 2008; Naninck et al., 2015; Karst et al., 2020). To examine if this early life experience affected chloride maturation in the young pups, we measured FRET ratios in layer 2/3 neurons in acute slices from the mPFC from control and ELS male mice at P9, immediately after the stress period (Fig 4A). In total, 443 and 470 neurons were included in the analysis obtained from 7 control and 7 ELS mice, respectively. As expected, average $[Cl^-]_i$ levels were higher in mPFC compared to hippocampal pyramidal cells at comparable age (~17.3 mM in P9 mPFC slices (Fig. 4C) to ~11.5 mM in DIV2-3 cultured hippocampal slices (Fig. 3C)). This likely reflects the delayed maturation of the PFC compared to the hippocampus (Amadeo et al., 2018; Karst et al., 2019). Average FRET ratios in layer 2/3 pyramidal cells in slices from SClm mice that experienced ELS were slightly lower compared to control, but this difference was not significant when comparing average FRET ratios per mouse (Fig 4B,C). However, when we analyzed the distribution of FRET ratios in individual cells, we observed a significant shift towards more cells with a lower FRET ratio in the ELS condition (Fig 4D). A small dependence of FRET ratio on soma depth was found for both conditions in acute prefrontal slices (Fig 4E,F). As this was different from our observations in slice cultures (Fig. 3E-G), we suspect it may reflect surface damage from slicing. Together our results show that ELS leads to an increase in neurons with high, immature chloride levels at P9 compared to control mice.

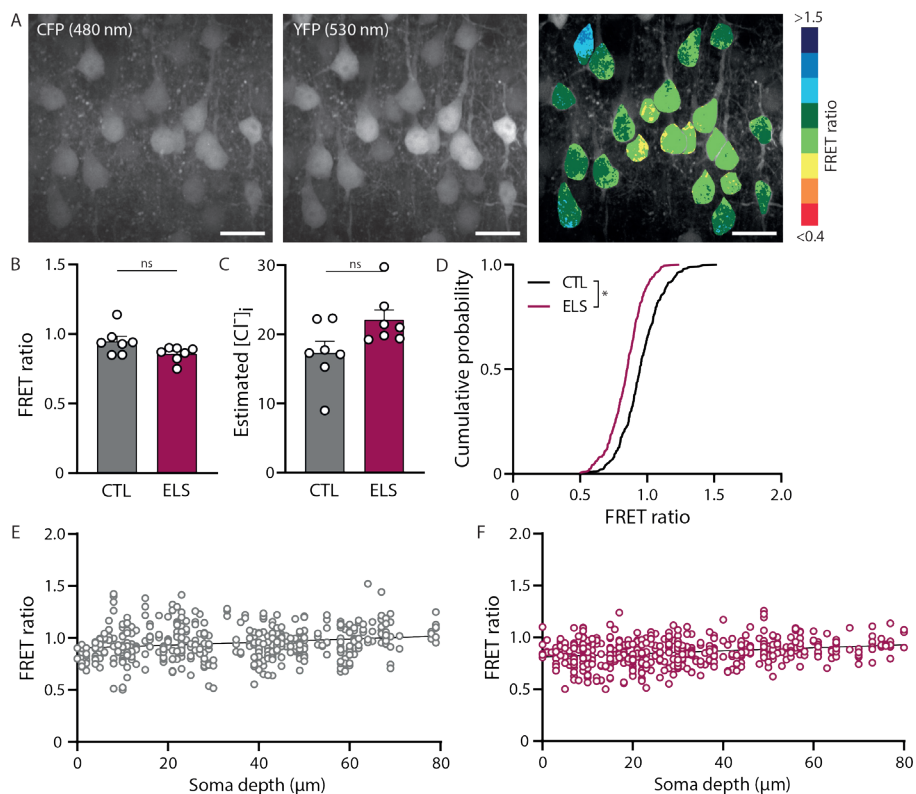


Figure 4. Higher [Cl⁻]_i in L2/3 cells of the mPFC from mice that experienced early life stress.

A) Two-photon image of layer 2/3 neurons of the medial PFC of an acute slice of a P9 SCLm mouse. Shown is the CFP and YFP fluorescence, and the corresponding FRET ratios. Individual cells are color-coded to their FRET ratios. Scale bar: 20 μm .

B) Average FRET ratios from control mice and from mice after ELS. Data from 7 mice in both groups ($p = 0.55$, T test). The average FRET ratios were significantly lower in the ELS condition when analyzed per slice ($p < 0.01$, T test) or per cell ($p < 0.0001$, MW test) (data not shown).

C) Average estimated [Cl⁻]_i as calculated from the FRET ratios in B ($p = 0.07$, MW test).

D) Cumulative distribution of individual FRET ratios in slices from control and ELS mice. For each mouse 50 cells were randomly selected, making a total of 350 plotted cells per condition ($p < 0.001$; KS test).

E) Individual FRET ratios plotted against soma depth in slices from control mice ($n = 443$ neurons). Line represents linear regression fit ($r = 0.035$; $p < 0.0001$).

F) Same as E for slices from mice after ELS ($n = 470$ neurons). Line represents linear regression fit ($r = 0.058$; $p < 0.0001$).

3.6 Discussion

In this study we performed two-photon chloride imaging using the SClm sensor to determine the time course of chloride maturation in cultured hippocampal slices and to examine alterations of the chloride development in the mPFC by ELS. Previous non-ratiometric chemical indicators, including 6-methoxy-N-(3-sulfopropyl)quinolinium (SPQ) and N-(ethoxycarbonylmethyl)-6-methoxyquinolinium bromide (MQAE) (Illsley and Verkman, 1987; Verkman et al., 1989), have the disadvantage that their fluorescence depends not only on $[Cl^-]_i$, but also on the dye concentration and optical thickness at each location, e.g. depth in the slice or in the brain. Therefore SPQ and MQAE allow for the assessment of acute changes in $[Cl^-]_i$ within the same neurons (Arosio and Ratto, 2014; Zajac et al., 2020), but cannot be used to study developmental changes which requires comparisons between animals and between slices. The SClm sensor has an improved affinity for chloride compared to its processor Clomeleon (Berglund et al., 2006), resulting in a more than fourfold improvement in signal to noise over Clomeleon (Grimley et al., 2013). Two-photon chloride imaging poses major advantages over perforated patch clamp recordings. Most importantly, chloride imaging allows for assessing of $[Cl^-]_i$ over time in multiple neurons simultaneously in a non-invasive manner. One important limitation of the SClm sensor is its sensitivity to intracellular pH (pH_i) (Lodovichi et al., 2022). However, we do not expect large changes in pH_i in our in vitro experiments, and pH_i remains fairly constant during postnatal development (Sulis Sato et al., 2017). Using SClm, we could directly measure changes in $[Cl^-]_i$ when we loaded 70 mM chloride into a neuron via the patch pipette and after addition of a GABA_A receptor agonist. This demonstrates that the SClm sensor reliably reports changes in intracellular chloride within the physiological range. Furthermore, we could detect subtle changes in the distribution of individual $[Cl^-]_i$ levels within the pyramidal cell population during normal and disturbed postnatal development. Subtle changes at the population level are physiologically relevant and would have been hard to pick up otherwise.

Although the advantages of direct chloride imaging using the SClm sensor are numerous, we found that the conversion of FRET ratios to absolute values of intracellular chloride concentrations was not very robust. In our hands, calibration using ionophores and varying extracellular chloride concentrations gave variable results. Variable FRET ratios, especially in the physiological range (5-10 mM), hampered reliable calibration to $[Cl^-]_i$. Compared to our cultured slices, cultured primary neurons are better accessible for ionophores. Cultured neurons are therefore expected to respond more consistently to changes in extracellular chloride levels during ionophore calibration (Grimley et al., 2013; Boffi et al., 2018), and this method is more unpredictable in cultured slices. In addition, strong regulation of intracellular chloride levels (Kaila et al., 2014; Rahmati et al., 2021) and variable resilience of neurons to the harsh calibration conditions may have hampered the calibration procedure in our slices. We therefore

resorted to using perforated patch clamp and inferred chloride concentrations from the reversal potential of GABA_A currents. Although our calibration curve was in good agreement with previous reports (Grimley et al., 2013; Rahmati et al., 2021), we noticed that small alterations in the fit strongly affect chloride level estimates. We therefore conclude that the SClm sensor is an excellent tool to measure relative changes in $[Cl^-]_i$, which are physiological relevant, but that conversion to absolute chloride concentrations should be interpreted with care. In our view, this disadvantage does not outweigh the significant benefits of using the SClm sensor to detect changes in neuronal chloride levels over time and between conditions. In recent years, genetically encoded fluorescent sensors have been developed which enable imaging of different molecules. Live imaging studies using these sensors, most prominently of intracellular calcium, have made great contributions to our understanding of intra- and intercellular signaling (Day-Cooney et al., 2022; Dong et al., 2022), despite the fact that calibration of most of these sensors to absolute concentrations remains notoriously difficult. We hope that current and future chloride sensors (Zajac et al., 2020; Lodovichi et al., 2022) will make a similar impact on our understanding of chloride homeostasis.

Using the SClm sensor, we have monitored the developmental decrease in neuronal chloride levels in organotypic hippocampal cultures from SClm mice. The SClm sensor proved much more sensitive than its precursor Clomeleon, which was previously used to determine chloride maturation in cultured neurons and in an *in vitro* epilepsy model (Kuner and Augustine, 2000; Dzhala and Staley, 2021). With the SClm sensor we could discern that neuronal chloride levels in our cultured slices show a clear reduction between DIV3 and DIV9 (equivalent to the second postnatal week *in vivo*), and that in some pyramidal cells chloride levels continue to decrease until DIV22. The large cell-to-cell differences that we observe have been previously reported (Stein et al., 2004; Yamada et al., 2004; Dzhala et al., 2012; Kirmse et al., 2015; Sulis Sato et al., 2017). The estimated $[Cl^-]_i$ values in our developing cultured slices are in good agreement with previous estimates in cultured hippocampal neurons (Kuner and Augustine, 2000; Tyzio et al., 2007), and acute hippocampal slices (Staley and Proctor, 1999; Tyzio et al., 2007). A recent study using LSSmClpHensor chloride sensor in the visual cortex *in vivo* (Sulis Sato et al., 2017) also showed a rapid reduction in $[Cl^-]_i$ during the first postnatal week, followed by a slow further decrease to mature levels.

Brain development is strongly influenced by external factors and early life experiences (Hensch, 2004; Miguel et al., 2019). Here we used ELS, an established model to interfere with early brain development with long-lasting consequences for psychopathological risks later in life (Teicher et al., 2016; Joëls et al., 2018; Bachiller et al., 2022; Catale et al., 2022). We used SClm to detect possible alterations in chloride maturation in the mPFC. We observed that ELS results in a shift towards higher (i.e. immature) chloride levels in individual layer 2/3 cells in the mPFC. This suggests that ELS delays the GABA shift in SClm mice, but we did not examine chloride levels at older ages. Our results are in

line with previous reports showing a delayed GABA shift in hippocampal neurons after prenatal maternal restraint stress and when newborn pups were repeatedly separated from their mother (Veerawatananan et al., 2016; Furukawa et al., 2017; Hu et al., 2017b). However, the effect on the GABA shift can be very sensitive to the type and timing of stress, and a different maternal separation paradigm results in an advance of the hippocampal GABA shift (Galanopoulou, 2008). Using the same ELS paradigm in C57/BL6 mice, we previously reported accelerated maturation of synaptic currents in layer 2/3 mPFC pyramidal cells (Karst et al., 2020), and decreased $[Cl^-]_i$ levels in young pups after ELS (Karst et al., 2019). Although we used the same stress paradigm and mice were housed in the same facility, the effect of ELS on $[Cl^-]_i$ was remarkably different between the SClm and WT mice. Chloride homeostasis is highly regulated and affected by many intracellular factors including the chloride buffering capacity (Rahmati et al., 2021), and we cannot exclude that the permanent presence of a chloride sensor induces subtle changes in the regulation of chloride homeostasis in neurons in SClm mice. However, the $[Cl^-]_i$ we report here in SClm (unstressed) controls (17.3 mM) was comparable to the chloride concentration that was previously measured by perforated patch in WT C57/BL6 control mice (18.8 mM) (Henk Karst, unpublished observations), suggesting that the difference cannot be explained by a difference in baseline chloride levels. The response to stress can differ substantially between mouse strains and C57BL/6 mice appear more resilient to stress in comparison to other strains (Murthy and Gould, 2018). Unfortunately, we did not directly compare the two mouse lines. A difference in ELS response may indicate a difference in genetic predisposition with possible consequences for stress responses and stress-related behavior (McIlwrick et al., 2016; Teicher et al., 2016; Joëls et al., 2018). The poor breeding performance of SClm mice may also reflect differences in stress response compared to C57BL/6 mice. Our results underscore that the developmental chloride trajectory appears incredibly sensitive to environmental factors and may differ between mouse lines. We advise to take these differences into account in behavioral experiments.

Our data demonstrate that the high sensitivity of the SClm sensor at relevant chloride concentrations allows detecting physiological alterations in neuronal chloride levels during normal and altered postnatal development. Although we also found some limitations, our study underscores that two-photon chloride imaging is a powerful technique to further illuminate the role of chloride signaling in the brain.

3.7 Author contributions

L.J.H., C.P., and C.J.W. designed research; L.J.H. and C.P. performed research; H.K. contributed unpublished reagents/analytic tools; L.J.H., C.P., S.U., and D.S. analyzed data; L.J.H., C.P., and C.J.W. wrote the paper.

3.8 Declaration of Interests

The authors declare no competing interests.

3.9 Acknowledgments

We thank Prof. Kevin Staley for providing the SuperClomeleon^{lox/-} mouse line and SClm AAV and Dr. Stefan Berger for the CamKII α ^{Cre/+} mice; several members of the Staley lab for helpful discussions; René van Dorland for his technical support with the AAV; and Prof. Marian Joëls for her constructive feedback on this manuscript.



3.10 References

- Amadeo, A., Coatti, A., Aracri, P., Ascagni, M., Iannantuoni, D., Modena, D., 2018. Postnatal Changes in K⁺/Cl⁻ Cotransporter-2 Expression in the Forebrain of Mice Bearing a Mutant Nicotinic Subunit Linked to Sleep-Related Epilepsy *Alida*. *Neuroscience* 386, 91–107. <https://doi.org/10.1016/j.neuroscience.2018.06.030>
- Arosio, D., Ratto, G.M., 2014. Twenty years of fluorescence imaging of intracellular chloride. *Front. Cell. Neurosci.* 8, 1–12. <https://doi.org/10.3389/fncel.2014.00258>
- Arosio, D., Ricci, F., Marchetti, L., Gualdani, R., Albertazzi, L., Beltram, F., 2010. Simultaneous intracellular chloride and pH measurements using a GFP-based sensor. *Nat. Methods* 7, 516–518. <https://doi.org/10.1038/nmeth.1471>
- Bachiller, S., Hidalgo, I., Garcia, M.G., Boza-Serrano, A., Paulus, A., Denis, Q., Haikal, C., Manouchehrian, O., Klementieva, O., Li, J.Y., Pronk, C.J., Gouras, G.K., Deierborg, T., 2022. Early-life stress elicits peripheral and brain immune activation differently in wild type and 5xFAD mice in a sex-specific manner. *J. Neuroinflammation* 19, 1–15. <https://doi.org/10.1186/s12974-022-02515-w>
- Ben-Ari, Y., Gaiarsa, J.-L., Tyzio, R., Khazipov, R., 2007. GABA: A Pioneer Transmitter That Excites Immature Neurons and Generates Primitive Oscillations. *Physiol. Rev.* 87, 1215–1284. <https://doi.org/10.1152/physrev.00017.2006>
- Berglund, K., Schleich, W., Krieger, P., Loo, L.S., Wang, D., Cant, N.B., Feng, G., Augustine, G.J., Kuner, T., 2006. Imaging synaptic inhibition in transgenic mice expressing the chloride indicator, Clomeleon. *Brain Cell Biol.* 35, 207–228. <https://doi.org/10.1007/s11068-008-9019-6>
- Boffi, J.C., Knabbe, J., Kaiser, M., Kuner, T., 2018. KCC2-dependent steady-state intracellular chloride concentration and pH in cortical layer 2/3 neurons of anesthetized and awake mice. *Front. Cell. Neurosci.* 12, 1–14. <https://doi.org/10.3389/fncel.2018.00007>
- Bormann, J., Hamill, O.P., Sakmann, B., 1987. Mechanism of anion permeation through channels gated by glycine and gamma-aminobutyric acid in mouse cultured spinal neurones. *J. Physiol.* 385, 243–286.
- Casanova, E., Fehsenfeld, S., Mantamadiotis, T., Lemberger, T., Greiner, E., Stewart, A.F., Schtz, G., 2001. A CamKIIa iCre BAC allows brain-specific gene inactivation. *Genesis* 31, 37–42. <https://doi.org/10.1002/gene.1078>
- Catale, C., Martini, A., Piscitelli, R.M., Senzasono, B., Iacono, L. Lo, Mercuri, N.B., Guatteo, E., Carola, V., 2022. Early-life social stress induces permanent alterations in plasticity and perineuronal nets in the mouse anterior cingulate cortex. *Eur. J. Neurosci.* online ahead of print. <https://doi.org/10.1111/ejn.15825>
- Day-Cooney, J., Dalangin, R., Zhong, H., Mao, T., 2022. Genetically encoded fluorescent sensors for imaging neuronal dynamics in vivo. *J. Neurochem.* 1–25. <https://doi.org/10.1111/jnc.15608>
- Dong, C., Zheng, Y., Long-Iyer, K., Wright, E.C., Li, Y., Tian, L., 2022. Fluorescence Imaging of Neural Activity, Neurochemical Dynamics, and Drug-Specific Receptor Conformation with Genetically Encoded Sensors. *Annu. Rev. Neurosci.* 45, 273–294. <https://doi.org/10.1146/annurev-neuro-110520-031137>
- Dzhala, V., Valeeva, G., Glykys, J., Khazipov, R., Staley, K., 2012. Traumatic Alterations in GABA Signaling Disrupt Hippocampal Network Activity in the Developing Brain. *J. Neurosci.* 32, 4017–4031. <https://doi.org/10.1523/JNEUROSCI.5139-11.2012>
- Dzhala, V.I., Staley, K.J., 2021. Kcc2 chloride transport contributes to the termination of ictal epileptiform activity. *eNeuro* 8, 1–16. <https://doi.org/10.1523/ENEURO.0208-20.2020>

- Furukawa, M., Tsukahara, T., Tomita, K., Iwai, H., Sonomura, T., Miyawaki, S., Sato, T., 2017. Neonatal maternal separation delays the GABA excitatory-to-inhibitory functional switch by inhibiting KCC2 expression. *Biochem. Biophys. Res. Commun.* 493, 1243–1249. <https://doi.org/10.1016/j.bbrc.2017.09.143>
- Galanopoulou, A.S., 2008. Dissociated gender-specific effects of recurrent seizures on GABA signaling in CA1 pyramidal neurons: Role of GABAA receptors. *J. Neurosci.* 28, 1557–1567. <https://doi.org/10.1523/JNEUROSCI.5180-07.2008>
- Glykys, J., Dzhalala, V.I., Kuchibhotla, K.V., Feng, G., Kuner, T., Augustine, G., Bacskaï, B., Staley, K., 2009. Differences in cortical vs. subcortical GABAergic signaling: a candidate mechanism of electroclinical dissociation of neonatal seizures. *Neuron.* 63, 657–672. <https://doi.org/10.1016/j.neuron.2009.08.022>
- Grimley, J.S., Li, L., Wang, W., Wen, L., Beese, L.S., Hellinga, H.W., Augustine, G.J., 2013. Visualization of Synaptic Inhibition with an Optogenetic Sensor Developed by Cell-Free Protein Engineering Automation. *J. Neurosci.* 33, 16297–16309. <https://doi.org/10.1523/JNEUROSCI.4616-11.2013>
- Hensch, T.K., 2004. Critical Period Regulation. *Annu. Rev. Neurosci.* 27, 549–579. <https://doi.org/10.1146/annurev.neuro.27.070203.144327>
- Hu, Yu, Z.L., Zhang, Y., Han, Y., Zhang, W., Lu, L., Shi, J., 2017. Bumetanide treatment during early development rescues maternal separation-induced susceptibility to stress. *Sci. Rep.* 7, 1–16. <https://doi.org/10.1038/s41598-017-12183-z>
- Illsley, N.P., Verkman, A.S., 1987. Membrane Chloride Transport Measured Using a Chloride-Sensitive Fluorescent Probe. *Biochemistry* 26, 1215–1219. <https://doi.org/10.1021/bi00379a002>
- Ishikawa, J., Nishimura, R., Ishikawa, A., 2015. Early-life stress induces anxiety-like behaviors and activity imbalances in the medial prefrontal cortex and amygdala in adult rats. *Eur. J. Neurosci.* 41, 442–453. <https://doi.org/10.1111/ejn.12825>
- Joëls, M., Karst, H., Sarabdjitsingh, R.A., 2018. The stressed brain of humans and rodents. *Acta Physiol.* 223, 1–10. <https://doi.org/10.1111/apha.13066>
- Kaila, K., 1994. Ionic basis of GABAA receptor channel function in the nervous system. *Prog. Neurobiol.* 42, 489–537. [https://doi.org/10.1016/0301-0082\(94\)90049-3](https://doi.org/10.1016/0301-0082(94)90049-3)
- Kaila, K., Price, T.J., Payne, J.A., Puskarjov, M., Voipio, J., 2014. Cation-chloride cotransporters in neuronal development, plasticity and disease. *Nat. Rev. Neurosci.* 15, 637–654. <https://doi.org/10.1038/nrn3819>
- Kaila, K., Voipio, J., Paalasmaa, P., Pasternack, M., Deisz, R.A., 1993. The role of bicarbonate in GABAA receptor-mediated IPSPs of rat neocortical neurones. *J. Physiol.* 464, 273–289.
- Karst, H., Sarabdjitsingh, R.A., van der Weerd, N., Feenstra, E., Damsteegt, R., Joëls, M., 2020. Age-dependent shift in spontaneous excitation-inhibition balance of infralimbic prefrontal layer II/III neurons is accelerated by early life stress, independent of forebrain mineralocorticoid receptor expression. *Neuropharmacology* 180, 1–12. <https://doi.org/10.1016/j.neuropharm.2020.108294>
- Karst, H., van Mourik, L.I., Joëls, M., 2019. Early life stress in mice causes a change in the excitation-inhibition balance in prefrontal cortex neurons during development, in: *Society for Neuroscience Abstracts.* p. 409.03.
- Kirmse, K., Kummer, M., Kovalchuk, Y., Witte, O.W., Garaschuk, O., Holthoff, K., 2015. GABA depolarizes immature neurons and inhibits network activity in the neonatal neocortex in vivo. *Nat. Commun.* 6, 1–13. <https://doi.org/10.1038/ncomms8750>
- Kuner, T., Augustine, G.J., 2000. A Genetically Encoded Ratiometric Indicator for Chloride. *Neuron* 27, 447–459. [https://doi.org/10.1016/s0896-6273\(00\)00056-8](https://doi.org/10.1016/s0896-6273(00)00056-8)
- Lodovichi, C., Ratto, G.M., Trevelyan, A.J., Arosio, D., 2022. Genetically encoded sensors for Chloride concentration. *J. Neurosci. Methods* 368, 109455. <https://doi.org/10.1016/j.jneumeth.2021.109455>

- Lohmann, C., Kessels, H.W., 2014. The developmental stages of synaptic plasticity. *J. Physiol.* 592, 13–31. <https://doi.org/10.1113/jphysiol.2012.235119>
- Mcllwrick, S., Rechenberg, A., Matthes, M., Burgstaller, J., Chen, Thomas Schwarzbauer, A., Touma, C., 2016. Genetic predisposition for high stress reactivity amplifies effects of early-life adversity. *Psychoneuroendocrinology* 70, 85–97.
- Mcklveen, J.M., Myers, B., Herman, J.P., 2015. The Medial Prefrontal Cortex: Coordinator of Autonomic, Neuroendocrine and Behavioural Responses to Stress. *J. Neuroendocrinol.* 27, 446–456. <https://doi.org/10.1111/jne.12272>
- Miguel, P., Pereira, L., Silveira, P., Meaney, M., 2019. Early environmental influences on the development of children's brain structure and function. 61, 1127–1133. <https://doi.org/10.1111/dmnc.14182>.
- Murata, Y., Colonnese, M.T., 2020. GABAergic interneurons excite neonatal hippocampus in vivo. *Sci. Adv.* 6, 1–10.
- Murthy, S., Gould, E., 2018. Early life stress in rodents: Animal models of illness or resilience? *Front. Behav. Neurosci.* 12, 1–5. <https://doi.org/10.3389/fnbeh.2018.00157>
- Naninck, E.F.G., Hoeijmakers, L., Kakava-Georgiadou, N., Meesters, A., Lazic, S.E., Lucassen, P.J., Korosi, A., 2015. Chronic early life stress alters developmental and adult neurogenesis and impairs cognitive function in mice. *Hippocampus* 25, 309–328. <https://doi.org/10.1002/hipo.22374>
- Peerboom, C., Wierenga, C.J., 2021. The postnatal GABA shift: A developmental perspective. *Neurosci. Biobehav. Rev.* 124, 179–192. <https://doi.org/10.1016/j.neubiorev.2021.01.024>
- Pressman, B., Fahim, M., 1982. Pharmacology and toxicology of the monovalent carboxylic ionophores. *Annu Rev Pharmacol Toxicol.* 22, 465–490. <https://doi.org/10.1146/annurev.pa.22.040182.002341>.
- Pylayeva-Gupta, Y., 2011. Activity-Dependent Validation of Excitatory vs. Inhibitory Synapses by Neuroligin-1 vs. Neuroligin-2. *Bone* 23, 1–7. <https://doi.org/10.1038/jid.2014.371>
- Rahmati, N., Normoyle, K.P., Glykys, J., Dzhalal, V.I., Lillis, K.P., Kahle, K.T., Raiyyani, R., Jacob, T., Staley, K.J., 2021. Unique actions of gaba arising from cytoplasmic chloride microdomains. *J. Neurosci.* 41, 4967–4975. <https://doi.org/10.1523/JNEUROSCI.3175-20.2021>
- Rice, C.J., Sandman, C.A., Lenjavi, M.R., Baram, T.Z., 2008. A novel mouse model for acute and long-lasting consequences of early life stress. *Endocrinology* 149, 4892–4900. <https://doi.org/10.1210/en.2008-0633>
- Rivera, C., Voipio, J., Payne, J. a, Ruusuvoori, E., Lahtinen, H., Lamsa, K., Pirvola, U., Saarma, M., Kaila, K., 1999. The K⁺/Cl⁻ co-transporter KCC2 renders GABA hyperpolarizing during neuronal maturation. *Nature* 397, 251–255. <https://doi.org/10.1038/16697>
- Romo-Parra, H., Treviño, M., Heinemann, U., Gutiérrez, R., 2008. GABA actions in hippocampal area CA3 during postnatal development: Differential shift from depolarizing to hyperpolarizing in somatic and dendritic compartments. *J. Neurophysiol.* 99, 1523–1534. <https://doi.org/10.1152/jn.01074.2007>
- Sernagor, E., Chabrol, F., Bony, G., Cancedda, L., 2010. Gabaergic control of neurite outgrowth and remodeling during development and adult neurogenesis: General rules and differences in diverse systems. *Front. Cell. Neurosci.* 4, 1–11. <https://doi.org/10.3389/fncel.2010.00011>
- Sík, A., Hájos, N., Gulácsi, A., Mody, I., Freund, T.F., 1998. The absence of a major Ca²⁺ signaling pathway in GABAergic neurons of the hippocampus. *Proc. Natl. Acad. Sci. U. S. A.* 95, 3245–3250. <https://doi.org/10.1073/pnas.95.6.3245>
- Staley, K.J., Proctor, W.R., 1999. Modulation of mammalian dendritic GABA(A) receptor function by the kinetics of Cl⁻ and HCO₃⁻ transport. *J. Physiol.* 519, 693–712. <https://doi.org/10.1111/j.1469-7793.1999.0693n.x>

- Stein, V., Hermans-Borgmeyer, I., Jentsch, T.J., Hübner, C.A., 2004. Expression of the KCl Cotransporter KCC2 Parallels Neuronal Maturation and the Emergence of Low Intracellular Chloride. *J. Comp. Neurol.* 468, 57–64. <https://doi.org/10.1002/cne.10983>
- Sulis Sato, S., Artoni, P., Landi, S., Cozzolino, O., Parra, R., Pracucci, E., Trovato, F., Szczurkowska, J., Luin, S., Arosio, D., Beltram, F., Cancedda, L., Kaila, K., Ratto, G.M., 2017. Simultaneous two-photon imaging of intracellular chloride concentration and pH in mouse pyramidal neurons in vivo. *Proc. Natl. Acad. Sci.* 114, E8770–E8779. <https://doi.org/10.1073/pnas.1702861114>
- Teicher, M.H., Samson, J.A., Anderson, C.M., Ohashi, K., 2016. The effects of childhood maltreatment on brain structure, function and connectivity. *Nat. Rev. Neurosci.* 17, 652–666. <https://doi.org/10.1038/nrn.2016.111>
- Tsien, J.Z., Chen, D.F., Gerber, D., Tom, C., Mercer, E.H., Anderson, D.J., Mayford, M., Kandel, E.R., Tonegawa, S., 1996. Subregion- and cell type-restricted gene knockout in mouse brain. *Cell* 87, 1317–1326. [https://doi.org/10.1016/S0092-8674\(00\)81826-7](https://doi.org/10.1016/S0092-8674(00)81826-7)
- Tyzio, R., Holmes, G.L., Ben-Ari, Y., Khazipov, R., 2007. Timing of the developmental switch in GABAA mediated signaling from excitation to inhibition in CA3 rat hippocampus using gramicidin perforated patch and extracellular recordings. *Epilepsia* 48, 96–105. <https://doi.org/10.1111/j.1528-1167.2007.01295.x>
- Veerawatananan, B., Surakul, P., Chutabhakdikul, N., 2016. Maternal restraint stress delays maturation of cation-chloride cotransporters and GABAA receptor subunits in the hippocampus of rat pups at puberty. *Neurobiol. Stress* 3, 1–7. <https://doi.org/10.1016/j.ynstr.2015.12.001>
- Verkman, A.S., Sellers, M.C., Chao, A.C., Leung, T., Ketcham, R., 1989. Synthesis and characterization of improved chloride-sensitive fluorescent indicators for biological applications. *Anal. Biochem.* 178, 355–361. [https://doi.org/10.1016/0003-2697\(89\)90652-0](https://doi.org/10.1016/0003-2697(89)90652-0)
- Wang, B.S., Feng, L., Liu, M., Liu, X., Cang, J., 2013. Environmental Enrichment Rescues Binocular Matching of Orientation Preference in Mice that Have a Precocious Critical Period. *Neuron* 80, 198–209. <https://doi.org/10.1016/j.neuron.2013.07.023>
- Yamada, J., Okabe, A., Toyoda, H., Kilb, W., Luhmann, H., Fukuda, A., 2004. Cl⁻ uptake promoting depolarizing GABA actions in immature rat neocortical neurones is mediated by NKCC1. *J. Physiol.* 557, 829–841.
- Zajac, M., Chakraborty, K., Saha, S., Mahadevan, V., Infield, D.T., Accardi, A., Qiu, Z., Krishnan, Y., 2020. What biologists want from their chloride reporters - A conversation between chemists and biologists. *J. Cell Sci.* 133. <https://doi.org/10.1242/jcs.240390>



4

Delaying the GABA shift indirectly affects membrane properties in the developing hippocampus

C. Peerboom¹, S. De Kater¹, N. Jonker¹, M.P.J.M. Rieter¹, T. Wijne¹ and C.J. Wierenga^{1,2}

¹ Cell Biology, Neurobiology and Biophysics, Biology department, Utrecht University, 3584CH, Utrecht, the Netherlands,

² Current address: Faculty of Science & Donders Institute, Radboud University, 6525 AJ, Nijmegen, the Netherlands

This chapter has been published in *Journal of Neuroscience* 2023, 43 (30), doi: 10.1523/JNEUROSCI.0251-23.2023

4.1 Abstract

During the first two postnatal weeks intraneuronal chloride concentrations in rodents gradually decrease, causing a shift from depolarizing to hyperpolarizing γ -aminobutyric acid (GABA) responses. The postnatal GABA shift is delayed in rodent models for neurodevelopmental disorders and in human patients, but the impact of a delayed GABA shift on the developing brain remain obscure. Here we examine the direct and indirect consequences of a delayed postnatal GABA shift on network development in organotypic hippocampal cultures made from 6 to 7-day old mice by treating the cultures for one week with VU0463271, a specific inhibitor of the chloride exporter KCC2. We verified that VU treatment delayed the GABA shift and kept GABA signaling depolarizing until day in vitro (DIV) 9. We found that the structural and functional development of excitatory and inhibitory synapses at DIV9 was not affected after VU treatment. In line with previous studies, we observed that GABA signaling was already inhibitory in control and VU-treated postnatal slices. Surprisingly, fourteen days after the VU treatment had ended (DIV21), we observed an increased frequency of spontaneous inhibitory post-synaptic currents in CA1 pyramidal cells, while excitatory currents were not changed. Synapse numbers and release probability were unaffected. We found that dendrite-targeting interneurons in the stratum Radiatum had an elevated resting membrane potential, while pyramidal cells were less excitable compared to control slices. Our results show that depolarizing GABA signaling does not promote synapse formation after P7, and suggest that postnatal intracellular chloride levels indirectly affect membrane properties in a cell-specific manner.

4.2 Significance Statement

During brain development the action of neurotransmitter GABA shifts from depolarizing to hyperpolarizing. This shift is a thought to play a critical role in synapse formation. A delayed shift is common in rodent models for neurodevelopmental disorders and in human patients, but its consequences for synaptic development remain obscure. Here, we delayed the GABA shift by one week in organotypic hippocampal cultures and carefully examined the consequences for circuit development. We find that delaying the shift has no direct effects on synaptic development, but instead leads to indirect, cell type-specific changes in membrane properties. Our data call for careful assessment of alterations in cellular excitability in neurodevelopmental disorders.

4.3 Introduction

During postnatal development of rodents intracellular chloride concentrations in neurons gradually decrease. Since GABA_A receptors mainly conduct chloride, the developmental decrease in intracellular chloride causes the reversal potential for GABA currents to gradually drop below resting membrane potential. As a result, the GABAergic driving force shifts from depolarizing in immature neurons to hyperpolarizing in mature neurons (Rivera et al., 1999; Hübner et al., 2001; Tyzio et al., 2007; Romo-Parra et al., 2008; Kirmse et al., 2015; Tsukahara et al., 2015; Sulis Sato et al., 2017; Murata and Colonnese, 2020). This GABA shift is a key event during development and is suggested to play a critical role in the formation and maturation of synapses (Leinekugel et al., 1997; Akerman and Cline, 2006; Wang and Kriegstein, 2008, 2011; Chancey et al., 2013; van Rheede et al., 2015; Oh et al., 2016).

The shift in postnatal chloride levels is the direct result of an increased function of the chloride exporter KCC2 (K-Cl cotransporter 2) relative to the chloride importer NKCC1 (Na-K-2Cl cotransporter 1) (Rivera et al., 1999; Gulyás et al., 2001; Yamada et al., 2004; Dzhala et al., 2005; Otsu et al., 2020). In humans, the shift in chloride transporter expression occurs during the first year after birth (Dzhala et al., 2005; Sedmak et al., 2016), but in some patients with neurodevelopmental disorders (NDDs) chloride homeostasis seems impaired and alterations in the expression of both NKCC1 and KCC2 have been widely reported (Talos et al., 2012; Duarte et al., 2013; Merner et al., 2015a; Ruffolo et al., 2016; Birey et al., 2022). In rodents, the GABA shift occurs during the first two postnatal weeks (Rivera et al., 1999; Stein et al., 2004; Tyzio et al., 2007; Romo-Parra et al., 2008; Kirmse et al., 2015; Sulis Sato et al., 2017; Murata and Colonnese, 2020). In many animal models for NDDs a delayed GABA shift and alterations in chloride cotransporter expression have been reported (He et al., 2014; Tyzio et al., 2014; Banerjee et al., 2016; Corradini et al., 2017; Fernandez et al., 2018; Roux et al., 2018; Lozovaya et al., 2019; Bertoni et al., 2021), suggesting this is a key feature of many NDDs. In NDD mouse models alterations in early spontaneous network activity are observed (Gonçalves et al., 2013; Cheyne et al., 2019), and coordination between excitatory and inhibitory transmission is impaired in adult mice (Gogolla et al., 2009; Antoine et al., 2019). These observations suggest that a delay in the GABA shift during early postnatal development disturbs synaptic connectivity and network development with consequences for adulthood (Meredith, 2015; Molnár et al., 2020). However, a direct link between the timing of the GABA shift and synaptic connectivity remains elusive.

Depolarizing, excitatory GABA signaling supports spontaneous oscillations in the immature rodent brain (Ben-Ari et al., 1989; Khazipov et al., 2004; Sipilä et al., 2006; Rheims et al., 2008; Spoljaric et al., 2019) and can induce the formation and maturation of excitatory synapses until the first week after birth (Leinekugel et al., 1997; Wang

and Kriegstein, 2008, 2011; van Rheede et al., 2015; Oh et al., 2016). After the GABA shift, the KCC2 protein takes over the synapse-promoting role, as it directly facilitates spine growth by promoting actin dynamics in spines and supports AMPA receptor insertion and confinement (Li et al., 2007; Gauvain et al., 2011; Fiumelli et al., 2013; Chevy et al., 2015; Puskarjov et al., 2017; Awad et al., 2018; Kesaf et al., 2020). The effect of depolarizing GABA on inhibitory synapses is less clear, as studies have reported both positive and negative effects (Chudotvorova et al., 2005; Akerman and Cline, 2006; Nakanishi et al., 2007; Wang and Kriegstein, 2008, 2011). It is important to note that the shift from depolarizing to hyperpolarizing GABA signaling does not necessarily go hand in hand with a shift from excitatory to inhibitory action. Depolarizing GABA can already have an inhibitory action and limit neuronal activity when GABA-mediated depolarization is subthreshold and opening of GABA_A receptors shunts excitatory inputs (Staley and Mody, 1992; Kirmse et al., 2015; Murata and Colonnese, 2020; Salmon et al., 2020). When GABA signaling becomes inhibitory, it restrains excitatory synapse formation (Kang, 2019; Salmon, 2020) and network oscillations disappear (Ben-Ari et al., 1989; Khazipov et al., 2004). Recent studies have suggested that depolarizing GABA is already inhibitory in the brain of newborn rodents after P3-7 (Kirmse et al., 2015; Valeeva et al., 2016; Murata and Colonnese, 2020). This would imply that the role of depolarizing GABA in promoting synapse formation is limited to the period before and up to the first week after birth.

Many NDD mouse models show a delay in the postnatal GABA shift, although the precise delay is variable. For instance, the GABA shift is delayed with three days in the cerebellum of mice exposed *in utero* to valproate (Roux et al., 2018), the delay is two to seven days in the hippocampus of Magel2 knock out mice (Bertoni et al., 2021), and six days in the cortex of fragile X mice (He et al., 2014). Longer delays have also been reported (Banerjee et al., 2016; Corradini et al., 2017; Fernandez et al., 2018; Lozovaya et al., 2019). Here, we carefully assessed the direct and indirect consequences of a delayed postnatal GABA shift on the development of synapses. We used hippocampal organotypic cultures, as in these slices the anatomy and the development of excitatory and inhibitory synapses is largely preserved compared to the *in vivo* situation (De Simoni, 2003). We treated the cultures with the KCC2 antagonist VU0463271 (VU) to block chloride extrusion for one week (from DIV1 to DIV8), while preserving the structural role of the KCC2 protein in spines (Li et al., 2007; Kesaf et al., 2020). VU treatment delayed the GABA shift without affecting expression levels of the chloride transporters. We found that excitatory and inhibitory synapses were not affected after one week of VU treatment. However, 14 days after the VU treatment had ended, we observed an increased frequency of spontaneous inhibitory postsynaptic currents (sIPSC), while excitatory postsynaptic currents (sEPSCs) were unaltered. We found that this was correlated with specific alterations in membrane excitability of pyramidal cells and interneurons. Our data suggest that delaying the GABA shift does not directly

affect synaptic development, but rather leads to indirect cell-type specific changes in membrane properties.

4.4 Materials and methods

Animals

All animal experiments were performed in compliance with the guidelines for the welfare of experimental animals issued by the Federal Government of the Netherlands and were approved by the Dutch Central Committee Animal experiments (CCD), project AVD1080020173847 and project AVD1150020184927. In this study we used male and female transgenic mice: GAD65-GFP mice (López-Bendito et al., 2004) (bred as a heterozygous line in a C57BL/6Jrj background), VGAT-Cre mice (JAX stock #028862) and SuperClomeleon (SCLm) mice. The SCLm mice (Herstel et al., 2022) are SuperClomeleon^{lox/-} mice (Rahmati et al., 2021), a gift from Kevin Staley (Massachusetts General Hospital, Boston, MA) crossed with CamKIIα^{Cre/-} mice (Tsien et al., 1996; Casanova et al., 2001). SCLm mice express the chloride sensor SCLm in up to 70% of the pyramidal neurons in the hippocampus (Casanova et al., 2001; Wang et al., 2013). VGAT-Cre mice express Cre recombinase expression in all inhibitory GABAergic neurons (Vong et al., 2011), and GAD65-GFP mice express GFP in ~20% of GABAergic interneurons in the CA1 region of the hippocampus (Wierenga et al., 2010). As we did not detect any differences between slices from male and female mice, all data were pooled.

Organotypic hippocampal culture preparation and VU treatment

Organotypic hippocampal cultures were made from P6-7 mice as described before (Hu et al., 2019; Herstel et al., 2022), based on Stoppini *et al.* (Stoppini et al., 1991). Mice were decapitated and their brain was rapidly placed in ice-cold Grey's Balanced Salt Solution (GBSS; containing (in mM): 137 NaCl, 5 KCl, 1.5 CaCl₂, 1 MgCl₂, 0.3 MgSO₄, 0.2 KH₂PO₄ and 0.85 Na₂HPO₄) with 25 mM glucose, 12.5 mM HEPES and 1 mM kynurenic acid (pH set at 7.2, osmolarity set at ~320 mOsm, sterile filtered). 400 μm thick transverse hippocampal slices were cut with a Mcllwain tissue chopper. Slices were placed on Millicell membrane inserts (Millipore) in wells containing 1 ml culture medium (consisting of 48% MEM, 25% HBSS, 25% horse serum, 25 mM glucose, and 12.5 mM HEPES, with an osmolarity of ~325 mOsm and a pH of 7.3 – 7.4). Slices were stored in an incubator (35°C with 5% CO₂). Culture medium was replaced by culture medium supplemented with 0.1% Dimethyl sulfoxide (DMSO, Sigma-Aldrich) or 1 μM VU VU0463271 (VU, Sigma-Aldrich, in 0.1 % DMSO) at DIV 1. In addition, a small drop of medium supplemented with DMSO or VU was carefully placed on top of the slices. In this way, cultures were treated 3 times per week until DIV8. From DIV8 onwards, cultures received normal culture medium 3 times per week. Experiments were performed at day in vitro 1-3 (DIV2), 7-8 (DIV8), 8-10 (DIV9) or 20-22 (DIV21). Please note that experiments at DIV9 were performed 1 to 55 hr after cessation of the

VU treatment, but within groups there was no correlation between measurements and DIV.

Lentivirus with KCC2 short hairpin

To transiently knock down KCC2 expression, a KCC2 short hairpin (SH) lentivirus was produced. HEK293T cells were maintained at a high growth rate in DMEM supplemented with 10% FCS and 1% pen/strep. At 1 day after plating, cells were transfected using PEI (Polysciences) with second-generation LV packaging plasmids (psPAX2 and 2MD2.G) and KCC2-SH-TetR-GFP (cloned from a KCC2-SH plasmid, a gift from Franck Polleux, Zuckerman Institute Columbia University, New York, USA) at a 1:1:1 molar ratio. Six hours after transfection, cells were washed once with PBS, and medium was replaced with DMEM containing 1% pen/strep. At 48 hours after transfection, the supernatant was harvested and briefly centrifuged at 700g to remove cell debris. The supernatant was concentrated using Amicon Ultra 15 100K MWCO columns (Milipore) and frozen at -80°C until infection. Virus was injected into the CA1 region of slice cultures at DIV 1 using a microinjector (Eppendorf, FemtoJet) aided by a stereoscopic microscope (Leica, M80). Medium was supplemented with 1 µg/ml doxycycline (Abcam). After injection, a 15 µl drop of doxycycline containing medium was added onto the slice. Medium was replaced 4 times with new medium containing doxycycline and a 15 µl drop of doxycycline containing medium was added onto the slice until immunohistochemistry or electrophysiology experiments at DIV8-10.

Electrophysiology and analysis

Organotypic cultures were transferred to a recording chamber and continuously perfused with carbonated (95% O₂, 5% CO₂) artificial cerebrospinal fluid (ACSF, in mM: 126 NaCl, 3 KCl, 2.5 CaCl₂, 1.3 MgCl₂, 26 NaHCO₃, 1.25 NaH₂PO₄, 20 glucose; with an osmolarity of ~310 mOsm) at a rate of approximately 1 ml/min. For acute treatments, ACSF containing 0.1% DMSO or 1 µM VU (dissolved in 0.1% DMSO) was bath applied for 5 minutes. Bath temperature was maintained at 29-32°C. Recordings were acquired using an MultiClamp 700B amplifier (Molecular Devices), filtered with a 3 kHz Bessel filter and stored using pClamp10 software.

Perforated patch clamp recordings were performed in CA1 pyramidal neurons. Recording pipettes with resistances of 2-4 MΩ were pulled from borosilicate glass capillaries (World Precision Instruments). The pipette tip was filled with gramicidin-free KCl solution (140 mM KCl and 10 mM HEPES, pH adjusted to 7.2 with KOH, and osmolarity 285 mOsm/l) and then backfilled with solution containing gramicidin (60 µg/ml, Sigma). Neurons were held at -65 mV and the access resistance of the perforated cells was monitored constantly before and during recordings. An access resistance of 50 MΩ was considered acceptable to start recording. Recordings were excluded if the resting membrane potential exceeded -50 mV or if the series resistance after the recording deviated more than 30% from its original value. GABAergic currents

were induced upon local application of 50 μM muscimol dissolved in HEPES-ACSF (containing in mM: 135 NaCl, 3 KCl, 2.5 CaCl_2 , 1.3 MgCl_2 , 1.25 $\text{Na}_2\text{H}_2\text{PO}_4$, 20 Glucose, and 10 HEPES) every 30s using a Picospritzer II. Muscimol responses were recorded in the presence of 1 μM TTX (Abcam) at holding potentials between -100 mV and -30 mV in 10 mV steps. We plotted response amplitude as a function of holding potential and calculated the chloride reversal potential from the intersection of the linear current-voltage curve with the x-axis.

We performed whole-cell patch clamp recordings from CA1 pyramidal neurons and GAD65-GFP interneurons in the *stratum Radiatum* (sRad) using borosilicate glass pipettes with resistances of 3–6 M Ω . For recordings of spontaneous inhibitory postsynaptic currents (sIPSCs), miniature inhibitory currents (mIPSCs) and evoked IPSCs (eIPSCs), pipettes were filled with a KCl-based internal solution (containing in mM: 70 K-gluconate, 70 KCl, 0.5 ethyleneglycol-bis(β -aminoethyl)-N,N,N',N'-tetraacetic Acid (EGTA), 4 Na_2 phosphocreatine, 4 MgATP, 0.4 NaGTP and 10 HEPES; pH adjusted to 7.2 with KOH) and ACSF was supplemented with 20 μM DNQX (Tocris) and 50 μM DL-APV (Tocris). For recordings of miniature IPSCs (mIPSCs), 1 μM TTX (Abcam) was also added to the ACSF. For recordings of spontaneous excitatory postsynaptic currents (sEPSCs), pipettes were filled with a K-gluconate-based internal solution (containing in mM: 140 K-gluconate, 4 KCl, 0.5 EGTA, 10 HEPES, 4 MgATP, 0.4 NaGTP, 4 Na_2 phosphocreatine, 30 Alexa 568 (Thermo Fisher Scientific); pH adjusted to 7.2 with KOH) and ACSF was supplemented with 6 μM gabazine (HelloBio). Membrane potential was clamped at -65 mV. sIPSCs and mIPSCs were recorded for 6 minutes, sEPSCs for 10 minutes. For recording of eIPSCs a glass electrode filled with ACSF and containing a stimulus electrode was positioned either in sRad or *stratum Pyramidale* (sPyr) of CA1 (respectively ~ 250 – 300 μm or ~ 50 μm from the recording electrode). Stimulus intensity was set at half maximum response. eIPSCs were recorded at least 30 times every 30s with 100 ms interval. Paired pulse ratios were calculated as the mean amplitude of all second responses divided by the mean amplitude of all first responses (Kim and Alger, 2001). The coefficient of variation was calculated as the standard deviation divided by the mean amplitude of the first responses ($n=15$ – 60). After recording of sEPSCs, we switched to current clamp to assess excitability. Current was injected at resting membrane potential ($I=0$) in 10 pA increments with a maximum of 200 pA to assess firing properties. The threshold potential was determined as the accompanying membrane potential at the start of the action potential. Cells were discarded if series resistance was above 35 M Ω or if the resting membrane potential exceeded -50 mV for pyramidal neurons and -40 mV for GAD65-GFP interneurons or if the series resistance after the recording deviated more than 30% from its original value.

Cell-attached recordings were performed using borosilicate glass pipettes of 3-5 M Ω , filled with a 150 mM NaCl-based solution. Modified ACSF with higher K⁺ and lower Ca²⁺ and Mg²⁺ levels (Maffei et al., 2004) was used to increase the baseline firing frequency (containing in mM: 126 NaCl, 3,5 KCl, 1.0 CaCl₂, 0.5 MgCl₂, 26 NaHCO₃, 1.25 Na₂H₂PO₄, 20 glucose). CA1 pyramidal neurons were sealed (≥ 1 G Ω) and voltage clamped at a holding current of 0 pA, to avoid affecting the firing activity of the cell (Perkins, 2006). Firing was recorded for 6 minutes before and after wash in of muscimol (50 μ M, Tocris).

All data were blinded before analysis. Network discharges were marked and removed from sEPSC recordings before event analysis. Events were selected using a template in Clampfit10 software. Further analysis was performed using custom-written MATLAB scripts. Rise time of sIPSCs was determined as the time between 10% and 90% of the peak value. The distribution of the rise times recorded in control conditions (generated from 100 randomly selected IPSCs per cell) was fitted with two Gaussians and their crossing point determined the separation between fast and slow IPSCs (Ruiter et al., 2020). We verified that the double Gaussian fit for the rise time distribution in VU conditions gave a similar separation value (control: 0.85 ms; VU: 0.95 ms) and our conclusions did not change by taking the VU separation value. The decay tau was fitted with a single exponential function. Only events with a goodness of fit $R^2 \geq 0.75$ were included.

Two-photon SuperClomeleon imaging and analysis

We performed two-photon chloride imaging in CA1 pyramidal cells using the SuperClomeleon sensor (Grimley et al., 2013) in cultured slices from SCLm mice (described above). To target GABAergic interneurons, we used an AAV approach in slices from VGAT-Cre mice. An adeno associated virus (AAV) 2/5 for Cre-dependent SCLm expression was prepared from a SCLM-DIO construct (kind gift from Thomas Kuner (Boffi et al., 2018)) using packaging plasmid pAAV2/5 (addgene_104964) and helper plasmid pAdDeltaF6 (addgene_112867). The virus was added on top of the CA1 region of organotypic hippocampal cultures from VGAT-Cre mice at DIV1 using a microinjector (Eppendorf, FemtoJet) aided by a stereoscopic microscope (Leica, M80). This resulted in widespread, but sparse SCLm expression in GABAergic neurons.

At the recording day, slices were transferred to a recording chamber and continuously perfused with carbonated (95% O₂, 5% CO₂) ACSF supplemented with 1 mM Trolox, at a rate of approximately 1 ml/min. Bath temperature was monitored and maintained at 30-32 °C. Two-photon imaging of CA1 pyramidal neurons or VGAT-positive interneurons in the CA1 area of the hippocampus was performed using a customized two-photon laser scanning microscope (Femto3D-RC, Femtonics, Budapest, Hungary) with a Ti:Sapphire femtosecond pulsed laser (MaiTai HP, Spectra-Physics) and a 60x water immersion objective (Nikon NIR Apochromat; NA 1.0) The CFP donor was excited at 840 nm. The emission light was split using a dichroic beam splitter at 505 nm and detected using two GaAsP photomultiplier tubes. We collected fluorescence emission

of Cerulean/CFP (485 ± 15 nm) and Topaz/YFP (535 ± 15 nm) in parallel. Of each slice from SClm mice, 2-5 image stacks were acquired in different fields of view. Of each VGAT-Cre slice 2-5 image stacks were acquired in different fields of view in both sPyr and sRad). The resolution was 8.1 pixels/ μm (1024×1024 pixels, $126 \times 126 \mu\text{m}$) with 1 μm z-steps.

Image analysis was performed using ImageJ software, as described before (Herstel et al., 2022). We manually determined regions of interest (ROIs) around individual neuron somata. To select a representative cell population in SClm slices, in each image z-stack we selected four z-planes at comparable depths in which three pyramidal cells were identified that varied in CFP brightness (bright, middle and dark). In VGAT-Cre slices with viral SClm expression, all visible neurons were analyzed (range: 1 to 9). We subtracted the mean fluorescence intensity of the background in the same image plane before calculating the fluorescence ratio of CFP and YFP. We limited our analysis to cells which were located within 450 pixels from the center of the image, as FRET ratios showed slight aberrations at the edge of our images. We excluded cells with a FRET ratio < 0.5 or > 1.6 to avoid unhealthy cells. FRET-colored images (as shown in Fig. 2D and 9A) were made in ImageJ. We first subtracted the average background and Gaussian filtered the CFP and YFP image z-stacks separately. Next, the acceptor (YFP) image was divided by the donor (CFP) image to get the ratiometric image. A mask was created by manually drawing ROIs for each soma in the image. An average projection of the ratiometric image was made in a specific z range and multiplied by the mask. Finally, the masked ratiometric image was combined with the grayscale image. Please note that these images were made for illustration purposes only, analysis was done on the raw data.

Protein extraction and Western Blot analysis

Organotypic hippocampal cultures were washed in cold PBS and subsequently lysed in cold protein extraction buffer containing: 150 mM NaCl, 10 mM EDTA 10 mM HEPES, 1% Triton-X100 and 1x protease and 1x phosphatase inhibitors cocktails (Complete Mini EDTA-free and phosSTOP, Roche). Lysates were cleared of debris by centrifugation (14,000 rpm, 1 min, 4°C) and measured for protein concentration before storage at -20°C until use. Lysates were denatured by adding loading buffer and heating to 95°C for 5 min. For each sample an equal mass of proteins was resolved on 4–15 % polyacrylamide gel (Bio-Rad). The proteins were then transferred (300 mA, 3h) onto ethanol-activated Immobilon-P PVDF membrane (Millipore) before blocking with 3% Bovine Serum Albumin in Tris- buffered saline-Tween (TBST, 20 mM Tris, 150 mM NaCl, 0.1% Tween-20) for 1 h. Primary antibodies used in this study were: mouse anti-NKCC1 (T4, Developmental Studies Hybridoma Bank, 1:1000), rabbit anti-KCC2 (07-432, Merck, 1:1000) and s940-pKCC2 (p1551-940, LuBioSciences, 1:1000), mouse anti-tubulin (T-5168, Sigma, 1:10000). Primary antibodies were diluted in blocking buffer and incubated with the blots overnight at 4°C under gentle rotation. The membrane was

washed 3 times 15 minutes with TBST before a 1h incubation of horseradish peroxidase (HRP)-conjugated antibodies (P0447 goat anti-mouse IgG HRP, Dako, 1:2500 or P0399 swine anti-rabbit IgG HRP, Dako, 1:2500), and washed 3 times 15 minutes in TBST again before chemiluminescence detection. For chemiluminescence detection, blots were incubated with Enhanced luminol-based Chemiluminescence substrate (Promega), and the exposure was captured using the ImageQuant 800 system (Amersham). Images were analyzed in ImageJ, by drawing rectangular boxes around each band and measuring average intensities. Protein levels were normalized to the Tubulin loading controls.

Immunohistochemistry, confocal microscopy and analysis

Organotypic hippocampal cultures were fixed 4 % paraformaldehyde solution in PBS for 30 minutes at room temperature. After washing slices in phosphate buffered saline (PBS), they were permeabilized for 15 minutes in 0.5 % Triton X-100 in PBS for 15 minutes, followed by 1 hour in a blocking solution consisting of 10 % normal goat serum and 0.2 % Triton X-100 in PBS. Slices were incubated in primary antibody solution at 4 °C overnight. The following primary antibodies were used: rabbit polyclonal anti-KCC2 (07-432, Merck, 1:1000), rabbit anti-VGAT (131003, Synaptic Systems, 1:1000), guinea pig anti-VGLUT (AB5905, Merck, 1:1000), mouse anti-NeuN (MAB377, Millipore, 1:500), guinea pig anti-NeuN Merck, 1:1000).

Slices were washed in PBS and incubated in secondary antibody solution for four hours at room temperature. Secondary antibodies used were: goat anti-mouse Alexa Fluor 467 (Life Technologies, A21236, 1:500), goat anti-rabbit Alexa Fluor 405 (Life Technologies, A31556, 1:500), goat anti-guinea pig Alexa Fluor 488 (A11073, Life Technologies, 1:1000) and Goat anti-guineapig Alexa Fluor 568 (A11075, Life Technologies, 1:500) Goat anti-rabbit Alexa fluor 647 (A21245, Life Technologies, 1:500). After another PBS wash, slices were mounted in Vectashield mounting medium (Vector labs).

Confocal images were taken on a Zeiss LSM-700 confocal laser scanning microscopy system with a Plan-Apochromat 40x 1.3 NA immersion objective for KCC2 staining and 63x 1.4 NA oil immersion objective for spines and VGLUT/VGAT staining. VGLUT/VGAT staining was imaged in the CA1 sPyr and sRad of each slice, KCC2 staining was imaged in two fields of view in the CA1 sPyr of each slice and spines were imaged on the second dendritic branch of the apical dendrite of each Alexa-568 filled neuron. Image stacks (1024x1024 pixels) were acquired at 6.55 pixels/ μm for KCC2 staining, 20.15 pixels/ μm for spines and 10.08 pixels/ μm for VGLUT/VGAT staining. Step size in z was 0.5 μm for spines and KCC2 staining and 0.4 μm for VGLUT/VGAT staining.

Confocal images were blinded before analysis. The number of dendritic spines on the second dendritic branch of the apical dendrite were counted using the multi-point tool in ImageJ. As we noticed that spine density was low near the base of dendrites,

the first 10 μm of the dendrites were excluded from analysis. For analysis of VGLUT and VGAT puncta a custom-made macro was used (Ruiter et al., 2020). Briefly, three z-planes were averaged and background was subtracted with rolling ball radius of 10 pixels. Puncta were then identified using watershed segmentation. For analysis of KCC2 levels in control and VU-treated slices, ROIs were drawn around 5 NeuN positive cell bodies, and this was repeated in 1-3 z-planes (depending on the depth of KCC2 signal) at comparable depths, to measure average KCC2 fluorescence of 5-15 neurons per image stack. For analysis of KCC2 levels in slices injected with KCC2-SH-TetR-GFP virus, ROIs were drawn around 3 GFP-positive and 3 GFP-negative NeuN positive cell bodies. This was repeated another z-plane (depending on the depth of KCC2 signal) at comparable depth, to measure KCC2 fluorescence in 6-12 neurons per image stack. We determined average fluorescent intensities in the ROI as well as within the ROIs after scaling it with 10 pixels ($\sim 1 \mu\text{m}$) in width to assess both the total and membrane fraction of KCC2.

Experimental design and statistical analyses

Statistical analysis was performed in Prism (Graphpad). Normality was tested using the D'Agostino & Pearson test. For the comparison of two groups we either used an unpaired Student's t test (UT; parametric), a Mann-Whitney test (MW; non-parametric), a paired Student's t test (PT; parametric) or a Wilcoxon signed-rank test (WSR; non-parametric). For comparison of two cumulative distributions we performed a Kolmogorov Smirnov test (KS; nonparametric). For comparison of multiple groups, a one way ANOVA (1W ANOVA; parametric) was used, followed by a Sidak's Multiple Comparisons posthoc test (SMC) or a Kruskal Wallis test (KW; nonparametric) was used, followed by a Dunn's Multiple Comparison posthoc test (DMC). For comparison of two variables in multiple groups a two way ANOVA (2W ANOVA; parametric) was performed, followed by a Sidak's Multiple Comparisons posthoc test (SMC). Data are presented as mean \pm standard error of the mean. Significance is reported as * $p < 0.05$; ** $p \leq 0.01$; *** $p \leq 0.001$.

4.5 Results

The GABA shift takes place in organotypic hippocampal cultures

We assessed the development of neuronal chloride levels in organotypic hippocampal cultures made from P6-7 mouse pups using gramicidin perforated patch recordings of CA1 pyramidal neurons. We recorded GABAergic currents in response to brief applications of the GABA_A receptor agonist muscimol and determined the GABA reversal potentials at DIV2, DIV9 and DIV21 (Fig. 1A). The GABA reversal potential (E_{GABA}) and GABAergic driving force (GABA DF) decreased gradually over this period (Fig. 1B, C), indicating that intracellular chloride homeostasis was still maturing in our slice cultures (Salmon et al., 2020; Herstel et al., 2022). The resting membrane potential (RMP) remained stable (Fig. 1D).

Intracellular chloride levels are determined by the relative expression level and activity of the chloride importer NKCC1 and the chloride exporter KCC2 (Rivera et al., 1999; Gulyás et al., 2001; Yamada et al., 2004; Banke and McBain, 2006; Otsu et al., 2020). We therefore determined the contribution of KCC2 to the GABA reversal potential. Application of KCC2 blocker VU0463271 (VU) in slices at DIV2 resulted only in a small depolarizing shift of E_{GABA} (Fig. 1E), and did not affect GABA driving force (Fig. 1F), while in DIV21 slices VU application triggered an acute elevation of E_{GABA} and GABA driving force (Fig. 1G, H). This suggests that KCC2 function increased with development *in vitro*, as expected (Salmon et al., 2020). We assessed the expression levels of NKCC1 and KCC2 in our slice cultures using Western blots. As the function of KCC2 is enhanced during development by phosphorylation at serine 940 (S940) (Lee et al., 2007; Mòdol et al., 2014), we also included a phospho-specific antibody to detect phosphorylated KCC2 (pKCC2) levels. The expression of NKCC1 and KCC2 increased in our organotypic cultures between DIV2 and DIV21 (Fig. 1I-L). For comparison with the developmental trajectory *in vivo*, we determined NKCC1, KCC2 and pKCC2 levels in hippocampal tissue from P6 and adult mice. NKCC1, KCC2 and pKCC2 expression increased from P6 to adulthood (Fig. 1I-N). We noted that KCC2 and pKCC2 expression in DIV21 slice cultures did not reach adult levels (Fig. 1K-N). Together, these data show that a clear GABA shift occurred *in vitro*, which is consistent with a previous report (Salmon et al., 2020) and our own previous analysis of chloride maturation in organotypic hippocampal cultures (Herstel et al., 2022).

VU treatment depolarizes GABA driving force and elevates intracellular chloride levels at DIV9

Having established that the GABA shift occurs during the first week *in vitro*, we set out to delay the shift with one week to mimic the delayed chloride development in NDD mouse models (He et al., 2014; Tyzio et al., 2014; Deidda et al., 2015b; Banerjee et al., 2016; Corradini et al., 2017; Fernandez et al., 2018; Roux et al., 2018; Lozovaya et al., 2019; Bertoni et al., 2021). We treated slices for one week (from DIV1 to DIV8) with VU0463271 (VU), a specific blocker of the chloride exporter KCC2 (Delpire et al., 2012), or with DMSO control. One week treatment with VU from resulted in a significant elevation of E_{GABA} in CA1 pyramidal neurons immediately after the VU treatment at DIV9 (Fig. 2A). The driving force for GABA signaling (GABA DF) also shifted to positive values (Fig. 2B), which were comparable to control slices at DIV2 (Fig. 1C). This indicates that GABA signaling remained depolarizing in VU-treated slices at DIV9. We assessed intracellular chloride levels in the CA1 pyramidal cell population using the chloride sensor SuperClomeleon (SCLm) (Grimley et al., 2013; Boffi et al., 2018; Rahmati et al., 2021). The SCLm sensor consists of two fluorescent proteins, Cerulean (CFP mutant) and Topaz (YFP mutant), joined by a flexible linker. Depending on the binding of chloride, Fluorescence Resonance Energy Transfer (FRET) occurs from the CFP donor to the YFP acceptor ((Grimley et al., 2013); Fig. 2C). We measured SCLm FRET ratios (fluorescence intensity of YFP/CFP) using two-photon microscopy. Measured FRET

ratios are independent of expression level and tissue depth (Herstel et al., 2022). We observed a prominent decrease in SClm FRET values in CA1 pyramidal neurons (Fig. 2D,E), reflecting an increase in chloride levels after VU treatment. When we analyzed the distribution of individual values we observed a clear increase in the fraction of cells with low FRET ratios (Fig. 2F). Together, these data show that VU treatment between DIV1 and DIV8 resulted in an elevation of intracellular chloride levels and depolarizing GABA signaling at DIV9.

Next, we assessed whether the expression levels of the chloride cotransporters NKCC1 and KCC2 were altered after the VU treatment. We did not find any significant difference in the levels of NKCC1, KCC2 or S940-pKCC2 between VU-treated and control slices at DIV9 (Fig. 2G,H). As Western blot only allows for assessment of total KCC2 levels and cannot distinguish between cytosolic KCC2 and KCC2 in the plasma membrane, we also examined KCC2 levels in treated and control slices using immunohistochemistry. We used NeuN to identify individual cell bodies and we estimated KCC2 levels in these cells. VU treatment did not significantly affect total or membrane KCC2 levels (Fig. 2I,J). We verified with shKCC2 that we could detect changes with this method. We reduced KCC2 levels in our slices using a Lentivirus containing an inducible shKCC2 construct. Expression of shKCC2 was induced in GFP-expressing cells by doxycycline treatment, resulting in a cell-specific elevation of GABA DF (data not shown, GABA DF=12.4±9.3 mV in GFP+ cells and -11.5±2.2 mV in GFP- cells, MW, $p=0.03$). We could clearly detect the reduction in KCC2 levels in dox-treated GFP+ cells using immunohistochemistry (Fig. 2K,L). Together, this indicates that blocking KCC2 function between DIV1 and DIV8 delayed the GABA shift without changing the expression or surface levels of KCC2.

As a positive control we produced a lentivirus expressing a short hairpin RNA (shRNA) against KCC2. To transiently knock down KCC2 expression, we injected a doxycycline (dox)-inducible KCC2-SH-TetR-GFP lentivirus in P6/7 organotypic hippocampal cultures. This resulted in local virus expression in many neurons around the injection site at DIV9/10 (Fig. 2K,L). Expression of KCC2-SH-TetR-GFP in combination with dox treatment resulted in a cell specific elevation of the GABA DF (Fig. 2M-O). We verified using immunohistochemistry against KCC2 that KCC2 expression was decreased in infected (GFP+) neurons compared to (GFP-) control cells in the same slice, and that this was specific for cultures in which dox was supplemented to the culture medium (Fig. 2P). This control shows that we are able to detect changes in EGABA and KCC2 expression levels with our methods.

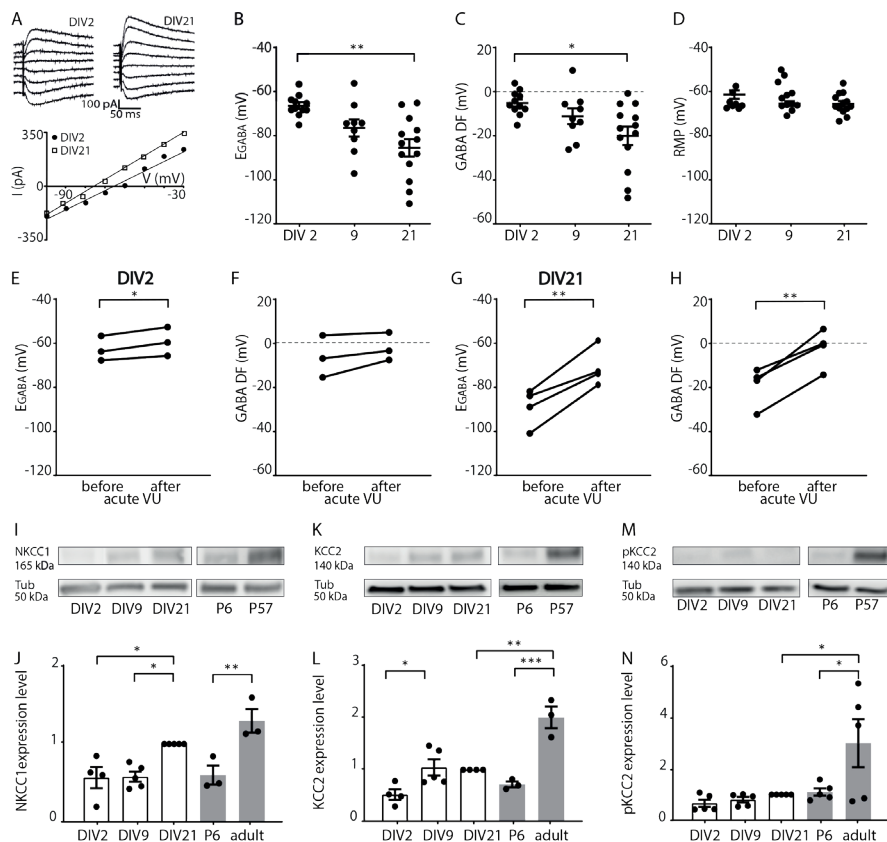


Figure 1. GABA shift is ongoing in organotypic hippocampal slice cultures.

A) Perforated patch clamp recordings in CA1 pyramidal cells in hippocampal slice cultures at DIV2 and DIV21. Responses to muscimol application were recorded at holding potentials from -100 to -30 mV with 10 mV increments and GABA reversal potential was determined from the intersection of the linear current-voltage curve with the x-axis.

B) The GABA reversal potential (E_{GABA}) recorded in cultured slices at DIV2, DIV9 and DIV21 (KW, $p=0.019$; DMC: DIV2 versus DIV9, $p=0.13$; DIV9 versus DIV21, $p=0.65$; DIV2 versus DIV21, $p=0.001$).

C) GABA Driving Force (GABA DF) during *in vitro* slice development (KW, $p=0.017$; DMC: DIV2 versus DIV9, $p=0.35$; DIV9 versus DIV21, $p=0.85$; DIV2 versus DIV21, $p=0.013$).

D) The resting membrane potential (RMP) during *in vitro* slice development (KW, $p=0.23$).

Data in B-D from 9-13 cells from 8-11 slices and 5-10 mice per group.

E,F) E_{GABA} (PT, $p=0.038$) and GABA DF (PT, $p=0.18$) values recorded in CA1 pyramidal cells at DIV2 before and after acute application of VU. Data from 3 cells, 3 slices and 3 mice per group.

G,H) E_{GABA} (PT, $p=0.009$) and GABA DF (PT, $p=0.006$) values recorded in CA1 pyramidal cells at DIV21 before and after acute application of VU. Data from 4 cells, 4 slices and 4 mice per group.

I) Western blot for NKCC1 protein content, measured in hippocampal slices cultures at DIV2, DIV9 and DIV21, and in acute slices from P6 and adult (P57) mice. Tubulin (Tub) was used as loading control.

J) Summary of data for NKCC1 expression levels. Protein levels were normalized to DIV21 values. (1W ANOVA, $p=0.0003$; SMC: DIV2 versus DIV9, $p>0.99$; DIV9 versus DIV21, $p=0.019$; DIV2 versus DIV21, $p=0.023$; DIV21 versus P57, $p=0.26$; P6 versus P57, $p=0.003$).

K) Western blot for KCC2 protein content, measured in hippocampal slices cultures at DIV2, DIV9 and DIV21, and in acute slices from P6 and adult (P57) mice. Tubulin (Tub) was used as loading control.

L) Summary of data for KCC2 expression levels. Protein levels were normalized DIV21 values. (1W ANOVA, $p<0.0001$; SMC: DIV2 versus DIV9, $p=0.045$; DIV9 versus DIV21, $p>0.99$; DIV2 versus DIV21, $p=0.10$; DIV21 versus P57, $p=0.0007$; P6 versus P57, $p=0.0001$).

M) Western blot for S940-pKCC2 (pKCC2) protein content, measured in hippocampal slices cultures at DIV2, DIV9 and DIV21, and in acute slices from P6 and adult (P57) mice. Tubulin (Tub) was used as loading control.

N) Summary of data for s940-pKCC2 (pKCC2) expression levels. Protein levels were normalized to DIV21 values. (1W ANOVA, $p=0.006$; SMC: DIV2 versus DIV9, $p>0.99$; DIV9 versus DIV21, $p>0.99$; DIV2 versus DIV21, $p=0.99$; DIV21 versus P57, $p=0.020$; P6 versus P57, $p=0.033$). Data in I-N from 3-5 experiments and 2-5 mice per group.

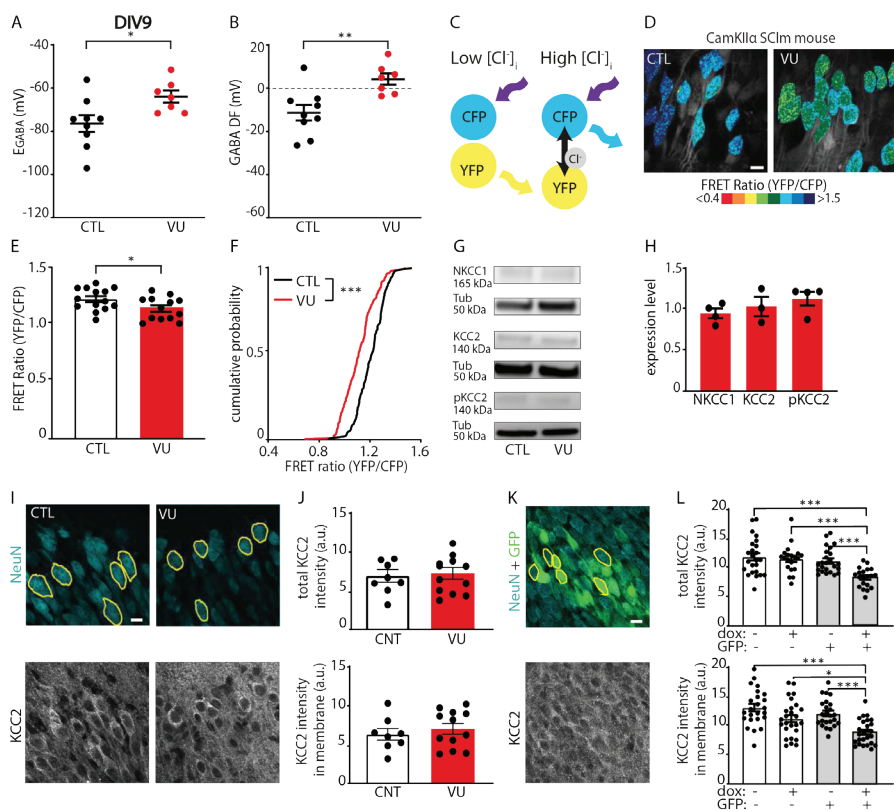


Figure 2. VU depolarizes GABA DF and increases intracellular chloride levels at DIV9.

A,B) GABA reversal potential (E_{GABA}) (MW, $p=0.016$) and GABA Driving Force (GABA DF) (MW, $p=0.005$) recorded in CA1 pyramidal cells at DIV9 in control (CTL) and VU-treated slices. Data from 7-9 cells, 6-8 slices and 3-5 animals per group.

C) Illustration of Fluorescence Resonance Energy Transfer (FRET) from CFP donor to YFP acceptor of the SCLm sensor. FRET ratios (YFP/CFP fluorescence) decrease with increasing chloride concentrations.

D) Two-photon images of SCLm FRET ratios in CA1 pyramidal neurons in CTL and VU-treated cultures at DIV9. Individual cells are color-coded to their FRET ratios. Scale bar: 10 μm .

E) Average SCLm FRET ratios in CTL and VU-treated cultures (UT, $p=0.041$). Data from 16-24 cells per slice, 13-14 slices and 6-8 mice per group.

F) Cumulative distribution of FRET ratios in individual cells in CTL and VU-treated cultures. (KS, $p<0.0001$). Data from 15 cells per slice, 13-14 slices and 6-8 mice per group.

G) Western blot of NKCC1, KCC2 and S940-pKCC2 (pKCC2) expression in CTL and VU-treated cultures. Tubulin (Tub) was used as loading control.

H) Summary of data for NKCC1, KCC2 and for s940-pKCC2 (pKCC2) expression levels at DIV9. Values in VU-treated cultures were normalized to the protein level in CTL cultures (NKCC1: MW, $p>0.99$; KCC2: MW, $p=0.70$; pKCC2: MW, $p=0.31$).

I) Confocal images of NeuN and KCC2 staining in CTL and VU-treated cultures with ROIs in yellow. Scale bar: 10 μm .

J) Total KCC2 levels (UT, $p=0.78$) and KCC2 levels in membrane (UT, $p=0.51$) in CTL and VU-treated cultures at DIV9. Each datapoint represents the mean KCC2 intensity of the 5-15 ROIs in one image. Data from 8-12 images, 4-6 slices and 3 mice per group.

K) Confocal images of NeuN and KCC2 staining in slices were infected with KCC2-SH-TetR-eGFP Lentivirus. Expression of shKCC2 was induced in GFP+ cells by doxycycline (dox) treatment.

L) Upper panel: Total KCC2 intensity in KCC2-SH-TetR-GFP positive and negative CA1 pyramidal neurons in slice cultures with or without dox treatment at DIV9 (KW, $p<0.0001$; DMC: GFP- dox- versus GFP- dox+, $p>0.99$; GFP- dox- versus GFP+ dox-, $p>0.99$; GFP- dox- versus GFP+ dox+, $p=0.0001$; GFP- dox+ versus GFP+ dox-, $p>0.99$; GFP- dox+ versus GFP+ dox+, $p=0.0003$; GFP+ dox- versus GFP+ dox+, $p=0.009$). Lower panel: KCC2 intensity in membrane in KCC2-SH-TetR-GFP positive and negative CA1 pyramidal neurons in slice cultures with or without dox treatment at DIV9 (KW, $p<0.0001$; DMC: GFP- dox- versus GFP- dox+, $p=0.20$; GFP- dox- versus GFP+ dox-, $p>0.99$; GFP- dox- versus GFP+ dox+, $p<0.0001$; GFP- dox+ versus GFP+ dox-, $p>0.99$; GFP- dox+ versus GFP+ dox+, $p=0.032$; GFP+ dox- versus GFP+ dox+, $p=0.0006$). Data from 23-24 cells, 3-4 slices and 3 mice per group.

Synaptic inputs and firing properties of CA1 pyramidal cells are not affected at DIV9 after VU treatment

Previous experimental studies in which the GABA shift was accelerated showed that depolarizing GABA facilitates excitatory synapse formation (Leinekugel et al., 1997; Akerman and Cline, 2006; Wang and Kriegstein, 2008, 2011; Chancey et al., 2013; van Rheede et al., 2015; Oh et al., 2016). This would predict that delaying the GABA shift, e.g. prolonging the period when GABA signaling is depolarizing, would result in an excess synapse growth.

To assess functional synapses, we recorded sEPSCs and sIPSCs in CA1 pyramidal cells using whole-cell patch clamp recordings (Fig. 3A,B). We found that sEPSC frequency, amplitudes, and kinetics were not different in CA1 pyramidal cells in VU-treated and control slices at DIV9 (Fig. 3C-F). There were also no changes in sIPSCs (Fig. 3G-J). In addition, we recorded action potential (AP) firing rates during current injections of increasing amplitude (Fig. 3K). Firing rates, resting membrane potential and action potential threshold were comparable in control and VU-treated slices (Fig. 3L-N).

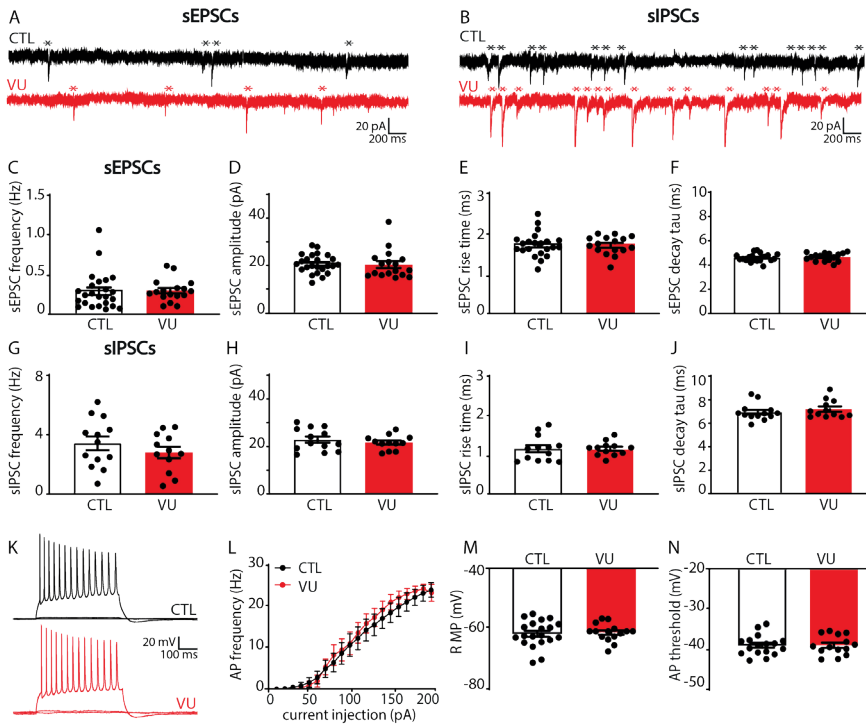


Figure 3. VU treatment does not change excitatory or inhibitory transmission and firing properties at DIV9.

A) sEPSC recordings from CA1 pyramidal cells in a control (CTL) and VU-treated culture at DIV9. sEPSCs are indicated with asterisks.

B) sIPSC recordings in CTL and VU-treated cultures at DIV9. sIPSCs are indicated with asterisks.

C-F) sEPSC frequency (MW, $p=0.36$), amplitude (MW, $p=0.45$), risetime (UT, $p=0.87$) and decay tau (UT, $p=0.53$) in CTL and VU-treated cultures at DIV9. Data from 16-24 cells, 11-15 slices and 10-12 mice per group.

G-J) sIPSC frequency (UT, $p=0.32$), amplitude (UT, $p=0.46$), risetime (UT, $p=0.99$) and decay tau (UT, $p=0.20$) in CTL and VU-treated cultures at DIV9. Data from 12-13 cells, 4-7 slices and 4-6 mice per group.

K) Example recordings of action potentials during current injections in CA1 pyramidal neurons in CTL and VU-treated cultures at DIV9.

L) Action potential firing rates in CTL and VU-treated cultures with increasing current injections at DIV9 (2W ANOVA, current injection: $p<0.001$, treatment: $p=0.24$). Data from 14-17 cells, 10-11 slices and 9-10 mice per group.

M,N) Resting membrane potential (RMP) (UT, $p=0.75$) and action potential (AP) threshold (UT, $p=0.98$) in CTL and VU-treated cultures at DIV9. Data from 14-20 cells, 10-11 slices and 9-10 mice per group.

Additionally, we assessed synaptic density by performing immunohistochemistry on VU-treated and control slices. Consistent with our electrophysiological data, the density and size of VGLUT and VGAT puncta in the *stratum Pyramidale* (sPyr) and *stratum Radiatum* (sRad) of the CA1 area were similar in VU-treated and control slices at DIV9 (Fig. 4A-J). Furthermore, we filled pyramidal neurons with Alexa-568 via a patch pipette to assess dendritic spines at which excitatory synapses are located (Sheng and Hoogenraad, 2007). Spine density of CA1 pyramidal neurons was similar in control and VU-treated slices (Fig. 4K,L).

Together, these data show that VU treatment from DIV1 to DIV8 induced a clear depolarizing shift in GABA signaling, but this did not affect excitatory and inhibitory synapses and firing properties in CA1 pyramidal cells at DIV9.

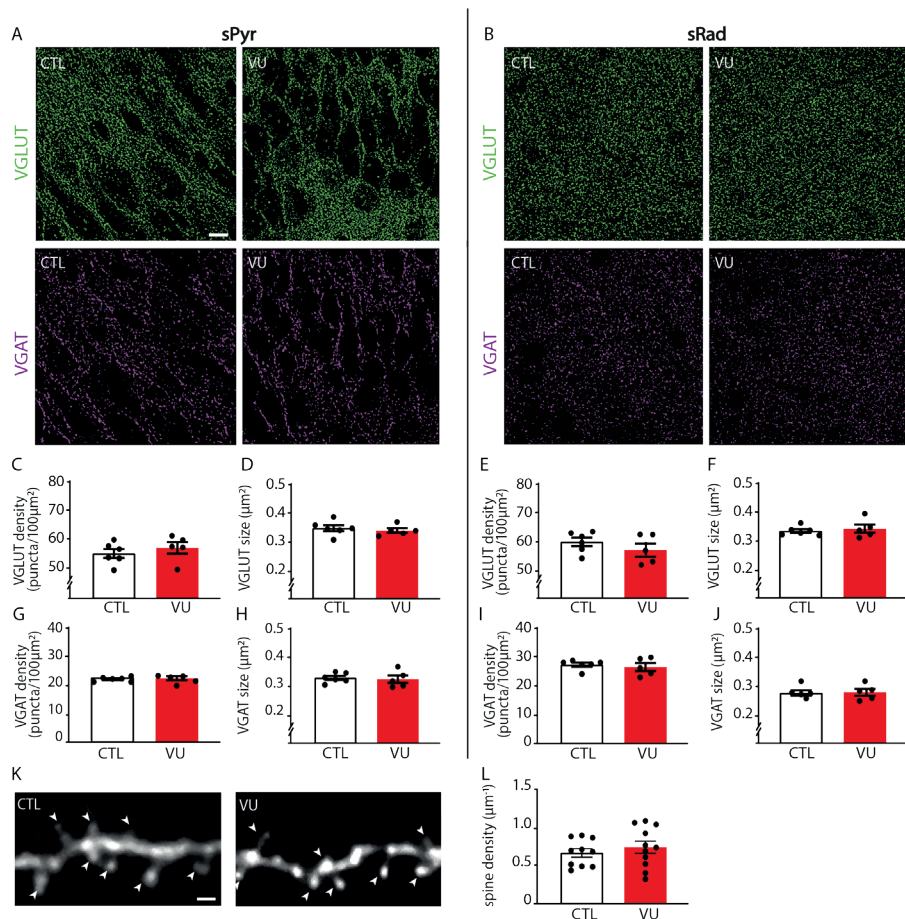


Figure 4. VU treatment does not change excitatory or inhibitory synapses at DIV9.

A,B) Thresholded images of VGLUT and VGAT puncta in the CA1 sPyr and sRad of control (CTL) and VU-treated cultures at DIV9. Scale bar: 10 µm.

C,D) Density (MW, $p=0.43$) and size (MW, $p=0.33$) of VGLUT puncta in the sPyr in CTL and VU-treated cultures at DIV9.

E,F) Density (MW, $p=0.27$) and size (MW, $p=0.83$) of VGLUT puncta in the sRad.

G,H) Density (MW, $p=0.96$) and size (MW, $p=0.54$) of VGAT puncta in the sPyr.

I,J) Density (MW, $p=0.89$) and size (MW, $p=0.84$) of VGAT puncta in the sRad. Data in C-J from 5-6 slices and 4-5 mice per group.

K) Example images of the apical dendrite of CA1 pyramidal neurons in CTL and VU-treated cultures at DIV9. Spines are indicated with arrowheads. Scale bar: 1 µm.

L) The average density of dendritic spines (UT, $p=0.82$) in CTL and VU-treated cultures at DIV9. Data from 10-11 cells, 6-8 slices and 6 mice per group.

Depolarizing GABA signaling in VU-treated slices acts inhibitory

As eluded to above, it is important to note that depolarizing GABA signaling does not necessarily mean that GABA acts inhibitory. Depolarizing GABA can have an inhibitory action and limit neuronal activity when the GABA-mediated depolarization is subthreshold and shunts excitatory inputs (Staley and Mody, 1992; Kirmse et al., 2015; Murata and Colonnese, 2020; Salmon et al., 2020). We noticed that during the sEPSC recordings, when GABA_A-mediated inhibitory currents were blocked with gabazine, network discharges often occurred. These discharges probably reflect periods of synchronous firing of pyramidal cells that can occur in the absence of fast GABA_A-mediated inhibition, when only the slower GABA_B-mediated inhibition is left to counteract excitatory synaptic transmission (Scanziani et al., 1994; Menendez De La Prida et al., 2006). The frequency and duration of these network discharges were not different in VU-treated and control slices at DIV9 (Fig. 5A-C). We directly assessed if depolarizing GABA was already inhibitory in our VU-treated slices. To determine the role of GABA in regulating action potential firing, we washed in GABA_A receptor agonist muscimol while recording spontaneous firing in cell-attached configuration. As spontaneous activity of hippocampal neurons is very low in standard artificial cerebral spinal fluid (ACSF), we used a modified ACSF with higher K⁺ and lower Ca²⁺ and Mg²⁺ levels, which elevates spontaneous firing (Maffei et al., 2004). Muscimol inhibited firing in control as well as in VU-treated slices at DIV8 (Fig. 5D-F). This indicates that GABA_A receptor-mediated signaling is inhibitory in both control and VU-treated slices at DIV8, despite being hyperpolarizing in control and depolarizing in VU-treated slices (Fig. 2B). This suggests that GABA signaling mostly acts inhibitory in hippocampal slice cultures from P6-7 mice, which is in line with previous reports in P6-9 acute hippocampal slices (Khalilov et al., 1997; Valeeva et al., 2016), cultured hippocampal slices at P5 DIV3-5 (Salmon et al., 2020) and *in vivo* recordings in the hippocampus after P3-7 (Valeeva et al., 2010; Murata and Colonnese, 2020). Together, our data suggest that depolarizing GABA signaling after the first postnatal week acts mostly inhibitory and does not contribute to synapse formation in the hippocampus.

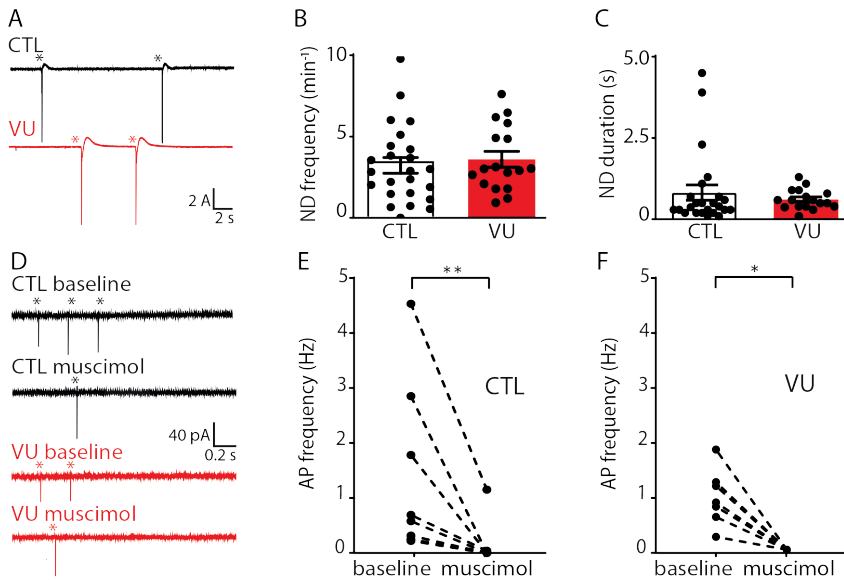


Figure 5. GABA is inhibitory in control and VU-treated slice cultures at DIV8 and DIV9.

A) Whole-cell voltage clamp recordings from CA1 pyramidal cells in the presence of gabazine in control (CTL) and VU-treated cultures at DIV9. Network discharges are indicated with asterisks. B,C) Network discharge (ND) frequency (MW, $p=0.61$) and duration (MW, $p=0.20$) in CTL and VU-treated cultures at DIV9. Data from 17-24 cells, 11-15 slices and 10-12 mice per group. D) Cell-attached recordings from CA1 pyramidal cells showing action potential (AP) firing in modified ACSF in CTL and VU-treated cultures at DIV8 before (baseline) and after muscimol wash in. APs are indicated with asterisks. E, F) Average AP frequency before and after muscimol wash in CTL and VU-treated cultures at DIV8. Muscimol decreases firing rates in CTL (WSR, $p=0.008$) and VU-treated (WSR, $p=0.016$) cultures at DIV8. Data from 7-8 cells, 7-8 slices and 3-4 mice per group. A MW was performed to compare baseline firing rates in CTL and VU-treated cultures (MW, $p=0.79$).

Indirect effects on inhibitory synaptic inputs in VU-treated slices at DIV21

Previous studies demonstrated that transient alterations in GABA function during early postnatal development can have long-lasting consequences for network function and ultimately behavior (He et al., 2018; Bertoni et al., 2021; Matsushima et al., 2022). We therefore assessed possible long-lasting consequences of the VU treatment on the CA1 network at DIV21. After DIV8, the VU treatment was stopped and cultures were maintained in normal medium until DIV21. We verified that at DIV21, E_{GABA} and GABA DF in CA1 pyramidal neurons in VU-treated slices were back to control levels (Fig. 6A,B), indicating that chloride levels were fully restored.

We performed whole-cell recordings in CA1 pyramidal cells to record sEPSCs and sIPSCs (Fig. 6C,D). Similar to DIV9, we found no differences in sEPSCs between control and VU-treated slices at DIV21 (Fig. 6E-H). Surprisingly, we observed that sIPSC frequency in VU-treated slices was increased compared to control slices at DIV21 (Fig. 6I), whereas sIPSC amplitudes were not different (Fig. 6J). When we analyzed the kinetics of the individual sIPSCs we noticed that sIPSCs in VU-treated slices had slightly larger rise times compared to control (Fig. 6K), while decay times were not different (Fig. 6L). The IPSC rise time depends on the location of synapse where the current originates from, with somatic synapses generating currents with faster rise times while currents from dendritic synapses will be slower due to dendritic filtering (Rall, 1967; Bekkers and Clements, 1999; Wierenga and Wadman, 1999; Ruitter et al., 2020). When we split slow and fast sIPSCs (Ruitter et al., 2020), we observed that the increase was most prominent in slow sIPSCs (Fig. 6M-P), possibly reflecting an increase in IPSCs originating from dendritic synapses.

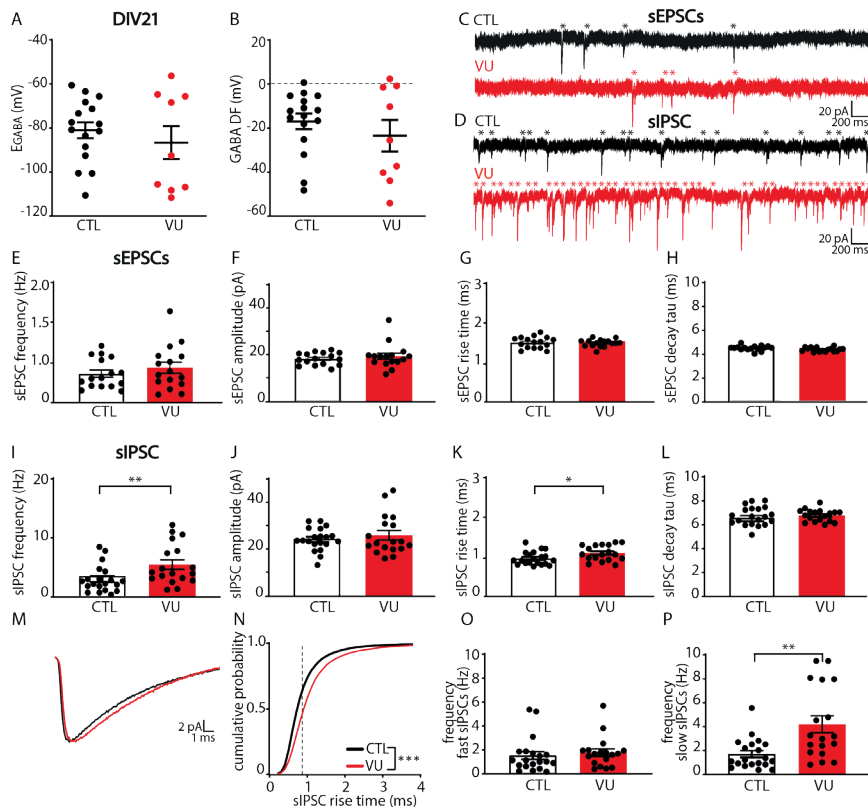


Figure 6. VU treatment does not affect excitatory transmission, but increases spontaneous inhibitory transmission at DIV21.

A,B) GABA reversal potential (E_{GABA}) (MW, $p=0.56$) and GABA Driving Force (GABA DF) (MW, $p=0.76$) recorded in CA1 pyramidal cells in control (CTL) and VU-treated cultures at DIV21, two weeks after cessation of treatment. Data from 9-16 cells, 3-10 slices and 3-10 mice per group.

C, D) sEPSC and sIPSC recordings from CA1 pyramidal cells in CTL and VU-treated cultures at DIV21. sEPSCs and sIPSCs are indicated with asterisks.

E-H) sEPSC frequency (UT, $p=0.26$), amplitude (MW, $p=0.59$), risetime (UT, $p=0.80$) and decay tau (UT, $p=0.94$) in CTL and VU-treated cultures at DIV21. Data from 16 cells, 9 slices and 9 mice per group.

I-L) sIPSC frequency (MW, $p=0.006$), amplitude (UT, $p=0.52$), risetime (UT, $p=0.026$) and decay tau (UT, $p=0.37$) in CTL and VU-treated cultures at DIV21.

M) Average sIPSC recorded in CA1 pyramidal cells in CTL and VU-treated cultures at DIV21.

N) Cumulative distribution of sIPSC risetimes in control and VU-treated cultures at DIV21 (KS, $p<0.0001$). Dotted line indicates value used to split fast from slow rise time sIPSCs.

O) Frequency of fast sIPSCs in CTL and VU-treated cultures at DIV21 (MW, $p=0.20$).

P) Frequency of fast slow sIPSCs in CTL and VU-treated cultures at DIV21 (MW, $p=0.003$). Data in I-P from 18-20 cells, 11-12 slices and 8-9 mice per group.

To assess whether the increase in inhibitory transmission after VU was activity dependent, we also measured mIPSCs in control and VU-treated slices at DIV21. We found that mIPSCs were not different in VU-treated and control slices (Fig. 7A-D), suggesting that VU treatment increased activity-dependent GABA release at DIV21. To assess possible changes in synaptic density, we determined the density and size of VGLUT and VGAT puncta in the CA1 area and we found no differences between control and VU-treated slices, both in sPyr and sRad (Fig. E-L). Spine density in CA1 pyramidal neurons was also not different in control and VU-treated slices at DIV21 (Fig. 7M,N). This indicates that excitatory and inhibitory synaptic density remained unaffected 14 days after the VU treatment and suggests that the observed increase in sIPSC frequency is due to an increased activity-dependent release from GABAergic terminals, possibly preferentially at dendritic inhibitory synapses.

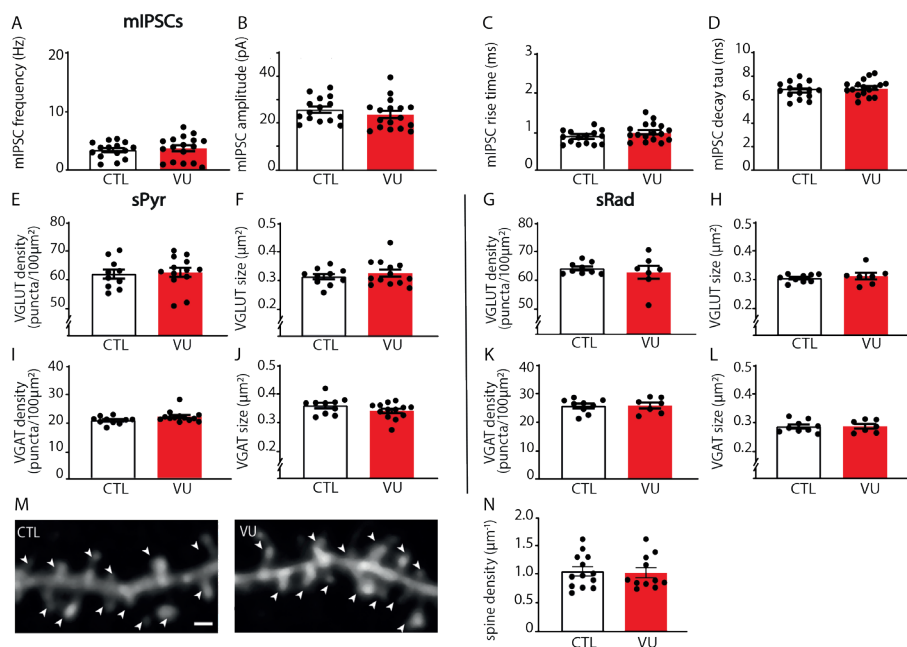


Figure 7. VU treatment does not affect mIPSCs, or excitatory and inhibitory synapses at DIV21.

A-D) mIPSC frequency (UT, $p=0.60$), amplitude (UT, $p=0.34$), risetime (UT, $p=0.077$) and decay tau (UT, $p=0.40$) recorded from CA1 pyramidal cells in CTL and VU-treated cultures at DIV21. Data from 15-17 cells, 9-12 slices and 6-9 mice per group.

E,F) Density (UT, $p=0.80$) and size (UT, $p=0.61$) of VGLUT puncta in the sPyr in CTL and VU-treated slices at DIV21.

G,H) Density (MW, $p=0.91$) and size (MW, $p=0.76$) of VGLUT puncta in the stratum Radiatum (sRad).

I,J) Density (MW, $p=0.078$) and size (UT, $p=0.14$) of VGAT puncta in the sPyr.

K,L) Density (MW, $p=0.76$) and size (MW, $p>0.99$) of VGAT puncta in the sRad. Data in E-L from 10-13 slices and 6-7 mice per group.

M) Maximal projection of confocal images of the apical dendrite of DIV21 CA1 pyramidal neurons in CTL and VU-treated cultures. Spines are indicated with arrowheads. Scale bar: $1 \mu\text{m}$.

N) Dendritic spine densities in control and VU-treated cultures at DIV21 (MW, $p=0.77$). Data from 10-11 cells, 8 slices and 7-8 mice per group.

Network discharges during sEPSC recordings were rare at DIV21 and not different between control and VU-treated slices (Fig. 8A-C). One week VU treatment did not affect firing properties (Fig. 8D,E) or resting membrane potential (RMP) (Fig. 8F) of CA1 pyramidal neurons at DIV21, but we observed a slight elevation of the action potential (AP) threshold in VU-treated slices at DIV21 (Fig. 8G). The relative AP threshold (defined as the difference between AP threshold and RMP, Fig. 8H) was not different VU-treated and control pyramidal cells. It is noteworthy that the AP threshold was not different when we recorded with high chloride internal solution, which resulted

in a more negative AP threshold (DMSO -41.9 ± 3.3 mV; VU -42.9 ± 3.4 mV; UT, $p=0.45$; data not shown). A similar decrease in AP threshold after chloride loading was recently described in CA3 pyramidal neurons (Sørensen et al., 2017), but the mechanism remained unresolved.

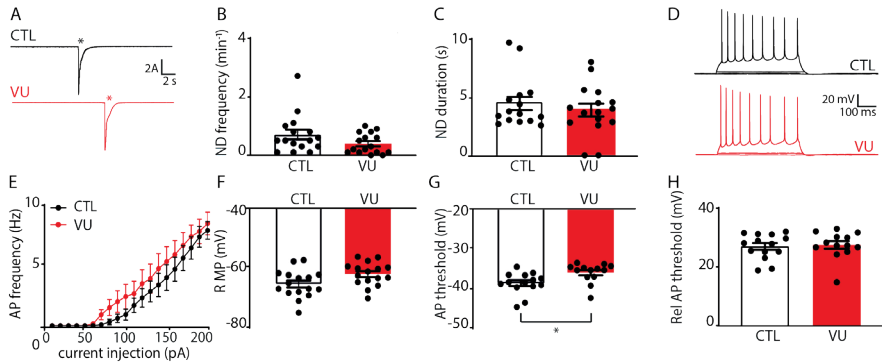


Figure 8. VU treatment increases the firing threshold of pyramidal neurons at DIV21.

A) Whole-cell voltage clamp recordings from CA1 pyramidal cells in control (CTL) and VU-treated cultures at DIV21, in the presence of gabazine. Network discharges are indicated with asterisks.

B, C) Network discharge (ND) frequency (MW, $p=0.14$) and duration (MW, $p=0.20$) in CTL and VU-treated cultures at DIV21. Data from 16 cells, 9 slices and 9 mice per group.

D) Whole-cell current clamp recordings of action potentials after current injections in CA1 pyramidal neurons in CTL and VU-treated cultures at DIV21.

E) Action potential firing rates in CTL and VU-treated cultures with increasing current injections at DIV21 (2W ANOVA, current injection: $p<0.001$, treatment: $p=0.36$). Data from 13-14 cells, 9 slices and 9 mice per group.

F-H) Resting membrane potential (RMP) (UT, $p=0.75$), action potential (AP) threshold (MW, $p=0.006$), and relative action potential (Rel AP) threshold (MW, $p=0.72$) in CTL and VU-treated cultures at DIV21. Data from 13-16 cells, 9 slices and 9 mice per group.

VU treatment does not affect chloride levels in interneurons at DIV9 or DIV21

Our data suggest that VU treatment specifically affected activity-dependent GABAergic transmission from interneurons to pyramidal neurons. We wondered if VU treatment affected chloride concentrations in inhibitory neurons in the same way as in pyramidal neurons. We therefore expressed the chloride sensor SClm (Grimley et al., 2013) specifically in GABAergic interneurons, using a Cre-dependent adeno associated virus (Boffi et al., 2018) in slices from VGAT-Cre mice. We measured SClm FRET ratios in cell bodies of GABAergic interneurons in sRad and sPyr (Fig. 9A). We observed that FRET values in interneurons were much lower compared to pyramidal cells at DIV9 (Fig. 2E), and clearly increased between DIV9 and DIV21 (Fig. 9B,C), reflecting

a decrease of intracellular chloride levels with development. This was remarkable as we previously showed that chloride levels in pyramidal neurons are already mature at DIV9 and remain relatively stable during this period (Herstel et al., 2022). When we normalized FRET ratios at DIV21 to DIV9 for interneurons and pyramidal neurons, the relative increase was $1.33 \pm 0.03\%$ in interneurons compared to $1.02 \pm 0.03\%$ in pyramidal neurons (UT, $p < 0.0001$). This suggests that the GABA shift occurs later in inhibitory neurons compared to excitatory neurons in the CA1 area, which is in line with previous reports (Patenaude et al., 2005; Otsu et al., 2020). Interestingly, and in clear contrast to pyramidal neurons (Fig. 2G,F), VU treatment from DIV1 to DIV8 did not affect SClm FRET values in interneurons at DIV9 (Fig. 9B-E), suggesting that the contribution of KCC2 to chloride levels in interneurons was minimal during the treatment period. FRET ratios increased similarly to DIV21 in VU-treated and control slices (Fig. 9B-E). These results indicate that the one week VU treatment had a differential effect on intracellular chloride levels in CA1 pyramidal and interneurons, probably because of cell type-specific timing of chloride maturation.

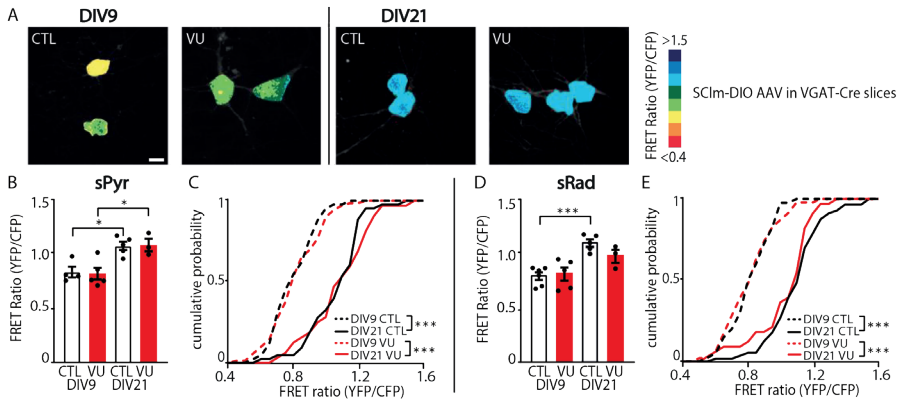


Figure 9. VU treatment does not change chloride concentrations in VGAT positive interneurons.

A) Images of SClm FRET ratios in CA1 sRad GABAergic interneurons in control (CTL) and VU-treated slices from VGAT-Cre mice at DIV9 and 21. Scale bar: 10 μm .

B) Average SClm FRET ratio in interneurons in the CA1 sPyr in CTL and VU-treated cultures at DIV9 and DIV21 (1W ANOVA, $p=0.002$; SMC: DIV9 DMSO versus DIV9 VU, $p=0.99$; DIV9 DMSO versus DIV21 DMSO, $p=0.015$; DIV9 VU versus DIV21 VU, $p=0.015$; DIV21 DMSO versus DIV21 VU, $p=0.97$).

C) Cumulative distribution of FRET ratios in individual sPyr interneurons in CTL and VU-treated cultures (KS, $p<0.0001$). Data in B,C from 32-69 cells, 3-5 slices and 3 mice per group.

D) Average SClm FRET ratio in interneurons in the CA1 sRad in CTL and VU-treated cultures at DIV9 and DIV21 (1W ANOVA, $p=0.02$; SMC: DIV9 DMSO versus DIV9 VU, $p=0.77$; DIV9 DMSO versus DIV21 DMSO, $p=0.0007$; DIV9 VU versus DIV21 VU, $p=0.12$; DIV21 DMSO versus DIV21 VU, $p=0.23$). An additional 1W ANOVA was performed to compare FRET ratios of individual cells in DIV9 VU versus DIV21 VU cultures and DIV21 DMSO versus DIV21 VU cultures (1W ANOVA, $p<0.0001$; SMC: DIV9 VU versus DIV21 VU, $p<0.0001$; DIV21 DMSO versus DIV21 VU, $p=0.37$).

E) Cumulative distribution of FRET ratios in individual interneurons the CA1 sRad VU-treated (KS, $p<0.0001$) and VU-treated cultures (KS, $p<0.0001$). An additional KS was performed to compare the distribution of FRET ratios in CTL and VU-treated cultures at DIV21 (KS, $p=0.63$). Data in D,E from 33-56 cells, 3-6 slices and 2-3 mice per group.

VU treatment results in elevated membrane potential in sRad interneurons at DIV21

As sIPSC frequency was increased in VU-treated slices at DIV21, while mIPSCs and VGAT puncta were unaffected, we wondered if release probability at GABAergic synapses was increased. We therefore assessed paired-pulse ratios (PPR) of evoked IPSCs in CA1 pyramidal cells after stimulation with an extracellular electrode in the sPyr or sRad (Fig. 10A), but PPR of IPSCs was similar in VU-treated and control slices (Fig. 10B,C). We also determined the coefficient of variation of the first IPSCs, another parameter that is dependent on release probability, but we did not find any difference between VU-treated and control slices (Fig. 10D,E). This suggests that IPSC release probability was not affected by VU treatment. We therefore wondered if the increase in sIPSC frequency in VU-treated slices could be due to an increased activity of GABAergic

cells at DIV21. Based on our observation of a specific increase in sIPSC with slow rise times in VU-treated slices (Fig. 6M-P), we focused on dendritically targeting GABAergic cells in the sRad. We performed whole-cell patch clamp recordings from GFP-labeled interneurons in the sRad in slices from GAD65-GFP mice, which are mostly reelin-positive and preferentially target pyramidal dendrites (Wierenga et al., 2008, 2010). We found that sEPSCs (Fig. 10F-H), and general firing properties (Fig. 10I,J) of sRad interneurons were not different in VU-treated and control slices at DIV21. Intriguingly, we observed that in VU-treated slices resting membrane potential of the GFP-labeled interneurons was slightly elevated (Fig. 10K). The AP threshold was not significantly altered (Fig. 10L), but the relative action potential threshold was lower in VU-treated slices compared to control (Fig. 10M). Input resistance was not different (DMSO $271.1 \pm 12.8 \text{ M}\Omega$; VU $244.2 \pm 13.2 \text{ M}\Omega$; UT, $p=0.15$). Together, this suggests that sRad interneurons in VU-treated slices receive normal excitatory synaptic input at DIV21, but that less input current is required to reach their firing threshold. We propose that this subtle alteration in membrane excitability contributes to the elevated sIPSC frequency that we observed after VU treatment at DIV21.

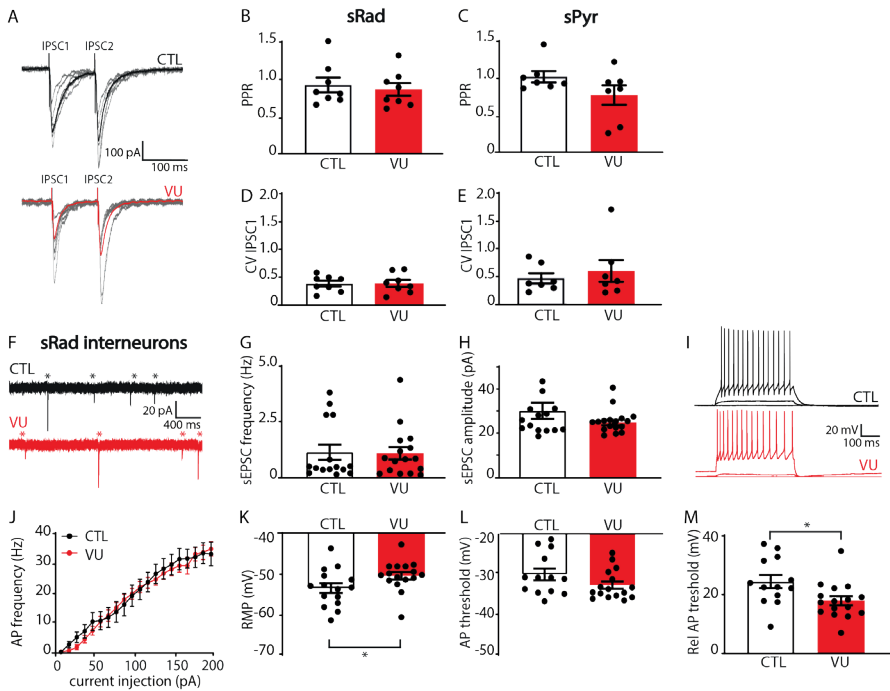


Figure 10. VU treatment results in elevated resting membrane potentials in sRad interneurons at DIV21.

A) Whole-cell voltage clamp recordings of evoked IPSCs in control (CTL) and VU-treated cultures at DIV21. Stimulation electrode was placed in the sRad. Average evoked IPSCs are shown in bold, individual traces are shown in grey.

B, C) Paired pulse ratios (PPR; IPSC2/IPSC1 amplitudes) evoked in sRad (MW, $p=0.65$) and sPyr (MW, $p=0.21$) in CTL and VU-treated cultures at DIV21.

D, E) Coefficient of variation (CV) of the first IPSCs evoked in sRad (MW, $p=0.96$) and sPyr (MW, $p=0.80$) in CTL and VU-treated cultures at DIV21. Data in B-E from 7-8 cells, 4-6 slices and 3-5 mice per group.

F) sEPSC recording in GFP-labeled interneurons in sRad from control (CTL) and VU-treated cultures from GAD65-GFP mice at DIV21. sEPSC are indicated with asterisks.

G, H) sEPSC frequency (MW; $p=0.85$) and amplitude (MW; $p=0.38$) in these interneurons. Data from 15-16 cells, 11 slices and 10 mice per group.

I) Whole-cell current clamp recordings of action potentials after current injections in sRad interneurons in CTL and VU-treated cultures at DIV21.

J) Action potential firing rates in sRad interneurons in CTL and VU-treated cultures at DIV21 (2W ANOVA, current injection: $p<0.001$, treatment: $p=0.42$).

K-M) Resting membrane potential (RMP) (MW, $p=0.023$), action potential (AP) threshold (UT, $p=0.11$), relative action potential (Rel AP) threshold (MW, $p=0.012$) in sRad interneurons in CTL and VU-treated cultures at DIV21. Data in J-M from 13-16 cells, 11 slices and 10 mice per group.

4.6 Discussion

There is accumulating evidence that the developmental GABA shift is often delayed in NDD patients (Talos et al., 2012; Duarte et al., 2013; Merner et al., 2015; Tang et al., 2016; Ruffolo et al., 2018; Wang et al., 2021; Birey et al., 2022) and in NDD animal models (He et al., 2014; Tyzio et al., 2014; Deidda et al., 2015b; Banerjee et al., 2016; Corradini et al., 2017; Fernandez et al., 2018; Roux et al., 2018; Lozovaya et al., 2019; Bertoni et al., 2021). Here, we used organotypic hippocampal cultures to examine the consequences of a delayed GABA shift for the developing CA1 network using the specific KCC2 blocker VU0463271 (VU). VU treatment between DIV1 and DIV8 increased intracellular chloride levels without affecting chloride transporter expression levels, thereby effectively delaying the GABA shift in CA1 pyramidal neurons. We found that VU treatment did not have a direct effect on synaptic currents and firing properties of CA1 pyramidal cells at DIV9. However, at DIV21, when chloride levels were fully normalized, we observed a remarkable increase in sIPSC frequency compared to control slices, while synapse numbers remained unaffected. We found that firing thresholds in CA1 pyramidal neurons were slightly elevated while dendrite-targeting interneurons showed an elevated resting membrane potential and lower firing threshold at DIV21. Together, this shows that a delay in the postnatal GABA shift does not directly affect synaptic development, but rather leads to indirect, cell type-specific changes in membrane properties that may contribute to altered network activity at a later time point.

In this study we used organotypic hippocampal cultures as a model system to study postnatal development. We demonstrate that the GABA shift occurs in slice cultures around the same time as it does *in vivo* (Valeeva et al., 2016; Sulis Sato et al., 2017; Murata and Colonnese, 2020; Salmon et al., 2020; Herstel et al., 2022). As previously reported, synapses continue to develop in these cultured slices. Indeed, sEPSC frequency and density of VGGLUT puncta and density of spines increased from DIV9 to DIV21 (De Simoni et al., 2003; Berry et al., 2012), while sEPSC amplitude decreased (De Simoni et al., 2003) and the frequency of sIPSCs and density of puncta VGAT remained mostly stable (De Simoni et al., 2003). VU treatment from DIV1 to DIV8 resulted in increased chloride levels in CA1 pyramidal cells at DIV9, that were comparable to untreated slices at DIV2. This indicates that the VU treatment effectively delayed chloride maturation and maintained depolarizing GABA signaling up to DIV9. Chloride maturation in interneurons occurs later compared to pyramidal cells and remained unaffected by the VU treatment. Importantly, VU treatment blocked KCC2 function without altering expression levels of the protein. This suggests that VU treatment altered intracellular chloride levels in pyramidal cells without interfering with the structural role of KCC2 proteins in spines (Li et al., 2007; Gauvain et al., 2011; Fiumelli et al., 2013; Chevy et al., 2015; Puskarjov et al., 2017; Awad et al., 2018; Kesaf et al., 2020), although we can never exclude that blocking chloride transport changes how KCC2 interacts with other proteins (Mahadevan et al., 2017; Smalley et al., 2020). Our experimental design

therefore allowed for selectively testing how intracellular chloride concentrations influence the developing CA1 network.

The first key finding from this study is that maintaining depolarizing GABA signaling until DIV9 did not have any direct effects on excitatory and inhibitory synaptic structure or function. Previous groundbreaking research has demonstrated that excitatory GABAergic signaling during prenatal and perinatal development promotes synapse formation and maturation (Leinekugel et al., 1997; Akerman and Cline, 2006; Nakanishi et al., 2007; Wang and Kriegstein, 2008, 2011; van Rheede et al., 2015; Oh et al., 2016). These studies were performed before P8, or when the GABA shift was accelerated. Our slices are made from P6-7 pups, when GABA signaling is still depolarizing. Here we show that prolonging the period of depolarizing GABA signaling during the second postnatal week does no longer affect synapse formation. We did not observe any difference in synapse number between control and VU-treated slices, at DIV9 nor at DIV21. This was corroborated by a parallel study, in which we treated slices for one week with furosemide (Peerboom et al, in preparation). These observations suggest that the synapse-promoting effect of depolarizing GABA signaling is restricted from embryonic development up to the first postnatal week.

Comparing our current results with previous literature suggests that the effect of chloride manipulation critically depends on whether GABAergic signaling is excitatory or inhibitory for network activity, which is only indirectly related to E_{GABA} . The effect of GABA signaling under physiological conditions does not only depend on the relation between E_{GABA} and the AP threshold, but also on the spatiotemporal distribution of glutamatergic and GABAergic inputs (Staley and Mody, 1992; Gao et al., 1998; Morita et al., 2006; Le Magueresse and Monyer, 2013; Kilb, 2021). With more (excitatory) synaptic activity, shunting inhibition will become more prominent (Woodruff et al., 2011; Branchereau et al., 2016). This means that the precise consequences of alterations in the postnatal GABA shift depend on the effect on local network activity (Wang and Kriegstein, 2011; Seja et al., 2012; Deidda et al., 2015a; Pisella et al., 2019). In our slices, even when GABA signaling was kept depolarizing, GABA signaling already had an inhibitory action on cellular and network activity. Although E_{GABA} in VU-treated slices was depolarized relative to RMP at DIV9 (Fig. 2B), it remained well below AP threshold (Fig. 3N). As a result, GABA signaling was inhibitory in both control and VU-treated slices (Fig. 5). It should be noted that we measured inhibitory GABA signaling after elevating network activity with modified ACSF, may have skewed GABAergic function towards more inhibitory action via activity-induced chloride changes (Raimondo et al., 2012; Branchereau et al., 2016; Kilb, 2021). However, network discharges were also observed in DMSO and VU treated slices during sEPSC recordings in normal ACSF (Fig. 5A), indicating a similar inhibitory action. Our results are in line with previous reports which argue that depolarizing GABAergic signaling is inhibitory in hippocampal slices from approximately P6-9 (Khalilov et al., 1997; Valeeva et al., 2016; Salmon et

al., 2020). Also in the hippocampus of living mice, depolarizing GABA was found to inhibit activity in the hippocampus from P7 onwards (Valeeva et al., 2010; Murata and Colonnese, 2020). This suggests that the situation in our slices recapitulates the *in vivo* situation well. However, it will be important to confirm our findings *in vivo* in future studies, especially since the precise consequences of altered chloride levels depend on local activity. Together, our results support the notion that depolarizing but inhibitory GABA signaling has limited contribution to postnatal synapse development in the hippocampus.

The second key finding from this study is that subtle, and cell type specific, alterations in membrane properties were observed two weeks after the VU treatment had ended. We found that CA1 pyramidal cells had a slightly increased firing threshold, and interneurons in the *sRad* showed a slightly elevated membrane potential, which reduced the amount of depolarization required to fire an AP. We speculate that together this will modify spontaneous network activity toward an increased inhibitory tone and contribute to the increased sIPSC frequency that we observed in VU-treated slices (Fig. 6I). It is important to note that our study does not address the possible contribution of other interneurons, for instance Oriens-Lacunosum Moleculare (OLM) interneurons (Leão et al., 2012). Interestingly, pharmacological inhibition of NKCC1 from P3 to P8 (resulting in decreased intracellular chloride levels) has been reported to transiently decrease inhibitory transmission in the visual cortex several weeks later (at P35) (Deidda et al., 2015a), suggesting that developing GABAergic transmission may be particularly sensitive to intracellular chloride levels.

It remains unclear how blocking KCC2 from DIV1 to DIV8 can alter membrane properties of neurons two weeks later. It is important to note that these indirect effects observed in slices cannot easily be translated to the *in vivo* situation as they will likely be influenced by *in vivo* activity patterns and neuromodulatory signaling. In addition, although we carefully selected VU for its highest selectivity to KCC2 (Delpire and Weaver, 2017) and lowest off-target effects, we cannot exclude that the latter may have contributed (Sivakumaran et al., 2015), for instance via the Translocator protein (TSPO) (Liu et al., 2017; Shi et al., 2022). However, it is interesting that our study adds to an increasing number of studies that demonstrate that intracellular chloride levels can modify ion channels, and therefore membrane excitability, in often unpredictable ways (Huang et al., 2012; Seja et al., 2012; Goutierre et al., 2019; Sinha et al., 2022). Most notably, it was shown that membrane levels of TASK-3 potassium channels are regulated via KCC2 (Goutierre et al., 2019) and that the chloride-dependent kinase WNK3 regulates inward rectifier potassium channels (Sinha et al., 2022). It will also be important to further examine the role of various chloride channels in membrane excitability (Jentsch, 2016; Jentsch and Pusch, 2018; Akita and Fukuda, 2020). Interestingly, effects seem to strongly depend on cell type (Seja et al., 2012) and timing of the chloride manipulation (Lim et al., 2021; Sinha et al., 2022). The changes in excitability that we observed at

DIV21 may therefore reflect a complex sequence of subtle adaptations of ion channel distribution that is likely specific per cell type and per brain region.

The present work shows that delaying the postnatal GABA shift by one week has no direct effects on synaptic development. Instead, we found evidence for indirect, cell type-specific changes in membrane properties, possibly via chloride-dependent regulation of ion channels, which may have long-term consequences for network activity and brain function. Our data call for careful assessment of alterations in cellular excitability in NDDs.

4.7 Author contributions

C.P., and C.J.W. designed research; C.P., S.K., N.J., M.R. and T.W., performed research and analyzed data; C.P., and C.J.W. wrote the paper.

4.8 Declaration of Interests

The authors declare no competing interests.

4.9 Acknowledgements

This research was supported by a TOP grant from ZonMW (#91216021) and by the Nederlandse Organisatie voor Wetenschappelijk Onderzoek (NWO; #OCENW. KLEIN.150). We thank Prof. Franck Polleux for providing the KCC2 short hairpin construct (Bortone and Polleux, 2009). We thank Prof. Thomas Kuner for providing the Cre-dependent SCLM construct (Boffi et al., 2018). We thank Prof. Kevin Staley for providing the SuperClomeleon^{lox/-} mouse line, Dr. Stefan Berger for the CamKII α ^{Cre/-} mice and Dr. Henk Karst for sharing these mice with us. We thank Dunya Selemangel for help with SuperClomeleon data analysis and René van Dorland for the AAV production and excellent technical support.

4.10 References

- Akerman, C.J., Cline, H.T., 2006. Depolarizing GABAergic conductances regulate the balance of excitation to inhibition in the developing retinotectal circuit in vivo. *J. Neurosci.* 26, 5117–5130. <https://doi.org/10.1523/JNEUROSCI.0319-06.2006>
- Akita, T., Fukuda, A., 2020. Intracellular Cl⁻ dysregulation causing and caused by pathogenic neuronal activity. *Pflugers Arch. Eur. J. Physiol.* 472, 977–987. <https://doi.org/10.1007/s00424-020-02375-4>
- Antoine, M.W., Langberg, T., Schnepel, P., Feldman, D.E., 2019. Increased Excitation-Inhibition Ratio Stabilizes Synapse and Circuit Excitability in Four Autism Mouse Models - supplemental. *Neuron* 101, 648–661.e4. <https://doi.org/10.1016/j.neuron.2018.12.026>
- Awad, P.N., Amegandjin, C.A., Szczurkowska, J., Carriço, J.N., Fernandes do Nascimento, A.S., Baho, E., Chattopadhyaya, B., Cancedda, L., Carmant, L., Di Cristo, G., 2018. KCC2 Regulates Dendritic Spine Formation in a Brain-Region Specific and BDNF Dependent Manner. *Cereb. Cortex* 1–14. <https://doi.org/10.1093/cercor/bhy198>
- Banerjee, A., Rikhye, R. V., Breton-Provencher, V., Tang, X., Li, C., Li, K., Runyan, C.A., Fu, Z., Jaenisch, R., Sur, M., 2016. Jointly reduced inhibition and excitation underlies circuit-wide changes in cortical processing in Rett syndrome. *Proc. Natl. Acad. Sci.* 113, E7287–E7296. <https://doi.org/10.1073/pnas.1615330113>
- Banke, T.G., McBain, C.J., 2006. GABAergic input onto CA3 hippocampal interneurons remains shunting throughout development. *J. Neurosci.* 26, 11720–11725. <https://doi.org/10.1523/JNEUROSCI.2887-06.2006>
- Bekkers, J.M., Clements, J.D., 1999. Quantal amplitude and quantal variance of strontium-induced asynchronous EPSCs in rat dentate granule neurons. *J. Physiol.* 516, 227–248. <https://doi.org/10.1111/j.1469-7793.1999.227aa.x>
- Ben-Ari, Y., Cherubini, E., Corradetti, R., Gaiarsa, J., 1989. Giant synaptic potentials in immature rat CA3 hippocampal neurones. *J. Physiol. Sep*, 303–325.
- Berry, C.T., Sceniak, M.P., Zhou, L., Sabo, S.L., 2012. Developmental Up-Regulation of Vesicular Glutamate Transporter-1 Promotes Neocortical Presynaptic Terminal Development. *PLoS One* 7. <https://doi.org/10.1371/journal.pone.0050911>
- Bertoni, A., Schaller, F., Tyzio, R., Gaillard, S., Santini, F., Xolin, M., Diabira, D., Vaidyanathan, R., Matarazzo, V., Medina, I., Hammock, E., Zhang, J., Chini, B., Gaiarsa, J.-L., Muscatelli, F., 2021. Oxytocin administration in neonates shapes the hippocampal circuitry and restores social behavior in a mouse model of autism. *Mol. Psychiatry* 26, 7582–7595. <https://doi.org/10.1038/s41380-021-01227-6>
- Birey, F., Li, M.Y., Gordon, A., Thete, M. V., Valencia, A.M., Revah, O., Paşca, A.M., Geschwind, D.H., Paşca, S.P., 2022. Dissecting the molecular basis of human interneuron migration in forebrain assembloids from Timothy syndrome. *Cell Stem Cell* 29, 248–264. e7. <https://doi.org/10.1016/j.stem.2021.11.011>
- Boffi, J.C., Knabbe, J., Kaiser, M., Kuner, T., 2018. KCC2-dependent steady-state intracellular chloride concentration and pH in cortical layer 2/3 neurons of anesthetized and awake mice. *Front. Cell. Neurosci.* 12, 1–14. <https://doi.org/10.3389/fncel.2018.00007>
- Bortone D, Polleux F (2009) KCC2 Expression Promotes the Termination of Cortical Interneuron Migration in a Voltage-Sensitive Calcium-Dependent Manner. *Neuron* 62:53–71 Available at: <http://dx.doi.org/10.1016/j.neuron.2009.01.034>.
- Branchereau, P., Cattaert, D., Delpy, A., Allain, A.E., Martin, E., Meyrand, P., 2016. Depolarizing GABA/glycine synaptic events switch from excitation to inhibition during frequency increases. *Sci. Rep.* 6, 1–19. <https://doi.org/10.1038/srep21753>

- Casanova, E., Fehsenfeld, S., Mantamadiotis, T., Lemberger, T., Greiner, E., Stewart, A.F., Schtz, G., 2001. A CamKII α iCre BAC allows brain-specific gene inactivation. *Genesis* 31, 37–42. <https://doi.org/10.1002/gene.1078>
- Chancey, J.H., Adlaf, E.W., Sapp, M.C., Pugh, P.C., Wadiche, J.I., Overstreet-Wadiche, L.S., 2013. GABA Depolarization Is Required for Experience-Dependent Synapse Unsilencing in Adult-Born Neurons. *J. Neurosci.* 33, 6614–6622. <https://doi.org/10.1523/JNEUROSCI.0781-13.2013>
- Chevy, Q., Heubl, M., Goutierre, M., Backer, S., Moutkine, I., Eugene, E., Bloch-Gallego, E., Levi, S., Poncer, J.C., 2015. KCC2 Gates Activity-Driven AMPA Receptor Traffic through Cofilin Phosphorylation. *J. Neurosci.* 35, 15772–15786. <https://doi.org/10.1523/JNEUROSCI.1735-15.2015>
- Cheyne, J.E., Zabouri, N., Baddeley, D., Lohmann, C., 2019. Spontaneous Activity Patterns Are Altered in the Developing Visual Cortex of the Fmr1 Knockout Mouse. *Front. Neural Circuits* 13, 1–8. <https://doi.org/10.3389/fncir.2019.00057>
- Chudotvorova, I., Ivanov, A., Rama, S., Christian, A.H., Pellegrino, C., 2005. Early expression of KCC2 in rat hippocampal cultures augments expression of functional GABA synapses 3, 671–679. <https://doi.org/10.1113/jphysiol.2005.089821>
- Corradini, I., Focchi, E., Rasile, M., Morini, R., Desiato, G., Tomasoni, R., Lizier, M., Ghirardini, E., Fesce, R., Morone, D., Barajon, I., Antonucci, F., Pozzi, D., Matteoli, M., 2017. Maternal Immune Activation Delays Excitatory-to-Inhibitory Gamma-Aminobutyric Acid Switch in Offspring. *Biol. Psychiatry* 83, 1–12. <https://doi.org/10.1016/j.biopsych.2017.09.030>
- De Simoni, A., Griesinger, C.B., Edwards, F.A., 2003. Development of rat CA1 neurones in acute versus organotypic slices: Role of experience in synaptic morphology and activity. *J. Physiol.* 550, 135–147. <https://doi.org/10.1113/jphysiol.2003.039099>
- Deidda, G., Allegra, M., Cerri, C., Naskar, S., Bony, G., Zunino, G., Bozzi, Y., Caleo, M., Cancedda, L., 2015a. Early depolarizing GABA controls critical-period plasticity in the rat visual cortex. *Nat. Neurosci.* 18, 87–96. <https://doi.org/10.1038/nn.3890>
- Deidda, G., Parrini, M., Naskar, S., Bozarth, I.F., Contestabile, A., Cancedda, L., 2015b. Reversing excitatory GABAAR signaling restores synaptic plasticity and memory in a mouse model of Down syndrome. *Nat. Med.* 21, 318–326. <https://doi.org/10.1038/nm.3827>
- Delpire, E., Baranczak, A., Waterson, A.G., Kim, K., Kett, N., Morrison, R.D., Scott Daniels, J., David Weaver, C., Lindsley, C.W., 2012. Further optimization of the K-Cl cotransporter KCC2 antagonist ML077: Development of a highly selective and more potent in vitro probe. *Bioorganic Med. Chem. Lett.* 22, 4532–4535. <https://doi.org/10.1016/j.bmcl.2012.05.126>
- Duarte, S.T., Armstrong, J., Roche, A., Ortez, C., Pérez, A., O'Callaghan, M. del M., Pereira, A., Sanmartí, F., Ormazábal, A., Artuch, R., Pineda, M., García-Cazorla, A., 2013. Abnormal Expression of Cerebrospinal Fluid Cation Chloride Cotransporters in Patients with Rett Syndrome. *PLoS One* 8, 1–7. <https://doi.org/10.1371/journal.pone.0068851>
- Dzhala, V.I., Talos, D.M., Sdrulla, D.A., Brumback, A.C., Mathews, G.C., Benke, T.A., Delpire, E., Jensen, F.E., Staley, K.J., 2005. NKCC1 transporter facilitates seizures in the developing brain. *Nat. Med.* 11, 1205–1213. <https://doi.org/10.1038/nm1301>
- Fernandez, A., Dumon, C., Guimond, D., Fernandez, A., Burnashev, N., Tyzio, R., Lozovaya, N., Ferrari, D.C., Bonifazi, P., Ben-Ari, Y., 2018. The GABA Developmental Shift Is Abolished by Maternal Immune Activation Already at Birth. *Cereb. Cortex* 29, 3982–3992. <https://doi.org/10.1093/cercor/bhy279>
- Fiumelli, H., Briner, A., Puskarjov, M., Blaesse, P., Belem, B., Dayer, A., Kaila, K., Martin, J., Vutskits, L., 2013. An Ion Transport-Independent Role for the Cation-Chloride Cotransporter KCC2 in Dendritic Spinogenesis In Vivo. *Cereb. Cortex* 23, 378–388.

- Gao, X.-B., Chen, G., van den Pol, A.N., 1998. GABA-Dependent Firing of Glutamate-Evoked Action Potentials at AMPA/Kainate Receptors in Developing Hypothalamic Neurons. *J. Neurophysiol.* 79, 716–726. <https://doi.org/10.1152/jn.1998.79.2.716>
- Gauvain, G., Chamma, I., Chevy, Q., Cabezas, C., Irinopoulou, T., Bodrug, N., Carnaud, M., Levi, S., Poncer, J.C., 2011. The neuronal K-Cl cotransporter KCC2 influences postsynaptic AMPA receptor content and lateral diffusion in dendritic spines. *Proc. Natl. Acad. Sci.* 108, 15474–15479. <https://doi.org/10.1073/pnas.1107893108>
- Gogolla, N., LeBlanc, J.J., Quast, K.B., Südhof, T.C., Fagiolini, M., Hensch, T.K., 2009. Common circuit defect of excitatory-inhibitory balance in mouse models of autism. *J. Neurodev. Disord.* 1, 172–181. <https://doi.org/10.1007/s11689-009-9023-x>
- Gonçalves, J.T., Anstey, J.E., Golshani, P., Portera-Cailliau, C., 2013. Circuit level defects in the developing neocortex of Fragile X mice. *Nat. Neurosci.* 16, 903–909. <https://doi.org/10.1038/nn.3415>
- Goutierre, M., Al Awabdh, S., Donneger, F., François, E., Gomez-Dominguez, D., Irinopoulou, T., Menendez de la Prida, L., Poncer, J.C., 2019. KCC2 Regulates Neuronal Excitability and Hippocampal Activity via Interaction with Task-3 Channels. *Cell Rep.* 28, 91–103. <https://doi.org/10.1016/j.celrep.2019.06.001>
- Grimley, J.S., Li, L., Wang, W., Wen, L., Beese, L.S., Hellinga, H.W., Augustine, G.J., 2013. Visualization of Synaptic Inhibition with an Optogenetic Sensor Developed by Cell-Free Protein Engineering Automation. *J. Neurosci.* 33, 16297–16309. <https://doi.org/10.1523/JNEUROSCI.4616-11.2013>
- Gulyás, A.I., Sík, A., Payne, J.A., Kaila, K., Freund, T.F., 2001. The KCl cotransporter, KCC2, is highly expressed in the vicinity of excitatory synapses in the rat hippocampus. *Eur. J. Neurosci.* 13, 2205–2217. <https://doi.org/10.1046/j.0953-816X.2001.01600.x>
- He, Q., Arroyo, E.D., Smukowski, S.N., Xu, J., Piochon, C., Savas, J.N., Portera-Cailliau, C., Contractor, A., 2018. Critical period inhibition of NKCC1 rectifies synapse plasticity in the somatosensory cortex and restores adult tactile response maps in fragile X mice. *Mol. Psychiatry* 24, 1732–1747. <https://doi.org/10.1038/s41380-018-0048-y>
- He, Q., Nomura, T., Xu, J., Contractor, A., 2014. The Developmental Switch in GABA Polarity Is Delayed in Fragile X Mice. *J. Neurosci.* 34, 446–450. <https://doi.org/10.1523/JNEUROSCI.4447-13.2014>
- Herstel, L.J., Peerboom, C., Uijtewaal, S., Selemangel, D., Karst, H., Wierenga, C.J., 2022. Using SuperClomeleon to measure changes in intracellular chloride during development and after early life stress. *Eneuro* November/D.
- Hu, H.Y., Kruijssen, D.L.H., Frias, C.P., Rózsza, B., Hoogenraad, C.C., Wierenga, C.J., 2019. Endocannabinoid Signaling Mediates Local Dendritic Coordination between Excitatory and Inhibitory Synapses. *Cell Rep.* 27, 666–675. e5. <https://doi.org/10.1016/j.celrep.2019.03.078>
- Huang, Y., Ko, H., Cheung, Z.H., Yung, K.K.L., Yao, T., Wang, J.J., Morozov, A., Ke, Y., Ip, N.Y., Yung, W.H., 2012. Dual actions of brain-derived neurotrophic factor on GABAergic transmission in cerebellar Purkinje neurons. *Exp. Neurol.* 233, 791–798. <https://doi.org/10.1016/j.expneurol.2011.11.043>
- Hübner, C. a, Stein, V., Hermans-Borgmeyer, I., Meyer, T., Ballanyi, K., Jentsch, T.J., 2001. Disruption of KCC2 reveals an essential role of K-Cl cotransport already in early synaptic inhibition. *Neuron* 30, 515–524.
- Jentsch, T.J., 2016. VRACs and other ion channels and transporters in the regulation of cell volume and beyond. *Nat. Rev. Mol. Cell Biol.* 17, 293–307. <https://doi.org/10.1038/nrm.2016.29>
- Jentsch, T.J., Pusch, M., 2018. CLC chloride channels and transporters: Structure, function, physiology, and disease. *Physiol. Rev.* 98, 1493–1590. <https://doi.org/10.1152/physrev.00047.2017>

- Kesaf, S., Khirug, S., Dinh, E., Saez Garcia, M., Soni, S., Orav, E., Delpire, E., Taira, T., Lauri, S.E., Rivera, C., 2020. The Kainate Receptor Subunit GluK2 Interacts With KCC2 to Promote Maturation of Dendritic Spines. *Front. Cell. Neurosci.* 14, 1–14. <https://doi.org/10.3389/fncel.2020.00252>
- Khalilov, I., Khazipov, R., Esclapez, M., Ben-Ari, Y., 1997. Bicuculline induces ictal seizures in the intact hippocampus recorded in vitro. *Eur. J. Pharmacol.* 319, 5–6. [https://doi.org/10.1016/S0014-2999\(96\)00964-8](https://doi.org/10.1016/S0014-2999(96)00964-8)
- Khazipov, R., Khalilov, I., Tyzio, R., Morozova, E., Ben-Ari, Y., Holmes, G.L., 2004. Developmental changes in GABAergic actions and seizure susceptibility in the rat hippocampus. *Eur. J. Neurosci.* 19, 590–600. <https://doi.org/10.1111/j.0953-816X.2003.03152.x>
- Kilb, W., 2021. When are depolarizing GABAergic responses excitatory? *Front. Mol. Neurosci.*
- Kim, J., Alger, B.E., 2001. Random Response Fluctuations Lead to Spurious Paired-Pulse Facilitation. *J. Neurosci.* 21, 9608–9618.
- Kirmse, K., Kummer, M., Kovalchuk, Y., Witte, O.W., Garaschuk, O., Holthoff, K., 2015. GABA depolarizes immature neurons and inhibits network activity in the neonatal neocortex in vivo. *Nat. Commun.* 6, 1–13. <https://doi.org/10.1038/ncomms8750>
- Le Magueresse, C., Monyer, H., 2013. GABAergic Interneurons Shape the Functional Maturation of the Cortex. *Neuron* 77, 388–405. <https://doi.org/10.1016/j.neuron.2013.01.011>
- Lee, H.H.C., Walker, J.A., Williams, J.R., Goodier, R.J., Payne, J.A., Moss, S.J., 2007. Direct protein kinase C-dependent phosphorylation regulates the cell surface stability and activity of the potassium chloride cotransporter KCC2. *J. Biol. Chem.* 282, 29777–29784. <https://doi.org/10.1074/jbc.M705053200>
- Leinekugel, X., Medina, I., Khalilov, I., Ben-Ari, Y., Khazipov, R., 1997. Ca²⁺ Oscillations Mediated by the Synergistic Excitatory Actions of GABA. *Neuron* 18, 243–255.
- Li, H., Khirug, S., Cai, C., Ludwig, A., Blaesse, P., Kolikova, J., Afzalov, R., Coleman, S.K., Lauri, S., Airaksinen, M.S., Keinänen, K., Khiroug, L., Saarma, M., Kaila, K., Rivera, C., 2007. KCC2 Interacts with the Dendritic Cytoskeleton to Promote Spine Development. *Neuron* 56, 1019–1033. <https://doi.org/10.1016/j.neuron.2007.10.039>
- Lim, W.M., Chin, E.W.M., Tang, B.L., Chen, T., Goh, E.L.K., 2021. WNK3 Maintains the GABAergic Inhibitory Tone, Synaptic Excitation and Neuronal Excitability via Regulation of KCC2 Cotransporter in Mature Neurons. *Front. Mol. Neurosci.* 14, 1–17. <https://doi.org/10.3389/fnmol.2021.762142>
- López-Bendito G, Sturgess K, Erdélyi F, Szabó G, Molnár Z, Paulsen O. Preferential origin and layer destination of GAD65-GFP cortical interneurons. *Cereb Cortex.* 2004 Oct;14(10):1122-33. doi: 10.1093/cercor/bhh072. Epub 2004 Apr 27. PMID: 15115742.
- Lozovaya, N., Nardou, R., Tyzio, R., Chiesa, M., Pons-Bennaceur, A., Eftekhari, S., Bui, T.T., Billon-Grand, M., Rasero, J., Bonifazi, P., Guimond, D., Gaiarsa, J.L., Ferrari, D.C., Ben-Ari, Y., 2019. Early alterations in a mouse model of Rett syndrome: the GABA developmental shift is abolished at birth. *Sci. Rep.* 9, 1–16. <https://doi.org/10.1038/s41598-019-45635-9>
- Maffei, A., Nelson, S.B., Turrigiano, G.G., 2004. Selective reconfiguration of layer 4 visual cortical circuitry by visual deprivation. *Nat. Neurosci.* 7, 1353–1359. <https://doi.org/10.1038/nn1351>
- Mahadevan V, Khademullah CS, Dargaei Z, Chevrier J, Uvarov P, Kwan J, Bagshaw RD, Pawson T, Emili A, De Koninck Y, Anggono V, Airaksinen M, Woodin MA (2017) Native KCC2 interactome reveals PACSIN1 as a critical regulator of synaptic inhibition. *Elife* 6:1–34
- Matsushima, T., Miura, M., Patzke, N., Toji, N., Wada, K., Ogura, Y., Homma, K.J., Sgadò, P., Vallortigara, G., 2022. Impaired Epigenesis of Imprinting Predispositions Causes Autism-like Behavioral Phenotypes in Domestic Chicks. *bioRxiv.*

- Menendez De La Prida, L., Huberfeld, G., Cohen, I., Miles, R., 2006. Threshold behavior in the initiation of hippocampal population bursts. *Neuron* 49, 131–142. <https://doi.org/10.1016/j.neuron.2005.10.034>
- Meredith, R.M., 2015. Sensitive and critical periods during neurotypical and aberrant neurodevelopment: A framework for neurodevelopmental disorders. *Neurosci. Biobehav. Rev.* 50, 180–188. <https://doi.org/10.1016/j.neubiorev.2014.12.001>
- Merner, N., Chandler, M., Bourassa, C., Liang, B., Khanna, A., Dion, P., Rouleau, G., Kahle, K., 2015. Regulatory domain or CpG site variation in SLC12A5, encoding the chloride transporter KCC2, in human autism and schizophrenia. *Front. Cell. Neurosci.* 9, 386.
- Merner, N.D., Chandler, M.R., Bourassa, C., Liang, B., Khanna, A.R., Dion, P., Rouleau, G.A., Kahle, K.T., 2015. Regulatory domain or CPG site variation in SLC12A5, encoding the chloride transporter KCC2, in human autism and schizophrenia. *Front. Cell. Neurosci.* 9, 1–10. <https://doi.org/10.3389/fncel.2015.00386>
- Mòdol, L., Casas, C., Llidó, A., Navarro, X., Pallarès, M., Darbra, S., 2014. Neonatal allopregnanolone or finasteride administration modifies hippocampal K⁺ Cl⁻ co-transporter expression during early development in male rats. *J. Steroid Biochem. Mol. Biol.* 143, 343–347. <https://doi.org/10.1016/j.jsbmb.2014.05.002>
- Molnár, Z., Luhmann, H.J., Kanold, P.O., 2020. Transient cortical circuits match spontaneous and sensory-driven activity during development. *Science* (80-.). 370. <https://doi.org/10.1126/science.abb2153>
- Morita, K., Tsumoto, K., Aihara, K., 2006. Bidirectional modulation of neuronal responses by depolarizing GABAergic inputs. *Biophys. J.* 90, 1925–1938. <https://doi.org/10.1529/biophysj.105.063164>
- Murata, Y., Colonnese, M.T., 2020. GABAergic interneurons excite neonatal hippocampus in vivo. *Sci. Adv.* 6, 1–10.
- Nakanishi, K., Yamada, J., Takayama, C., Oohira, A., Fukuda, A., 2007. NKCC1 Activity Modulates Formation of Functional Inhibitory Synapses in Cultured Neocortical Neurons. *Synapse* 411, 401–411. <https://doi.org/10.1002/syn>
- Oh, W.C., Lutz, S., Castillo, P.E., Kwon, H.B., 2016. De novo synaptogenesis induced by GABA in the developing mouse cortex - supplemental. *Science* (80-.). 353, 1037–1040. <https://doi.org/10.1126/science.aaf5206>
- Otsu, Y., Donneger, F., Schwartz, E.J., Poncer, J.C., 2020. Cation–chloride cotransporters and the polarity of GABA signalling in mouse hippocampal parvalbumin interneurons. *J. Physiol.* 598, 1–16. <https://doi.org/10.1113/JP279221>
- Patenaude, C., Massicotte, G., Lacaille, J.C., 2005. Cell-type specific GABA synaptic transmission and activity-dependent plasticity in rat hippocampal stratum radiatum interneurons. *Eur. J. Neurosci.* 22, 179–188. <https://doi.org/10.1111/j.1460-9568.2005.04207.x>
- Perkins, K.L., 2006. Cell-attached voltage-clamp and current-clamp recording and stimulation techniques in brain slices. *J. Neurosci. Methods* 154, 1–18. <https://doi.org/10.1016/j.jneumeth.2006.02.010>
- Pisella, Gaiarsa, Diabira, Zhang, Khalilov, Duan, Kahle, Medina, 2019. Impaired regulation of KCC2 phosphorylation leads to neuronal network dysfunction and neurodevelopmental pathology. *Sci. Signal.* 12. <https://doi.org/10.1126/scisignal.aay0300>
- Puskarjov, M., Fiumelli, H., Briner, A., Bodogan, T., Demeter, K., Laco, C., Mavrovic, M., Blaesse, P., Kaila, K., Vutskits, L., 2017. K-Cl Cotransporter 2–mediated Cl⁻ Extrusion Determines Developmental Stage–dependent Impact of Propofol Anesthesia on Dendritic Spine. *Anesthesiology* 126, 1–13.
- Rahmati, N., Normoyle, K.P., Glykys, J., Dzhalal, V.I., Lillis, K.P., Kahle, K.T., Raiyyani, R., Jacob, T., Staley, K.J., 2021. Unique actions of gaba arising from cytoplasmic chloride microdomains. *J. Neurosci.* 41, 4967–4975. <https://doi.org/10.1523/JNEUROSCI.3175-20.2021>

- Rall, W., 1967. Distinguishing Theoretical Synaptic Potentials Computed for Different Soma-Dendritic Distributions of Synaptic. *J Neurophysiol.* sep 30, 1138–68.
- Rheims, S., Minlebaev, M., Ivanov, A., Represa, A., Khazipov, R., Holmes, G.L., Ben-Ari, Y., Zilberter, Y., 2008. Excitatory GABA in rodent developing neocortex in vitro. *J. Neurophysiol.* 100, 609–619. <https://doi.org/10.1152/jn.90402.2008>
- Rivera, C., Voipio, J., Payne, J. a, Ruusuvuori, E., Lahtinen, H., Lamsa, K., Pirvola, U., Saarna, M., Kaila, K., 1999. The K⁺/Cl⁻ co-transporter KCC2 renders GABA hyperpolarizing during neuronal maturation. *Nature* 397, 251–255. <https://doi.org/10.1038/16697>
- Romo-Parra, H., Treviño, M., Heinemann, U., Gutiérrez, R., 2008. GABA actions in hippocampal area CA3 during postnatal development: Differential shift from depolarizing to hyperpolarizing in somatic and dendritic compartments. *J. Neurophysiol.* 99, 1523–1534. <https://doi.org/10.1152/jn.01074.2007>
- Roux, S., Lohof, A., Ben-Ari, Y., Poulain, B., Bossu, J.-L., 2018. Maturation of GABAergic Transmission in Cerebellar Purkinje Cells Is Sex Dependent and Altered in the Valproate Model of Autism. *Front. Cell. Neurosci.* 12, 1–14. <https://doi.org/10.3389/fncel.2018.00232>
- Ruffolo, G., Cifelli, P., Roseti, C., Thom, M., van Vliet, E.A., Limatola, C., Aronica, E., Palma, E., 2018. A novel GABAergic dysfunction in human Dravet syndrome. *Epilepsia* 59, 2106–2117. <https://doi.org/10.1111/epi.14574>
- Ruffolo, G., Iyer, A., Cifelli, P., Roseti, C., Mühlebner, A., van Scheppingen, J., Scholl, T., Hainfellner, J., Feucht, M., Krsek, P., Zamecnik, J., Jansen, F., Spliet, W., Limatola, C., Aronica, E., Palma, E., 2016. Functional aspects of early brain development are preserved in tuberous sclerosis complex (TSC) epileptogenic lesions. *Neurobiol. Dis.* 95, 93–101.
- Ruiter, M., Herstel, L.J., Wierenga, C.J., Ma, T., 2020. Reduction of Dendritic Inhibition in CA1 Pyramidal Neurons in Amyloidosis Models of Early Alzheimer's Disease. *J. Alzheimer's Dis.* 78, 951–964. <https://doi.org/10.3233/JAD-200527>
- Salmon, C.K., Pribiag, H., Gizowski, C., Farmer, W.T., Cameron, S., Jones, E. V., Mahadevan, V., Bourque, C.W., Stellwagen, D., Woodin, M.A., Murai, K.K., 2020. Depolarizing GABA Transmission Restrains Activity-Dependent Glutamatergic Synapse Formation in the Developing Hippocampal Circuit. *Front. Cell. Neurosci.* 14, 1–16. <https://doi.org/10.3389/fncel.2020.00036>
- Scanziani, M., Debanne, D., Müller, M., Gähwiler, B.H., Thompson, S.M., 1994. Role of excitatory amino acid and GABA_B receptors in the generation of epileptiform activity in disinhibited hippocampal slice cultures. *Neuroscience* 61, 823–832. [https://doi.org/10.1016/0306-4522\(94\)90405-7](https://doi.org/10.1016/0306-4522(94)90405-7)
- Sedmak, G., Puskarjov, N.J.-M.M., Ulamec, M., Krušlin, B., Kaila, K., Judaš, M., 2016. Developmental Expression Patterns of KCC2 and Functionally Associated Molecules in the Human Brain. *Cereb. Cortex* 27, 4060–4072. <https://doi.org/10.1093/cercor/bhw218>
- Seja, P., Schonewille, M., Spitzmaul, G., Badura, A., Klein, I., Rudhard, Y., Wisden, W., Hübner, C.A., De Zeeuw, C.I., Jentsch, T.J., 2012. Raising cytosolic Cl⁻ in cerebellar granule cells affects their excitability and vestibulo-ocular learning. *EMBO J.* 31, 1217–1230. <https://doi.org/10.1038/emboj.2011.488>
- Sheng, M., Hoogenraad, C.C., 2007. The postsynaptic architecture of excitatory synapses: A more quantitative view. *Annu. Rev. Biochem.* 76, 823–847. <https://doi.org/10.1146/annurev.biochem.76.060805.160029>

- Sinha, A.S., Wang, T., Watanabe, M., Hosoi, Y., Sohara, E., Akita, T., Uchida, S., Fukuda, A., 2022. WNK3 kinase maintains neuronal excitability by reducing inwardly rectifying K⁺ conductance in layer V pyramidal neurons of mouse medial prefrontal cortex. *Front. Mol. Neurosci.* 15. <https://doi.org/10.3389/fnmol.2022.856262>
- Sipila, S.T., Schuchmann, S., Voipio, J., Yamada, J., Kaila, K., 2006. The cation-chloride cotransporter NKCC1 promotes sharp waves in the neonatal rat hippocampus 3, 765–773. <https://doi.org/10.1113/jphysiol.2006.107086>
- Smalley JL, Kontou G, Choi C, Ren Q, Albrecht D, Abiraman K, Santos MAR, Bope CE, Deeb TZ, Davies PA, Brandon NJ, Moss SJ (2020) Isolation and Characterization of Multi-Protein Complexes Enriched in the K-Cl Cotransporter 2 From Brain Plasma Membranes. *Front Mol Neurosci* 13:1–16.
- Sørensen, A.T., Ledri, M., Melis, M., Ledri, L.N., Andersson, M., Kokaia, M., 2017. Altered chloride homeostasis decreases the action potential threshold and increases hyperexcitability in hippocampal neurons. *eNeuro* 4, 1–10. <https://doi.org/10.1523/ENEURO.0172-17.2017>
- Spoljaric, I., Spoljaric, A., Mavrovic, M., Seja, P., Puskarjov, M., Kaila, K., 2019. KCC2-Mediated Cl⁻ Extrusion Modulates Spontaneous Hippocampal Network Events in Perinatal Rats and Mice. *Cell Rep.* 26, 1073-1081.e3. <https://doi.org/10.1016/j.celrep.2019.01.011>
- Staley, K.J., Mody, I., 1992. Shunting of excitatory input to dentate gyrus granule cells by a depolarizing GABA(A) receptor-mediated postsynaptic conductance. *J. Neurophysiol.* 68, 197–212. <https://doi.org/10.1152/jn.1992.68.1.197>
- Stein, V., Hermans-Borgmeyer, I., Jentsch, T.J., Hübner, C.A., 2004. Expression of the KCl Cotransporter KCC2 Parallels Neuronal Maturation and the Emergence of Low Intracellular Chloride. *J. Comp. Neurol.* 468, 57–64. <https://doi.org/10.1002/cne.10983>
- Stoppini, L., Buchs, P.A., Muller, D., 1991. A simple method for organotypic cultures of nervous tissue. *J. Neurosci. Methods* 37, 173–182. [https://doi.org/10.1016/0165-0270\(91\)90128-M](https://doi.org/10.1016/0165-0270(91)90128-M)
- Sulis Sato, S., Artoni, P., Landi, S., Cozzolino, O., Parra, R., Pracucci, E., Trovato, F., Szczurkowska, J., Luin, S., Arosio, D., Beltram, F., Cancedda, L., Kaila, K., Ratto, G.M., 2017. Simultaneous two-photon imaging of intracellular chloride concentration and pH in mouse pyramidal neurons in vivo. *Proc. Natl. Acad. Sci.* 114, E8770–E8779. <https://doi.org/10.1073/pnas.1702861114>
- Talos, D.M., Sun, H., Kosaras, B., Joseph, A., Folkerth, R.D., Poduri, A., Madsen, J.R., Black, P.M., Jensen, F.E., 2012. Altered inhibition in tuberous sclerosis and type IIb cortical dysplasia. *Ann. Neurol.* 71, 539–551. <https://doi.org/10.1002/ana.22696>
- Tang, X., Kim, J., Zhou, L., Wengert, E., Zhang, L., Wu, Z., Carrameu, C., Muotri, A.R., Marchetto, M.C.N., Gage, F.H., Chen, G., 2016. KCC2 rescues functional deficits in human neurons derived from patients with Rett syndrome. *Proc. Natl. Acad. Sci.* 113, 751–756. <https://doi.org/10.1073/pnas.1524013113>
- Tsien, J.Z., Chen, D.F., Gerber, D., Tom, C., Mercer, E.H., Anderson, D.J., Mayford, M., Kandel, E.R., Tonegawa, S., 1996. Subregion- and cell type-restricted gene knockout in mouse brain. *Cell* 87, 1317–1326. [https://doi.org/10.1016/S0092-8674\(00\)81826-7](https://doi.org/10.1016/S0092-8674(00)81826-7)
- Tsukahara, T., Masuhara, M., Iwai, H., Sonomura, T., Sato, T., 2015. Repeated stress-induced expression pattern alterations of the hippocampal chloride transporters KCC2 and NKCC1 associated with behavioral abnormalities in female mice. *Biochem. Biophys. Res. Commun.* 465, 145–151. <https://doi.org/10.1016/j.bbrc.2015.07.153>

- Tyzio, R., Holmes, G.L., Ben-Ari, Y., Khazipov, R., 2007. Timing of the developmental switch in GABA mediated signaling from excitation to inhibition in CA3 rat hippocampus using gramicidin perforated patch and extracellular recordings. *Epilepsia* 48, 96–105. <https://doi.org/10.1111/j.1528-1167.2007.01295.x>
- Tyzio, R., Nardou, R., Ferrari, D., Tsintsadze, T., Shahrokhi, A., Eftekhari, S., Khalilov, I., Tsintsadze, V., Brouchoud, C., Chazal, G., Lemonnier, E., Lozovaya, N., Burnashev, N., Y., B.-A., 2014. Oxytocin-Mediated GABA Inhibition During Delivery Attenuates Autism Pathogenesis in Rodent Offspring. *Science* (80-.). 343, 675–680.
- Valeeva, G., Abdullin, A., Tyzio, R., Skorinkin, A., Nikolski, E., Ben-Ari, Y., Khazipov, R., 2010. Temporal coding at the immature depolarizing gabaergic synapse. *Front. Cell. Neurosci.* 4, 1–12. <https://doi.org/10.3389/fncel.2010.00017>
- Valeeva, G., Tressard, T., Mukhtarov, M., Baude, A., Khazipov, R., 2016. An Optogenetic Approach for Investigation of Excitatory and Inhibitory Network GABA Actions in Mice Expressing Channelrhodopsin-2 in GABAergic Neurons. *J. Neurosci.* 36, 5961–5973. <https://doi.org/10.1523/JNEUROSCI.3482-15.2016>
- van Rheede, J.J., Richards, B.A., Akerman, C.J., 2015. Sensory-Evoked Spiking Behavior Emerges via an Experience-Dependent Plasticity Mechanism. *Neuron* 87, 1050–1062. <https://doi.org/10.1016/j.neuron.2015.08.021>
- Vong, L., Ye, C., Yang, Z., Choi, B., Chua, S., Lowell, B.B., 2011. Leptin Action on GABAergic Neurons Prevents Obesity and Reduces Inhibitory Tone to POMC Neurons. *Neuron* 71, 142–154. <https://doi.org/10.1016/j.neuron.2011.05.028>
- Wang, B.S., Feng, L., Liu, M., Liu, X., Cang, J., 2013. Environmental Enrichment Rescues Binocular Matching of Orientation Preference in Mice that Have a Precocious Critical Period. *Neuron* 80, 198–209. <https://doi.org/10.1016/j.neuron.2013.07.023>
- Wang, D.D., Kriegstein, A.R., 2011. Blocking early GABA depolarization with bumetanide results in permanent alterations in cortical circuits and sensorimotor gating deficits. *Cereb. Cortex* 21, 574–587. <https://doi.org/10.1093/cercor/bhq124>
- Wang, D.D., Kriegstein, A.R., 2008. GABA Regulates Excitatory Synapse Formation in the Neocortex via NMDA Receptor Activation. *J. Neurosci.* 28, 5547–5558. <https://doi.org/10.1523/JNEUROSCI.5599-07.2008>
- Wang, T., Shan, L., Miao, C., Xu, Z., Jia, F., 2021. Treatment Effect of Bumetanide in Children With Autism Spectrum Disorder: A Systematic Review and Meta-Analysis. *Front. Psychiatry* 12, 1–11. <https://doi.org/10.3389/fpsy.2021.751575>
- Wierenga, C.J., Becker, N., Bonhoeffer, T., 2008. GABAergic synapses are formed without the involvement of dendritic protrusions. *Nat. Neurosci.* 11, 1044–1052. <https://doi.org/10.1038/nn.2180>
- Wierenga, C.J., Müllner, F.E., Rinke, I., Keck, T., Stein, V., Bonhoeffer, T., 2010. Molecular and electrophysiological characterization of GFP-expressing ca1 interneurons in GAD65-GFP mice. *PLoS One* 5, 1–11. <https://doi.org/10.1371/journal.pone.0015915>
- Wierenga, C.J., Wadman, W.J., 1999. Miniature inhibitory postsynaptic currents in CA1 pyramidal neurons after kindling epileptogenesis. *J. Neurophysiol.* 82, 1352–1362. <https://doi.org/10.1152/jn.1999.82.3.1352>
- Woodruff, A.R., McGarry, L.M., Vogels, T.P., Inan, M., Anderson, S.A., Yuste, R., 2011. State-dependent function of neocortical chandelier cells. *J. Neurosci.* 31, 17872–17886. <https://doi.org/10.1523/JNEUROSCI.3894-11.2011>
- Yamada, J., Okabe, A., Toyoda, H., Kilb, W., Luhmann, H., Fukuda, A., 2004. Cl⁻ uptake promoting depolarizing GABA actions in immature rat neocortical neurones is mediated by NKCC1. *J. Physiol.* 557, 829–841.



5

Treatment with furosemide indirectly increases inhibitory transmission in the developing hippocampus

C. Peerboom¹, T. Wijne¹ and C.J. Wierenga^{1,2}

¹ Cell Biology, Neurobiology and Biophysics, Biology department, Utrecht University, 3584CH, Utrecht, the Netherlands,

² Current address: Faculty of Science & Donders Institute, Radboud University, 6525 AJ, Nijmegen, the Netherlands

BioRxiv (preprint) doi: <https://doi.org/10.1101/2023.07.11.548438>

5.1 Abstract

During the first two postnatal weeks intraneuronal chloride concentrations in rodents gradually decrease, causing a shift from depolarizing to hyperpolarizing γ -aminobutyric acid (GABA) responses. GABAergic depolarization in the immature brain is crucial for the formation and maturation of excitatory synapses, but when GABAergic signaling becomes inhibitory it no longer promotes synapse formation. Here we examined the role of chloride transporters in developing postnatal hippocampal neurons using furosemide, an inhibitor of the chloride importer NKCC1 and chloride exporter KCC2 with reported anticonvulsant effects. We treated organotypic hippocampal cultures made from 6 to 7-day old mice with 200 μ M furosemide and assessed its effect on inhibitory synapses. Using perforated patch clamp recordings we found that the GABA reversal potential was depolarized after acute furosemide application, but after a week of furosemide treatment the GABA reversal potential was more hyperpolarized compared to control. However, we did not detect a change in chloride levels using the chloride sensor SuperClomeleon. Expression levels of the chloride cotransporters were unaffected after one week furosemide treatment. This suggests that furosemide inhibited KCC2 acutely, but sustained application resulted in (additional) inhibition of NKCC1, though we cannot exclude additional changes in HCO_3^- levels. We then assessed the effects of accelerating the GABA shift by furosemide treatment on inhibitory synapses onto CA1 pyramidal cells. Directly after cessation of furosemide treatment at DIV9, inhibitory synapses were not affected. However at DIV21, two weeks after ending the treatment, we found that the frequency of inhibitory currents was increased, possibly due to an increased number of inhibitory synapses in the *stratum Radiatum*. In addition, we found evidence for cell shrinkage in CA1 pyramidal neurons in furosemide-treated slices at DIV21. Our results suggest that furosemide indirectly promotes the development of inhibitory synapses. The furosemide-induced increase in inhibitory transmission might constitute an additional mechanism via which furosemide reduces seizure susceptibility in the epileptic brain.

5.2 Introduction

γ -Aminobutyric acid (GABA) is the main inhibitory, hyperpolarizing neurotransmitter in the adult brain, but during early development GABA actually depolarizes neurons. Ionotropic GABA_A receptors primarily conduct chloride (~70%), but also some HCO₃⁻ (~30%), (Kaila et al., 2014). While HCO₃⁻ levels remain constant, intracellular chloride levels decrease during brain development (Kaila et al., 2014). The decrease in chloride causes the reversal potential (E_{GABA}) to gradually drop below resting membrane potential. As a result, the GABAergic driving force shifts from depolarizing in immature neurons to hyperpolarizing in the mature brain (Rivera et al., 1999; Hübner et al., 2001; Tyzio et al., 2007; Romo-Parra et al., 2008; Kirmse et al., 2015; Tsukahara et al., 2015; Sulis Sato et al., 2017; Murata and Colonnese, 2020). The decrease in chloride levels is the direct result of an increased function of the chloride exporter KCC2 (K-Cl cotransporter 2) relative to the chloride importer NKCC1 (Na-K-2Cl cotransporter 1) (Rivera et al., 1999; Gulyás et al., 2001; Yamada et al., 2004; Dzhala et al., 2005; Otsu et al., 2020). In humans, the shift in chloride transporter expression occurs during the first year after birth (Dzhala et al., 2005; Sedmak et al., 2016). In rodents, GABA shifts during the first two postnatal weeks (Rivera et al., 1999; Stein et al., 2004; Tyzio et al., 2007; Romo-Parra et al., 2008; Kirmse et al., 2015; Sulis Sato et al., 2017; Murata and Colonnese, 2020).

Depolarizing GABA signaling plays a critical role in the formation and maturation of excitatory synapses in the developing brain (Leinekugel et al., 1997; Akerman and Cline, 2006; Wang and Kriegstein, 2008, 2011; Chancey et al., 2013; van Rheede et al., 2015; Oh et al., 2016). However, after the first postnatal week, GABA becomes inhibitory and it no longer promotes synapse formation (Salmon et al., 2020; Peerboom et al., 2023). Here we examined the role of chloride transporters in developing postnatal hippocampal neurons using furosemide, a well-known inhibitor of chloride transport. Low furosemide concentrations (100-1000 μM) have been employed previously to acutely block KCC2 and elevate chloride concentrations in (slice) cultures (Thompson and Gahwiler, 1989; Jarolimek et al., 1999; Deeb et al., 2013; Wright et al., 2017), as furosemide has a preference for inhibiting KCC2 over NKCC1 (IC₅₀ ~30 μM for rat NKCC1 and IC₅₀ ~10 μM for rat KCC2, expressed in *Xenopus* oocytes (Orlov et al., 2015)). In addition, furosemide can inhibit $\alpha 6$ - and $\alpha 4$ -subunit containing GABA_A receptors (Thompson and Gahwiler, 1989; Pearce, 1993; Korpi et al., 1995), and proteins that regulate neuronal HCO₃⁻ levels (Halligan et al., 1991; Temperini et al., 2009; Ruusuvuori, E. & Kaila, 2014; Uwera et al., 2015). Moreover, furosemide was shown to inhibit activity-induced swelling of epileptic brain tissue (Hochman et al., 1995; Gutschmidt et al., 1999; Hochman, 2012).

Furosemide is commonly used as a diuretic, but has anti-epileptic actions as well. A case-control study on hypertension and epilepsy showed that diuretics including furosemide protected patients with hypertension against an increased risk on

seizures in later life (Hesdorffer et al., 1996). Subsequently, the antiepileptic effects of furosemide were demonstrated in animal models (Hochman et al., 1995; Gutschmidt et al., 1999; Holtkamp et al., 2003; Barbaro et al., 2004; Viitanen et al., 2010; Hochman, 2012; Uwera et al., 2015; Chen et al., 2022). Since then, several epidemiological and experimental studies have reported anticonvulsant actions of furosemide, but because of its wide range of actions, the mechanism behind furosemide's anti-epileptic effects remains mostly unclear (Hesdorffer et al., 1996; Staley, 2002; Maa et al., 2011).

We examined the effects of 200 μM furosemide in P6/7 organotypic hippocampal cultures. We found that acute furosemide application depolarized GABA reversal potential in DIV21 slices, in line with inhibition of KCC2. In contrast, furosemide treatment from DIV1 to DIV8 hyperpolarized the GABA reversal potential. We did not detect changes in intracellular chloride levels using the chloride sensor SuperClomeleon and expression levels of the chloride-cotransporters were unaffected after furosemide-treatment, possibly due to reduced sensor sensitivity at low chloride levels. We suggest that sustained application of furosemide resulted in inhibition of NKCC1, but we cannot exclude changes in HCO_3^- levels. We then assessed the consequences of accelerating the GABA shift through furosemide treatment on inhibitory transmission. We found that inhibitory synapses were not affected directly after furosemide treatment at DIV9. However at DIV21, when E_{GABA} had normalized, inhibitory currents were strongly increased in furosemide-treated slices, possibly via an increased number of inhibitory synapses in the *stratum Radiatum*. In addition, we found clues for shrinkage of CA1 pyramidal neurons in furosemide-treated slices at DIV21. Our results suggest that furosemide indirectly promotes inhibitory transmission. The increase in inhibitory transmission might constitute a new mechanism via which furosemide can reduce seizures in the epileptic brain.

5.3 Methods

Animals

All animal experiments were performed in compliance with the guidelines for the welfare of experimental animals issued by the Federal Government of the Netherlands and were approved by the Dutch Central Committee Animal experiments (CCD), project AVD1080020173847 and project AVD1150020184927. In this study we used male and female transgenic mice: GAD65-GFP mice (López-Bendito et al., 2004) (bred as a heterozygous line in a C57BL/6Jrj background), C57BL/6Jrj littermates, and SuperClomeleon (SCLm) mice. The SCLm mice (Herstel et al., 2022) are SuperClomeleon^{lox/-} mice (Rahmati et al., 2021), a gift from Kevin Staley (Massachusetts General Hospital, Boston, MA) crossed with CamKII α ^{Cre/-} mice (Tsien et al., 1996; Casanova et al., 2001). SCLm mice express the chloride sensor SCLm in up to 70% of the pyramidal neurons in the hippocampus (Casanova et al., 2001; Wang et al., 2013). GAD65-GFP mice express GFP in ~20% of GABAergic interneurons in the CA1 region of

the hippocampus (Wierenga et al., 2010). As we did not detect any differences between slices from male and female mice as well as from GAD65-GFP mice and C57BL/6JRj littermates, all data were pooled.

Organotypic hippocampal culture preparation and furosemide treatment

Organotypic hippocampal cultures were made from P6-7 mice as described before (Hu et al., 2019; Herstel et al., 2022), based on the *Stoppini method* (Stoppini et al., 1991). Mice were decapitated and their brain was rapidly placed in ice-cold Grey's Balanced Salt Solution (GBSS; containing (in mM): 137 NaCl, 5 KCl, 1.5 CaCl₂, 1 MgCl₂, 0.3 MgSO₄, 0.2 KH₂PO₄ and 0.85 Na₂HPO₄) with 25 mM glucose, 12.5 mM HEPES and 1 mM kynurenic acid (pH set at 7.2, osmolality set at ~320 mOsm, sterile filtered). 400 µm thick transverse hippocampal slices were cut with a McIlwain tissue chopper. Slices were placed on Millicell membrane inserts (Millipore) in wells containing 1 ml culture medium (consisting of 48% MEM, 25% HBSS, 25% horse serum, 25 mM glucose, and 12.5 mM HEPES, with an osmolality of ~325 mOsm and a pH of 7.3 – 7.4). Slices were stored in an incubator (35°C with 5% CO₂). Culture medium was replaced by culture medium supplemented with 0.1% dimethyl sulfoxide (DMSO, Sigma-Aldrich) or 200 µM furosemide (furosemide, Merck, in 0.1 % DMSO). In addition, a small drop of medium supplemented with DMSO or furosemide was carefully placed on top of the slices. In this way, cultures were treated 3 times per week until DIV8. From DIV8 onwards, cultures received normal culture medium 3 times per week. Experiments were performed at day in vitro 1-3 (DIV2), 8-10 (DIV9) or 20-22 (DIV21). Please note that perforated patch experiments at DIV9 were performed 1 to 55 hr after cessation of the furosemide treatment, but experimental results did not correlate with hours after treatment or with the addition of furosemide to ACSF during the perforated patch recording.

Electrophysiology and analysis

Organotypic cultures were transferred to a recording chamber and continuously perfused with carbonated (95% O₂, 5% CO₂) artificial cerebrospinal fluid (ACSF, in mM: 126 NaCl, 3 KCl, 2.5 CaCl₂, 1.3 MgCl₂, 26 NaHCO₃, 1.25 NaH₂PO₄, 20 glucose; with an osmolality of ~310 mOsm) at a rate of approximately 1 ml/min. For acute application, ACSF containing 0.1% DMSO or 200 µM furosemide (dissolved in 0.1% DMSO) was bath applied for 5 minutes. Bath temperature was maintained at 29-32°C. Recordings were acquired using an MultiClamp 700B amplifier (Molecular Devices), filtered with a 3 kHz Bessel filter and stored using pClamp10 software.

Perforated patch clamp recordings were performed in CA1 pyramidal neurons. Recording pipettes with resistances of 2-4 MΩ were pulled from borosilicate glass capillaries (World Precision Instruments). The pipette tip was filled with gramicidin-free KCl solution (140 mM KCl and 10 mM HEPES, pH adjusted to 7.2 with KOH, and osmolality 285 mOsm/l) and then backfilled with solution containing gramicidin (60 µg/ml, Sigma). Neurons were held at -65 mV and the access resistance of the

perforated cells was monitored constantly before and during recordings by a 5 mV seal test. An access resistance of 50 M Ω was considered acceptable to start recording. Recordings were excluded if the resting membrane potential exceeded -50 mV or if the series resistance after the recording deviated more than 30% from its original value. GABA_A currents were induced upon local application of 50 μ M muscimol dissolved in HEPES-ACSF (containing in mM: 135 NaCl, 3 KCl, 2.5 CaCl₂, 1.3 MgCl₂, 1.25 Na₂H₂PO₄, 20 Glucose, and 10 HEPES) every 30 sec using a Picospritzer II. Muscimol responses were recorded in the presence of 1 μ M TTX (Abcam) at holding potentials between -100 mV and -30 mV in 10 mV steps. We plotted response amplitude as a function of holding potential and calculated the chloride reversal potential from the intersection of the linear current-voltage curve with the x-axis. To assess the size of GABA_A currents independent of holding and reversal potential, we calculated the slope of the current-voltage-plot.

For recordings of spontaneous inhibitory postsynaptic currents (sIPSCs) and miniature inhibitory currents (mIPSCs) we performed whole-cell patch clamp recordings from CA1 pyramidal neurons using borosilicate glass pipettes with resistances of 3-6 M Ω . Pipettes were filled with a KCl-based internal solution (containing in mM: 70 Kgluconate, 70 KCl, 0.5 ethyleneglycol- bis(β -aminoethyl)-N,N,N',N'-tetraacetic Acid (EGTA), 4 Na₂phosphocreatine, 4 MgATP, 0.4 NaGTP and 10 HEPES; pH adjusted to 7.2 with KOH) and ACSF was supplemented with 20 μ M DNQX (Tocris) and 50 μ M DL-APV (Tocris). For recordings of miniature IPSCs (mIPSCs), 1 μ M TTX (Abcam) was also added to the ACSF. sIPSCs and mIPSCs were recorded for 6 minutes. For wash in experiments, an sIPSC baseline was recorded for 6 minutes and compared to sIPSCs after 20 minutes wash in of 1 μ M TTX (Abcam), 0.2 μ M K252a (Tocris), 5 μ M AM251 (Sigma) or 1 μ M agatoxin-IVA (smartox-biotech), again for 6 minutes. Membrane capacitance and series resistance were monitored during the recordings by a 5 mV seal test. Cells were discarded if series resistance was above 35 M Ω or if the resting membrane potential exceeded -50 mV or if the series resistance after the recording deviated more than 30% from its original value.

All data were blinded before analysis. Events were selected using a template in Clampfit10 software. Further analysis was performed using custom-written MATLAB scripts. Rise time of sIPSCs was determined as the time between 10% and 90% of the peak value. The decay tau was fitted with a single exponential function. Only events with a goodness of fit $R^2 \geq 0.75$ were included.

Two-photon SuperClomeleon imaging and analysis

We performed two-photon chloride imaging in CA1 pyramidal cells using the SuperClomeleon sensor (Grimley et al., 2013) in cultured slices from SClm mice (Herstel et al., 2022). The SClm sensor consists of Cerulean (a CFP mutant) and Topaz (a YFP mutant) joined by a flexible linker. In the absence of chloride, Fluorescence Resonance

Energy Transfer (FRET) occurs from the CFP donor to the YFP acceptor. Chloride binding to YFP increases the distance between the fluorophores and decreases FRET (Grimley et al., 2013).

At the recording day, slices were transferred to a recording chamber and continuously perfused with carbonated (95% O₂, 5% CO₂) ACSF supplemented with 1 mM Trolox, at a rate of approximately 1 ml/min. Bath temperature was monitored and maintained at 30-32 °C. Two-photon imaging of CA1 pyramidal neurons or VGAT-positive interneurons in the CA1 area of the hippocampus was performed using a customized two-photon laser scanning microscope (Femto3D-RC, Femtonics, Budapest, Hungary) with a Ti:Sapphire femtosecond pulsed laser (MaiTai HP, Spectra-Physics) and a 60x water immersion objective (Nikon NIR Apochromat; NA 1.0). The CFP donor was excited at 840 nm. The emission light was split using a dichroic beam splitter at 505 nm and detected using two GaAsP photomultiplier tubes. We collected fluorescence emission of Cerulean/CFP (485 ± 15 nm) and Topaz/YFP (535 ± 15 nm) in parallel. Of each slice from SClm mice, 2-5 image stacks were acquired in different fields of view. The resolution was 8.1 pixels/μm (1024x1024 pixels, 126x126 μm) with 1 μm z-steps.

Image analysis was performed using ImageJ software, as described before (Herstel et al., 2022). We manually determined regions of interest (ROIs) around individual neuron somata. To select a representative cell population in SClm slices, in each image z-stack we selected four z-planes at comparable depths in which three pyramidal cells were identified that varied in CFP brightness (bright, middle and dark). We subtracted the mean fluorescence intensity of the background in the same image plane before calculating the fluorescence ratio of CFP and YFP. We limited our analysis to cells which were located within 450 pixels from the center of the image, as FRET ratios showed slight aberrations at the edge of our images. We excluded cells with a FRET ratio < 0.5 or > 1.6 to avoid unhealthy cells.

Protein extraction and Western Blot analysis

Organotypic hippocampal cultures were washed in cold PBS and subsequently lysed in cold protein extraction buffer containing: 150 mM NaCl, 10 mM EDTA 10 mM HEPES, 1% Triton-X100 and 1x protease and 1x phosphatase inhibitors cocktails (Complete Mini EDTA-free and phosSTOP, Roche). Lysates were cleared of debris by centrifugation (14,000 rpm, 1 min, 4°C) and measured for protein concentration before storage at -20°C until use. Lysates were denatured by adding loading buffer and heating to 95°C for 5 min. For each sample an equal mass of proteins was resolved on 4-15 % polyacrylamide gel (Bio-Rad). The proteins were then transferred (300 mA, 3h) onto ethanol-activated Immobilon-P PVDF membrane (Millipore) before blocking with 3% Bovine Serum Albumin in Tris- buffered saline-Tween (TBST, 20 mM Tris, 150 mM NaCl, 0.1% Tween-20) for 1 h. Primary antibodies used in this study were: mouse anti-NKCC1 (T4, Developmental Studies Hybridoma Bank, 1:1000), rabbit anti-KCC2 (07-432,

Merck, 1:1000) and s940-pKCC2 (p1551-940, LuBioSciences, 1:1000), mouse anti-tubulin (T-5168, Sigma, 1:10000). Primary antibodies were diluted in blocking buffer and incubated with the blots overnight at 4 °C under gentle rotation. The membrane was washed 3 times 15 minutes with TBST before a 1h incubation of horseradish peroxidase (HRP)-conjugated antibodies (P0447 goat anti-mouse IgG HRP, Dako, 1:2500 or P0399 swine anti-rabbit IgG HRP, Dako, 1:2500), and washed 3 times 15 minutes in TBST again before chemiluminescence detection. For chemiluminescence detection, blots were incubated with Enhanced luminol-based Chemiluminescence substrate (Promega), and the exposure was captured using the ImageQuant 800 system (Amersham). Images were analyzed in ImageJ, by drawing rectangular boxes around each band and measuring average intensities. Protein levels were normalized to the Tubulin loading controls.

Immunohistochemistry, confocal microscopy and analysis

Slices were fixed 4 % paraformaldehyde solution in PBS for 30 minutes at room temperature. After washing slices in phosphate buffered saline (PBS), they were permeabilized for 15 minutes in 0.5 % Triton X-100 in PBS for 15 minutes, followed by 1 hour in a blocking solution consisting of 10 % normal goat serum and 0.2 % Triton X-100 in PBS. Slices were incubated in primary antibody solution at 4 °C overnight. The following primary antibodies were used: rabbit polyclonal anti-KCC2 (07-432, Merck, 1:1000), rabbit anti-VGAT (131003, Synaptic Systems, 1:1000), guinea pig anti-VGLUT (AB5905, Merck, 1:1000), mouse anti-NeuN (MAB377, Millipore, 1:500), guinea pig anti-NeuN (ABN90, Merck, 1:1000). Slices were washed in PBS and incubated in secondary antibody solution for four hours at room temperature. Secondary antibodies used were: goat anti-mouse Alexa Fluor 467 (Life Technologies, A21236, 1:500), goat anti-rabbit Alexa Fluor 405 (A31556, Life Technologies, 1:500), goat anti-guinea pig Alexa Fluor 488 (A11073, Life Technologies, 1:1000) and Goat anti-guineapig Alexa Fluor 568 (A11075, Life Technologies, 1:500) Goat anti-rabbit Alexa fluor 647 (A21245, Life Technologies, 1:500). After another PBS wash, slices were mounted in Vectashield mounting medium (Vector labs).

Confocal images were taken on a Zeiss LSM-700 confocal laser scanning microscopy system with a Plan-Apochromat 40x 1.3 NA immersion objective for KCC2 staining and 63x 1.4 NA oil immersion objective for inhibitory synapse staining. KCC2 staining was imaged in two fields of view in the CA1 *sPyr* of each slice. Inhibitory synapses were imaged in the CA1 *sPyr* and *sRad* of each slice. Image stacks (1024x1024 pixels) were acquired at 6.55 pixels/ μm for KCC2 staining, 10.08 pixels/ μm for VGLUT/VGAT staining. Step size in z was 0.5 μm for KCC2 staining and 0.4 μm for inhibitory synapse staining.

Confocal images were blinded before analysis. For the analysis of KCC2 levels in control and furosemide-treated slices, ROIs were drawn around 5 NeuN positive cell bodies and this was repeated in 1-3 z-planes (depending on the depth of KCC2 signal) at

comparable depths, to measure average KCC2 fluorescence of 5-15 neurons per image stack. For analysis of inhibitory synapses a custom-made macro was used (Ruiter et al., 2020). Briefly, three Z-planes were averaged and background was subtracted with rolling ball radius of 10 pixels. VGAT puncta were identified using watershed segmentation. PV and CB1R channels were thresholded and colocalization with VGAT puncta was analyzed.

Statistical Analyses

Statistical analysis was performed in Prism (Graphpad). Normality was tested using the D'Agostino & Pearson test. For the comparison of two groups we either used an unpaired Student's t test (UT; parametric), a Mann-Whitney test (MW; non-parametric), a paired Student's t test (PT; parametric) or a Wilcoxon signed-rank test (WSR; non-parametric). For comparison of multiple groups, a Kruskal Wallis test (KW; nonparametric) was used, followed by a Dunn's Multiple Comparison posthoc test (DMC) or a two way ANOVA (2W ANOVA; parametric), followed by a Sidak's Multiple Comparisons posthoc test (SMC). Data are presented as mean \pm standard error of the mean. Significance is reported as * $p < 0.05$; ** $p \leq 0.01$; *** $p \leq 0.001$.

5.4 Results

Furosemide depolarizes GABA responses acutely, but hyperpolarizes GABA responses after one week treatment.

We set out to manipulate the GABA shift with furosemide in organotypic hippocampal cultures. We used perforated patch recordings upon muscimol application in CA1 pyramidal neurons of cultured hippocampal slices to record the reversal potential of GABA_A receptor currents. Acute administration of 200 μ M furosemide in DIV2 slices did not affect the GABA reversal potential (E_{GABA}) (Fig. 1A) or GABA driving force (GABA DF) (Fig. 1B), in agreement with a low expression of KCC2 at this age (Salmon et al., 2020; Peerboom et al., 2023). At DIV21, when KCC2 expression is high (Salmon et al., 2020; Peerboom et al., 2023), acute furosemide application elevated E_{GABA} and GABA DF (Fig. 1C,D), in line with previous reports on acute application of furosemide (Thompson and Gahwiler, 1989; Jarolimek et al., 1999; Deeb et al., 2013; Wright et al., 2017) and in line with acute inhibition of KCC2 by the specific KCC2 blocker VU0463271 (VU) in slices at the same developmental stage (Peerboom et al., 2023). We then treated cultured hippocampal slices from DIV1 to DIV8 with 200 μ M furosemide. Surprisingly, we observed a strong hyperpolarization of E_{GABA} and a negative shift of the GABA DF after one week furosemide treatment at DIV9 (Fig. 1E,F). Since furosemide has been shown to inhibit $\alpha 6$ - and $\alpha 4$ -subunit containing GABA_A receptors (Thompson and Gahwiler, 1989; Pearce, 1993; Korpi et al., 1995), we checked if GABA_A receptor inhibition may have interfered with our measurements of E_{GABA} and GABA DF. As a rough indication, we determined the slope of the current-voltage (IV) plot to assess GABA response amplitudes independently of holding potential and reversal potential.

However, IV-slopes were not different (MW, $p=0.46$), suggesting that furosemide did not have a major effect on GABA_A receptors.

A hyperpolarizing shift in E_{GABA} suggest that furosemide treatment decreased intraneuronal chloride or HCO_3^- levels. To further examine intracellular chloride levels after furosemide treatment, we used the chloride sensor SuperClomeleon (SCLm) (Grimley et al., 2013; Boffi et al., 2018; Rahmati et al., 2021; Herstel et al., 2022). Remarkably, SCLm FRET ratios in CA1 pyramidal neurons were not different in furosemide-treated and control cultures (Fig. 1G,H). The discrepancy between our results from perforated patch recordings and SCLm imaging may be due to the decreased sensitivity of the SCLm sensor for low chloride levels (Grimley et al., 2013; Herstel et al., 2022). Alternatively, it may reflect concomitant changes in chloride and HCO_3^- , as SCLm displays substantial pH-sensitivity (Grimley et al., 2013; Boffi et al., 2018; Lodovichi et al., 2022). These possibilities are discussed in more detail in the discussion section.

To examine if furosemide treatment made GABA signaling hyperpolarizing by changing chloride cotransporter expression, we assessed total NKCC1, KCC2 or S940-pKCC2 protein levels in control and furosemide-treated slices using Western blots. No significant changes in the levels of NKCC1, KCC2 or S940-pKCC2 were observed (Fig. 1I,J). In addition, we examined KCC2 localization in treated and control slices using immunohistochemistry. We used NeuN to identify individual cell bodies and we estimated KCC2 levels in somata and membranes. We previously showed that we can detect reduction in KCC2 levels after shRNA using these methods (Peerboom 2023). Furosemide treatment did not significantly affect KCC2 levels in somata or membranes of CA1 pyramidal neurons (Fig. 1K,L). Together, this indicates that furosemide treatment during DIV1 to DIV8 hyperpolarized GABA signaling without changing the expression or surface levels of KCC2, nor by changing expression levels of NKCC1 and S940-pKCC2. These results suggest that furosemide treatment hyperpolarized E_{GABA} via inhibition of both chloride transporters KCC2 and NKCC1 without altering their expression.

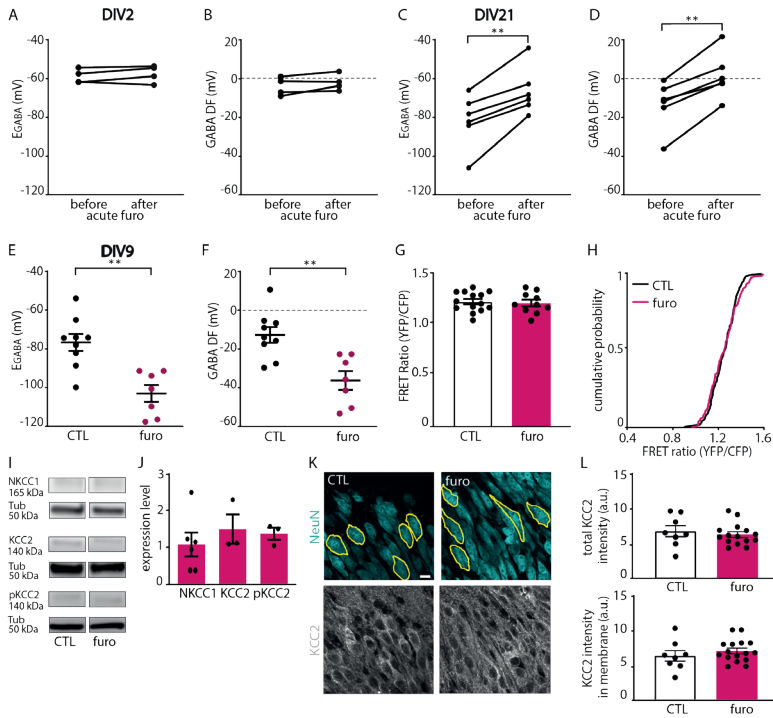


Figure 1. Furosemide acutely depolarizes the GABAergic driving force, but results in hyperpolarization after one week treatment.

A, B) GABA reversal potential (E_{GABA}) (PT, $p=0.33$) and GABA Driving Force (GABA DF) (PT, $p=0.19$) values recorded in CA1 pyramidal cells at DIV2 before and after acute application of furosemide. Data from 4 cells, 4 slices and 4 mice.

C, D) E_{GABA} (MW, $p=0.004$) and GABA DF (MW, $p=0.002$) values recorded in CA1 pyramidal cells at DIV21 before and after acute application of furosemide. Data from 6 cells, 5 slices and 5 mice.

E, F) E_{GABA} (MW, $p=0.001$) and GABA DF (MW, $p=0.005$) recorded in CA1 pyramidal cells at DIV9 in control (CTL) and furosemide-treated slices. Data from 7-9 cells, 5-8 slices and 4-5 mice per group.

G) Average SCLm FRET ratios in CTL and furosemide-treated slice cultures (UT, $p=0.75$). Data from 10-14 slices and 6-10 mice per group.

H) Cumulative distribution of FRET ratios in individual cells in CTL and furosemide-treated cultures. (KS, $p=0.23$). Data from 15 randomly selected cells per slice.

I) Western blots of NKCC1, KCC2 and S940-pKCC2 (pKCC2) protein levels in CTL and furosemide-treated slice cultures. Tubulin (Tub) was used as loading control.

J) Summary of data for NKCC1, KCC2 and for s940-pKCC2 (pKCC2) protein levels. Values were normalized to the protein level in CTL cultures (NKCC1: MW, $p>0.99$; KCC2: MW, $p=0.70$; pKCC2: MW, $p=0.48$). Data from 3-5 experiments and 3 mice per group.

K) Confocal images of NeuN and KCC2 staining in CTL and furosemide-treated cultures. Yellow lines indicate the outlines of individual cells. Scale bar: 10 μ m.

L) Total KCC2 levels (UT, $p=0.55$) and KCC2 levels in membrane (UT, $p=0.37$) in CTL and furosemide-treated cultures. Each datapoint represents the mean KCC2 intensity of all neurons in one image. Data from 8-17 images, 4-8 slices and 3 mice per group.

Furosemide does not affect inhibitory synapses at DIV9, but increases the number of inhibitory synapses at DIV21.

The results above show that one week of furosemide treatment hyperpolarized E_{GABA} , thereby accelerating the GABA shift. Next, we assessed the consequences of this accelerated GABA shift on inhibitory transmission. We recorded spontaneous and miniature inhibitory currents (sIPSCs and mIPSCs) from CA1 pyramidal cells in control and furosemide-treated slices at DIV9. We found that the frequency, amplitude, rise and decay kinetics of sIPSCs and the membrane capacitance (C_m) of CA1 pyramidal neurons were similar in control and furosemide-treated slices at DIV9 (Fig. 2A-E). This indicates that GABA signaling does not directly affect the development of inhibitory synapses at this developmental stage, which is in line with our recent study (Peerboom et al., 2023).

When recording sIPSCs, we noticed that the sIPSC frequency slightly increased with ~20% during 20 minutes of recording in both control and furosemide-treated slices (Fig. 2F,G). When we washed in TTX to block neuronal activity in control slices, this 'run-up' was prevented (Fig. 2H), indicating that the run-up is activity dependent. However, TTX did not prevent the run-up in furosemide-treated slices, suggesting that the run up had different mechanisms in control and furosemide-treated slices (Fig. 2I). We considered the possibility that the activity-dependent run up is due to release of activity-dependent factors, such as endocannabinoids or BDNF. We therefore assessed the contribution of TrkB, the BDNF receptor, and CB1, the endocannabinoid receptor, in control and furosemide-treated slices using TrkB antagonist K252a, and CB1 receptors antagonist AM251 respectively. We found that sIPSCs were enhanced after wash in K252a, but not AM251. This suggests that there is ongoing suppression of GABA release by BDNF, while endocannabinoid signaling does not have a prominent role on GABA release in our slices at DIV9. There was no differential contribution of BDNF and endocannabinoid signaling between control and furosemide-treated slices (Fig. 2J). We also blocked presynaptic P/Q calcium channels with agatoxin-IVA (aga) (Goswami et al., 2012), but this did not significantly alter sIPSC frequency in control and furosemide-treated slices (Fig. 2J). It thereby remains unclear why the run up of sIPSCs was different after furosemide treatment.

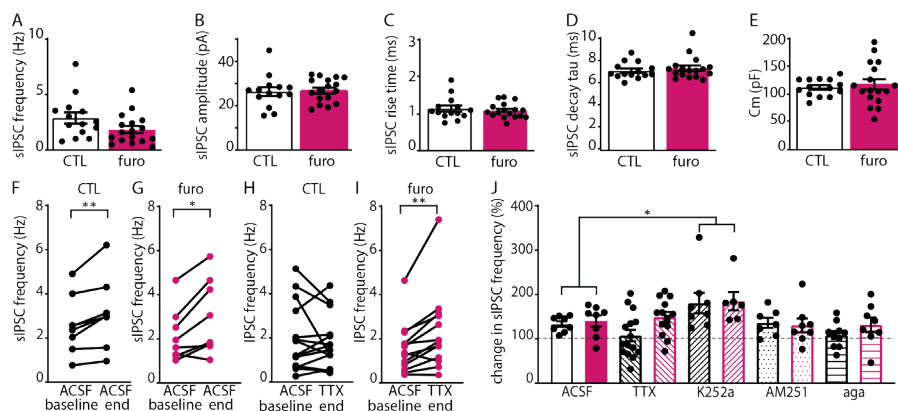


Figure 2. Furosemide does not affect inhibitory transmission at DIV9.

A-E) sIPSC frequency (MW, $p=0.084$), amplitude (UT, $p=0.83$), risetime (MW, $p=0.80$) and decay tau (MW, $p=0.57$) and membrane capacitance (C_m) (UT, $p=0.63$) in control (CTL) and furosemide-treated slice cultures at DIV9. Data from 14-17 cells, 9 slices and 9 mice per group.

F-I) sIPSC frequency after ACSF wash in as a control CTL (WSR, $p=0.008$) and furosemide-treated (WSR, $p=0.002$) slice cultures at DIV9. sIPSC frequency after TTX wash in of in CTL (WSR, $p=0.80$) and furosemide-treated WSR, ($p=0.002$) slice cultures at DIV9. Data from 8-15 cells, 8-15 slices and 7-10 mice per group.

J) Change in sIPSC frequency after ACSF wash in as a control, versus after wash in of TTX, K252a, AM251 and agatoxin-IVA (aga) to block neuronal activity, BDNF, endocannabinoids and P/Q calcium channels respectively in control and furosemide-treated slices at DIV9 (2W ANOVA, treatment $p=0.18$, blocker $p=0.002$; SMC, control versus TTX, $p=0.95$; control versus K252a, $p=0.020$; control versus AM251, $p=0.99$; control versus agatoxin-IVA (aga), $p=0.82$). Data from 7-15 cells, 7-15 slices and 4-10 mice per group.

Two weeks after ending the treatment at DIV21, E_{GABA} and GABA DF in pyramidal neurons had normalized and reached control levels (Fig. 3A,B). As we previously found that a transient elevation of chloride using VU treatment from DIV1 to DIV8 resulted in indirect changes in inhibitory transmission (Peerboom et al., 2023), we also recorded inhibitory transmission at DIV21 (Fig. 3C,D). We observed that the sIPSC amplitude was significantly increased in furosemide-treated slices, while the frequency, rise and decay time of the sIPSCs were not affected (Fig. 3E-H). In addition, we found that cell capacitance of CA1 pyramidal cells was decreased in furosemide-treated slices compared to control slices (Fig. 3I). To assess whether the changes in inhibitory transmission were activity-dependent, we also recorded mIPSCs. The mIPSCs frequency was increased in furosemide-treated slices at DIV21, while amplitude, rise and decay time were not different (Fig. 3J-M). This suggests that the increase in sIPSC amplitude may be explained by an increase in inhibitory synapses. Interestingly, a difference in membrane capacitance was no longer detected when recording mIPSCs in the presence of TTX (Fig. 3N). This may reflect a change in activity-dependent cell

swelling after furosemide treatment (Hochman et al., 1995; Gutschmidt et al., 1999; Hochman, 2012).

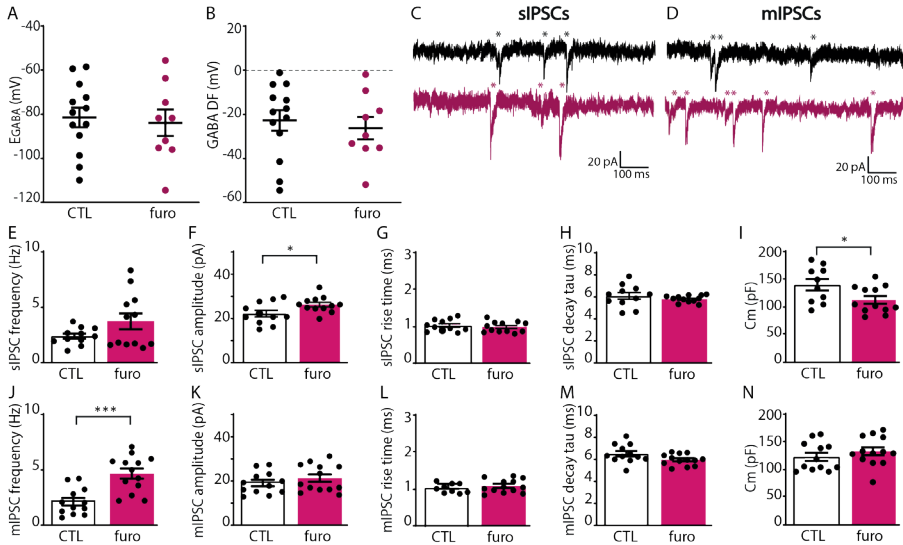


Figure 3. Furosemide increases inhibitory transmission at DIV21.

A,B) GABA reversal potential (E_{GABA}) (MW, $p=0.56$) and GABA Driving Force (GABA DF) (MW, $p=0.76$) in control (CTL) and furosemide-treated slice cultures at DIV21. Data from 9-13 cells, 9 slices and 9 mice per group.

C) sIPSC recording from CA1 pyramidal cells in CTL and furosemide-treated organotypic cultures at DIV21. sIPSCs are indicated with *.

D) mIPSC recording from CA1 pyramidal cells in control and furosemide-treated organotypic cultures at DIV21. mIPSCs are indicated with *.

E-H) sIPSC frequency (UT, $p=0.10$), amplitude (UT, $p=0.034$), risetime (UT, $p=0.54$) and decay tau (UT, $p=0.34$) in CTL and furosemide-treated slice cultures at DIV21. Data from 11-12 cells, 5-6 slices and 3-5 mice per group.

I) Membrane capacitance (C_m) of CA1 pyramidal cells in CTL and furosemide-treated slice cultures at DIV21 (UT, $p=0.035$). Data from 11-12 cells, 5-6 slices and 3-5 mice per group.

J-M) mIPSC frequency (UT, $p=0.0002$), amplitude (UT, $p=0.34$), risetime (MW, $p=0.73$) and decay tau (UT, $p=0.06$) in CTL and furosemide-treated organotypic cultures at DIV21. Data from 11-12 cells, 5-6 slices and 3-5 mice per group. Data from 12-13 cells, 5 slices and 4 mice per group.

N) Membrane capacitance (C_m) of CA1 pyramidal cells in the presence of TTX in CTL and furosemide-treated slice cultures at DIV21 (UT, $p=0.35$). Data from 12-13 cells, 5 slices and 4 mice per group.

We also compared C_m in sIPSC (I) versus mIPSC (N) recordings in CTL slice cultures (UT, $p=0.16$) and C_m in sIPSC (I) versus mIPSC (N) recordings in furosemide-treated slices (UT, $p=0.068$).

Our observation that the amplitude, but not frequency, of sIPSCs was increased in furosemide-treated slices, while mIPSC frequency, and not amplitude, was increased, suggest that the number of inhibitory synapses is increased in furosemide-treated slices. To assess synapse numbers, we used immunohistochemistry to visualize inhibitory synapses in *stratum Pyramidale* (*sPyr*) and *stratum Radiatum* (*sRad*) using the vesicular GABA transporter VGAT. In addition, we stained for CB1 receptors (CB1R) and parvalbumin (PV), to identify inhibitory synapses from specific interneuron subtypes (Fig. 4A,B, Fig. 5A,B). The density and size of VGAT puncta in the CA1 area were similar in control and furosemide-treated slices at DIV9 (Fig. 4C-F) and we did not observe any differences in the density of CB1R+ and PV+ VGAT puncta (Fig. 4G-I). At DIV21 however, we observed an increased density and reduced size of VGAT puncta in the *sRad* in furosemide-treated slices compared to controls (Fig. 5E,F), but not *sPyr* (Fig. 5C,D). This suggests that the number of inhibitory synapses in the dendritic region was increased at DIV21 in furosemide-treated slices. The density of PV- and CB1R-positive puncta were not different in furosemide-treated and control slices (Fig. 5G-I), suggesting that the increase in VGAT puncta is due to an increase in synapses from another interneuron subtype.

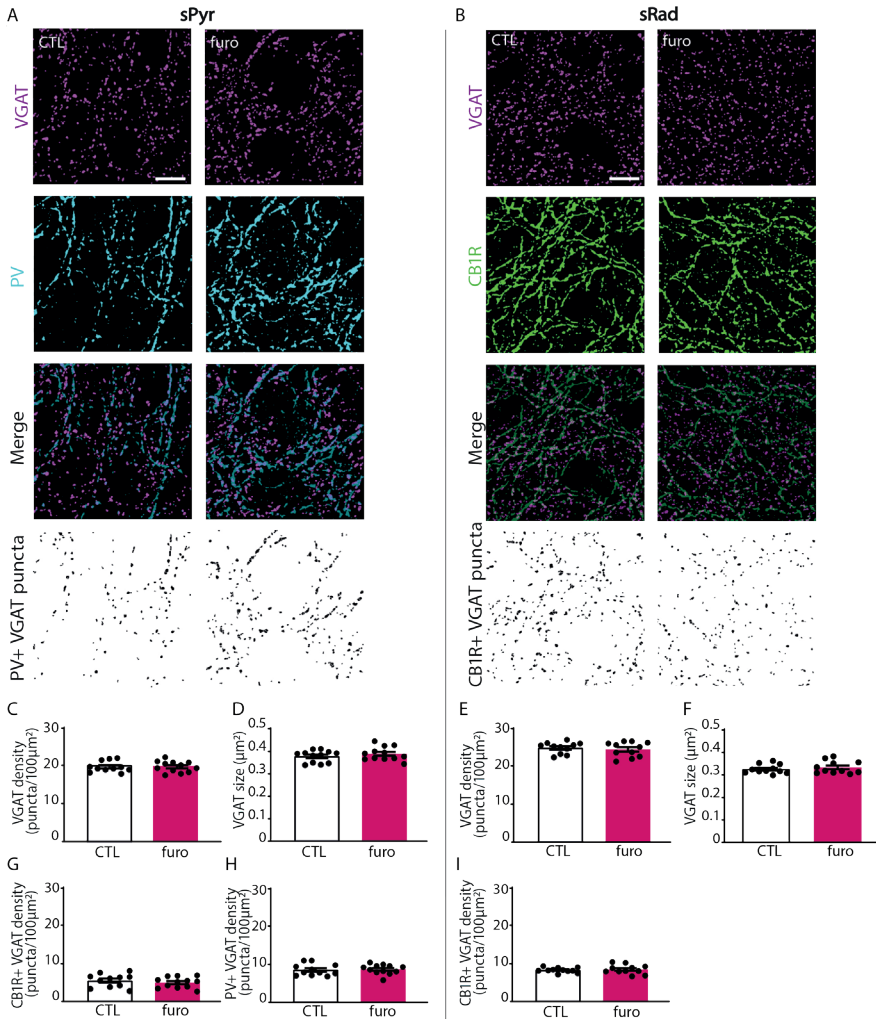


Figure 4. Furosemide does not affect inhibitory synapses at DIV9.

A,B) VGAT, PV and CB1R immunofluorescence in the CA1 *stratum Pyramidale* (sPyr) and *stratum Radiatum* (sRad) of control (CTL) and furosemide-treated organotypic cultures at DIV9. Scale bar=10 µm.

C,D) The density (UT, $p=0.50$) and size (UT, $p=0.47$) of VGAT puncta in the sPyr of CTL and furosemide-treated organotypic cultures at DIV9.

E,F) The density (UT, $p=0.59$) and size (UT, $p=0.46$) of VGAT puncta in sRad of CTL and furosemide-treated organotypic cultures at DIV9.

G,H) The density of CB1R-positive VGAT puncta (UT, $p=0.43$) and PV positive VGAT puncta (UT, $p=0.82$) in sPyr of CTL and furosemide-treated organotypic cultures at DIV9.

I) The density of CB1R-positive VGAT puncta (UT, $p=0.68$) in sRad of CTL and furosemide-treated organotypic cultures at DIV9.

Data in C-I from 11-12 images, 6 slices and 2 mice per group.

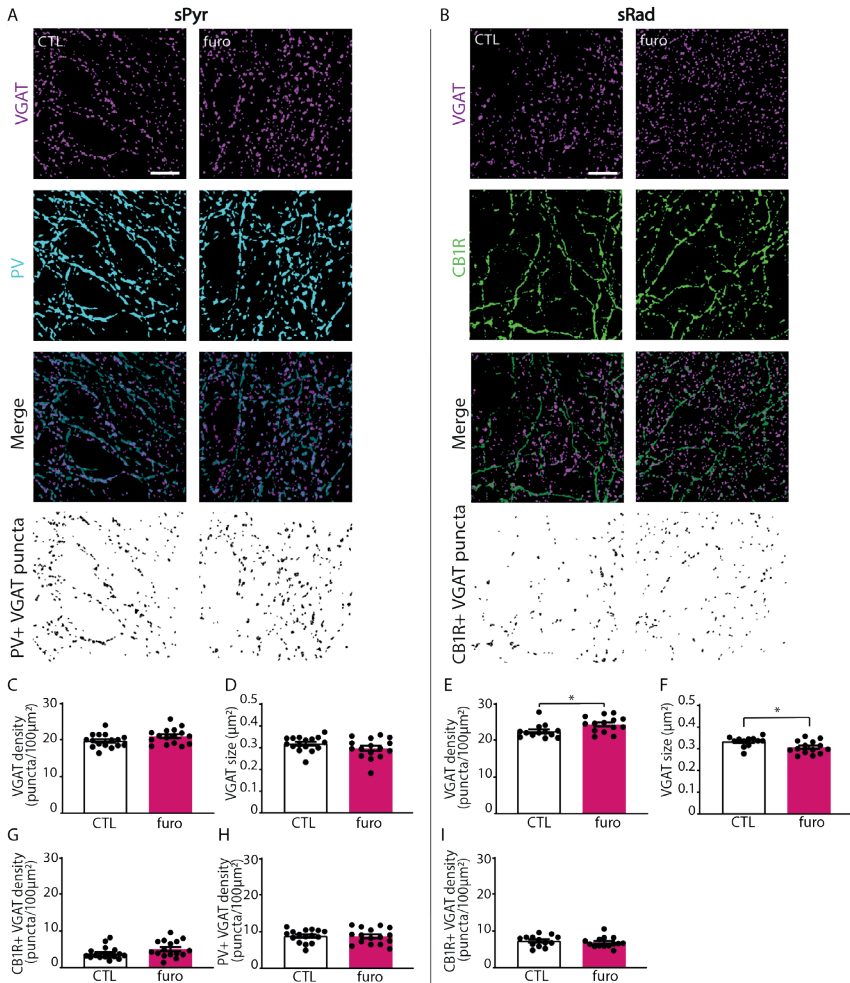


Figure 5. Furosemide increases the number of inhibitory synapses at DIV21 in *sRad*.

A,B) VGAT, PV and CB1R immunofluorescence in the CA1 *stratum Pyramidale* (*sPyr*) and *stratum Radiatum* (*sRad*) of control (CTL) and furosemide-treated organotypic cultures at DIV21. Scale bar=10 µm.

C,D) The density (UT, $p=0.09$) and size (UT, $p=0.14$) of VGAT puncta in *sPyr* of CTL and furosemide-treated organotypic cultures at DIV21. Data from 16 images, 8 slices and 3 mice per group.

E,F) The density (MW, $p=0.019$) and size (MW, $p=0.015$) of VGAT puncta in *sRad* of CTL and furosemide-treated organotypic cultures at DIV21. Data from 13 images, 7 slices and 3 mice per group.

G,H) The density of CB1R (UT, $p=0.11$) and PV positive VGAT puncta (UT, $p=0.89$) in *sPyr* of CTL and furosemide-treated organotypic cultures at DIV21. Data from 16 images, 8 slices and 3 mice per group.

I) The density of CB1R-positive VGAT puncta (MW, $p=0.30$) in *sRad* of CTL and furosemide-treated organotypic cultures at DIV21. Data from 13 images, 7 slices and 3 mice per group.

5.5 Discussion

In this study, we used furosemide to manipulate the GABA shift. Unexpectedly, we observed that one week treatment with furosemide had the opposite effect compared to acute application. While acute application of furosemide depolarized the reversal potential for GABA signaling (E_{GABA}), one week furosemide treatment resulted in a strong hyperpolarizing shift of E_{GABA} . This shift was not accompanied by a change in SuperClomeleon (SCLm) FRET ratios or chloride co-transporter expression. We observed that sIPSCs were not affected by the hyperpolarization of E_{GABA} after furosemide treatment at DIV9, consistent with the notion that GABA signaling in the second postnatal week no longer affects synapse formation (Wang and Kriegstein, 2011; Peerboom et al., 2023). However, we found that at DIV21, two weeks after ending furosemide treatment, inhibitory currents were increased, likely through an increase of the number of inhibitory synapses in *sRad*. Moreover, we found clues for cell shrinkage in CA1 pyramidal neurons in furosemide-treated slices at DIV21. Together, these results show that accelerating the GABA shift with furosemide does not directly affect the development of inhibitory synapses. Furosemide treatment seemed to have altered cell volume regulation and increased inhibitory transmission two weeks later.

Effect of furosemide on neuronal chloride levels

The depolarizing effect of acute furosemide application at DIV21 is comparable to that of acute inhibition of KCC2 by specific KCC2 blocker VU0463271 (VU) in slices at the same developmental stage (Peerboom et al., 2023), suggesting that acutely applied furosemide merely inhibited KCC2. At the concentration used here (200 μM), furosemide is expected to block both KCC2 and NKCC1 (Orlov et al., 2015). However, NKCC1 maintains chloride levels only until approximately P15-21 (Romo-Parra et al., 2008; Sulis Sato et al., 2017; Salmon et al., 2020). Previous studies reporting a depolarizing effect of furosemide acutely applied the compound to (slice) cultures at a developmental stage equal to P14 or later (Thompson and Gahwiler, 1989; Jarolimek et al., 1999; Deeb et al., 2013; Wright et al., 2017). Thus, in our slices at DIV21 (prepared from P6 and P7 mice), NKCC1 may no longer affect chloride levels, and therefore furosemide may act only via KCC2 at DIV21.

In stark contrast, furosemide treatment from DIV1 to DIV8 resulted in hyperpolarizing E_{GABA} , suggestive of NKCC1 block. We checked that furosemide treatment did not affect expression levels of chloride transporters. To assess if the furosemide-induced hyperpolarization of E_{GABA} is indeed mediated by inhibition of NKCC1, perforated patch experiments should be performed during wash in of NKCC1 blocker bumetanide (Owens et al., 1996; Romo-Parra et al., 2008; Sulis Sato et al., 2017). If furosemide hyperpolarized E_{GABA} via NKCC1, wash in of bumetanide should not result in a further hyperpolarization of E_{GABA} in furosemide-treated slices, but would hyperpolarize E_{GABA} in controls.

If furosemide treatment indeed hyperpolarized E_{GABA} by blocking NKCC1, we would expect to observe an increase in SClm FRET ratios (reflecting a decrease in chloride levels) after furosemide treatment, which was not the case. However, the sensitivity of the SClm sensor is reduced at chloride concentrations below ~ 5 mM (Grimley et al., 2013; Boffi et al., 2018; Herstel et al., 2022). This raises the possibility that chloride levels in our slices at DIV9 are too low to detect a further decrease by furosemide treatment with the SClm sensor.

Possible effect of furosemide on pH

In addition to blocking chloride transporters, furosemide may also interfere with enzymes that are involved in HCO_3^- regulation (Halligan et al., 1991; Temperini et al., 2009; Uwera et al., 2015). GABA_A receptors are permeable for chloride and HCO_3^- ions with a permeability of around 70% and 30% respectively (Kaila et al., 2014). The reversal potential of HCO_3^- ($E_{\text{HCO}_3^-}$) is maintained by pH-regulatory proteins at around -10 mV (Kaila et al., 2014), which is much more positive than the chloride reversal potential (E_{Cl}). As a result, E_{GABA} is slightly more positive than E_{Cl} and the flow of chloride through GABA_A receptors is accompanied by an outflow of HCO_3^- (Kaila et al., 2014). This raises the possibility that the hyperpolarization of E_{GABA} together with a lack of change in SClm FRET ratios after furosemide treatment reflect changes in intracellular HCO_3^- levels. If furosemide would decrease intraneuronal HCO_3^- levels, the outflow of HCO_3^- upon GABA_A receptor activation would be reduced, and E_{GABA} would become more negative. Previous studies have suggested that furosemide can inhibit the $\text{Cl}^-/\text{HCO}_3^-$ anion exchanger AE3 (Halligan et al., 1991; Uwera et al., 2015). AE3 exchanges intracellular HCO_3^- for extracellular chloride, thereby lowering intracellular pH and increasing intracellular chloride concentrations in response to intracellular alkali loads (Gonzalez-Islas et al., 2009; Pfeffer et al., 2009; Romero et al., 2013). Furosemide can also block carbonic anhydrase (CA) (Temperini et al., 2009), which is a cytosolic enzyme that mediates the conversion of HCO_3^- ($\text{CO}_2 + \text{H}_2\text{O} \rightleftharpoons \text{HCO}_3^- + \text{H}^+$) to buffer intraneuronal pH after alkali or acid loads (Ruusuvaori, E. & Kaila, 2014). To our knowledge there are no studies directly examining the contribution of AE3 or CA to E_{GABA} . Theoretically, inhibition of AE3 by furosemide would decrease intracellular chloride levels while increasing HCO_3^- , which have opposing effects on E_{GABA} . Inhibition of CA would in theory reduce the contribution of $E_{\text{HCO}_3^-}$ to E_{GABA} and result in a negative shift of E_{GABA} towards E_{Cl} . If the hyperpolarization of E_{GABA} was solely due to changing HCO_3^- levels without changing chloride, pH values would be unphysiologically low. A strong decrease in pH would decrease IPSC frequency and amplitude and increase IPSC rise and decay time (Mozrzymas et al., 2003; Dietrich and Morad, 2010), while we observed that IPSCs were unaffected at DIV9. This suggests that no major change in pH levels occurred. We therefore deem it unlikely that furosemide induced large pH changes. However, a small decrease in intracellular pH would decrease SClm FRET ratios (Grimley et al., 2013; Boffi et al., 2018; Lodovichi et al., 2022), which may have obscured an increase in FRET ratios due to a decrease in chloride levels. We therefore

conclude that furosemide treatment most likely resulted in a decrease in chloride levels, but our data do not exclude a subtle change in pH regulation. To measure the contributions of AE3 and CA to the furosemide-induced hyperpolarization of E_{GABA} , AE3 inhibitor 4,4'-diisothiocyanatostilbene-2,2'-disulfonic acid (DIDS) (Uwera et al., 2015) and CA inhibitor ethoxzolamide (EZA) (Ruusuvoori et al., 2004; Rivera et al., 2005) should be washed in during perforated patch experiments. If furosemide treatment induced a hyperpolarization of E_{GABA} by blocking AE3 or CA, wash in of DIDS or EZA would not result in further hyperpolarization of E_{GABA} in furosemide-treated slices, but it would alter E_{GABA} in controls. To test if furosemide treatment altered the pH in our slices additional experiments would be required, using a fluorescent pH sensor, such as 2',7'-Bis-(2-Carboxyethyl)-5-(and-6)-Carboxyfluorescein, Acetoxymethyl Ester (BCECF) (Ruusuvoori et al., 2004). Another option would be the LSSmClopHensor, which allows for simultaneous measurement of intracellular chloride concentrations and pH. However, it should be noted that the sensitivity of LSSmClopHensor is limited at low chloride concentrations (Sulis Sato et al., 2017), which will hamper chloride measurements.

Possible effect of furosemide on cell volume regulation

We observed that the membrane capacitance of CA1 pyramidal neurons was reduced in furosemide-treated slices compared to control slices at DIV21 (Fig. 2E,S). A reduction in whole cell membrane capacitance may reflect a reduction in cell size (Taylor, 2012). Remarkably, neuronal capacitance was not affected when neuronal activity was blocked during mIPSC recordings (compare Fig. 3I and 3N), suggesting that the difference in membrane capacitance reflected activity-dependent cell shrinkage. Previous studies have shown that furosemide inhibits activity-induced changes in the volume of neuronal tissue during epilepsy (Hochman et al., 1995; Gutschmidt et al., 1999; Hochman, 2012). It has been shown that this effect is mainly mediated by inhibition of NKCC1 on glia (Ransom et al., 1985; Hochman, 2012). Glia disperse local, activity-induced elevations in potassium and chloride ions which are followed by water and result in glial swelling (Ransom et al., 1985; Hochman et al., 1995; Gutschmidt et al., 1999; Hochman, 2012). Our results suggest that furosemide may indirectly inhibit the activity-induced swelling of neurons as well.

In interpreting our results and that of previous studies, it is hard to disentangle the versatile pharmacological profile of furosemide and the many roles for neuronal chloride, as chloride levels also regulate cell volume (Jentsch and Pusch, 2018) and possibly cellular excitability (Huang et al., 2012; Seja et al., 2012; Jentsch and Pusch, 2018; Goutierre et al., 2019; Sinha et al., 2022; Peerboom et al., 2023). To disentangle the roles of chloride, GABA, cell volume and excitability in brain development, the consequences of treatments with specific KCC2 (Peerboom et al., 2023), NKCC1 (Wang and Kriegstein, 2011), AE3 and CA inhibitors, osmolytes and excitability modulators on network development should be studied and compared.

Furosemide treatment indirectly increased inhibitory transmission

We observed that sIPSCs were not affected by the hyperpolarization of E_{GABA} at DIV9, immediately after the furosemide treatment (Fig. 2A-E). These results confirm previous studies reporting that synapse formation is mostly independent from GABA signaling after the first postnatal week (Wang and Kriegstein, 2011; Peerboom et al., 2023).

More surprisingly, we found that furosemide treatment resulted in an increase in inhibitory transmission at DIV21. The amplitude of sIPSCs and the frequency of mIPSCs were strongly increased, and this was associated with an increased density of inhibitory synapses in *sRad* in furosemide-treated slices compared to control slices. However, one should be cautious in interpreting synaptic density in the two conditions, as furosemide treatment may have induced overall cell shrinkage, which would increase the apparent density. To assess synaptic densities independently of cell shrinkage, the density of synapses along the dendrites (Feng et al., 2021) or per soma (Bijlsma et al., 2022) should be assessed. The indirect effect on inhibitory synapses is reminiscent of our other recent study, although the underlying mechanism seems different. When we treated slice cultures with VU, a specific blocker of the chloride exporter KCC2, to delay the postnatal GABA shift and maintain a depolarizing E_{GABA} until DIV8, we also observed an indirect increase in sIPSC frequency at DIV21, but in this case without affecting mIPSCs or synapse numbers, and possibly via altered excitability of a subset of GABAergic cells (Peerboom et al., 2023). These results underscore the need for a better understanding of the role of chloride as an intracellular messenger in developing neurons. Our current results suggest that furosemide treatment indirectly increases inhibitory transmission, which adds to its previously described anticonvulsant action.

5.6 Author contributions

C.P., and C.J.W. designed research; C.P and T.W., performed research and analyzed data; C.P., and C.J.W. wrote the paper.

5.7 Declaration of Interests

The authors declare no competing interests.

5.8 Acknowledgements

We thank Prof. Thomas Kuner for providing the Cre-dependent SCLM construct (Boffi et al., 2018). We thank Prof. Kevin Staley for providing the SuperClomeleon^{lox/-} mouse line, Dr. Stefan Berger for the CamKII $\alpha^{\text{Cre/-}}$ mice and Dr. Henk Karst for sharing these mice with us. We thank Dunya Selemangel for help with superclomeleon data analysis and René van Dorland for the AAV production and excellent technical support.

5.9 References

- Akerman, C.J., Cline, H.T., 2006. Depolarizing GABAergic conductances regulate the balance of excitation to inhibition in the developing retinotectal circuit in vivo. *J. Neurosci.* 26, 5117–5130. <https://doi.org/10.1523/JNEUROSCI.0319-06.2006>
- Barbaro, N.M., Takahashi, D.K., Baraban, S.C., 2004. A potential role for astrocytes in mediating the antiepileptic actions of furosemide in vitro. *Neuroscience* 128, 655–663. <https://doi.org/10.1016/j.neuroscience.2004.07.007>
- Bijlsma, A., Omrani, A., Spoelder, M., Verharen, J.P.H., Bauer, L., Cornelis, C., de Zwart, B., van Dorland, R., Vanderschuren, L.J.M.J., Wierenga, C.J., 2022. Social Play Behavior Is Critical for the Development of Prefrontal Inhibitory Synapses and Cognitive Flexibility in Rats. *J. Neurosci.* 42, 8716–8728. <https://doi.org/10.1523/JNEUROSCI.0524-22.2022>
- Boffi, J.C., Knabbe, J., Kaiser, M., Kuner, T., 2018. KCC2-dependent steady-state intracellular chloride concentration and pH in cortical layer 2/3 neurons of anesthetized and awake mice. *Front. Cell. Neurosci.* 12, 1–14. <https://doi.org/10.3389/fncel.2018.00007>
- Casanova, E., Fehsenfeld, S., Mantamadiotis, T., Lemberger, T., Greiner, E., Stewart, A.F., Schtz, G., 2001. A CamKII α iCre BAC allows brain-specific gene inactivation. *Genesis* 31, 37–42. <https://doi.org/10.1002/gene.1078>
- Chancey, J.H., Adlaf, E.W., Sapp, M.C., Pugh, P.C., Wadiche, J.I., Overstreet-Wadiche, L.S., 2013. GABA Depolarization Is Required for Experience-Dependent Synapse Unsilencing in Adult-Born Neurons. *J. Neurosci.* 33, 6614–6622. <https://doi.org/10.1523/JNEUROSCI.0781-13.2013>
- Chen, L., Yu, J., Wan, L., Wu, Z., Wang, G., Hu, Z., Ren, L., Zhou, J., Qian, B., Zhao, X., Zhang, J., Liu, X., 2022. Furosemide prevents membrane KCC2 downregulation during convulsant stimulation in the hippocampus. *IBRO Neurosci. Reports* 12, 355–365. <https://doi.org/10.1016/j.ibneur.2022.04.010>
- Deeb, T.Z., Nakamura, Y., Frost, G.D., Davies, P.A., Moss, S.J., 2013. Disrupted Cl⁻ homeostasis contributes to reductions in the inhibitory efficacy of diazepam during hyperexcited states. *Eur. J. Neurosci.* 38, 2453–2467. <https://doi.org/10.1111/ejn.12241>
- Dietrich, C.J., Morad, M., 2010. Synaptic acidification enhances GABAA signaling. *J. Neurosci.* 30, 16044–16052. <https://doi.org/10.1523/JNEUROSCI.6364-09.2010>
- Dzhala, V.I., Talos, D.M., Sdrulla, D.A., Brumback, A.C., Mathews, G.C., Benke, T.A., Delpire, E., Jensen, F.E., Staley, K.J., 2005. NKCC1 transporter facilitates seizures in the developing brain. *Nat. Med.* 11, 1205–1213. <https://doi.org/10.1038/nm1301>
- Feng, T., Alicea, C., Pham, V., Kirk, A., Pieraut, S., 2021. Experience-dependent inhibitory plasticity is mediated by CCK1 basket cells in the developing dentate gyrus. *J. Neurosci.* 41, 4607–4619. <https://doi.org/10.1523/JNEUROSCI.1207-20.2021>
- Gonzalez-Islas, C., Chub, N., Wenner, P., 2009. NKCC1 and AE3 appear to accumulate chloride in embryonic motoneurons. *J. Neurophysiol.* 101, 507–518. <https://doi.org/10.1152/jn.90986.2008>
- Goswami, S.P., Bucurenciu, I., Jonas, P., 2012. Miniature IPSCs in hippocampal granule cells are triggered by voltage-gated Ca²⁺ channels via microdomain coupling. *J. Neurosci.* 32, 14294–14304. <https://doi.org/10.1523/JNEUROSCI.6104-11.2012>

- Goutierre, M., Al Awabdh, S., Donneger, F., François, E., Gomez-Dominguez, D., Irinopoulou, T., Menendez de la Prida, L., Poncer, J.C., 2019. KCC2 Regulates Neuronal Excitability and Hippocampal Activity via Interaction with Task-3 Channels. *Cell Rep.* 28, 91–103. <https://doi.org/10.1016/j.celrep.2019.06.001>
- Grimley, J.S., Li, L., Wang, W., Wen, L., Beese, L.S., Hellinga, H.W., Augustine, G.J., 2013. Visualization of Synaptic Inhibition with an Optogenetic Sensor Developed by Cell-Free Protein Engineering Automation. *J. Neurosci.* 33, 16297–16309. <https://doi.org/10.1523/JNEUROSCI.4616-11.2013>
- Gulyás, A.I., Sík, A., Payne, J.A., Kaila, K., Freund, T.F., 2001. The KCl cotransporter, KCC2, is highly expressed in the vicinity of excitatory synapses in the rat hippocampus. *Eur. J. Neurosci.* 13, 2205–2217. <https://doi.org/10.1046/j.0953-816X.2001.01600.x>
- Gutschmidt, K.U., Stenkamp, K., Buchheim, K., Heinemann, U., Meierkord, H., 1999. Anticonvulsant actions of furosemide in vitro. *Neuroscience* 91, 1471–1481. [https://doi.org/10.1016/S0306-4522\(98\)00700-3](https://doi.org/10.1016/S0306-4522(98)00700-3)
- Halligan, R.D., Shelat, H., Kahn, A.M., 1991. Na⁺-independent Cl⁻-HCO₃⁻ exchange in sarcolemmal vesicles from vascular smooth muscle. *Am J Physiol* 260, C347–54.
- Herstel, L.J., Peerboom, C., Uijtewaal, S., Selemangel, D., Karst, H., Wierenga, C.J., 2022. Using SuperClomeleon to measure changes in intracellular chloride during development and after early life stress. *Eneuro* November/D.
- Hesdorffer, D.C., Hauser, W.A., Annegers, J.F., Rocca, W.A., 1996. Severe, uncontrolled hypertension and adult-onset seizures: A case-control study in Rochester, Minnesota. *Epilepsia* 37, 736–741. <https://doi.org/10.1111/j.1528-1157.1996.tb00644.x>
- Hochman, D.W., 2012. The extracellular space and epileptic activity in the adult brain: Explaining the antiepileptic effects of furosemide and bumetanide. *Epilepsia* 53, 18–25. <https://doi.org/10.1111/j.1528-1167.2012.03471.x>
- Hochman, D.W., Baraban, S.C., Owens, J.W.M., Schwartzkroin, P.A., 1995. Dissociation of synchronization and excitability in furosemide blockade of epileptiform activity. *Science* (80-.). 270, 99–102. <https://doi.org/10.1126/science.270.5233.99>
- Holtkamp, M., Matzen, J., Buchheim, K., Walker, M.C., Meierkord, H., 2003. Furosemide terminates limbic status epilepticus in freely moving rats. *Epilepsia* 44, 1141–1144. <https://doi.org/10.1046/j.1528-1157.2003.14003.x>
- Hu, H.Y., Kruijssen, D.L.H., Frias, C.P., Rózsa, B., Hoogenraad, C.C., Wierenga, C.J., 2019. Endocannabinoid Signaling Mediates Local Dendritic Coordination between Excitatory and Inhibitory Synapses. *Cell Rep.* 27, 666–675. e5. <https://doi.org/10.1016/j.celrep.2019.03.078>
- Huang, Y., Ko, H., Cheung, Z.H., Yung, K.K.L., Yao, T., Wang, J.J., Morozov, A., Ke, Y., Ip, N.Y., Yung, W.H., 2012. Dual actions of brain-derived neurotrophic factor on GABAergic transmission in cerebellar Purkinje neurons. *Exp. Neurol.* 233, 791–798. <https://doi.org/10.1016/j.expneurol.2011.11.043>
- Hübner, C. a, Stein, V., Hermans-Borgmeyer, I., Meyer, T., Ballanyi, K., Jentsch, T.J., 2001. Disruption of KCC2 reveals an essential role of K-Cl cotransport already in early synaptic inhibition. *Neuron* 30, 515–524.
- Jarolimek, W., Lewen, A., Misgeld, U., 1999. A furosemide-sensitive K⁺ -Cl⁻ cotransporter counteracts intracellular Cl⁻ accumulation and depletion in cultured rat midbrain neurons. *J. Neurosci.* 19, 4695–4704. <https://doi.org/10.1523/jneurosci.19-12-04695.1999>
- Jentsch, T.J., Pusch, M., 2018. CLC chloride channels and transporters: Structure, function, physiology, and disease. *Physiol. Rev.* 98, 1493–1590. <https://doi.org/10.1152/physrev.00047.2017>
- Kaila, K., Price, T.J., Payne, J.A., Puskarjov, M., Voipio, J., 2014. Cation-chloride cotransporters in neuronal development, plasticity and disease. *Nat. Rev. Neurosci.* 15, 637–654. <https://doi.org/10.1038/nrn3819>

- Kirmse, K., Kummer, M., Kovalchuk, Y., Witte, O.W., Garaschuk, O., Holthoff, K., 2015. GABA depolarizes immature neurons and inhibits network activity in the neonatal neocortex in vivo. *Nat. Commun.* 6, 1–13. <https://doi.org/10.1038/ncomms8750>
- Korpi, E.R., Kuner, T., Seeburg, P.H., Luddens, H., 1995. Selective antagonist for the cerebellar granule cell-specific g-aminobutyric acid type A receptor. *Mol. Pharmacol.* 47, 283–289.
- Leinekugel, X., Medina, I., Khalilov, I., Ben-Ari, Y., Khazipov, R., 1997. Ca²⁺ Oscillations Mediated by the Synergistic Excitatory Actions of GABA. *Neuron* 18, 243–255.
- Lodovichi, C., Ratto, G.M., Trevelyan, A.J., Arosio, D., 2022. Genetically encoded sensors for Chloride concentration. *J. Neurosci. Methods* 368, 109455. <https://doi.org/10.1016/j.jneumeth.2021.109455>
- López-Bendito G, Sturgess K, Erdélyi F, Szabó G, Molnár Z, Paulsen O. Preferential origin and layer destination of GAD65-GFP cortical interneurons. *Cereb Cortex.* 2004 Oct;14(10):1122-33. doi: 10.1093/cercor/bhh072. Epub 2004 Apr 27. PMID: 15115742.
- Maa, E.H., Kahle, K.T., Walcott, B.P., Spitz, M.C., Staley, K.J., 2011. Diuretics and epilepsy: Will the past and present meet? *Epilepsia* 52, 1559–1569. <https://doi.org/10.1111/j.1528-1167.2011.03203.x>
- Mozrzymas, J., Zarnowska, E., Pytel, M., Mercik, K., 2003. Modulation of GABAA receptors by hydrogen ions reveals synaptic GABA transient and a crucial role of the desensitization process. *J. Neurosci.* 23, 7981–7992.
- Murata, Y., Colonnese, M.T., 2020. GABAergic interneurons excite neonatal hippocampus in vivo. *Sci. Adv.* 6, 1–10.
- Oh, W.C., Lutz, S., Castillo, P.E., Kwon, H.B., 2016. De novo synaptogenesis induced by GABA in the developing mouse cortex - supplemental. *Science (80-.)*. 353, 1037–1040. <https://doi.org/10.1126/science.aaf5206>
- Orlov, S.N., Koltsova, S. V, Kapilevich, L. V, Gusakova, S. V, Dulin, N.O., 2015. NKCC1 and NKCC2: The pathogenetic role of cation-chloride cotransporters in hypertension 2, 186–196. <https://doi.org/10.1016/j.gendis.2015.02.007.NKCC1>
- Otsu, Y., Donneger, F., Schwartz, E.J., Poncer, J.C., 2020. Cation–chloride cotransporters and the polarity of GABA signalling in mouse hippocampal parvalbumin interneurons. *J. Physiol.* 598, 1–16. <https://doi.org/10.1113/JP279221>
- Owens, D.F., Boyce, L.H., Davis, M.B.E., Kriegstein, A.R., 1996. Excitatory GABA responses in embryonic and neonatal cortical slices demonstrated by gramicidin perforated-patch recordings and calcium imaging. *J. Neurosci.* 16, 6414–6423.
- Pearce, R.A., 1993. Physiological evidence for two distinct GABAA responses in rat hippocampus. *Neuron* 10, 189–200. [https://doi.org/10.1016/0896-6273\(93\)90310-N](https://doi.org/10.1016/0896-6273(93)90310-N)
- Peerboom, C., Kater, S. De, Jonker, N., Rieter, M., Wijne, T., Wierenga, C.J., 2023. Delaying the GABA shift indirectly affects membrane properties in the developing hippocampus. [bioRxiv](https://doi.org/10.1101/2023.08.15.551111).
- Pfeffer, C.K., Stein, V., Keating, D.J., Maier, H., Rinke, I., Rudhard, Y., Hentschke, M., Rune, G.M., Jentsch, T.J., Hubner, C.A., 2009. NKCC1-Dependent GABAergic Excitation Drives Synaptic Network Maturation during Early Hippocampal Development. *J. Neurosci.* 29, 3419–3430. <https://doi.org/10.1523/JNEUROSCI.1377-08.2009>
- Rahmati, N., Normoyle, K.P., Glykys, J., Dzhalal, V.I., Lillis, K.P., Kahle, K.T., Raiyyani, R., Jacob, T., Staley, K.J., 2021. Unique actions of gaba arising from cytoplasmic chloride microdomains. *J. Neurosci.* 41, 4967–4975. <https://doi.org/10.1523/JNEUROSCI.3175-20.2021>
- Ransom, B., Yamate, C., Connors, B., 1985. Activity-dependent in rat optic nerve: a developmental study. *J. Neurosci.* 5, 532–535.

- Rivera, C., Voipio, J., Kaila, K., 2005. Two developmental switches in GABAergic signalling: The K⁺-Cl⁻ cotransporter KCC2 and carbonic anhydrase CAVII. *J. Physiol.* 562, 27–36. <https://doi.org/10.1113/jphysiol.2004.077495>
- Rivera, C., Voipio, J., Payne, J. a, Ruusuvuori, E., Lahtinen, H., Lamsa, K., Pirvola, U., Saarna, M., Kaila, K., 1999. The K⁺/Cl⁻ co-transporter KCC2 renders GABA hyperpolarizing during neuronal maturation. *Nature* 397, 251–255. <https://doi.org/10.1038/16697>
- Romero, M.F., Chen, A.P., Parker, M.D., Boron, W.F., 2013. The SLC4 family of bicarbonate (HCO₃⁻) transporters. *Mol. Aspects Med.* 34, 159–182. <https://doi.org/10.1016/j.mam.2012.10.008>
- Romo-Parra, H., Treviño, M., Heinemann, U., Gutiérrez, R., 2008. GABA actions in hippocampal area CA3 during postnatal development: Differential shift from depolarizing to hyperpolarizing in somatic and dendritic compartments. *J. Neurophysiol.* 99, 1523–1534. <https://doi.org/10.1152/jn.01074.2007>
- Ruiter, M., Herstel, L.J., Wierenga, C.J., Ma, T., 2020. Reduction of Dendritic Inhibition in CA1 Pyramidal Neurons in Amyloidosis Models of Early Alzheimer's Disease. *J. Alzheimer's Dis.* 78, 951–964. <https://doi.org/10.3233/JAD-200527>
- Ruusuvuori, E. & Kaila, K., 2014. Carbonic Anhydrase: Mechanism, Regulation, Links to Disease, and Industrial Applications, Springer.
- Ruusuvuori, E., Li, H., Huttu, K., Palva, J.M., Smirnov, S., Rivera, C., Kaila, K., Voipio, J., 2004. Carbonic Anhydrase Isoform VII Acts As A Molecular Switch in the Development of Synchronous Gamma-Frequency Firing of Hippocampal CA1 Pyramidal Cells. *J. Neurosci.* 24, 2699–2707. <https://doi.org/10.1523/JNEUROSCI.5176-03.2004>
- Salmon, C.K., Pribrag, H., Gizowski, C., Farmer, W.T., Cameron, S., Jones, E. V., Mahadevan, V., Bourque, C.W., Stellwagen, D., Woodin, M.A., Murai, K.K., 2020. Depolarizing GABA Transmission Restrains Activity-Dependent Glutamatergic Synapse Formation in the Developing Hippocampal Circuit. *Front. Cell. Neurosci.* 14, 1–16. <https://doi.org/10.3389/fncel.2020.00036>
- Sedmak, G., Puskarjov, N.J.-M.M., Ulamec, M., Krušlin, B., Kaila, K., Judaš, M., 2016. Developmental Expression Patterns of KCC2 and Functionally Associated Molecules in the Human Brain. *Cereb. Cortex* 27, 4060–4072. <https://doi.org/10.1093/cercor/bhw218>
- Seja, P., Schonewille, M., Spitzmaul, G., Badura, A., Klein, I., Rudhard, Y., Wisden, W., Hübner, C.A., De Zeeuw, C.I., Jentsch, T.J., 2012. Raising cytosolic Cl⁻ in cerebellar granule cells affects their excitability and vestibulo-ocular learning. *EMBO J.* 31, 1217–1230. <https://doi.org/10.1038/emboj.2011.488>
- Sinha, A.S., Wang, T., Watanabe, M., Hosoi, Y., Sohara, E., Akita, T., Uchida, S., Fukuda, A., 2022. WNK3 kinase maintains neuronal excitability by reducing inwardly rectifying K⁺ conductance in layer V pyramidal neurons of mouse medial prefrontal cortex. *Front. Mol. Neurosci.* 15. <https://doi.org/10.3389/fnmol.2022.856262>
- Staley, K.J., 2002. Diuretics as Antiepileptic Drugs: Should We Go with the Flow? *Epilepsy Curr.* 2, 39–40. <https://doi.org/10.1046/j.1535-7597.2002.00013.x>
- Stein, V., Hermans-Borgmeyer, I., Jentsch, T.J., Hübner, C.A., 2004. Expression of the KCl Cotransporter KCC2 Parallels Neuronal Maturation and the Emergence of Low Intracellular Chloride. *J. Comp. Neurol.* 468, 57–64. <https://doi.org/10.1002/cne.10983>
- Stoppini, L., Buchs, P.A., Muller, D., 1991. A simple method for organotypic cultures of nervous tissue. *J. Neurosci. Methods* 37, 173–182. [https://doi.org/10.1016/0165-0270\(91\)90128-M](https://doi.org/10.1016/0165-0270(91)90128-M)

- Sulis Sato, S., Artoni, P., Landi, S., Cozzolino, O., Parra, R., Pracucci, E., Trovato, F., Szczurkowska, J., Luin, S., Arosio, D., Beltram, F., Cancedda, L., Kaila, K., Ratto, G.M., 2017. Simultaneous two-photon imaging of intracellular chloride concentration and pH in mouse pyramidal neurons in vivo. *Proc. Natl. Acad. Sci.* 114, E8770–E8779. <https://doi.org/10.1073/pnas.1702861114>
- Taylor, A.L., 2012. What we talk about when we talk about capacitance measured with the voltage-clamp step method. *J. Comput. Neurosci.* 32, 167–175. <https://doi.org/10.1007/s10827-011-0346-8>
- Temperini, C., Cecchi, A., Scozzafava, A., Supuran, C.T., 2009. Carbonic anhydrase inhibitors. Comparison of chlorthalidone, indapamide, trichloromethiazide, and furosemide X-ray crystal structures in adducts with isozyme II, when several water molecules make the difference. *Bioorganic Med. Chem.* 17, 1214–1221. <https://doi.org/10.1016/j.bmc.2008.12.023>
- Thompson, S.M., Gahwiler, B.H., 1989. Activity-dependent disinhibition. II. Effects of extracellular potassium, furosemide, and membrane potential on E(Cl)- in hippocampal CA3 neurons. *J. Neurophysiol.* 61, 512–523. <https://doi.org/10.1152/jn.1989.61.3.512>
- Tsien, J.Z., Chen, D.F., Gerber, D., Tom, C., Mercer, E.H., Anderson, D.J., Mayford, M., Kandel, E.R., Tonegawa, S., 1996. Subregion- and cell type-restricted gene knockout in mouse brain. *Cell* 87, 1317–1326. [https://doi.org/10.1016/S0092-8674\(00\)81826-7](https://doi.org/10.1016/S0092-8674(00)81826-7)
- Tsukahara, T., Masuhara, M., Iwai, H., Sonomura, T., Sato, T., 2015. Repeated stress-induced expression pattern alterations of the hippocampal chloride transporters KCC2 and NKCC1 associated with behavioral abnormalities in female mice. *Biochem. Biophys. Res. Commun.* 465, 145–151. <https://doi.org/10.1016/j.bbrc.2015.07.153>
- Tyzio, R., Holmes, G.L., Ben-Ari, Y., Khazipov, R., 2007. Timing of the developmental switch in GABAA mediated signaling from excitation to inhibition in CA3 rat hippocampus using gramicidin perforated patch and extracellular recordings. *Epilepsia* 48, 96–105. <https://doi.org/10.1111/j.1528-1167.2007.01295.x>
- Uwera, J., Nedergaard, S., Andreasen, M., 2015. A novel mechanism for the anticonvulsant effect of furosemide in rat hippocampus in vitro. *Brain Res.* 1625, 1–8. <https://doi.org/10.1016/j.brainres.2015.08.014>
- van Rheede, J.J., Richards, B.A., Akerman, C.J., 2015. Sensory-Evoked Spiking Behavior Emerges via an Experience-Dependent Plasticity Mechanism. *Neuron* 87, 1050–1062. <https://doi.org/10.1016/j.neuron.2015.08.021>
- Viitanen, T., Ruusuvuori, E., Kaila, K., Voipio, J., 2010. The K⁺-Cl⁻ cotransporter KCC2 promotes GABAergic excitation in the mature rat hippocampus. *J. Physiol.* 588, 1527–1540. <https://doi.org/10.1113/jphysiol.2009.181826>
- Wang, B.S., Feng, L., Liu, M., Liu, X., Cang, J., 2013. Environmental Enrichment Rescues Binocular Matching of Orientation Preference in Mice that Have a Precocious Critical Period. *Neuron* 80, 198–209. <https://doi.org/10.1016/j.neuron.2013.07.023>
- Wang, D.D., Kriegstein, A.R., 2011. Blocking early GABA depolarization with bumetanide results in permanent alterations in cortical circuits and sensorimotor gating deficits. *Cereb. Cortex* 21, 574–587. <https://doi.org/10.1093/cercor/bhq124>
- Wang, D.D., Kriegstein, A.R., 2008. GABA Regulates Excitatory Synapse Formation in the Neocortex via NMDA Receptor Activation. *J. Neurosci.* 28, 5547–5558. <https://doi.org/10.1523/JNEUROSCI.5599-07.2008>
- Wierenga, C.J., Müllner, F.E., Rinke, I., Keck, T., Stein, V., Bonhoeffer, T., 2010. Molecular and electrophysiological characterization of GFP-expressing ca1 interneurons in GAD65-GFP mice. *PLoS One* 5, 1–11. <https://doi.org/10.1371/journal.pone.0015915>

Wright, R., Newey, S.E., Ilie, A., Wefelmeyer, W., Raimondo, J. V., Ginham, R., McIlhinney, R.A.J., Akerman, C.J., 2017. Neuronal Chloride Regulation via KCC2 Is Modulated through a GABA B Receptor Protein Complex. *J. Neurosci.* 37, 5447–5462. <https://doi.org/10.1523/JNEUROSCI.2164-16.2017>

Yamada, J., Okabe, A., Toyoda, H., Kilb, W., Luhmann, H., Fukuda, A., 2004. Cl⁻ uptake promoting depolarizing GABA actions in immature rat neocortical neurones is mediated by NKCC1. *J. Physiol.* 557, 829–841.



6

Discussion

Carlijn Peerboom

During my PhD, I aimed to improve our understanding of the role of the GABA shift in brain development.

In **chapter 2** we summarized the current knowledge on the developmental GABA shift. We describe how every step in brain development is guided by GABA signaling. It remains unclear what triggers the GABA shift under normal conditions and why the timing of the GABA shift is altered in neurodevelopmental disorders (NDDs). It will be important to improve our understanding of GABAergic signaling in brain development, as it may open up strategies to alleviate behavioral impairments in NDDs in the future.

In **chapter 3** we used the SuperClomeleon (SCLm) sensor to study chloride levels in neurons in the developing hippocampus and prefrontal cortex. We could measure a developmental decrease in chloride in hippocampal cultures and found an increase in chloride in slices of the prefrontal cortex from mice that experienced early life stress. Although conversion from SCLm fluorescence to absolute chloride concentrations proved difficult, our work shows that the SCLm sensor is a powerful tool to measure physiological changes in chloride levels in brain slices.

In **chapter 4** we found that delaying the GABA shift in cultured brain slices using KCC2 blocker VU0463271 (VU) did not directly affect the function and structure of synapses and neurons, but did increase inhibitory transmission and induce subtle, cell-specific alterations in neuronal membrane properties two weeks later. This chapter underlines a role of chloride beyond synapse formation and implicates a link between chloride levels and membrane conductance.

In **chapter 5** we accelerated the GABA shift with furosemide, an inhibitor of both chloride co-transporters that has anti-epileptic effects. The function and structure of inhibitory synapses were not affected directly after treatment, further confirming that GABA no longer affects synapse formation in the second week after birth. Two weeks later however, inhibitory transmission was increased, presumably due to an increase in the number of inhibitory synapses. This chapter raises attention to a potential link between chloride regulation and the regulation of pH and cell volume during development.

Together, these results underline that the GABA shift plays a crucial, but complex role in brain development. In this chapter I will discuss in more detail 1) technical considerations and advancements, 2) how environmental factors can steer the timing of the GABA shift 3) how the timing of the GABA shift may direct brain development, 4) implications of our findings on furosemide as a possible treatment for epilepsy and 5) implications of our findings for neurodevelopmental disorders.

6.1 Technical considerations and advancements

In this paragraph I will highlight the strengths and weaknesses of the methods used to follow the developmental chloride trajectory. In addition, I will discuss advancements that may further improve our understanding of the GABA shift. In particular, I will discuss the development of chloride indicators, which will make it easier to follow the chloride development in many neurons as well as CRISPR/Cas9-mediated genome editing, which may enable us to follow NKCC1, KCC2 and other proteins involved in the GABA shift in living brain tissue in the future.

Sensors for intraneuronal chloride concentrations

Throughout this thesis, we assessed chloride levels from the GABA reversal potential (E_{GABA}) using perforated patch clamp recordings and the recently developed chloride sensor SuperClomeleon (SCLm) (chapter 3, 4, 5). Perforated patch clamp allows for measuring the GABA reversal potential (E_{GABA}), but not for direct measurement of the chloride reversal potential (E_{Cl}). GABA_A currents are primarily mediated by chloride (~70%), but also by HCO₃⁻ (~30%). As the exact contribution of the reversal potential of HCO₃⁻ (E_{HCO_3}) to E_{GABA} in any given neuron is unknown, E_{GABA} cannot exactly be converted to E_{Cl} and perforated patch clamp only allows for estimations of intracellular chloride concentrations (Herstel et al., 2022; Kaila et al., 2014). Unfortunately, the SCLm sensor did not allow us to measure chloride concentrations with more accuracy. In chapter 3 we show that calibration of SCLm with ionophores and varying extracellular chloride concentrations is extremely variable. Therefore, conversion from SCLm FRET ratios to chloride concentrations comes with large degree of uncertainty (Herstel et al., 2022). Hence, both perforated patch clamp and SCLm imaging allow for measurements of changes in chloride, rather than absolute chloride concentrations.

Another major disadvantage of perforated patch clamp recordings is that they are very labor intensive. It is challenging to measure chloride concentrations in large populations of neurons, while big individual differences can exist between neurons and many recordings may be required to get a good population estimate (Sulis Sato et al., 2017; Tyzio et al., 2007). In this aspect, SCLm imaging poses advantages over perforated patch clamp. In chapter 3, we showed that SCLm sensor allows assessment of chloride in multiple neurons simultaneously and for measurement of changes in chloride levels within a neuron over time (Herstel et al., 2022). Nonetheless, we also identified issues of SCLm chloride imaging. First of all, the stress sensitivity in young SCLm mice may differ from other mouse lines such as C57BL/6, which could influence chloride development in these mice (Herstel et al., 2022; Karst et al., 2023). In addition, the sensitivity of the SCLm sensor is reduced at low chloride concentrations, which are physiologically very relevant (Boffi et al., 2018; Grimley et al., 2013; Herstel et al., 2022). This may be an issue in development and in disorders, as changes in chloride are often subtle (chapter 4, 5).

Thanks to rapid recent technological developments, various chloride indicators have been developed. In addition to the SClm sensor, there are the non-ratiometric chloride sensors 6-methoxy-N-(3-sulfopropyl)quinolinium (SPQ), N-(ethoxycarbonylmethyl)-6-methoxyquinolinium bromide (MQAE) and 6-methoxy-N-ethylquinolinium iodide (MEQ). These molecules can be excited and return to their ground state when hitting chloride. An increase in chloride concentration thus causes a simple decrease in sensor fluorescence. SPQ, MQAE and MEQ can be used to monitor acute changes in chloride, but these sensors are not very useful when studying chloride levels during brain development, since their fluorescence not only depends on chloride concentrations, but also on the dye concentration and optical thickness (Arosio and Ratto, 2014). In addition, various ratiometric chloride sensors have been developed over the last decade. SClm is a derivative from its precursor Clomeleon. Due to a shorter linker, a brighter donor (Cerulean rather than CFP in Clomeleon) and mutations in the Topaz fluorophore (Grimley et al., 2013), SClm has a chloride affinity with more physiological relevance (Kd 13.6-24.6 mM (Boffi et al., 2018; Grimley et al., 2013; Herstel et al., 2022)) compared to Clomeleon (Kd 87-167 mM (Berglund et al., 2006; Dzhalal et al., 2012; Kuner and Augustine, 2000)). Another very similar ratiometric probe, called Cl-Sensor, consists of a chloride sensitive, triple-mutated YFP fluorophore coupled to a chloride-insensitive CFP. However, Cl-Sensor's affinity (Kd 46.4 mM) is also lower than that of SClm (Batti et al., 2013).

An important disadvantage of the SClm sensor is its pH sensitivity. As described in chapter 5, furosemide treatment may have changed bicarbonate levels and pH, which could have affected SClm FRET ratios. We do not expect changes in pH during development (chapter 3) (Herstel et al., 2022; Sulis Sato et al., 2017), or after inhibition of KCC2 by VU treatment (chapter 4), but optimally SClm imaging should always be supplemented with measurements of intracellular pH. Neuronal pH is often overlooked, but important when studying chloride development and the GABA_A shift. Not only are chloride and bicarbonate levels linked via GABA_A receptors and common transporters (Kaila et al., 2014) but, like chloride, pH is also a powerful ionic modulator of neuronal excitability (Ruusuvuori et al., 2004). To allow for simultaneous pH and chloride measurements, the LSSmClpHensor has been developed (Lodovichi et al., 2022; Paredes et al., 2016; Sulis Sato et al., 2017). This sensor consists of a pH- and chloride-sensitive GFP mutant (E²GFP), and an ion/pH-insensitive red fluorescent protein, LSSmKate2, that is used as a reference. E²GFP allows for ratiometric measurement of intracellular pH. pH can be assessed by collecting fluorescence at at least two different excitation wavelengths. In addition, E²GFP fluorescence is lost upon chloride binding. This quenching of E²GFP can be measured at an additional excitation wavelength (Lodovichi et al., 2022; Paredes et al., 2016; Sulis Sato et al., 2017). The need for sequential acquisition of three rather than two excitation wavelengths, goes hand in hand with a slightly reduced time resolution and a more laborious analysis compared to SClm. The affinity and sensitivity to low chloride concentrations of

LSSmClopHensor (Kd 14.3 mM (Paredes et al., 2016)) seem quite comparable to those of SClm (Kd 13.6-24.6 mM (Boffi et al., 2018; Grimley et al., 2013; Herstel et al., 2022)). Thereby, major advantage of the LSSmClopHensor over the SClm and perforated patch clamp is concomitant chloride and pH measurement. In the future, it would be ideal if their affinity for chloride can be further improved, especially at low, mature chloride concentrations.

In conclusion, SClm offers advantages over perforated patch clamp, allowing for measuring changes in chloride levels over prolonged time periods and in many neurons simultaneously. However, cautiousness is required when using SClm regarding a possibly altered stress response in young SClm mice (chapter 3), SClm's limited sensitivity to low chloride levels, and its pH sensitivity (chapter 5). We hope that these issues will be addressed in a next generation of chloride sensors. The high throughput of chloride imaging compared to perforated patch clamp recordings could be highly advantageous in advancing our understanding of the role chloride in the brain. For example, expression of a sensitive chloride sensor in a cell type specific manner will be very informative to follow the GABA shift in different cell types (chapter 4). Improved sensor sensitivity and decreased pH-dependency would also be required for to measure furosemide's effect of on chloride levels and pH (chapter 5). While with perforated patch clamp it would be a tremendous task to measure the effect of furosemide on NKCC1, KCC2, and enzymes that regulate HCO_3^- levels, it will be feasible to do this with chloride imaging.

CRISPR/Cas9-mediated genome editing to studying endogenous protein distributions in slice cultures

To study molecular changes, such as the change in the chloride transporters that mediate the GABA shift during brain development, western blots of lysed tissue and immunohistochemistry on fixed tissue are commonly used (chapter 4, 5). Though these techniques allow for examining changes in overall expression of proteins of interest, as well as in the localization of these proteins in fixed tissue, they do not allow for visualization of endogenous protein dynamics in living cells. Also, they fully depend on the availability of specific antibodies. To follow proteins in living cells recombinant expression constructs are commonly used. However, as expression of the protein of interest is no longer under control of the endogenous transcription and translation machinery, overexpression artifacts such as altered protein localization, and consequential effects on cell morphology and function, are common (Ratz et al., 2015). To label endogenous proteins without affecting expression levels, CRISPR/Cas9-mediated genome editing can be used. CRISPR (Clustered Regularly Interspaced Short Palindromic Repeats) refers to repeating DNA sequences found in bacteria and archaea (Ishino et al., 1987; Jansen et al., 2002). Cas9 (or "CRISPR-associated protein 9") is an enzyme that uses CRISPR sequences as a guide to recognize and create blunt-ended double strand breaks in the DNA. CRISPR-Cas9 gene editing allows for tagging

endogenous proteins by incorporation of a unique guide RNA (gRNA) target sequence that leads Cas9 and a donor sequence (e.g. a fluorescence label such as GFP) to a genomic locus of interest (Knott and Doudna, 2018).

However, using CRISPR/Cas9 in neurons is not trivial. The integration of the DNA relies on homologous recombination; the exchange of two similar DNA molecules which mostly occurs during cell division, and is therefore extremely inefficient, if not impossible in post-mitotic neurons. To overcome this problem, a toolbox called ORANGE (Open Resource for the Application of Neuronal Genome Editing) has been recently developed by the MacGillavry lab (Willems et al., 2020). ORANGE employs homology-independent targeted integration to integrate knock in sequences in postmitotic cells. ORANGE knock ins can be delivered in dissociated hippocampal cultures using two lentiviruses, one containing the Cas9 protein and the other containing the gRNA (Willems et al., 2020). However, using this method to follow proteins in brain tissue proved more difficult. During my PhD project, we have attempted to optimize ORANGE labeling of endogenous proteins in cultured brain slices for two-photon live imaging.

We started by producing two lentivirus containing a gRNA for gephyrin and neuroligin-2 (NL2), key molecules in inhibitory synapses (Favuzzi and Rico, 2018; Pouloupoulos et al., 2009), along with a GFP donor sequence and a dsRed tag. Co-application of these viruses along with a Cas9 lentivirus in primary cultures, resulted in multiple neurons on a coverslip expressing the gRNA vector, as indicated by the dsRed cell fill (Fig. 1A-D). However, only a small proportion of dsRed positive neurons exhibited GFP-positive gephyrin or NL2 puncta. In addition, knock in puncta were rather weak and not easily discerned by eye. We therefore amplified the GFP signal by doing an immunostaining with an GFP-antibody. This seemed to improve detection of knock in neurons in a pilot experiment (Fig. 1C,D). We also tried to follow GFP-labeled NL2 and gephyrin puncta in live (and thus unstained) neurons using two-photon microscopy. However, it was difficult to distinguish knock ins from autofluorescent debris that leaked into the GFP channel (examples in Fig. 1E,F). These pilot experiments show that for live imaging of proteins in brain slices experiments brighter fluorescent tags are required. For example the GFP-tag could be changed to a 'spaghetti monster' fluorescent protein (Viswanathan et al., 2015). In addition, it will be important to validate that puncta followed under the two photon microscope represent true labeling of endogenous proteins. To do so, immunostaining should be performed for the proteins of interest after live imaging. To find the imaged neurons back after staining, dissociated neurons can be cultured on a grid and the image area in a slice can be marked with a scar made with high laser power (Liang et al., 2021).

We then tested the labelling of NL2 and glutamate receptor A1 (GluA1) as a positive control in slice cultures. Using a double lentiviral approach, only 0-1 knock-in neurons were found per slice. A double AAV approach to label gephyrin or GluA1 improved efficiency only slightly, with 0-4 knock-in neurons per slice. However, reliable live imaging using two photon microscopy requires a higher knock-in efficiency. We therefore performed a pilot experiment in which we added AAV containing a gephyrin gRNA, a GFP donor sequence and an mCherry-KASH tag onto slices of H11Cas9 mice, which express Cas9 in all cells (Jackson labs #28239). In this case, many neurons expressed the viral gRNA construct, as indicated by expression of mCherry-KASH (Fig. 1G). In each slice, more than ten knock-ins were found in the CA1 area (Fig. 1G). This pilot experiment indicates that the use of transgenic mice which express Cas9 enhances knock in efficiency and that Cas9 availability was a limiting factor in the dual-virus approach in slices. It is striking that even after GFP-antibody staining, the number of knock in neurons compared to the number of neurons expressing the gRNA (indicated by the expression of a dsRed in dissociated neurons and mCherry in slices) seems lower in slice cultures (Fig. 1G) than in neuronal cultures (Fig. 1C,D). This suggests that integration of the donor sequence is decreased in slice cultures compared to in dissociated cultures, and this might (partly) explain why a double viral strategy is sufficient for generating knock ins in dissociated neurons, but not in slices. Using slices from H11Cas9 mice instead, brings us one step closer to visualize the building blocks of the brain and their developmental trajectory in the highest detail. For example, ORANGE-mediated protein labeling could be useful in finding the sequence of molecules that are thought to regulate the timing of the GABA shift (chapter 2).

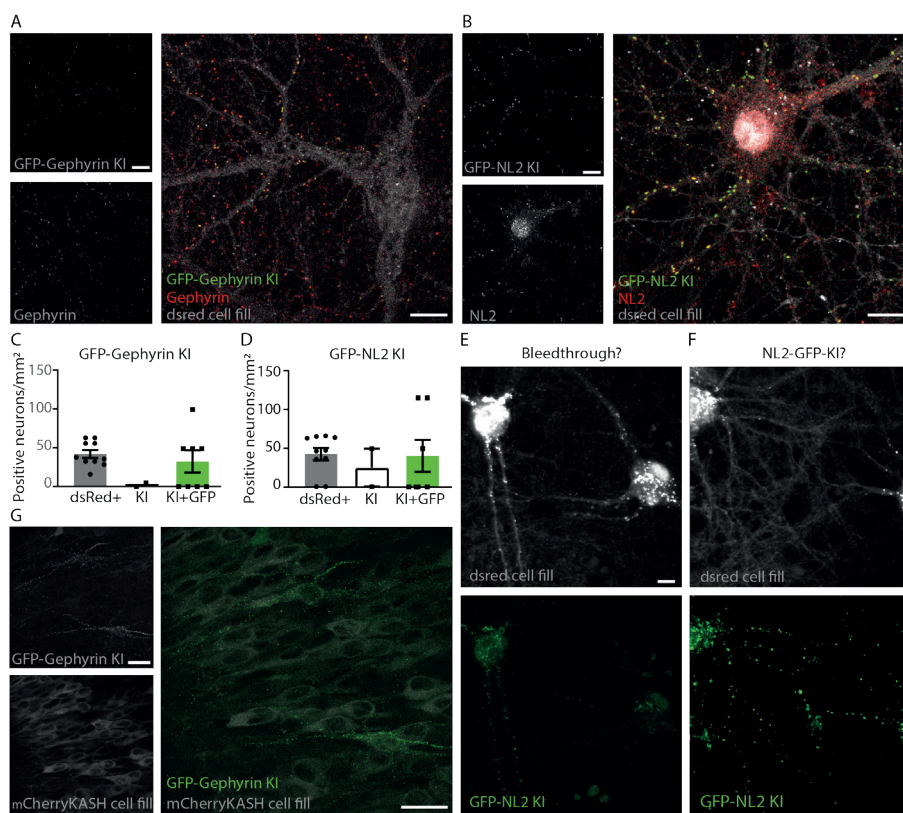


Figure 1. CRISPR/Cas9-based genome editing to study protein distribution in neuronal and slice cultures.

A,B) Example images of GFP-gephyrin and GFP-NL2 knock ins in dissociated hippocampal neurons. Scale bar: 10 μ m.

C,D) Quantification of dsRed positive neurons (expressing the gRNA vector) and GFP-gephyrin and GFP-NL2 knock ins in dissociated hippocampal neurons without and with GFP antibody staining.

E, F) Examples of GFP puncta in dissociated hippocampal neurons under the two photon microscope. Scale bar: 10 μ m. While GFP puncta of the neuron in E seem autofluorescent bleed through from the dsred channel, GFP puncta of the neuron in F might represent a GFP-NL2 knock in.

G) Example of GFP-gephyrin knock ins in slices from a H11Cas9 mice. Scale bar: 50 μ m

Methods used for the experiments in this section

Animals

All animal experiments were performed in compliance with the guidelines for the welfare of experimental animals issued by the Federal Government of the Netherlands and were approved by the Dutch Central Committee Animal experiments (CCD), project AVD1080020173404 and AVD1080020173847. For dissociated neuronal cultures, male and female Wistar rats were used (Janvier Labs). Dissociated neuronal cultures were prepared as described in (Cunha-Ferreira et al., 2018). For slice cultures, we used C57BL/6JRj and H11Cas9 mice (Jackson labs #28239m) of both sexes. H11Cas9 mice express *S. pyogenes* cas9 gene (hSpCas9) under control of a CAG promoter, resulting in global expression of Cas9 (Jackson labs #28239) and were kindly provided by Maarten Kole (Netherlands Institute for Neuroscience, Amsterdam, The Netherlands). Slice cultures were prepared as described in chapters 3, 4 and 5.

Virus production and infection

GFP-Gephyrin adeno-associated virus (AAV) was a gift from Fred de Winter (Netherlands institute for Neuroscience, Amsterdam, The Netherlands). Lentivirus was produced using HEK293T cells, maintained at a high growth rate in DMEM supplemented with 10% FCS and 1% pen/strep. At 1 day after plating, cells were transfected using PEI (Polysciences) with second-generation LV packaging plasmids (psPAX2 and 2MD2.G) and one of the following pFUGW constructs at a 1:1:1 molar ratio: pFUGW-Cas9 (Willems, 2020), pFUGW-GFP-gephyrin and pFUGW-GFP-NL2 (by insertion of a gephyrin- or NL2- guide sequence in pOrange (Willems, 2020) and cloning the pOrange construct into pFUGW (Addgene #14883). For primary cultures, 0.5-2 μ l virus was added per coverslip at DIV1. Neurons were used for live-imaging under the two-photon microscope at DIV16-21 or fixed at DIV14-18 and directly mounted or used for immunocytochemistry. For organotypic hippocampal slice cultures, virus was injected into the CA1 region at DIV1 using an Eppendorf Femtojet injector. Slices were fixed at DIV16-20 and directly mounted with VectaShield (Vector Laboratories).

Two-photon imaging

At DIV16-21, primary neurons were transferred to a recording chamber and continuously perfused with carbonated (95% O₂, 5% CO₂) ACSF, supplemented with 1 mM Trolox at a rate of approximately 1 ml/min. Bath temperature was monitored and maintained at 30-32°C. Two-photon imaging was performed using a customized two-photon laser scanning microscope (Femto3D-RC, Femtonics, Budapest, Hungary) with a Ti-Sapphire femtosecond pulsed laser (MaiTai HP, Spectra-Physics) at 950 nm to excite GFP and dsRed simultaneously. The emission light was split using a dichroic beam splitter at 550 nm and detected using two GaAsP photomultiplier tubes. Images were acquired using a 60x water immersion objective (Nikon NIR Aplanachromat; NA 1.0) at a resolution of 8.1 pixels/ μ m (1024x1024 pixels, 126x126 μ m) with 1 μ m steps.

Immunostainings

Primary neurons were fixed at DIV14-18 using 4% PFA and 4% sucrose in phosphate buffered saline (PBS), for 10 minutes at room temperature (RT). Neurons were washed three times in PBS containing 0.1 M glycine (PBS/Gly). Part of the neuronal cultures were directly mounted using Vectashield mounting medium (Vector labs). Other neuronal were used for immunocytochemistry and blocked for one hour in 10% normal goat serum and 0.1% Triton X-100 in PBS/Gly at 37°C. Neurons were incubated in primary antibodies in 5% normal goat serum and 0.1% Triton X-100 at 4°C overnight. The following primary antibodies were used: mouse anti-GFP (A-11120, ThermoFisher 1:500), rabbit anti-GFP (ab290, Abcam, 1:2000), mouse anti-Gephyrin (147 011, Synaptic Systems, 1:1000), rabbit anti-NL2 (129 203, Synaptic Systems, 1:500). Cultures were washed three times for 5 minutes with PBS/Gly and incubated with secondary antibodies in % normal goat serum and 0.1% Triton X-100 for 1 hour at RT and slices in PBS. Secondary antibodies were: Goat anti-mouse Alexa fluor 488 (A11029, Life Technologies, 1:500), goat anti-rabbit Alexa fluor 488 (A11034, Life Technologies, 1:1000) goat anti-rabbit Alexa fluor 647 (A21245, Life Technologies, 1:1000) Goat anti-mouse Alexa fluor 647 (A21236 Life Technologies, 1:1000). Coverslips were washed three times for 5 minutes in PBS/Gly, dipped in milliQ water (MQ), and mounted using Vectashield mounting medium (Vector labs).

Slices were fixed in at DIV16-20 in a 4% paraformaldehyde solution in PBS for 30 minutes at RT. Some slices were directly mounted, others were stained according to the protocol described in chapter 3, using the antibodies described for primary cultures above. Primary cultures and slices were imaged on a Zeiss LSM-700 confocal laser scanning microscopy system with a 63x NA 1.4 oil objectives. Z-stacks were acquired with a step size of 0.4 μ m at 10.08 pixels/ μ m.

6.2 Effects of the environment on the timing of the GABA shift

In chapter 2, we assessed the applicability of the SClm sensor to examine the effects of early life stress (ELS) on chloride levels in the medial prefrontal cortex (mPFC) (Herstel et al., 2022). We induced stress in dams and pups (Ivy et al., 2008) using a limited bedding material paradigm from P2 to P9, a period that roughly corresponds to the last trimester in human brain development (Chini and Hanganu-Opatz, 2021; Clancy et al., 2001). Prenatal exposure to maternal stress is considered an important risk factor for behavioral and mental health problems in later life (Joëls et al., 2018; Van den Bergh et al., 2020). For instance, prenatal stress is associated with a significant increase in ADHD risk, with an effect size varying between 1 and 22% (Ronald et al., 2011; Van den Bergh et al., 2020; Van Den Bergh and Marcoen, 2004). We found that ELS resulted in increased (more immature) chloride levels in mPFC neurons at P9, suggesting that ELS delayed the GABA shift in SClm mice (Herstel et al., 2022). It remains unknown if the contribution of early life stress to the development psychopathology in later life occurs via an altered GABA shift in both rodents and humans. To examine this possibility, the consequences of rescuing the GABA shift during ELS in rodents should be examined by pharmacologically inhibiting NKCC1. In addition, it would be informative to study the association between maternal stress and NKCC1/KCC2 expression in fetal and neonatal postmortem tissue or neonatal cerebrospinal fluid samples in humans.

These effects of ELS on neuronal chloride levels also underline that the developmental chloride trajectory is not completely pre-defined by genes, but responsive to environmental factors. ELS delayed the GABA shift in SClm mice, but the mechanism by which stress steers the GABA shift remains unclear. In contrast, various studies show that an environment enriched in sensory and social stimuli can accelerate the GABA shift (Baroncelli et al., 2017; He et al., 2010). Environmental enrichment is thought to do so by elevating the levels of the insulin-like growth factor-1 (IGF1). IGF1 is released in an activity-dependent manner and decreases the NKCC1/KCC2 expression ratio (Baroncelli et al., 2017; Cao et al., 2011). If similar mechanisms are present in humans, our understanding of behavioral and mental health problems may benefit from further elucidation of the links between sensory input, stress, the GABA shift and brain development.

6.3 Effects of the timing of the GABA shift on brain development and possible mechanisms

We assessed the consequences of a delayed and accelerated GABA shift in hippocampal slice cultures in chapters 4 and 5 using KCC2 blocker VU and chloride cotransporter blocker furosemide respectively. Interestingly, altering the GABA shift did not have any immediate effects on synapse development, while previous studies in which the GABA shift was advanced or GABA signaling was enhanced show that depolarizing and

excitatory GABAergic signaling can induce the formation and maturation of excitatory synapses before and right after birth (Leinekugel et al., 1997; Oh et al., 2016; Wang and Kriegstein, 2011, 2008). These studies led to the idea that depolarizing GABA is required for synapse formation. However, a recent study challenged this idea, by showing that excitatory synapses were not affected by enhanced GABA_A receptor function through propofol treatment in organotypic cultures in which GABA was depolarizing but inhibitory (Salmon et al., 2020). In our slice cultures, GABA also had an inhibitory action on cellular and network activity presumably by being shunting, even when it was kept depolarizing by VU (chapter 4). Together, these results suggest that depolarizing and excitatory GABA promotes excitatory transmission, but that this function is gradually lost after the first postnatal week when chloride levels decrease, and depolarizing GABA becomes inhibitory.

It will be important to verify this hypothesis in living rodents, as activity patterns in the intact brain will differ from those *in vitro*. Recent methodologies combining electrophysiology with calcium imaging, chemogenetics and/or optogenetics (Kirmse et al., 2015; Murata and Colonnese, 2020; Valeeva et al., 2016), enable measurement of the effect of GABA on cell and network activity during development of living animals. These methods have been used also to show that depolarizing GABA also inhibits activity from P7 onwards in the hippocampus of living mice (Murata and Colonnese, 2020; Valeeva et al., 2010), suggesting that GABA signaling in slices recapitulates the *in vivo* situation well.

That GABA no longer promotes excitatory transmission after the first postnatal week, does not mean that the timing of the shift to hyperpolarizing GABA during the second week after birth, is not important for brain development. Two weeks after delaying this shift with VU treatment, we found cell specific alterations in neuronal membrane properties. While CA1 pyramidal cells displayed an elevated action potential threshold, *stratum Radiatum* interneurons exhibited an depolarized resting membrane potential after VU treatment (chapter 4). Although experimental evidence is scarce, a few recent studies have reported chloride-mediated regulation of ion channels in a cell-specific manner (Goutierre et al., 2019; Huang et al., 2012; Jentsch and Pusch, 2018; Seja et al., 2012; Sinha et al., 2022). For instance, depolarized membrane potentials were also found after increases in chloride through knock out of KCC2 in cerebellar granule, but not Purkinje cells (Seja et al., 2012). The mechanism by which knock out of KCC2 affected membrane potentials remains unknown. Therefore, this finding may also be a result of disturbed structural interactions between KCC2 and ion channels (Goutierre et al., 2019), or may be indicative of chloride regulating the expression or function of ion channels that mediate membrane properties. To determine if the expression of ion channels is altered after VU- (and possibly furosemide-) treatment, a quantitative proteomics approach could be used in future experiments.

In addition, we found increases in inhibitory transmission two weeks after ending VU- and furosemide treatment. While VU treatment resulted in increased activity-dependent GABA release (without a change in the number of GABAergic synapses), we observed an increase in activity-independent GABA release (and probably an increase in the number of synapses) after furosemide. These results show that in the second week after birth, depolarizing and inhibitory GABA still affects GABAergic inhibition, but in an indirect manner.

It remains unclear how alterations in the shift to hyperpolarizing GABA alter inhibitory transmission later on. Various studies show that in the embryonic brain, formation and function of GABAergic synapses is highly dependent on GABA plays itself (Arama et al., 2015; Chattopadhyaya et al., 2007; Nguyen and Nicoll, 2018; Nicholson et al., 2018; Oh and Smith, 2019; Panzanelli et al., 2011). However, alterations in inhibitory transmission after prenatal manipulations of GABA signaling likely result from alterations in the synaptogenic effects of GABA rather than from altered GABA signaling. Moreover, we show that the effects of delaying and accelerating the GABA shift are not opposite. This suggests that the alterations in inhibitory transmission are due to alterations in local network activity, rather than the presence or absence of hyperpolarizing GABA.

We should also keep the possibility in mind that off-target effects may have contributed to the effects of VU and furosemide. VU can inhibit $\alpha 1$ -adrenergic receptors (IC₅₀ 0.35 μ M) and mitochondrial translocator protein (IC₅₀ 0.2 μ M). While we do not expect $\alpha 1$ -adrenergic receptor activation in our hippocampal slices, as they lack adrenergic input, VU may have inhibited TSPO. However, TSPO is primarily expressed by microglia and activation of TSPO increases microglial pruning of spines (Shi et al., 2022). Since spines were not affected by VU treatment in our slices (chapter 4), we do not expect that the effects of VU are a result of inhibition of TSPO. To demonstrate that this is the case, VU could be administered to slice cultures of TSPO knock out mice (Shi et al., 2022). We would expect VU to affect inhibitory transmission in a similar manner in the presence and absence of TSPO. Ideally, the effects of treatments with another, more specific KCC2 inhibitor on inhibitory transmission should be assessed to confirm that if the effect of VU is indeed mediated by inhibition of KCC2. However, VU is the most specific KCC2 inhibitor available at this moment. For instance, ((dihydroindenyl)oxy)alkanoic acid (DIOA) is also commonly used to block KCC2, but DIOA has been shown to affect cell viability (Delpire and Weaver, 2017). Decreasing KCC2 expression would represent a more specific alternative to pharmacological inhibition of KCC2. However, previous studies in hippocampal neurons at a similar stage of development as our slices have shown that suppression of KCC2 expression affects the function of excitatory synapses, by interfering with structural interactions between KCC2 and synaptic proteins, independently of KCC2 transporter function (Chevy et al., 2015; Gauvain et al., 2011). By treating our slices with VU and furosemide, we could study the consequences of altering the GABA shift without interfering with the structural

roles of KCC2. Our results suggest that the effects of KCC2 inhibition with VU deviate from those of reducing KCC2 expression.

Furosemide may have various off-target effects, besides the chloride cotransporters. Furosemide can inhibit $\alpha 6$ - and $\alpha 4$ -subunit containing GABA_A receptors (Korpi et al., 1995; Pearce, 1993; Thompson and Gahwiler, 1989), though we found no evidence for such inhibition happening in our slices (chapter 5). Instead, furosemide may have inhibited NKCC1, and possibly proteins that regulate neuronal HCO₃⁻ levels, including the Cl⁻/HCO₃⁻ anion exchanger (AE3) and/or carbonic anhydrase (CA) (chapter 5). Moreover, furosemide can inhibit activity-induced changes in cell volume, and may have done so in our slices (chapter 5). The effects of slice treatments with NKCC1 inhibitor bumetanide, AE3 inhibitor 4,4'- diisothiocyanatostilbene-2,2'-disulfonic acid (DIDS) (Uwera et al., 2015), CA inhibitor ethoxzolamide (EZA) (Rivera et al., 2005; Ruusuvaori et al., 2004) or osmolyte mannitol (Glykys et al., 2019) on inhibitory transmission at DIV21 would be informative to define the mechanism by which furosemide increased inhibitory transmission.

To summarize, depolarizing GABA is crucial for synapse formation before birth and up to approximately P7. After the first postnatal week, depolarizing and inhibitory GABA no longer promotes synapse formation, but indirectly regulates neuronal membrane properties and inhibitory transmission. In addition, chloride levels may be important for regulating cell volume at this time.

6.4 Implications for furosemide as a possible treatment for epilepsy

We examined the consequences of inhibiting NKCC1 and KCC2 for one week using furosemide in cultured hippocampal slices (chapter 5). Epidemiological and experimental studies have suggested that furosemide may have clinically relevant anticonvulsant actions (Hesdorffer et al., 2001, 1996; Maa et al., 2011; Staley, 2002). However, the versatile pharmacological profile of furosemide as well as the central homeostatic functions of its targets make it challenging to determine the exact mechanisms behind furosemide's anticonvulsant effects. Proposed explanations include inhibition of NKCC1-dependent glial swelling (thereby reducing ephaptic neuronal synchronization) (Gutschmidt et al., 1999; Hochman, 2012; Hochman et al., 1995), hyperpolarization of E_{GABA} (enhancing GABAergic inhibitory effect) (Chen et al., 2022) inhibition of KCC2-dependent increase in intraneuronal potassium (thereby depolarizing membrane potentials and promoting action potential firing) (Gutschmidt et al., 1999; Viitanen et al., 2010), inhibition of AE3 (decreasing activity-induced intracellular acidification and thereby suppressing epileptic activity) (Uwera et al., 2015; Xiong et al., 2000) and enhancement of inward rectifying potassium currents in glia (reducing the accumulation of extracellular potassium and thereby

reducing membrane potential depolarization) (Barbaro et al., 2004). Our results show that one week of furosemide treatment in organotypic cultures makes GABA more hyperpolarizing, which indirectly seems to promote the development of inhibitory synapses and to inhibit cell volume regulation (chapter 5). This indirect increase in inhibitory transmission, might constitute an additional mechanism via which furosemide can reduce seizure susceptibility. It will be important to examine if furosemide can also promote the formation of inhibitory synapses in the adult, and especially the epileptic brain.

6.5 Implications for the role of an altered GABA shift in neurodevelopmental disorders

During my PhD, I examined the consequences of delaying the GABA shift, to better understand the role of a delayed GABA shift in neurodevelopmental disorders (NDDs). NDDs represent a broad range of neurological and psychiatric conditions, including attention deficit hyperactivity disorder (ADHD), autism spectrum disorder (ASD), Down, Dravet, Fragile X, Prader-Willi, Rett and Timothy syndrome, and Tuberous Sclerosis Complex, which all manifest in the first three years after birth. In tissue and cerebrospinal fluid samples from Dravet, Rett, Timothy syndrome and Tuberous Sclerosis Complex patients, increased GABAergic depolarization and alterations in NKCC1 and/or KCC2 expression have been found, implicating a delayed GABA shift (Birey et al., 2022; Cherubini et al., 2022; Duarte et al., 2013; Ruffolo et al., 2018; Talos et al., 2012). Rodent models for NDDs also display alterations in the expression and function of NKCC1 and/or KCC2 (chapter 2) (Cherubini et al., 2022; Peerboom and Wierenga, 2021) along with a delayed GABA shift, though the length of the delay is variable. For instance, the GABA shift is delayed with three days in the cerebellum of mice exposed *in utero* to valproate (Roux et al., 2018), two to seven days in the hippocampus of a Prader Willi mouse model (Magel2 knock out) (Bertoni et al., 2021), and six days in the cortex of Fragile X mice (FMRP knock out) (He et al., 2018, 2014). Even longer delays have been reported in models for Rett syndrome and in maternal immune activation models for ASD (Banerjee et al., 2016; Corradini et al., 2017; Fernandez et al., 2018; Lozovaya et al., 2019) and in Down syndrome mice GABA remains depolarizing in adulthood (Deidda et al., 2015). Persistent GABAergic depolarization may most likely have different consequences than those of the delayed GABA shift studied here.

Rodent models for neurodevelopmental disorders often display a prolongation of excitatory GABA signaling

In chapter 4 we delayed the GABA shift in organotypic cultures by treating them for one week with VU and found that GABA signaling was depolarizing but inhibitory after VU treatment. We found that VU treatment indirectly affected inhibitory transmission and membrane properties (chapter 4), suggesting that GABA signaling indirectly regulates

inhibition and excitability in the second postnatal week. This role of depolarizing but inhibitory GABA differs from the role of depolarizing, excitatory GABA, which promotes the formation and maturation of excitatory synapses up to postnatal day 7 (Leinekugel et al., 1997; Oh et al., 2016; Wang and Kriegstein, 2011, 2008). This finding underlines the importance of assessing GABA's effect on activity when studying the GABA shift. Unfortunately, in many studies examining the GABA shift in rodent models for NDDs, GABA's effect on activity is not assessed. Other studies have reported a prolongation of the period during which GABA signaling is excitatory in NDD models (Corradini et al., 2017; Fernandez et al., 2018; Lozovaya et al., 2019; Roux et al., 2018; Tyzio et al., 2014).

Given the role of excitatory GABA in the formation of excitatory synapses, we would expect that prolonging of the period during which GABA is excitatory, would induce an overproduction of excitatory synapses (Leinekugel et al., 1997; Oh et al., 2016; Wang and Kriegstein, 2011, 2008), which may induce NDD-related behavior. However, a recent study puts this reasoning into doubt. In this study the consequences of a delayed GABA shift were examined in KCC2E/+ mice. These mice carry phosphomimetic mutations T906E and T1007E. As a result, the shift from excitatory to inhibitory GABA in hippocampal CA3 pyramidal neurons is delayed from approximately P10 to P20 in KCC2E/+ mice. KCC2E/+ CA3 pyramidal neurons displayed a transient increase in excitatory transmission along with a decrease in inhibitory transmission (Pisella et al., 2019). This suggests that delaying the shift from depolarizing and excitatory GABA to inhibitory GABA, does have no long term effects on transmission, while delaying the shift from depolarizing but inhibitory to hyperpolarizing GABA indirectly and specifically increases inhibitory transmission (chapter 4). In addition, KCC2E/+ mice display impaired social behavior. Interestingly, administration of the NKCC1 inhibitor bumetanide from P6 till P15 (which restored the GABA shift) restored the transient alterations in synaptic transmission in KCC2E/+ mice, but did not rescue behavior (Pisella et al., 2019). This suggests that prolongation of the period during which GABA is excitatory may have other, yet unknown consequences on the network, possibly in other brain areas than the hippocampus, that alter sociability. Alternatively, the alterations in KCC2 phosphorylation by itself, rather than the delayed GABA shift, may have altered sociability in KCC2E/+ mice. To see if prolongation of GABAergic excitation without interfering with KCC2 phosphorylation, indeed results in an overgrowth of excitatory synapses, it would be informative to prolong the period during which GABA is excitatory by treating younger slice cultures (e.g. from P3 pups) with VU in future experiments. As a next step, it would be very interesting to assess the behavioral consequences of administering VU to living animals of various ages (Raol et al., 2020). These experiments can further improve our understanding of the consequences of a mistimed GABA shift to the network and to behavior in NDDs.

Translatability of our findings to rodent models for neurodevelopmental disorders

We found increased inhibitory transmission and cell type specific alterations in neuronal membrane properties two weeks after the ending of the VU treatment. Rodent models for NDDs that display a delayed GABA shift commonly also show aberrant inhibitory transmission. In some rodent models with a delayed GABA shift, including those for Prader-Willi and Down syndrome, increases in adult inhibition have been reported (Bertoni et al., 2021; Ramamoorthi and Lin, 2011). However, many models, including those for ASD (prenatal exposure to antiepileptics and infections), Fragile X, and Tuberous Sclerosis display decreased inhibitory transmission in adulthood (Antoine et al., 2019; Griego et al., 2022; Qi et al., 2022; Ramamoorthi and Lin, 2011). Then again, the mutations that cause NDDs often directly interfere with the function of inhibitory synapses, and so may prenatal exposure to valproic acid and inflammation (D'Hulst and Kooy, 2007; Fu et al., 2012; Fukuchi et al., 2009; Ramamoorthi and Lin, 2011; Shin Yim et al., 2017). Moreover, our brain is set up with various mechanisms to coordinate excitation and inhibition after perturbations (Herstel and Wierenga, 2021; Maffei and Fontanini, 2009; Turrigiano and Nelson, 2004), which could indicate that changes in excitation and inhibition may well be compensatory to, rather than driving, altered network function (Antoine et al., 2019). Our data suggest that changes in membrane excitability may also contribute to altered brain development. Unfortunately, membrane properties are not well characterized in development and in NDD rodent models. Some alterations in membrane properties in NDD mouse models have been reported (Antoine et al., 2019; Bódi et al., 2022; Olmos-Serrano et al., 2010; Patrich et al., 2016), but again it remains unclear whether they represent direct consequences of the mutations or prenatal exposure of specific NDD models or if they are a consequence of an altered GABA shift. It also remains unclear if altered membrane properties contribute to NDD phenotypes. Interestingly, a recent study in a neural network-controlled robot suggests that variability in excitability between neurons indeed causes in NDD phenotypes, including excessive synaptic wiring, hypersensitive information processing, and behavioral alterations such as clumsiness, reduced generalization, and inflexibility (Idei et al., 2020).

Translatability of our findings to patients with neurodevelopmental disorders

It also remains unclear how the consequences of a delayed GABA shift in rodents, extrapolate to NDD patients. It is important to know that brain development at birth in rodents roughly corresponds to human development at the beginning of the last trimester (GW 28) of gestation (Chini and Hanganu-Opatz, 2021; Clancy et al., 2001). The change in expression profiles of NKCC1 and KCC2 during the last trimester, resembles chloride co-transporter expression in the first postnatal weeks birth of rodents (Dzhala et al., 2005; Sedmak et al., 2016) and the electroencephalogram (EEG) in healthy newborns (Kharod et al., 2019) resembles the stage in rodents where GABAergic signaling is inhibitory already (Vanhatalo et al., 2005). This suggest that in the typically developing human brain, GABA shifts already before birth. We remain unsure to what

extent the consequences of a delayed postnatal GABA shift in rodents, resemble the situation in NDD patients, in which the GABA shift may be delayed until after birth.

A clue for a causal role of a delayed GABA shift in NDDs across species, is the potential of NKCC1 inhibitor bumetanide to improve behavioral manifestations in children with NDDs and in animal models. A potential treatment is of major importance especially in autism, as at this moment there is no medication available that improves ASD's core symptoms. Bumetanide blocks chloride importer NKCC1 and is thereby thought to reinstate GABAergic hyperpolarization instead of depolarization. In NDD models, postnatal bumetanide improves some, but not all behavioral phenotypes (Deidda et al., 2015; He et al., 2018; Matsushima et al., 2022; Savardi et al., 2020). Likewise, bumetanide ameliorates a subset of behavioral alterations in a subset of children with NDDs, especially those with a paradoxical response to GABA-enforcing drugs (van Andel et al., 2022; Wang et al., 2021). Thus, it seems that bumetanide is beneficial for a subset of NDD patients in which GABAergic signaling may remain excitatory. This suggests that sustained GABAergic excitation can profoundly affect brain function and alter brain development in both mice and men, but these studies do not offer additional insight in the contribution of a delayed GABA shift in NDDs.

Historically, pharmacological interventions in NDDs are chosen on basis of specific diagnoses. This approach completely ignores the heterogeneity in NDD etiologies as well as the commonalities in symptoms across disorders. Still, the field typically searches for treatments that helps all children diagnosed with a specific disorder. Only recently, endeavors have emerged to personalize therapeutic interventions across disorders, using genetic and neurophysiological prediction markers (Geertjens et al., 2022; Sprengers et al., 2021; van Eeghen et al., 2022). The identification of patients most likely to respond to certain treatments is likely to benefit from a better understanding of the consequences of careful manipulations of the GABA shift. For example, we found that delaying the shift from depolarizing (but inhibitory) to hyperpolarizing GABA results in increased GABA inhibition (chapter 4). If the same mechanism holds true in human brain development, we would predict that patients that show genetic or neurophysiological indications for such a delay, may be especially likely to benefit from GABA-repressing agents. It would be wonderful if a more precise understanding of the environmental and molecular causes and consequences in NDDs will help stratify NDD treatments in the future.

6.6 Concluding remarks

We often think of our brain as the organ that makes us who we are. Our brain allows us to experience the outside world and to respond to our environments through emotions, thoughts, ideas and actions. But we tend to forget that the reverse is also true. Brain development is not only guided by our genes, which make sure

that key events are pre-programmed, but also by our experiences, which allows for adaptability. This thesis offers new insights into the adaptability of the GABA shift and the consequences of altered timing of the GABA shift during brain development. GABA signaling is important throughout brain development, but its role does not only simply depend on being de- or hyperpolarizing. Local network activity can make depolarizing GABA inhibitory when GABA-mediated depolarization is subthreshold and opening of GABA_A receptors will shunt excitatory inputs. After P7, inhibitory GABA indirectly regulates neuronal excitability and inhibitory transmission. In addition, chloride levels may regulate cell volume and possibly pH at this time. We are only beginning to understand how genetic mutations and early life experience that alter the timing of the GABA shift, can push brain development into different directions. I hope that a more precise understanding of the consequences of a mistimed GABA shift will be useful for the development of targeted therapies to alleviate behavioral burden in neurodevelopmental disorders.

6.7 References

- Antoine, M.W., Langberg, T., Schnepel, P., Feldman, D.E., 2019. Increased Excitation-Inhibition Ratio Stabilizes Synapse and Circuit Excitability in Four Autism Mouse Models - supplemental. *Neuron* 101, 648-661.e4. <https://doi.org/10.1016/j.neuron.2018.12.026>
- Arama, J., Abitbol, K., Goffin, D., Fuchs, C., Sihra, T.S., Thomson, A.M., Jovanovic, J.N., 2015. GABAA receptor activity shapes the formation of inhibitory synapses between developing medium spiny neurons. *Front. Cell. Neurosci.* 9, 1–18. <https://doi.org/10.3389/fncel.2015.00290>
- Arosio, D., Ratto, G.M., 2014. Twenty years of fluorescence imaging of intracellular chloride. *Front. Cell. Neurosci.* 8, 1–12. <https://doi.org/10.3389/fncel.2014.00258>
- Banerjee, A., Rikhye, R.V., Breton-Provencher, V., Tang, X., Li, C., Li, K., Runyan, C.A., Fu, Z., Jaenisch, R., Sur, M., 2016. Jointly reduced inhibition and excitation underlies circuit-wide changes in cortical processing in Rett syndrome. *Proc. Natl. Acad. Sci.* 113, E7287–E7296. <https://doi.org/10.1073/pnas.1615330113>
- Barbaro, N.M., Takahashi, D.K., Baraban, S.C., 2004. A potential role for astrocytes in mediating the antiepileptic actions of furosemide in vitro. *Neuroscience* 128, 655–663. <https://doi.org/10.1016/j.neuroscience.2004.07.007>
- Baroncelli, L., Cenni, M.C., Melani, R., Deidda, G., Landi, S., Narducci, R., Cancedda, L., Maffei, L., Berardi, N., 2017. Early IGF-1 primes visual cortex maturation and accelerates developmental switch between NKCC1 and KCC2 chloride transporters in enriched animals. *Neuropharmacology* 113, 167–177. <https://doi.org/10.1016/j.neuropharm.2016.02.034>
- Batti, L., Mukhtarov, M., Audero, E., Ivanov, A., Paolicelli, O., Zurborg, S., Gross, C., Bregestovski, P., Heppenstall, P.A., 2013. Transgenic mouse lines for non-invasive ratiometric monitoring of intracellular chloride. *Front. Mol. Neurosci.* 6, 1–14. <https://doi.org/10.3389/fnmol.2013.00011>
- Berglund, K., Schleich, W., Krieger, P., Loo, L.S., Wang, D., Cant, N.B., Feng, G., Augustine, G.J., Kuner, T., 2006. Imaging synaptic inhibition in transgenic mice expressing the chloride indicator, Clomeleon. *Brain Cell Biol.* 35, 207–228. <https://doi.org/10.1007/s11068-008-9019-6>
- Bertoni, A., Schaller, F., Tyzio, R., Gaillard, S., Santini, F., Xolin, M., Diabira, D., Vaidyanathan, R., Matarazzo, V., Medina, I., Hammock, E., Zhang, J., Chini, B., Gaiarsa, J.-L., Muscatelli, F., 2021. Oxytocin administration in neonates shapes the hippocampal circuitry and restores social behavior in a mouse model of autism. *Mol. Psychiatry* 26, 7582–7595. <https://doi.org/10.1038/s41380-021-01227-6>
- Birey, F., Li, M.Y., Gordon, A., Thete, M. V., Valencia, A.M., Revah, O., Paşca, A.M., Geschwind, D.H., Paşca, S.P., 2022. Dissecting the molecular basis of human interneuron migration in forebrain assembloids from Timothy syndrome. *Cell Stem Cell* 29, 248-264. e7. <https://doi.org/10.1016/j.stem.2021.11.011>
- Bódi, V., Májer, T., Kelemen, V., Világi, I., Szűcs, A., Varró, P., 2022. Alterations of the Hippocampal Networks in Valproic Acid-Induced Rat Autism Model. *Front. Neural Circuits* 16, 1–12. <https://doi.org/10.3389/fncir.2022.772792>
- Boffi, J.C., Knabbe, J., Kaiser, M., Kuner, T., 2018. KCC2-dependent steady-state intracellular chloride concentration and pH in cortical layer 2/3 neurons of anesthetized and awake mice. *Front. Cell. Neurosci.* 12, 1–14. <https://doi.org/10.3389/fncel.2018.00007>

- Cao, P., Maximov, A., Südhof, T.C., 2011. Activity-dependent IGF-1 exocytosis is controlled by the Ca²⁺-sensor synaptotagmin-10. *Cell* 145, 300–311. <https://doi.org/10.1016/j.cell.2011.03.034>
- Chattopadhyaya, B., Di Cristo, G., Wu, C.Z., Knott, G., Kuhlman, S., Fu, Y., Palmiter, R.D., Huang, Z.J., 2007. GAD67-Mediated GABA Synthesis and Signaling Regulate Inhibitory Synaptic Innervation in the Visual Cortex. *Neuron* 54, 889–903. <https://doi.org/10.1016/j.neuron.2007.05.015>
- Chen, L., Yu, J., Wan, L., Wu, Z., Wang, G., Hu, Z., Ren, L., Zhou, J., Qian, B., Zhao, X., Zhang, J., Liu, X., 2022. Furosemide prevents membrane KCC2 downregulation during convulsant stimulation in the hippocampus. *IBRO Neurosci. Reports* 12, 355–365. <https://doi.org/10.1016/j.ibneur.2022.04.010>
- Cherubini, E., Di Cristo, G., Avoli, M., 2022. Dysregulation of GABAergic Signaling in Neurodevelopmental Disorders: Targeting Cation-Chloride Co-transporters to Re-establish a Proper E/I Balance. *Front. Cell. Neurosci.* 15, 1–20. <https://doi.org/10.3389/fncel.2021.813441>
- Chevy, Q., Heubl, M., Goutier, M., Backer, S., Moutkine, I., Eugene, E., Bloch-Gallego, E., Levi, S., Poncer, J.C., 2015. KCC2 Gates Activity-Driven AMPA Receptor Traffic through Cofilin Phosphorylation. *J. Neurosci.* 35, 15772–15786. <https://doi.org/10.1523/JNEUROSCI.1735-15.2015>
- Chini, M., Hanganu-Opatz, I.L., 2021. Prefrontal Cortex Development in Health and Disease: Lessons from Rodents and Humans. *Trends Neurosci.* 44, 227–240. <https://doi.org/10.1016/j.tins.2020.10.017>
- Clancy, B., Darlington, R.B., Finlay, B.L., 2001. Translating developmental time across mammalian species. *Neuroscience* 105, 7–17. [https://doi.org/10.1016/S0306-4522\(01\)00171-3](https://doi.org/10.1016/S0306-4522(01)00171-3)
- Corradini, I., Focchi, E., Rasile, M., Morini, R., Desiato, G., Tomasoni, R., Lizier, M., Ghirardini, E., Fesce, R., Morone, D., Barajon, I., Antonucci, F., Pozzi, D., Matteoli, M., 2017. Maternal Immune Activation Delays Excitatory-to-Inhibitory Gamma-Aminobutyric Acid Switch in Offspring. *Biol. Psychiatry* 83, 1–12. <https://doi.org/10.1016/j.biopsych.2017.09.030>
- Cunha-Ferreira, I., Chazeau, A., Buijs, R.R., Stucchi, R., Will, L., Pan, X., Adolfs, Y., van der Meer, C., Wolthuis, J.C., Kahn, O.I., Schätzle, P., Altelaar, M., Pasterkamp, R.J., Kapitein, L.C., Hoogenraad, C.C., 2018. The HAUS Complex Is a Key Regulator of Non-centrosomal Microtubule Organization during Neuronal Development. *Cell Rep.* 24, 791–800. <https://doi.org/10.1016/j.celrep.2018.06.093>
- D’Hulst, C., Kooy, R.F., 2007. The GABA Receptor: a novel target for treatment of fragile X? *Trends Neurosci.* 30, 425–431. <https://doi.org/10.1016/j.tins.2007.06.003>
- Deidda, G., Parrini, M., Naskar, S., Bozarth, I.F., Contestabile, A., Cancedda, L., 2015. Reversing excitatory GABAAR signaling restores synaptic plasticity and memory in a mouse model of Down syndrome. *Nat. Med.* 21, 318–326. <https://doi.org/10.1038/nm.3827>
- Delpire, E., Weaver, C.D., 2017. Challenges of finding novel drugs targeting the K-Clcotransporter 7, 1624–1627.
- Duarte, S.T., Armstrong, J., Roche, A., Ortez, C., Pérez, A., O’Callaghan, M. del M., Pereira, A., Sanmartí, F., Ormazábal, A., Artuch, R., Pineda, M., García-Cazorla, A., 2013. Abnormal Expression of Cerebrospinal Fluid Cation Chloride Cotransporters in Patients with Rett Syndrome. *PLoS One* 8, 1–7. <https://doi.org/10.1371/journal.pone.0068851>
- Dzhala, V., Valeeva, G., Glykys, J., Khazipov, R., Staley, K., 2012. Traumatic Alterations in GABA Signaling Disrupt Hippocampal Network Activity in the Developing Brain. *J. Neurosci.* 32, 4017–4031. <https://doi.org/10.1523/JNEUROSCI.5139-11.2012>

- Dzhala, V.I., Talos, D.M., Sdrulla, D.A., Brumback, A.C., Mathews, G.C., Benke, T.A., Delpire, E., Jensen, F.E., Staley, K.J., 2005. NKCC1 transporter facilitates seizures in the developing brain. *Nat. Med.* 11, 1205–1213. <https://doi.org/10.1038/nm1301>
- Favuzzi, E., Rico, B., 2018. Molecular diversity underlying cortical excitatory and inhibitory synapse development. *Curr. Opin. Neurobiol.* 53, 8–15. <https://doi.org/10.1016/j.conb.2018.03.011>
- Fernandez, A., Dumon, C., Guimond, D., Fernandez, A., Burnashev, N., Tyzio, R., Lozovaya, N., Ferrari, D.C., Bonifazi, P., Ben-Ari, Y., 2018. The GABA Developmental Shift Is Abolished by Maternal Immune Activation Already at Birth. *Cereb. Cortex* 29, 3982–3992. <https://doi.org/10.1093/cercor/bhy279>
- Fu, C., Cawthon, B., Clinkscapes, W., Bruce, A., Winzenburger, P., Ess, K.C., 2012. GABAergic interneuron development and function is modulated by the Tsc1 gene. *Cereb. Cortex* 22, 2111–2119. <https://doi.org/10.1093/cercor/bhr300>
- Fukuchi, M., Nii, T., Ishimaru, N., Minamino, A., Hara, D., Takasaki, I., Tabuchi, A., Tsuda, M., 2009. Valproic acid induces up- or down-regulation of gene expression responsible for the neuronal excitation and inhibition in rat cortical neurons through its epigenetic actions. *Neurosci. Res.* 65, 35–43. <https://doi.org/10.1016/j.neures.2009.05.002>
- Gauvain, G., Chamma, I., Chevy, Q., Cabezas, C., Irinopoulou, T., Bodrug, N., Carnaud, M., Levi, S., Poncer, J.C., 2011. The neuronal K-Cl cotransporter KCC2 influences postsynaptic AMPA receptor content and lateral diffusion in dendritic spines. *Proc. Natl. Acad. Sci.* 108, 15474–15479. <https://doi.org/10.1073/pnas.1107893108>
- Geertjens, L., Cristian, G., Haspels, E., Ramautar, J., van der Wilt, G.J., Verhage, M., Bruining, H., 2022. Single-case experimental designs for bumetanide across neurodevelopmental disorders: BUDDI protocol. *BMC Psychiatry* 22, 1–11. <https://doi.org/10.1186/s12888-022-04033-8>
- Glykys, J., Duquette, E., Rahmati, N., Duquette, K., Staley, K.J., 2019. Mannitol decreases neocortical epileptiform activity during early brain development via cotransport of chloride and water. *Neurobiol. Dis.* 125, 163–175. <https://doi.org/10.1016/j.nbd.2019.01.024>
- Goutierre, M., Al Awabdh, S., Donneger, F., François, E., Gomez-Dominguez, D., Irinopoulou, T., Menendez de la Prida, L., Poncer, J.C., 2019. KCC2 Regulates Neuronal Excitability and Hippocampal Activity via Interaction with Task-3 Channels. *Cell Rep.* 28, 91–103. <https://doi.org/10.1016/j.celrep.2019.06.001>
- Griego, E., Segura-Villalobos, D., Lamas, M., Galván, E.J., 2022. Maternal immune activation increases excitability via downregulation of A-type potassium channels and reduces dendritic complexity of hippocampal neurons of the offspring. *Brain. Behav. Immun.* 105, 67–81. <https://doi.org/10.1016/j.bbi.2022.07.005>
- Grimley, J.S., Li, L., Wang, W., Wen, L., Beese, L.S., Hellinga, H.W., Augustine, G.J., 2013. Visualization of Synaptic Inhibition with an Optogenetic Sensor Developed by Cell-Free Protein Engineering Automation. *J. Neurosci.* 33, 16297–16309. <https://doi.org/10.1523/JNEUROSCI.4616-11.2013>
- Gutschmidt, K.U., Stenkamp, K., Buchheim, K., Heinemann, U., Meierkord, H., 1999. Anticonvulsant actions of furosemide in vitro. *Neuroscience* 91, 1471–1481. [https://doi.org/10.1016/S0306-4522\(98\)00700-3](https://doi.org/10.1016/S0306-4522(98)00700-3)
- He, Q., Arroyo, E.D., Smukowski, S.N., Xu, J., Piochon, C., Savas, J.N., Portera-Cailliau, C., Contractor, A., 2018. Critical period inhibition of NKCC1 rectifies synapse plasticity in the somatosensory cortex and restores adult tactile response maps in fragile X mice. *Mol. Psychiatry* 24, 1732–1747. <https://doi.org/10.1038/s41380-018-0048-y>
- He, Q., Nomura, T., Xu, J., Contractor, A., 2014. The Developmental Switch in GABA Polarity Is Delayed in Fragile X Mice. *J. Neurosci.* 34, 446–450. <https://doi.org/10.1523/JNEUROSCI.4447-13.2014>

- He, S., Ma, J., Liu, N., Yu, X., 2010. Early enriched environment promotes neonatal GABAergic neurotransmission and accelerates synapse maturation. *J. Neurosci.* 30, 7910–7916. <https://doi.org/10.1523/JNEUROSCI.6375-09.2010>
- Herstel, L.J., Peerboom, C., Uijtewaal, S., Selemangel, D., Karst, H., Wierenga, C.J., 2022. Using SuperClomeleon to measure changes in intracellular chloride during development and after early life stress. *Eneuro* November/D.
- Herstel, L.J., Wierenga, C.J., 2021. Network control through coordinated inhibition. *Curr. Opin. Neurobiol.* 67, 34–41. <https://doi.org/10.1016/j.conb.2020.08.001>
- Hesdorffer, D.C., Hauser, W.A., Annegers, J.F., Rocca, W.A., 1996. Severe, uncontrolled hypertension and adult-onset seizures: A case-control study in Rochester, Minnesota. *Epilepsia* 37, 736–741. <https://doi.org/10.1111/j.1528-1157.1996.tb00644.x>
- Hesdorffer, D.C., Stables, J.P., Allen Hauser, W., Annegers, J.F., Cascino, G., 2001. Are certain diuretics also anticonvulsants? *Ann. Neurol.* 50, 458–462. <https://doi.org/10.1002/ana.1136>
- Hochman, D.W., 2012. The extracellular space and epileptic activity in the adult brain: Explaining the antiepileptic effects of furosemide and bumetanide. *Epilepsia* 53, 18–25. <https://doi.org/10.1111/j.1528-1167.2012.03471.x>
- Hochman, D.W., Baraban, S.C., Owens, J.W.M., Schwartzkroin, P.A., 1995. Dissociation of synchronization and excitability in furosemide blockade of epileptiform activity. *Science* (80-.). 270, 99–102. <https://doi.org/10.1126/science.270.5233.99>
- Huang, Y., Ko, H., Cheung, Z.H., Yung, K.K.L., Yao, T., Wang, J.J., Morozov, A., Ke, Y., Ip, N.Y., Yung, W.H., 2012. Dual actions of brain-derived neurotrophic factor on GABAergic transmission in cerebellar Purkinje neurons. *Exp. Neurol.* 233, 791–798. <https://doi.org/10.1016/j.expneurol.2011.11.043>
- Idei, H., Murata, S., Yamashita, Y., Ogata, T., 2020. Homogeneous Intrinsic Neuronal Excitability Induces Overfitting to Sensory Noise: A Robot Model of Neurodevelopmental Disorder. *Front. Psychiatry* 11, 1–15. <https://doi.org/10.3389/fpsy.2020.00762>
- Ishino, Y., Shinagawa, H., Makino, K., Amemura, M., Nakamura, A., 1987. Nucleotide sequence of the iap gene, responsible for alkaline phosphatase isoenzyme conversion in *Escherichia coli*, and identification of the gene product. *J. Bacteriol.* 169, 5429–5433. <https://doi.org/10.1128/jb.169.12.5429-5433.1987>
- Ivy, A.S., Brunson, K.L., Sandman, C., Baram, T.Z., 2008. Dysfunctional nurturing behavior in rat dams with limited access to nesting material: a clinically relevant model for early-life stress. *Neuroscience* 154, 1132–1142.
- Jansen, R., Van Embden, J.D.A., Gaastra, W., Schouls, L.M., 2002. Identification of genes that are associated with DNA repeats in prokaryotes. *Mol. Microbiol.* 43, 1565–1575. <https://doi.org/10.1046/j.1365-2958.2002.02839.x>
- Jentsch, T.J., Pusch, M., 2018. CLC chloride channels and transporters: Structure, function, physiology, and disease. *Physiol. Rev.* 98, 1493–1590. <https://doi.org/10.1152/physrev.00047.2017>
- Joëls, M., Karst, H., Sarabdjitsingh, R.A., 2018. The stressed brain of humans and rodents. *Acta Physiol.* 223, 1–10. <https://doi.org/10.1111/apha.13066>
- Kaila, K., Price, T.J., Payne, J.A., Puskarjov, M., Voipio, J., 2014. Cation-chloride cotransporters in neuronal development, plasticity and disease. *Nat. Rev. Neurosci.* 15, 637–654. <https://doi.org/10.1038/nrn3819>
- Karst, H., Droogers, W.J., Weerd, N. Van Der, Damsteegt, R., Kroonenburg, N. Van, Sarabdjitsingh, R.A., Jo, M., 2023. Neuropharmacology Acceleration of GABA-switch after early life stress changes mouse prefrontal glutamatergic transmission 234. <https://doi.org/10.1016/j.neuropharm.2023.109543>

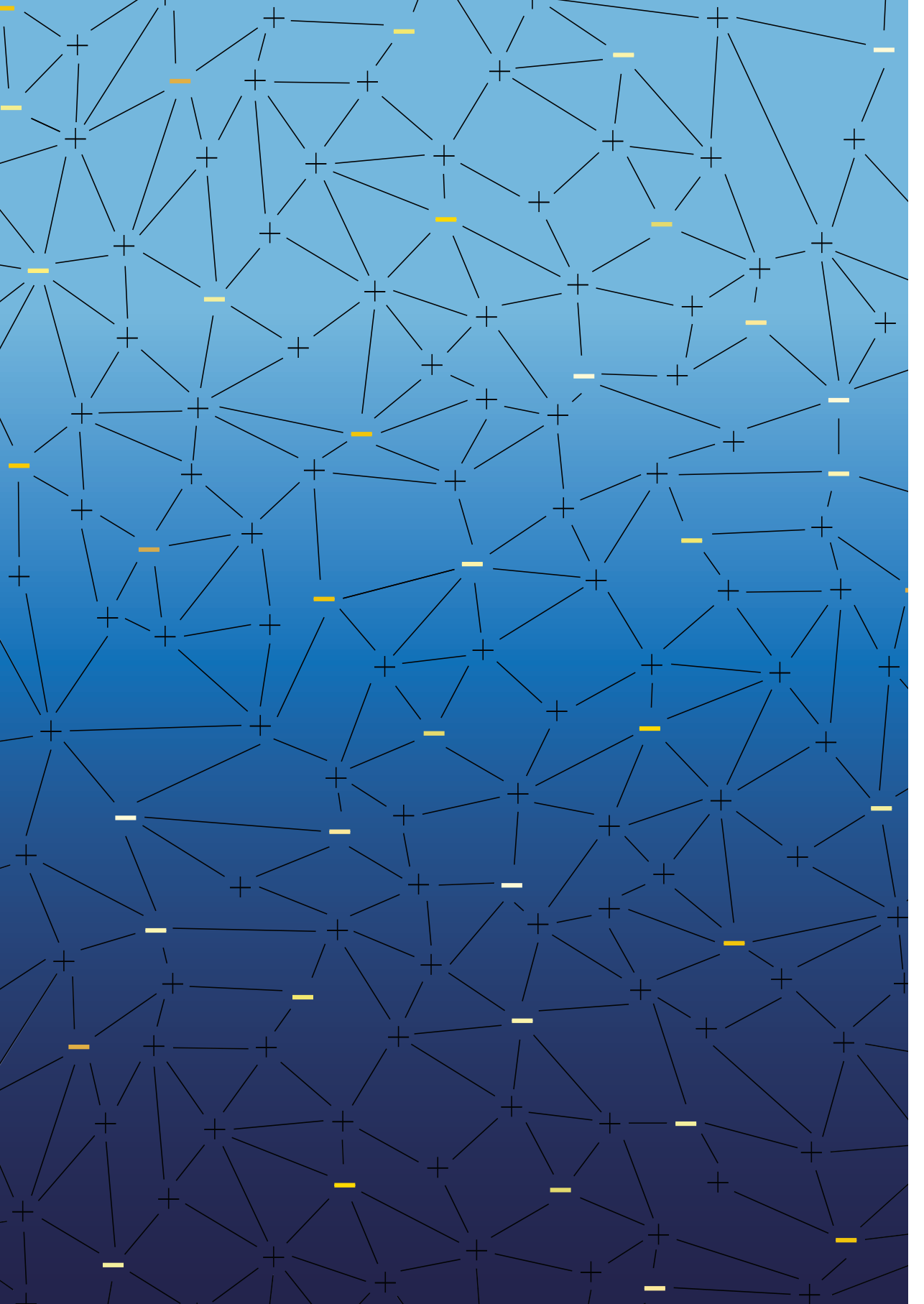
- Kharod, S.C., Kang, S.K., Kadam, S.D., 2019. Off-Label Use of Bumetanide for Brain Disorders: An Overview. *Front. Neurosci.* 13, doi: 10.3389/fnins.2019.00310. <https://doi.org/10.3389/fnins.2019.00310>
- Kirmse, K., Kummer, M., Kovalchuk, Y., Witte, O.W., Garaschuk, O., Holthoff, K., 2015. GABA depolarizes immature neurons and inhibits network activity in the neonatal neocortex in vivo. *Nat. Commun.* 6, 1–13. <https://doi.org/10.1038/ncomms8750>
- Knott, G.J., Doudna, J.A., 2018. CRISPR-Cas guides the future of genetic engineering. *Science* (80-.). 361, 866–869. <https://doi.org/10.1126/science.aat5011>
- Korpi, E.R., Kuner, T., Seeburg, P.H., Luddens, H., 1995. Selective antagonist for the cerebellar granule cell-specific g-aminobutyric acid type A receptor. *Mol. Pharmacol.* 47, 283–289.
- Kuner, T., Augustine, G.J., 2000. A Genetically Encoded Ratiometric Indicator for Chloride. *Neuron* 27, 447–459. [https://doi.org/10.1016/s0896-6273\(00\)00056-8](https://doi.org/10.1016/s0896-6273(00)00056-8)
- Leinekugel, X., Medina, I., Khalilov, I., Ben-Ari, Y., Khazipov, R., 1997. Ca²⁺ Oscillations Mediated by the Synergistic Excitatory Actions of GABA. *Neuron* 18, 243–255.
- Liang, J., Kruijssen, D.L., Verschuuren, A.C., Voeselek, B.J., Benavides, F.F., Gonzalez, M.S., Ruiter, M., Wierenga, C.J., 2021. Axonal CB1 receptors mediate inhibitory bouton formation via cAMP increase and PKA. *J. Neurosci.* JN-RM-0851-21. <https://doi.org/10.1523/jneurosci.0851-21.2021>
- Lodovichi, C., Ratto, G.M., Trevelyan, A.J., Arosio, D., 2022. Genetically encoded sensors for Chloride concentration. *J. Neurosci. Methods* 368, 109455. <https://doi.org/10.1016/j.jneumeth.2021.109455>
- Lozovaya, N., Nardou, R., Tyzio, R., Chiesa, M., Pons-Bennaceur, A., Eftekhari, S., Bui, T.T., Billon-Grand, M., Rasero, J., Bonifazi, P., Guimond, D., Gaiarsa, J.L., Ferrari, D.C., Ben-Ari, Y., 2019. Early alterations in a mouse model of Rett syndrome: the GABA developmental shift is abolished at birth. *Sci. Rep.* 9, 1–16. <https://doi.org/10.1038/s41598-019-45635-9>
- Maa, E.H., Kahle, K.T., Walcott, B.P., Spitz, M.C., Staley, K.J., 2011. Diuretics and epilepsy: Will the past and present meet? *Epilepsia* 52, 1559–1569. <https://doi.org/10.1111/j.1528-1167.2011.03203.x>
- Maffei, A., Fontanini, A., 2009. Network homeostasis: a matter of coordination. *Curr. Opin. Neurobiol.* 19, 168–173. <https://doi.org/10.1016/j.conb.2009.05.012>
- Matsushima, T., Miura, M., Patzke, N., Toji, N., Wada, K., Ogura, Y., Homma, K.J., Sgadò, P., Vallortigara, G., 2022. Impaired Epigenesis of Imprinting Predispositions Causes Autism-like Behavioral Phenotypes in Domestic Chicks. *bioRxiv*.
- Murata, Y., Colonnese, M.T., 2020. GABAergic interneurons excite neonatal hippocampus in vivo. *Sci. Adv.* 6, 1–10.
- Nguyen, Q.A., Nicoll, R.A., 2018. The GABA_A Receptor β Subunit Is Required for Inhibitory Transmission. *Neuron* 98, 718–725.e3. <https://doi.org/10.1016/j.neuron.2018.03.046>
- Nicholson, M.W., Sweeney, A., Pekle, E., Alam, S., Ali, A.B., Duchon, M., Jovanovic, J.N., 2018. Diazepam-induced loss of inhibitory synapses mediated by PLC δ /Ca²⁺/calcineurin signalling downstream of GABA_A receptors. *Mol. Psychiatry* 23, 1851–1867. <https://doi.org/10.1038/s41380-018-0100-y>
- Oh, W.C., Lutz, S., Castillo, P.E., Kwon, H.B., 2016. De novo synaptogenesis induced by GABA in the developing mouse cortex - supplemental. *Science* (80-.). 353, 1037–1040. <https://doi.org/10.1126/science.aaf5206>
- Oh, W.C., Smith, K.R., 2019. Activity-dependent development of GABAergic synapses. *Brain Res.* 1707, 18–26. <https://doi.org/10.1016/j.brainres.2018.11.014>

- Olmos-Serrano, J.L., Paluszkiwicz, S.M., Martin, B.S., Kaufmann, W.E., Corbin, J.G., Huntsman, M.M., 2010. Defective GABAergic Neurotransmission and Pharmacological Rescue of Neuronal Hyperexcitability in the Amygdala in a Mouse Model of Fragile X Syndrome. *J. Neurosci.* 30, 9929–9938. <https://doi.org/10.1523/jneurosci.1714-10.2010>
- Panzanelli, P., Gunn, B.G., Schlatter, M.C., Benke, D., Tyagarajan, S.K., Scheiffele, P., Belelli, D., Lambert, J.J., Rudolph, U., Fritschy, J.M., 2011. Distinct mechanisms regulate GABA A receptor and gephyrin clustering at perisomatic and axo-axonic synapses on CA1 pyramidal cells. *J. Physiol.* 589, 4959–4980. <https://doi.org/10.1113/jphysiol.2011.216028>
- Paredes, J.M., Idilli, A.I., Mariotti, L., Losi, G., Arslanbaeva, L.R., Sato, S.S., Artoni, P., Szczurkowska, J., Cancedda, L., Ratto, G.M., Carmignoto, G., Arosio, D., 2016. Synchronous Bioimaging of Intracellular pH and Chloride Based on LSS Fluorescent Protein. *ACS Chem. Biol.* 11, 1652–1660. <https://doi.org/10.1021/acscchembio.6b00103>
- Patrich, E., Piontkewitz, Y., Peretz, A., Weiner, I., Attali, B., 2016. Maternal immune activation produces neonatal excitability defects in offspring hippocampal neurons from pregnant rats treated with poly I:C. *Sci. Rep.* 6, 1–12. <https://doi.org/10.1038/srep19106>
- Pearce, R.A., 1993. Physiological evidence for two distinct GABAA responses in rat hippocampus. *Neuron* 10, 189–200. [https://doi.org/10.1016/0896-6273\(93\)90310-N](https://doi.org/10.1016/0896-6273(93)90310-N)
- Peerboom, C., Wierenga, C.J., 2021. The postnatal GABA shift: A developmental perspective. *Neurosci. Biobehav. Rev.* 124, 179–192. <https://doi.org/10.1016/j.neubiorev.2021.01.024>
- Pisella, Gaiarsa, Diabira, Zhang, Khalilov, Duan, Kahle, Medina, 2019. Impaired regulation of KCC2 phosphorylation leads to neuronal network dysfunction and neurodevelopmental pathology. *Sci. Signal.* 12. <https://doi.org/10.1126/scisignal.aay0300>
- Poulopoulos, A., Aramuni, G., Meyer, G., Soykan, T., Hoon, M., Papadopoulos, T., Zhang, M., Paarmann, I., Fuchs, C., Harvey, K., Jedlicka, P., Schwarzacher, S.W., Betz, H., Harvey, R.J., Brose, N., Zhang, W., Varoqueaux, F., 2009. Neuroligin 2 Drives Postsynaptic Assembly at Perisomatic Inhibitory Synapses through Gephyrin and Collybistin. *Neuron* 63, 628–642. <https://doi.org/10.1016/j.neuron.2009.08.023>
- Qi, C., Chen, A., Mao, H., Hu, E., Ge, J., Ma, G., Ren, K., Xue, Q., Wang, W., Wu, S., 2022. Excitatory and Inhibitory Synaptic Imbalance Caused by Brain-Derived Neurotrophic Factor Deficits During Development in a Valproic Acid Mouse Model of Autism. *Front. Mol. Neurosci.* 15, 1–19. <https://doi.org/10.3389/fnmol.2022.860275>
- Ramamoorthi, K., Lin, Y., 2011. The contribution of GABAergic dysfunction to neurodevelopmental disorders. *Trends Mol. Med.* 17, 452–462. <https://doi.org/10.1016/j.molmed.2011.03.003>
- Raol, Y.H., Joksimovic, S.M., Sampath, D., Matter, B.A., Lam, P.M., Kompella, U.B., Todorovic, S.M., González, M.I., 2020. The role of KCC2 in hyperexcitability of the neonatal brain. *Neurosci. Lett.* 738, 1–8. <https://doi.org/10.1016/j.neulet.2020.135324>
- Ratz, M., Testa, I., Hell, S.W., Jakobs, S., 2015. CRISPR/Cas9-mediated endogenous protein tagging for RESOLFT super-resolution microscopy of living human cells. *Sci. Rep.* 5, 1–6. <https://doi.org/10.1038/srep09592>
- Rivera, C., Voipio, J., Kaila, K., 2005. Two developmental switches in GABAergic signalling: The K⁺-Cl⁻ cotransporter KCC2 and carbonic anhydrase CAVII. *J. Physiol.* 562, 27–36. <https://doi.org/10.1113/jphysiol.2004.077495>
- Ronald, A., Pennell, C.E., Whitehouse, A.J.O., 2011. Prenatal maternal stress associated with ADHD and autistic traits in early childhood. *Front. Psychol.* 1, 1–8. <https://doi.org/10.3389/fpsyg.2010.00223>

- Roux, S., Lohof, A., Ben-Ari, Y., Poulain, B., Bossu, J.-L., 2018. Maturation of GABAergic Transmission in Cerebellar Purkinje Cells Is Sex Dependent and Altered in the Valproate Model of Autism. *Front. Cell. Neurosci.* 12, 1–14. <https://doi.org/10.3389/fncel.2018.00232>
- Ruffolo, G., Cifelli, P., Roseti, C., Thom, M., van Vliet, E.A., Limatola, C., Aronica, E., Palma, E., 2018. A novel GABAergic dysfunction in human Dravet syndrome. *Epilepsia* 59, 2106–2117. <https://doi.org/10.1111/epi.14574>
- Ruusuvuori, E., Li, H., Huttu, K., Palva, J.M., Smirnov, S., Rivera, C., Kaila, K., Voipio, J., 2004. Carbonic Anhydrase Isoform VII Acts As A Molecular Switch in the Development of Synchronous Gamma-Frequency Firing of Hippocampal CA1 Pyramidal Cells. *J. Neurosci.* 24, 2699–2707. <https://doi.org/10.1523/JNEUROSCI.5176-03.2004>
- Salmon, C.K., Pribiag, H., Gizowski, C., Farmer, W.T., Cameron, S., Jones, E. V., Mahadevan, V., Bourque, C.W., Stellwagen, D., Woodin, M.A., Murai, K.K., 2020. Depolarizing GABA Transmission Restrains Activity-Dependent Glutamatergic Synapse Formation in the Developing Hippocampal Circuit. *Front. Cell. Neurosci.* 14, 1–16. <https://doi.org/10.3389/fncel.2020.00036>
- Savardi, A., Borgogno, M., Narducci, R., La Sala, G., Ortega, J.A., Summa, M., Armirotti, A., Bertorelli, R., Contestabile, A., De Vivo, M., Cancedda, L., 2020. Discovery of a Small Molecule Drug Candidate for Selective NKCC1 Inhibition in Brain Disorders. *Chem* 6, 2073–2096. <https://doi.org/10.1016/j.chempr.2020.06.017>
- Sedmak, G., Puskarjov, N.J.-M.M., Ulapec, M., Krušlin, B., Kaila, K., Judaš, M., 2016. Developmental Expression Patterns of KCC2 and Functionally Associated Molecules in the Human Brain. *Cereb. Cortex* 27, 4060–4072. <https://doi.org/10.1093/cercor/bhw218>
- Seja, P., Schonewille, M., Spitzmaul, G., Badura, A., Klein, I., Rudhard, Y., Wisden, W., Hübner, C.A., De Zeeuw, C.I., Jentsch, T.J., 2012. Raising cytosolic Cl⁻ in cerebellar granule cells affects their excitability and vestibulo-ocular learning. *EMBO J.* 31, 1217–1230. <https://doi.org/10.1038/emboj.2011.488>
- Shi, Y., Cui, M., Ochs, K., Brendel, M., Strübing, F.L., Briel, N., Eckenweber, F., Zou, C., Banati, R.B., Liu, G.J., Middleton, R.J., Rupprecht, R., Rudolph, U., Zeilhofer, H.U., Rammes, G., Herms, J., Dorostkar, M.M., 2022. Long-term diazepam treatment enhances microglial spine engulfment and impairs cognitive performance via the mitochondrial 18 kDa translocator protein (TSPO). *Nat. Neurosci.* 25, 317–329. <https://doi.org/10.1038/s41593-022-01013-9>
- Shin Yim, Y., Park, A., Berrios, J., Lafourcade, M., Pascual, L.M., Soares, N., Yeon Kim, J., Kim, S., Kim, H., Waisman, A., Littman, D.R., Wickersham, I.R., Harnett, M.T., Huh, J.R., Choi, G.B., 2017. Reversing behavioural abnormalities in mice exposed to maternal inflammation. *Nature* 549, 482–487. <https://doi.org/10.1038/nature23909>
- Sinha, A.S., Wang, T., Watanabe, M., Hosoi, Y., Sohara, E., Akita, T., Uchida, S., Fukuda, A., 2022. WNK3 kinase maintains neuronal excitability by reducing inwardly rectifying K⁺ conductance in layer V pyramidal neurons of mouse medial prefrontal cortex. *Front. Mol. Neurosci.* 15. <https://doi.org/10.3389/fnmol.2022.856262>
- Sprengers, J.J., van Aniel, D.M., Zuithoff, N.P.A., Keijzer-Veen, M.G., Schulp, A.J.A., Scheepers, F.E., Lilien, M.R., Oranje, B., Bruining, H., 2021. Bumetanide for Core Symptoms of Autism Spectrum Disorder (BAMBI): A Single Center, Double-Blinded, Participant-Randomized, Placebo-Controlled, Phase-2 Superiority Trial. *J. Am. Acad. Child Adolesc. Psychiatry* 60, 865–876. <https://doi.org/10.1016/j.jaac.2020.07.888>
- Staley, K.J., 2002. Diuretics as Antiepileptic Drugs: Should We Go with the Flow? *Epilepsy Curr.* 2, 39–40. <https://doi.org/10.1046/j.1535-7597.2002.00013.x>

- Sulis Sato, S., Artoni, P., Landi, S., Cozzolino, O., Parra, R., Pracucci, E., Trovato, F., Szczurkowska, J., Luin, S., Arosio, D., Beltram, F., Cancedda, L., Kaila, K., Ratto, G.M., 2017. Simultaneous two-photon imaging of intracellular chloride concentration and pH in mouse pyramidal neurons in vivo. *Proc. Natl. Acad. Sci.* 114, E8770–E8779. <https://doi.org/10.1073/pnas.1702861114>
- Talos, D.M., Sun, H., Kosaras, B., Joseph, A., Folkerth, R.D., Poduri, A., Madsen, J.R., Black, P.M., Jensen, F.E., 2012. Altered inhibition in tuberous sclerosis and type 11b cortical dysplasia. *Ann. Neurol.* 71, 539–551. <https://doi.org/10.1002/ana.22696>
- Thompson, S.M., Gahwiler, B.H., 1989. Activity-dependent disinhibition. II. Effects of extracellular potassium, furosemide, and membrane potential on E(Cl⁻) in hippocampal CA3 neurons. *J. Neurophysiol.* 61, 512–523. <https://doi.org/10.1152/jn.1989.61.3.512>
- Turrigiano, G.G., Nelson, S.B., 2004. Homeostatic plasticity in the developing nervous system. *Nat. Rev. Neurosci.* 5, 97–107. <https://doi.org/10.1038/nrn1327>
- Tyzio, R., Holmes, G.L., Ben-Ari, Y., Khazipov, R., 2007. Timing of the developmental switch in GABA mediated signaling from excitation to inhibition in CA3 rat hippocampus using gramicidin perforated patch and extracellular recordings. *Epilepsia* 48, 96–105. <https://doi.org/10.1111/j.1528-1167.2007.01295.x>
- Tyzio, R., Nardou, R., Ferrari, D., Tsintsadze, T., Shahrokhi, A., Eftekhari, S., Khalilov, I., Tsintsadze, V., Brouchoud, C., Chazal, G., Lemonnier, E., Lozovaya, N., Burnashev, N., Y., B.-A., 2014. Oxytocin-Mediated GABA Inhibition During Delivery Attenuates Autism Pathogenesis in Rodent Offspring. *Science* (80-). 343, 675–680.
- Uwera, J., Nedergaard, S., Andreasen, M., 2015. A novel mechanism for the anticonvulsant effect of furosemide in rat hippocampus in vitro. *Brain Res.* 1625, 1–8. <https://doi.org/10.1016/j.brainres.2015.08.014>
- Valeeva, G., Abdullin, A., Tyzio, R., Skorinkin, A., Nikolski, E., Ben-Ari, Y., Khazipov, R., 2010. Temporal coding at the immature depolarizing gabaergic synapse. *Front. Cell. Neurosci.* 4, 1–12. <https://doi.org/10.3389/fncel.2010.00017>
- Valeeva, G., Tressard, T., Mukhtarov, M., Baude, A., Khazipov, R., 2016. An Optogenetic Approach for Investigation of Excitatory and Inhibitory Network GABA Actions in Mice Expressing Channelrhodopsin-2 in GABAergic Neurons. *J. Neurosci.* 36, 5961–5973. <https://doi.org/10.1523/JNEUROSCI.3482-15.2016>
- van Andel, D.M., Sprengers, J.J., Keijzer-Veen, M.G., Schulp, A.J.A., Lillien, M.R., Scheepers, F.E., Bruining, H., 2022. Bumetanide for Irritability in Children With Sensory Processing Problems Across Neurodevelopmental Disorders: A Pilot Randomized Controlled Trial. *Front. Psychiatry* 13, 1–13. <https://doi.org/10.3389/fpsy.2022.780281>
- Van Den Bergh, B.R.H., Marcoen, A., 2004. High antenatal maternal anxiety is related to ADHD symptoms, externalizing problems, and anxiety in 8- and 9-year-olds. *Child Dev.* 75, 1085–1097. <https://doi.org/10.1111/j.1467-8624.2004.00727.x>
- Van den Bergh, B.R.H., van den Heuvel, M.I., Lahti, M., Braeken, M., de Rooij, S.R., Entringer, S., Hoyer, D., Roseboom, T., Räikkönen, K., King, S., Schwab, M., 2020. Prenatal developmental origins of behavior and mental health: The influence of maternal stress in pregnancy. *Neurosci. Biobehav. Rev.* 117, 26–64. <https://doi.org/10.1016/j.neubiorev.2017.07.003>
- van Eeghen, A.M., Bruining, H., Wolf, N.I., Bergen, A.A., Houtkooper, R.H., van Haelst, M.M., van Karnebeek, C.D., 2022. Personalized medicine for rare neurogenetic disorders: can we make it happen? *Cold Spring Harb. Mol. Case Stud.* 8, 1–14. <https://doi.org/10.1101/mcs.a006200>

- Vanhatalo, S., Matias Palva, J., Andersson, S., Rivera, C., Voipio, J., Kaila, K., 2005. Slow endogenous activity transients and developmental expression of K⁺-Cl⁻ cotransporter 2 in the immature human cortex. *Eur. J. Neurosci.* 22, 2799–2804. <https://doi.org/10.1111/j.1460-9568.2005.04459.x>
- Viitanen, T., Ruusuvuori, E., Kaila, K., Voipio, J., 2010. The K⁺-Cl⁻ cotransporter KCC2 promotes GABAergic excitation in the mature rat hippocampus. *J. Physiol.* 588, 1527–1540. <https://doi.org/10.1113/jphysiol.2009.181826>
- Viswanathan, S., Williams, M.E., Bloss, E.B., Stasevich, T.J., Speer, C.M., Nern, A., Pfeiffer, B.D., Hooks, B.M., Li, W.P., English, B.P., Tian, T., Henry, G.L., Macklin, J.J., Patel, R., Gerfen, C.R., Zhuang, X., Wang, Y., Rubin, G.M., Looger, L.L., 2015. High-performance probes for light and electron microscopy. *Nat. Methods* 12, 568–576. <https://doi.org/10.1038/nmeth.3365>
- Wang, D.D., Kriegstein, A.R., 2011. Blocking early GABA depolarization with bumetanide results in permanent alterations in cortical circuits and sensorimotor gating deficits. *Cereb. Cortex* 21, 574–587. <https://doi.org/10.1093/cercor/bhq124>
- Wang, D.D., Kriegstein, A.R., 2008. GABA Regulates Excitatory Synapse Formation in the Neocortex via NMDA Receptor Activation. *J. Neurosci.* 28, 5547–5558. <https://doi.org/10.1523/JNEUROSCI.5599-07.2008>
- Wang, T., Shan, L., Miao, C., Xu, Z., Jia, F., 2021. Treatment Effect of Bumetanide in Children With Autism Spectrum Disorder: A Systematic Review and Meta-Analysis. *Front. Psychiatry* 12, 1–11. <https://doi.org/10.3389/fpsy.2021.751575>
- Willems, J., de Jong, A.P.H., Scheefhals, N., Mertens, E., Catsburg, L.A.E., Poorthuis, R.B., de Winter, F., Verhaagen, J., Meye, F.J., MacGillavry, H.D., 2020. Orange: A CRISPR/Cas9-based genome editing toolbox for epitope tagging of endogenous proteins in neurons. *PLoS Biology*. <https://doi.org/10.1371/journal.pbio.3000665>
- Xiong, Z.Q., Saggau, P., Stringer, J.L., 2000. Activity-dependent intracellular acidification correlates with the duration of seizure activity. *J. Neurosci.* 20, 1290–1296. <https://doi.org/10.1523/jneurosci.20-04-01290.2000>



Addendum

Carlijn Peerboom

Summary

Our brain is a fascinatingly complex organ that enables us to process information from the outside world and to respond through actions, thoughts, ideas and emotions. Our brain is comprised of a complex network of millions of brain cells (neurons), and their connections (synapses). Neurons come in two types: excitatory and inhibitory. When an excitatory neuron is active, it will send positive electrical signals through its excitatory synapses to the next neurons in the network. When an inhibitory neuron is active, it will provide subsequent neurons with negative electrical signals via its inhibitory synapses. Thus, our brains process information through a constantly changing combination of positive and negative electrical signals, processed by a network of neurons and synapses. All positive and negative signals simultaneously received by a brain cell, determine whether the cell will become active itself and will pass its electrical signals on to the next cells in the network.

The architecture of the adult brain is set up during brain development, which starts already in the womb. Genes provide the blueprint for the first steps in network formation, by dictating which neurons and synapses should be generated. In addition, network development is directed by spontaneous, electrical neuronal activity. When neurons are simultaneously active or active right after each other, they will make extra and stronger connections with each other. Since all electrical signals are still excitatory, the fetal neuronal network grows very quickly. Excitatory signals stimulate neuronal proliferation, synapse formation and synaptic strengthening in the immature brain. At this time, excitation is mainly provided by a substance called gamma-aminobutyric acid or GABA.

Only later on, sensory experiences start affecting the electrical activity in the network. The outside world affects network development in this way. Around the same time, GABA is changing from being excitatory, to providing electrical inhibition. Excitation is now provided by another signaling molecule, called glutamate. Inhibition enables the brain to handle an enormous amount of external stimuli in a controlled manner by filtering out irrelevant inputs and only passing on relevant stimuli.

The gradual developmental change in the function of GABA from excitation to inhibition is called the GABA shift. During my PhD, I studied the GABA shift in brain slices from mice. Brain development in mice and humans is very similar, though much faster in mice. In comparison: humans spend nine months in the womb, a mouse only three weeks. In humans, GABA shifts during the last three months of pregnancy, in mice during the first two weeks after birth.

To measure the GABA shift in murine brain slices, we tested a new sensor. We could discern the GABA shift by comparing dozens of neurons in slices of different ages. In addition, we used the sensor to investigate the effect of early life stress on the GABA shift. We saw that stress delayed the GABA shift in young mice. This study underlines the role of experience in brain development, which allows for adaptability, but also leads to vulnerability.

We also investigated the consequences of accelerating and delaying the GABA shift. Previous studies have shown that the excitatory GABA promotes synapse formation. Therefore, we expected that a delayed GABA shift would result in an overproduction of synapses. However, this is not what we observed when we delayed the GABA shift in slices from one week-old mice. We saw that the delayed GABA shift did not affect synapses, but found indirect changes in the neurons' electrical properties. This work is important for neurodevelopmental disorders such as autism, in which the GABA shift often seems delayed. Our research shows that such a delay affects further brain development.

We are only beginning to understand how genetic mutations and early life experiences affect the timing of the GABA shift and push brain development into different directions. I hope that this thesis contributes to our understanding of brain development. I think that we will better understand our brain and neurodevelopmental disorders and gain insights for therapeutic interventions, by continuing combining basic and clinical research in brain development in the future.

Nederlandse samenvatting

Ons brein is een fascinerend orgaan, dat ons in staat stelt informatie uit de wereld om ons heen te verwerken en daarop te reageren met emoties, gedachten, ideeën en acties. Ons brein bestaat uit een ingewikkeld netwerk van miljoenen hersencellen en hun verbindingen, ook wel synapsen genoemd. We kunnen hersencellen indelen in twee soorten: stimulerend en remmend. Als een stimulerende hersencel actief is, zal hij via zijn stimulerende synapsen, positieve elektrische signalen afgeven aan de volgende hersencellen in het netwerk. Als een remmende hersencel actief is, zal hij via zijn remmende synapsen, zorgen voor negatieve elektrische signalen in volgende hersencellen. Onze hersenen verwerken informatie dus door middel van een continu veranderende combinatie van positieve en negatieve elektrische signalen doorgegeven in een netwerk van hersencellen en synapsen. Al de positieve en negatieve signalen die een cel tegelijkertijd ontvangt, bepalen samen of een hersencel zelf actief wordt en elektrische signalen doorgeeft aan de volgende cellen in het netwerk.

De aanleg van de hersenen begint al in de baarmoeder. De eerste stappen van de hersenontwikkeling worden vooral bepaald door genen, die dicteren welke hersencellen en synapsen aangemaakt moeten worden. Daarnaast wordt de ontwikkeling van het netwerk beïnvloedt door de spontane, elektrische activiteit van de hersencellen. Als hersencellen tegelijk of vlak na elkaar actief zijn, zullen ze extra en sterkere verbindingen met elkaar gaan maken. Het jonge netwerk kan zich enorm snel ontwikkelen, omdat alle elektrische signalen in het brein nog stimulerend zijn. De stimulerende signalen helpen hersencellen om zich te vermenigvuldigen, om meer verbindingen met elkaar te maken en om al bestaande synapsen te versterken. De stimulatie in het jonge brein wordt vooral verzorgd door een stof die gamma-amino boterzuur of GABA genoemd wordt.

Pas later in de ontwikkeling, zullen via zintuigen prikkels van buitenaf de elektrische activiteit in het netwerk gaan bepalen. Zo kan ook de buitenwereld de ontwikkeling van het netwerk beïnvloeden. Ongeveer tegelijkertijd, zal GABA niet meer stimuleren, maar zorgen voor elektrische remming. De stimulerende signalen worden dan verzorgd door een andere stof, glutamaat. Op die manier kan het brein op een gecontroleerde manier omgaan met al de prikkels van buiten; prikkels die belangrijk zijn moeten worden doorgegeven en onbelangrijke prikkels worden weggefilterd.

De geleidelijke verandering in de functie van GABA, van stimulatie naar remming, die tijdens de ontwikkeling plaats vindt, wordt de GABA shift, of de GABA overgang genoemd. Tijdens mijn PhD heb ik de overgang van GABA bestudeerd in plakjes van muizenhersenen. De hersenontwikkeling van muizen en mensen lijkt erg op elkaar, al gaat de ontwikkeling in de muis veel sneller. Ter vergelijking: een mens spendeert

negen maanden in de baarmoeder, een muis maar drie weken. De overgang van GABA gebeurt bij mensen tijdens de laatste drie maanden van de zwangerschap en bij muizen tijdens de eerste twee weken na de geboorte.

Om de overgang van GABA te volgen in muizen hersenplakjes, hebben we een nieuwe sensor getest. We konden de overgang van GABA meten, door het signaal van de sensor in tientallen hersencellen in plakjes van verschillende leeftijden te vergelijken. Bovendien hebben we het effect van stress op de overgang van GABA met de sensor onderzocht. We zagen dat stress in jonge muizen de overgang van GABA vertraagd. Deze studie benadrukt dat hersenenontwikkeling niet alleen gestuurd wordt door genen, maar ook door ervaringen, wat het brein flexibel, maar tegelijk ook kwetsbaar maakt.

We hebben ook onderzocht hoe we de overgang van GABA in muizen hersenplakjes kunnen manipuleren en wat de consequenties van een versnelde en vertraagde overgang van GABA zijn. Eerdere studies hebben laten zien dat de stimulerende werking van GABA belangrijk is voor de vorming van synapsen. Op basis daarvan verwachtten we dat als de overgang van GABA vertraagd is, er teveel synapsen gevormd zouden worden. Maar wij vonden iets anders. We vonden dat de overgang van GABA, synapsen niet meer beïnvloedt in plakjes van muizen van een week oud. Maar vertraging van de overgang van GABA heeft wel een indirect effect op de elektrische eigenschappen van hersencellen. Dit werk is van belang voor patiënten met ontwikkelingsstoornissen zoals autisme, waarin de overgang van GABA veelal vertraagd lijkt. Ons onderzoek laat zien dat zo'n vertraging de verdere ontwikkeling van het brein verandert.

Op dit moment beginnen we pas te begrijpen hoe genen en ervaringen de overgang van GABA beïnvloeden en hersenontwikkeling verschillende richtingen op duwen. Ik hoop dat dit proefschrift bijdraagt aan ons begrip van hersenontwikkeling en daarmee ook van ontwikkelingsstoornissen. Ik denk dat we, door fundamenteel en klinisch onderzoek naar hersenontwikkeling te blijven combineren, ons brein en ontwikkelingsstoornissen steeds beter zullen begrijpen en inzicht zullen krijgen in behandel mogelijkheden.

Curriculum Vitae

Carlijn Peerboom was born on the 22nd of January 1993 in Geleen, the Netherlands. In 2011, she obtained her Gymnasium diploma (cum laude) at the Graaf Huyn College in Geleen. She completed a Bachelor's in Biomedical Sciences at Leiden University and the Karolinska Institutet in Stockholm. She then pursued a Master's in Biomedical Sciences with a focus on Neuroscience and Science Communication at Leiden University. Carlijn joined the lab of Joke Meijer to investigate neuronal firing rhythms in the brain's circadian clock. She followed the Leiden Science Communication and Society Programme and did an internship in science journalism at the editorial office of New Scientist in Amsterdam. She then joined the lab of Frances Edwards in London to investigate the role of microglia in the early synaptic alterations in a novel mouse model of amyloidopathy. Driven by an interest in electrophysiology, synaptic transmission and neurological diseases, Carlijn joined the lab of Corette Wierenga in 2017 to pursue her PhD. The results of her research are presented in this thesis.

List of publications

Peerboom C, Wijne T, Wierenga CJ. 2023. Treatment with furosemide indirectly increases inhibitory transmission in the developing hippocampus. *BioRxiv* (preprint) doi: <https://doi.org/10.1101/2023.07.11.548438>

Peerboom C, De Kater S, Jonker N, Rieter MPJM, Wijne T, Wierenga CJ. 2023. Delaying the GABA shift indirectly affects membrane properties in the developing hippocampus. *J Neurosci*. 2023 Jul 26;43(30):5483-5500. doi: [10.1523/JNEUROSCI.0251-23.2023](https://doi.org/10.1523/JNEUROSCI.0251-23.2023).

Herstel LJ*, **Peerboom C***, Uijtewaal S, Selemangel D, Karst H, Wierenga CJ. Using SuperClomeleon to Measure Changes in Intracellular Chloride during Development and after Early Life Stress. *eNeuro*. 2022 Dec 23;9(6). doi: [10.1523/ENEURO.0416-22.2022](https://doi.org/10.1523/ENEURO.0416-22.2022).
* contributed equally.

Peerboom C, Wierenga CJ. The postnatal GABA shift: A developmental perspective. *Neurosci Biobehav Rev*. 2021 May;124:179-192. doi: [10.1016/j.neubiorev.2021.01.024](https://doi.org/10.1016/j.neubiorev.2021.01.024).

Benitez DP, Jiang S, Wood J, Wang R, Hall CM, **Peerboom C**, Wong N, Stringer KM, Vitanova KS, Smith VC, Joshi D, Saito T, Saido TC, Hardy J, Hanrieder J, De Strooper B, Salih DA, Tripathi T, Edwards FA, Cummings DM. Knock-in models related to Alzheimer's disease: synaptic transmission, plaques and the role of microglia. *Mol Neurodegener*. 2021 Jul 15;16(1):47. doi: [10.1186/s13024-021-00457-0](https://doi.org/10.1186/s13024-021-00457-0).

Acknowledgements

Promoveren doe je niet alleen. Graag wil ik hier iedereen bedanken die me de afgelopen vijf jaar heeft aangemoedigd, geholpen en gesteund.

Allereerst wil ik graag mijn promotoren bedanken. Corette, bedankt voor een plek in jouw lab. Jouw ongekeerde enthousiasme, positiviteit en doorzettingsvermogen hebben mij regelmatig door de tegenvallers, die ook bij een PhD horen, heen gesleept. Bovendien heb je mij altijd veel vrijheid gegeven in de invulling van mijn onderzoek en dat heb ik als super stimulerend ervaren. Een samenwerking, summerschool of conferentie? Jij stond daar altijd voor open. Ik probeer wat van jouw onbevanging mee te nemen naar mijn toekomst! Anna, jouw scherpe blik maakte mijn project beter en mijzelf scherper. Dank voor je toewijding en support.

Graag wil ik ook alle leden van de lees- en promotiecommissie bedanken voor het lezen en beoordelen van dit proefschrift: Freek Hoebeek, Nael Nadif Kasri, Geeske van Woerden, Peter Burbach, Maarten Kole en in het bijzonder Christian Lohmann. In 2019 werd ik hartelijk door jouw lab ontvangen, om perforated patch experimenten te komen doen in slices van de visuele cortex. Monique had in utero electroporaties gedaan om NKCC1 tot overexpressie te brengen en ik was super benieuwd of we ook op die manier chloride levels konden manipuleren. Helaas gooide de Covid pandemie roet in het eten en moesten we mijn experimenten afblazen. Echter, toen ik een aantal jaar later, tegen het eind van een PhD plots een amplifier nodig had, kon ik weer op het Lohmann lab rekenen. Enorm bedankt!

Henk, wij leerden elkaar al tijdens het begin van mijn PhD kennen, toen ik van plan was om perforated patch recordings te gaan doen, en jij die techniek net onder de knie bleek te hebben. Ook gedurende de rest van mijn PhD heb ik nog veel van jouw fingerspitzengefühl voor elektrofysiologie mogen leren. Bovendien zocht jij contact met het Wierengalab toen je muizen met een chloride sensor naar Utrecht wilde halen en je je af vroeg of wij daar met onze two-photon microscoop niet wat plaatjes van konden maken. Dat laatste bleek nog niet zo simpel als gedacht. Gelukkig schoot Lotte al snel te hulp. Enorm veel dank voor al jouw doorzettingsvermogen en mentale support als de calibratie weer eens niet lukte. Samen hebben we, met hulp van Sten, Dunya en Marian, de voors en tegens van het meten van chloride levels in jonge Superclomeleon muizen in kaart gebracht en met de rest van de wereld kunnen delen. Enorm bedankt allemaal!

René, Bart, Zehra, Jian, Maria, Marvin, Dennis, Hai Yin, Elske and Cátia, thanks for making my time in the Wierenga lab a lot of fun and thanks for being such amazing colleagues! I learnt so much from all of you! You were always there for support when the slices were acting weird, the set up seemed about to explode, a virus needed to be prepared, the electricity went off, a poster or presentation needed improvement, or a borrel needed organization. Bedankt voor alles!

Thanks as well to Vicky, Renate, Hilgo, and Martien. I really enjoyed our TOP meetings and your wild, out-of-the-box ideas for my project and for potential collaborations. Your helped me putting my work into a broader context, which was super useful and a lot of fun.

Thanks also to Manon, Milena, Yolanda, Jelmer, Robbelien, Wouter, Wilco, Daphne, Josiah, Saishree, Klara, Wendy, Arthur, Niels, Katerina, Derk, Nicky, Cynthia, Lisa, Marijn, Robin, Jorian, Dipti, Fangrui, Lilian, Babet, Joyce, Harriet, Mai Dan, Ha, Chun Hei, Noortje, Anna, Albert, Jey, Ginny, Florian, Harold, Lukas, Mike, Sander, Martin, Lena, Ron, Esther, and Eugene, Ilya, Phebe and Bart. It was such a pleasure to get to know all of you! Thanks for all your help and support during my PhD and thanks for bringing so much fun to the lunch breaks and borrels.

Deze thesis was er ook nooit geweest zonder de talentvolle en enthousiaste studenten die ik de afgelopen jaren heb mogen begeleiden. Sam, Marijn, Nikki en Tessel, hartelijk dank voor al jullie hulp, doorzettingsvermogen en gezelligheid. Jullie hielpen me orde in de chaos te scheppen, experimenten af te ronden en brachten een berg aan nieuwe inzichten en goede vragen. Ik wens jullie allen het allerbeste voor jullie toekomst!

Thanks so much to my paranympths, Ate and Nazmiye. The two of you manage to always put a smile on my face. I hope that this protocol also works on the day of my defense! Thanks so much for all the support and laughter in and around the Kruyt.

Dank ook aan alle Hospital Hero's, met Charlotte en Nicolle in het bijzonder. Het schrijven van nieuwsberichten en het brainstormen over de app heeft mijn PhD-periode enorm verrijkt! Ik wens jullie en stichting Hospital Hero het allerbeste voor de toekomst.

Heel veel dank ook voor Christien, Eva, Giulia, Sofja, Melanie, Emilie, Marijn, Caroline, Aglaia, Door, Loes, Stephanie, Renee, Judith, Melissa, Diana, Josta, Kiki, Linda, Esmé, Eveline en Anne-Floor. Wat ben ik blij met al jullie lieve vriendinnen! Jullie inzichten wisten mijn de PhD stress altijd te relativeren en jullie knuffels, humor en gezelligheid zijn me heel erg dierbaar.

Acknowledgements

Bedankt ook aan alle Lowlanders. Mijn PhD begon en eindigt (zo ongeveer) met jullie in een tentje om me heen. Heel erg bedankt voor de fijne etentjes, feestjes en festivals! Ik heb niet zo vaak zo hard gelachen als in een poncho onder een picknicktafel met een bakje kibbeling en jullie aan mijn zijde.

Veel dank ook aan al lieve mijn familie! Of ik nu in Geleen en omstreken was, of (alweer) ging verhuizen, jullie stonden altijd voor me klaar. Speciale dank ook voor Hannah, wat was het fijn om samen met jou Utrechter te zijn!

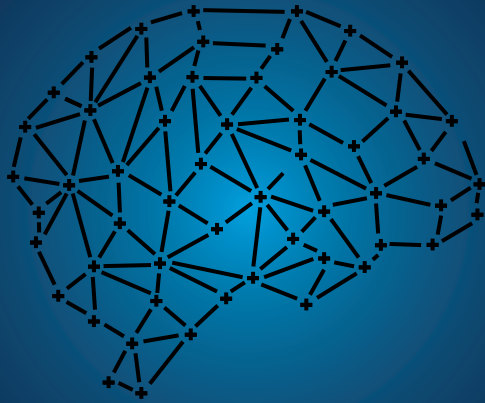
Thanks as well to Igor, Jonathan, Anatoly, Maayan and Itamar and all other family and friends in Israel for welcoming me so kindly into your homes. I hope we will meet again soon and cannot wait to meet little Be'eri!

Lieve papa, mama, Felix en Megan. Enorm veel dank voor alle support. Juist als het even tegenzat, realiseerde ik me maar weer hoe blij ik met jullie ben! Bedankt voor alles.

Last, maar zeker niet least, lieve Boris: wat ben ik blij dat onze wegen elkaar in het Kruyt-gebouw kruisten! Met jou is het leven leuker, voelen de lasten lichter, en klinkt metal mooier (tenminste, soms).

Heel veel dank!

Carlijn Peerboom,
Utrecht 2023



UMC Utrecht



Universiteit Utrecht

ISBN 978-94-6483-284-6